Bio-Modification of Non-Biological Surfaces with Function-Spacer-Lipid Constructs by Methods Including Bioprinting

Katie Barr

Thesis submitted in fulfilment of the degree of Doctorate of Philosophy

Auckland University of Technology

Auckland

New Zealand

2013

Table of Contents

List of figures

List of tables

Attestation of Authorship

"I hereby declare that this submission is my own work and that, to the best of my knowledge and belief, it contains no material previously published or written by another person (except where explicitly defined in the acknowledgments), nor material which to a substantial extent has been submitted for the award of any other degree or diploma of a university or other institution of higher learning."

Katie Barr

Auckland

2013

Acknowledgements

Firstly I would like to thank my supervisor Steve Henry for his guidance, support and enthusiasm throughout this research. It's been an exciting time and I thank him for this opportunity. I would also like to thank my supervisors Olaf Diegel and Stephen Parker for their support and assistance along the way.

I would like to thank the Foundation for Research Science and Technology for the TIF three year PhD scholarship, the Manchester Trust for my fourth year PhD scholarship, and AUT for the laptop scholarship.

Thank you to my colleagues at KODE Biotech Ltd, including Laurel King, Debbie Blake and Eleanor Williams and my fellow PhD students Caroline Oliver and Sarvani Komarraju who have made this a fun time, and provided encouragement along the way.

Finally, thanks to James and my family for their continued support, patience and confidence in me.

Abstract

The ability to immobilise biomolecules on solid surfaces whilst retaining their function is the foundation of microarrays, biosensors and other miniaturised assays that provide convenient ways of analysing binding reactions of molecules with their ligands. The stability, sensitivity, cost and ease of use are important considerations when designing these systems, with the immobilisation of the biomolecule to a surface being the key to success. Miniaturised assays can allow multiplex analysis of various samples from protein interactions, carbohydrate recognition events, DNA hybridisation and cell immobilisation. They can enable fast, high-throughput and efficient testing for diagnostics, environmental testing and research purposes, as well as enabling production of whole-cell arrays to tissue engineering. The drive to miniaturisation and integration has advanced the need for effective and stable attachment of biomolecules to solid surfaces which allow high probe density and high signal to noise ratio whilst maintaining the activity of the molecule.

KODE™ technology is a surface engineering technology that enables modification of a cell or virion surface without causing harm. This is achieved with Function-Spacer-Lipid (FSL) constructs that embed into the membrane. They contain a functional head group that conveys a desirable attribute to the cell or virion, which include carbohydrate or peptide antigens, fluorescent markers, whole proteins or useful molecules for attachment, e.g. biotin. This research set out to determine if FSL constructs could modify non-biological surfaces as well as biological ones.

The aims of this research were to establish whether FSL constructs could be attached to non-biological surfaces, and if so what the mechanisms of attachment and the limitations might be and what methods could be used to deliver the molecules to the surface. Inkjet printing was investigated as the primary delivery method, as it is becoming a popular approach to apply biological molecules to surfaces. It is a non-contact, precise, flexible and fast technique which lends itself well to this field where precise patterning, sample and waste volume and cost are important factors. The water soluble advantages of FSL constructs make their use as a "bioink" attractive and this method proved to be successful at applying FSLs to surfaces.

FSL constructs were successfully applied to various surfaces including papers, polymers, metals, modified cellulose materials and natural fibres. All surfaces were able to attach the FSLs. The stability of the attachment was shown to be unchanged after 8 months at room temperature. Some detergents and solvents were able to remove the FSLs from the surface, indicating particular limitations of the attachment. Variations of

the FSL structure gave insights into the attachment mechanisms which indicated that the amphiphilic nature of these constructs is important, with hydrophobic forces causing adsorption of these constructs onto solid surfaces.

Investigations into possible applications of FSL modified surfaces included mapping monoclonal antibodies against different blood group antigens, assessing disease markers in solid phase and attaching recombinant proteins to surfaces. The surface selected as optimal for bioassays was paper due to low background staining and high sensitivity when used in immunoassays. FSL constructs appear to allow orientated immobilisation of biomolecules, spaced away from the surface. Good correlation to serological results using the same constructs was observed, indicating the solid phase FSL assays can provide accurate results.

Cells and kodecytes were also shown to be immobilised onto solid surfaces through FSL attachment. Through linker molecules, red blood cells were attached to microspheres, paper, plastic and other surfaces which themselves were modified with FSLs. This is a potential novel method for producing cellular arrays, cellular bandages and for other applications needing precise attachment of cells. Further research will reveal other types of cells able to be used in this way.

In summary it was discovered that FSL constructs were able to modify non-biological surfaces with carbohydrate antigens, peptide markers and biotin, adding functionality to a wide variety of surfaces. This now opens up the potential to use FSLs as a universal surface modification technology by providing a fast, simple and easily controlled approach for biomolecule immobilisation.

Abbreviations

BSA	Bovine serum albumin
CMG	Carboxymethylglycine
DOD	Drop-on-demand
DOPE	Dioleoylphosphatidylethanolamine
EIA	Enzyme immunoassay
ELISA	Enzyme-linked immunosorbent assay
FSL	Function-Spacer-Lipid KODE™ construct
GOD	Glucose oxidase
HLA	Human Leukocyte Antigen
HRP	Horseradish peroxidase
Ig	Immunoglobulin
μPADs	Microfluidic paper-based analytical devices
PBS	Phosphate buffered saline
PEG	Polyethylene glycol
pFSL-EIA	Printed FSL enzyme immunoassay
RBC	Red blood cell (erythrocyte)
SAMs	Self-assembled monolayers
SEM	Scanning electron microscope
TLC	Thin layer chromatography

Chapter 1 Introduction

Immobilisation of biological molecules onto non-biological solid surfaces is an important way of examining and utilising the binding properties of certain ligands with their binding partners. These immobilisation methods, capable of preserving biological activity, have applications from microarrays to tissue engineering and regenerative medicine, and are providing valuable research tools for understanding these biomolecular recognition mechanisms. As well as research tools they are becoming established platforms for diagnostic assays, biosensors and bioreactors with applications in environmental testing, biomedical devices and point-of-care systems. The ability to functionalise surfaces in specific patterns or areas allows multiplex detection of analytes, hybridisation of DNA or selective patterning of cells and tissues, and these varied platforms are becoming more accessible as the repertoire of applications increases.

1.1 Bio-modification of non-biological surfaces with biological molecules

1.1.1 Immobilisation principles

The growing trend towards miniaturisation and integration in biological devices has advanced the technologies focussed on immobilisation of biological molecules onto solid surfaces. The ability to attach and pattern proteins, carbohydrates, DNA, lipids, cells and tissues in a "bio-chip" or "bio-platform" has been of increasing interest in recent years as it allows smaller test samples, higher sensitivity and higher throughput. The demand for high probe density, maintenance of biological activity and ease of preparation and use, has led to the development and establishment of a variety of methods for attaching biomolecules to non-biological surfaces.

The main considerations for choosing an immobilisation method are the surface chemistry, the distance of the biomolecule from the surface, the density of the probes, the structure of the biomolecule and the ability of the biomolecule to remain functional and undenatured. There are advantages and disadvantages of all methods but there is likely to be an optimum method for each probe molecule which preserves the greatest activity, allows for the highest attachment density and produces the best signal to noise ratio, where the unique chemistry and stability of the molecules have been considered.

The main techniques for immobilising biological molecules onto an insoluble matrix are

- Adsorption
- Covalent bonding
- Cross-linking
- Entrapment
- Affinity interactions

Figure 1 shows a schematic representation of these techniques. These methods of immobilisation are not independent techniques as they are increasingly being incorporated together to achieve the optimal immobilisation. In fact, although comprehensive, this list is not definitive as certain authors chose to classify them differently (Prieto-Simon et al., 2008; Sassolas et al., 2012; Sheldon, 2007). Sensitivity, stability, reproducibility and cost are all factors that influence the choice of immobilisation method to produce an outcome best suited to the intended application.

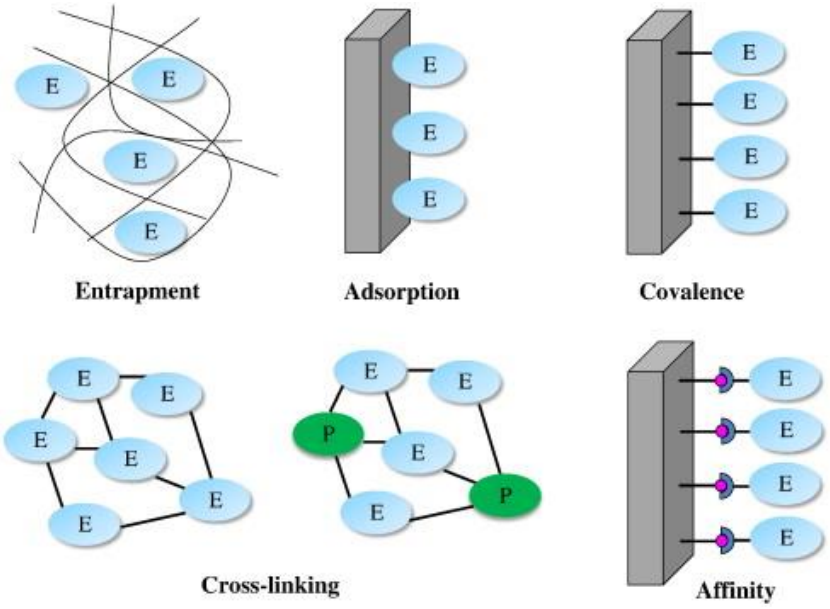

Figure 1. Schematic representation of the main different methods of immobilisation, E= enzyme, P= inert protein (Sassolas et al., 2012).

Adsorption

Adsorption involves the physical attachment to a matrix of a soluble molecule and relies on the non-specific physical interaction between the molecule and the surface. It is the easiest method of immobilisation as it requires no modification of the surface or the biomolecule, however it is a weak reaction and the problem of the loss of the molecule through desorption, especially in aqueous solutions, can occur (Brady & Jordaan, 2009; Wan et al., 2013). It was among the first immobilisation methods and has been used to immobilise enzymes, antibodies and glycans. The adsorption mechanisms involve hydrogen bonding, van de Waals interactions, ionic and electrostatic interactions, which are intrinsic advantages of the adsorption process as there is no requirement of functionalisation of the surface and it does not create a harsh environment for the biomolecule. However, this loose binding is susceptible to temperature and pH change and the surface is also vulnerable to non-specific binding. Although this is a simple strategy, it can be hard to control (Kong & Hu, 2012; Rabe et al., 2011).

The surface characteristics determine the nature of the binding between the adsorbate (the substance adsorbed) and the adsorbent (the material on which adsorption can occur). Most

surfaces used for physical adsorption are polymer based with polystyrene and nitrocellulose being the common ones. Native organic and inorganic surfaces are usually able to adsorb proteins easily (Ekblad & Liedberg, 2010). However surfaces that bind biomolecules readily will also be susceptible to non-specific binding and so blocking of the free sites will also be required.

Polymer surfaces

The interaction of proteins with surfaces has been widely studied due to its common occurrence. It is a fundamental phenomenon of a complicated nature which has attracted a great amount of interest. Proteins are mostly amphiphilic and hence favour adsorption onto the surface over remaining in the bulk solution (Gray, 2004; Hlady & Buijs, 1996). Surfaces such as polystyrene, polyvinylidene fluoride (PVDF) and nitrocellulose, have been routinely used for enzyme-linked immunosorbent assays (ELISAs) and microarrays. However this weak attachment is easily disrupted and peptides must be larger than 15 residues to be adsorbed (Angenendt et al., 2002; Butler et al., 1992; Uttamchandani & Yao, 2008). Plastic surfaces can achieve high signal uniformity and reproducibility with immobilised antibodies, although hydrophobic polymer coatings on surfaces can increase the detection limit (Angenendt et al., 2002). Alternatively, modifying peptides with a hydrophobic residue can increase the binding to polystyrene for use in ELISAs. This can reduce the peptide size limitation for binding to these surfaces (Pyun et al., 1997), as proteins are known to adsorb through hydrophobic interactions (Datta et al., 2013; Di Risio & Yan, 2009).

Although a fast and simple process, protein adsorption on polystyrene surfaces can lead to alteration of the protein structure, reducing the amount of active protein available for capturing binding partners (Butler et al., 1992). Proteins undergo conformational change upon adsorption to surfaces due to the change in free energy state which induces a relaxed structure of the molecule. This change can lead to a decrease in the biological activity of the protein due to random orientation of the molecule, which can reduce the accessibility of the binding sites (Rabe et al., 2011).

Some of the first carbohydrate microarrays were spotted onto nitrocellulose and polystyrene surfaces (D. Wang et al., 2002; Willats et al., 2002). Glycan microarrays are becoming a common technique in glycomics, only emerging in the last 10 years as an extension of the DNA and protein microarrays developed earlier. Glycans are present in large numbers and in great diversity on the cell surface and have a variety of functions including cell communication, cell adhesion and high involvement in the immune response (Horlacher & Seeberger, 2008; Shin et al., 2005). Being able to study their structure and binding capabilities is therefore of great importance. Polysaccharides adsorbed onto nitrocellulose-coated glass slides were shown to be capable of specifically detecting monoclonal antibodies with various epitopes (D. Wang et al., 2002). The efficiency was affected by the size of the molecules, where larger molecules were

retained more effectively than small ones, similar to peptides on hydrophobic surfaces. This is due to the cooperative effect of a greater number of interactions per molecule of larger glycans (Kralovec et al., 1996).

The adsorption of carbohydrates onto oxidised polystyrene has also been investigated (Willats et al., 2002). Polysaccharides and glycoproteins arrayed onto its surface bind initially through hydrogen and ionic binding which captured the molecules, followed by hydrophobic forces stabilising the binding due to the removal of water between the hydrophobic surface and the carbohydrate. These microarrays were stable and reproducible and were shown to preserve their antigenicity by assessment with a panel of monoclonal antibodies. Poly-L-lysine coated slides are also popular for attachment of biomolecules and have shown efficient and uniform attachment of polysaccharides in a non-covalent manner (Shipp & Hsieh-Wilson, 2007). Poly-L-lysine slides carry dense amino groups creating a positive charged surface and so are also capable of binding DNA through electrostatic interactions (Venkatasubbarao, 2004).

Oligosaccharides are generally quite hydrophilic, impeding adsorption onto solid polymer surfaces. Attaching lipids to carbohydrates to create neoglycolipids can overcome this, allowing robust non-covalent attachment to solid surfaces suitable for glycans arrays. Diverse oligosaccharides were attached in this way and efficiency of this immobilisation was found to be high, regardless of the size of the molecule (Feizi et al., 2003; Fukui et al., 2002). Bryan et al, (2002) have also linked lipids to glycans, and successfully immobilised them on polystyrene surfaces through hydrophobic bonding. Polyfluorinated hydrocarbons linked to carbohydrates have been spotted onto Teflon-like slides and shown strong attachment to this surface, creating microarrays suitable for protein attachment studies (Chang et al., 2010). Another approach to immobilise glycans is through polyacrylamide glycoconjugates. The physical adsorption occurs through van der Waals interactions, but again larger molecules attach with greater efficiency than smaller ones (Galanina et al., 2012); a limitation of the adsorption process.

Inorganic surfaces

Silica, glass and other non-organic surfaces are well known for absorbing biomolecules, especially proteins (Sharma et al., 2003). The adsorption sites on a silica surface are active hydroxyl groups. Lysozyme, a well characterised protein, has been repeatedly used as a model enzyme for understanding protein adsorption. Bovine serum albumin (BSA) has similarly been studied due to its high concentration in serum. These proteins adsorb to silica mainly by electrostatic interactions. At pH 7 lysozyme adsorbs to silica in a monolayer, whereas at pH 4 lower adsorption is observed. This also results in a different orientation of this enzyme where a lower pH resulted in sloping away from the surface as opposed to the flat orientation at pH 7 (Parida et al., 2006). BSA adsorbs to silica to a much higher degree when the pH equals the isoelectric point (pI) of the protein compared to at a lower pH (Rabe et al., 2011). R-phycoerythrin, another protein studied on silica, was also influenced by the ionic strength,

where as the pH approached the pI of the protein, the molecule adsorbed more readily leading to complete and permanent adsorption below the pI. DNA adsorption to silica was shown to be due to intermolecular electrostatic forces, dehydration and hydrogen bonding (Parida et al., 2006).

Lysozyme has been shown to adsorb onto a charged silica surface via a specific arginine residue. This residue is positively charged at pH 7 and the protein is able to penetrate the water layer on the surface due to this long flexible side group, suggesting hydrophobic and electrostatic interactions are at play in protein adsorption (Kubiak-Ossowska & Mulheran, 2010; Salis et al., 2010).

Glucose oxidase (GOD) has been adsorbed onto a nanostructured TiO_2 surface for use as a biosensor. This material has advantages of large surface area, good stability, biocompatibility and enabled high enzyme loading of GOD (Cui et al., 2013). Ultrafast adsorption of lysozyme onto nanoporous silica has shown and advantage of large pores of the silica over smaller ones (J. Sun et al., 2006). Lipases adsorbed onto a hydrophobic octadecyl-sepabeads have shown retained activity and good stability (Cunha et al., 2008; J. M. Palomo et al., 2004). This adsorption method was compared to covalent bonding which showed high immobilisation yields but complete loss of activity, probably due to restricted activity or inaccessibility of the active site. The hydrophobicity of the surface enabled high yield through physical adsorption providing a low cost, simple and effective immobilisation procedure.

Covalent bonding

Covalent attachment utilises the reactive groups of the biomolecule to bind it to the surface and is the most stable bond for immobilisation. Common functional groups used are carboxyl, hydroxyl and amino which allow direct binding to a functionalised membrane. It is important that these functional groups are not required for the activity of the biomolecule. Covalent methods are robust, providing stable immobilisation with no leakage from the membrane and high density coverage. However, they can require harsh conditions which may affect the structure and therefore activity of the immobilised molecule and often involve long and complex protocols (Gao et al., 2012; Prieto-Simon et al., 2008). The binding is generally non-specific which can lead to random immobilisation or multiple site binding, reducing the activity of the biomolecule due to denaturation or blocking of the active site. Covalent binding can occur on inorganic carriers (glass, silicon, titanium), natural polymers (cellulose) and synthetic polymers (nylon, polystyrene) (Smith, 2004). Surface modification of polymers for covalent attachment is becoming increasingly popular due to the different surface functionalities that can be added, and the ability to select a polymer with the bulk properties desired for the end use (Goddard & Hotchkiss, 2007).

Functional groups

Chemically modified surfaces are commonly used to immobilise biomolecules. These functionalities include epoxides, amines, aldehydes, thiols, maleimides, azides, hydrazides and N-Hydroxysuccinimide (NHS) esters and can be chemically linked to native or modified proteins, carbohydrates, DNA or other molecules (Larsen et al., 2006; S. Park et al., 2013). The most common way of covalently immobilising proteins is through the primary amine of the N terminal or the numerous lysine residues on the molecules surface to amine reactive surfaces (D. S. Wilson & Nock, 2002). Proteins, however can have lysine residues spread over their surface which can lead to multiple binding sites on the protein and hence ineffective immobilisation (MacBeath & Schreiber, 2000). Amino functionalisation of carbohydrates is used frequently to bind glycans to derivatised surfaces (Larsen et al., 2006) whereas many different groups are used to functionalise DNA probes to covalently bind them to the surface (Sassolas et al., 2008; V. Singh et al., 2011). Some examples of functional groups used for immobilisation are shown used in Figure 2.

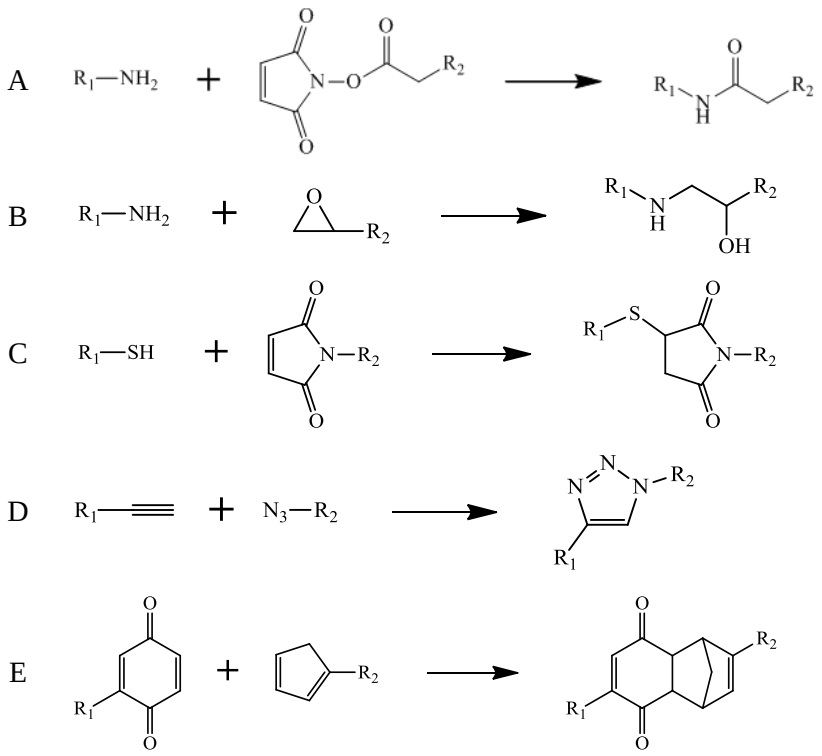

Figure 2. Examples of covalent coupling chemistries for immobilising biomolecules to surfaces. A) NHS ester with amines, B) epoxides with amines, C) maleimides with thiols, D) alkynes with azides and E) Diels-Alder cycloaddition (Horlacher & Seeberger, 2008).

Carbohydrates are commonly modified with reactive groups by reductive amination of the aldehyde group of the terminal reducing sugar. These reactive groups include amines, thiols, cyclopentadiene and azide which are able to be coupled to specific functional groups on the surface (Gao et al., 2012). Park et al, (2004; 2002) have shown the production of glycans arrays using maleimide-linked sugars covalently attached to thiol derivatised glass surfaces. The

mono- and disaccharides allowed investigation into the binding reactions of lectins with carbohydrates in a high throughput manner. An alternative is to use amine reactive NHS to couple amine-modified glycans to glass surfaces (Seo et al., 2010). This results in the formation of stable amide bonds and has produced sensitive arrays of more than 200 glycans (Blixt et al., 2004). Binding antibodies to a gold electrode for immunosensors can be prepared through this NHS coupling of the protein to a carboxyl activated surface. Greater sensitivity and hence signal to noise ratio is achieved compared to physical adsorption of the protein, due to increased antibody loading and a more reproducible orientation on the surface (Salam & Tothill, 2009).

Proteins and carbohydrates can be immobilised through activated hydroxyl groups located on the surface. Hydroxyl functionalised glass effectively bound to the reducing end of underivatised sugars via glycosidic bonds. Subsequent binding of fluorescent lectins demonstrated the applicability of this attachment method for specific and sensitive carbohydrate array fabrication (Nan et al., 2009). Electrospun polymer fibrous materials provide a large surface area for protein immobilisation with activation of hydroxyl groups on the fibre surface enabling the covalent attachment of lipases. This proved a robust method for biosensor fabrication and showed greatly improved stability compared to the free enzyme (Huang et al., 2008).

Oxidation of cellulose to generate aldehyde groups on the surface can be used to immobilise biomolecules. The carbonyl group can react with primary amines, found on the terminus of proteins, DNA or other biomolecules. A fluorescein labelled DNA aptamer has been reported to bind via an amino group on its 3' terminal. Compared to physical adsorption this technique was a strong and robust attachment (Su et al., 2007) with the cellulose providing a favourable surface for the aptamer activity. This ATP-binding aptamer allows detection of ATP using fluorescence in a system which switches between binding ATP and a quencher.

Epoxy-activated supports are popular for immobilising enzymes as they are able to bind to a multitude of different reactive groups (e.g. amino, hydroxyl or thiol) forming a strong bond. They can be reacted under favourable conditions for proteins, minimising inactivation and affording simple procedures (Mateo et al., 2000). First the enzyme is adsorbed onto the surface through hydrophobic interactions, followed by covalent attachment to the epoxy groups (Mateo, Palomo et al., 2007). However at neutral pH this binding can be slow, so in order to increase the binding rate and efficiency multifunctionalised epoxy supports have been developed which contain amines or thiols along with the epoxy which promote the initial adsorption of the proteins. Lectin attachment to epoxy-functionalised glass slides was carried out to produce super-microarrays. These platforms, capable of multiple simultaneous analyses due to duplication of arrays on each slide, showed highly consistent binding affinities of carbohydrates with high selectivity (X. Wang et al., 2013). Glycans have also been immobilised on epoxy

derivatised glass slides to enable characterisation of carbohydrate-binding proteins. The process of fluorescent labelling of glycans by reductive amination forms amines capable of reacting with the epoxide groups on the surface and provides a stable attachment of labelled glycans (de Boer et al., 2007).

Microspheres can be modified with various functionalities on their surface for covalent attachment of biomolecules. Lipase has been immobilised on microspheres through epoxy binding reactions and showed increased reactivity, reusability and stability compared to the free lipase (Lei et al., 2009). Indeed, immobilisation on microspheres offers advantages over planar surfaces due to their efficiency in bioassays. Commercial products are available with various activated epoxy supports for this use (Mateo et al., 2007; Mateo et al., 2003).

Silanisation of glass or silica can be achieved through the Si-OH groups and is a common method for covalent attachment of capture molecules through the terminal group of the silane (Aissaoui et al., 2011; Seidel & Niessner, 2008; Weetall, 1993). This terminal group can be aldehydes, amines, epoxides or thiols which are able to react with the modified biomolecules or directly with the amine groups of proteins in the case of aldehyde and epoxy surfaces. The main silanes used for biomolecule immobilisation are aminopropyltriethoxysilane (amino-silane) mercaptopropyltrimethoxysilane (thiol-silane) and glycidoxypropyltrimethoxysilane (epoxy-silane). Using 3-glycidoxypropyltrimethoxysilane to add epoxy groups on to the surface allowed immobilisation of urease through its amino groups in mild conditions (Pijanowska et al., 2003). Thiol terminated silanes enable maleimide containing molecules to be immobilised (Bhatia et al., 1989) and aldehyde silanes can react with the amines on proteins (MacBeath & Schreiber, 2000). Amino-silane functionalised silica magnetic nanospheres have been linked to the amino group of proteins using glutaraldehyde as linker, creating an effective and low cost platform for purification, immunoassay and other binding reactions (X. Liu et al., 2004). Glycan microarrays can be created by a condensation reaction between the carbohydrate aldehyde and an amine- modified glass surface (Yates et al., 2003).

Immobilisation of DNA through silanisation of the surface is common (Homs, 2002). Amine-modified oligonucleotides can be attached to a silica biosensor through amine-silanes and glutaraldehyde (W. Wang et al., 2013) and even silanising the DNA molecules themselves can allow direct attachment onto glass surfaces for compatibility with spotting techniques (Ravi Kumar, 2000).

Attachment of non-derivatised biomolecules for use in arrays avoids the time consuming modification of linking functional groups. Native carbohydrate immobilisation offers flexibility and diversity of covalently attached molecules for assessment of their role in essential biological processes (Song & Pohl, 2009). Highly reactive hydrazide groups are capable of binding to free reducing sugars (Godula & Bertozzi, 2010) and have been utilised to chemically join naturally

sourced glycans to surfaces. Using a gold or glass hydrazide modified surface, arrays of carbohydrates are able to probe binding proteins or bacteria (S. Park et al., 2009; Zhi et al.,2006). Similarly, aminooxyacetyl can bind to the reducing end of carbohydrates to create an oxime bond and the retained binding capabilities of these immobilised molecules have been demonstrated (X. Zhou & Zhou, 2006). These are simple, site specific methods capable of attaching structurally diverse glycans of different sizes to surfaces.

The random orientation of covalent bonding immobilisation can block activity or cause denaturing of the molecule. Site specific immobilisation can mitigate this effect by orientating the biomolecule in a reproducible and uniform arrangement, with the active site away from the membrane surface leaving it exposed to the sample solution. A covalent method available is site-directed mutagenesis to introduce a cysteine into the protein using recombinant methods. Cysteines contain an SH group which, when introduced to an area of the protein away from the active site, allows the thiol to bind to a gold or disulphide activated surface, causing site-specific immobilisation (Butterfield et al., 2001). This leaves the active site presented on the surface in such a way that it is available for interaction with its target molecule. It has been successful in increasing the activity of immobilised enzymes when compared to randomly orientated covalent binding, and hence can improve the reactions of biosensors and bioreactors (Hernandez & Fernandez-Lafuente, 2011). A similar method employs a polyethylene glycol (PEG) spacer containing *N*-hydroxysuccinimide (NHS) on one end and a maleimide group on the other. The NHS is coupled to an amino-functionalised surface. This functionalisation is achieved on mica or glass through silanisation with an amino-silane and leaves the thiol-reactive maleimide end of the PEG molecule free to bind to cysteines on a protein surface. This creates optimally orientated immobilisation and utilises a stable and reproducible coupling (Zimmermann et al., 2010).

PEG coupled to NHS at one end and acryloyl monomer at the other has been used to covalently attach cell adhesive peptides to a hydrogel. The NHS reacts with Arg-Gly-Asp (RGD) peptides attaching PEG to the biomolecule. The monomer part of the construct can then be photo-polymerised to form a hydrogel and the immobilised peptides used to attach cell surfaces. A concentration gradient of the RGD peptide was used to study stem cell adhesion and spreading, utilising the biocompatible properties of the hydrogel (Z. Liu et al., 2012).

Photochemical immobilisation

Photochemical immobilisation activates photosensitive reagents on biomolecules or material surfaces, generating reactive sites able to form covalent bonds with the target (Sigrist et al., 1995). It is a non-invasive procedure that does not cause denaturation of the biomolecule. Peptides, enzymes and DNA have been immobilised in this way and were able to bind ligands or hybridise effectively. Cellulose, made photoreactive by a thermochemical reaction with 1-fluoro-2-nitro-4-aziobenzene, creates highly reactive nitrene upon exposure to UV, which can

covalently bind a protein. GOD was bound using this method to show increased stability over the native enzyme. A comparison assessment of this technique against general adsorption of antibodies on polystyrene was carried out using an immunoassay test. The increased reactions of the photochemically linked protein demonstrate the advantage of this covalent binding. The C or N terminal of any protein is capable of reacting with the nitrene making this a broad-spectrum technique (Bora et al., 2006). A simpler method involves applying UV radiation to a droplet of protein solution on a glass slide. This removes the need for dispensing the molecules accurately. Arrays of Fab fragments were created on a quartz surface by using UV to disrupt disulphide bridges allowing the free thiol groups to react with the surface (Duroux et al., 2007). The resolution of the arrays is limited only by the focal point of the laser allowing spots of dimensions down to 20 µm. Patterning of biomolecules is also realised easily with this method by masking techniques or direct writing. A level of control is also afforded by applying different time periods of light, creating differing amounts of immobilised protein (Herbert et al., 1997). Perfluorophenyl azide modified surfaces were shown to attach carbohydrates through light activation. These unmodified sugars retained their binding abilities and showed specificity when incubated with various lectins, establishing a general method for carbohydrate immobilisation (H. Wang et al., 2011). An advantage of photoimmobilisation is the ability to optimise the pH, temperature and environment to the biomolecule rather than the chemical reaction conditions, since thermochemical reactions can require harsh and possibly denaturing agents (Sigrist et al., 1995).

Self-assembled monolayers

Self-assembled monolayers (SAMs) are formed by the spontaneous adsorption of organic molecules onto a surface. They are extremely ordered and easy to prepare and are hence very useful for surface functionalisation. They are the result of multiple interplays between the substrate and adsorbant which guide the self-assembly. These include intermolecular van der Waals and hydrophobic interactions which stabilise the structure along with other intramolecular forces (Grönbeck et al., 2000; Ulman, 1996; Vericat et al., 2010). The adsorption of thiols onto gold is well documented and has become a standard method for attaching biomolecules onto electrodes for use in biosensors (Chaki & Vijayamohanan, 2002). SAM formation involves initial physiosorption followed by covalent chemisorption of the sulphur group, and the formation of the densely packed phase (Vericat et al., 2010). By tailoring the terminal group the binding properties can be altered to allow attachment of various molecules such that covalent, non-covalent and affinity binding can occur on the monolayer

Amine groups of lysine residues of proteins are commonly used for attachment to SAMs. Carboxylic acid as the SAM terminal group can be activated by via an N-hydroxysuccinimide (NHS) ester and covalently linked to the amine. DNA can also be coupled using this NHS ester reaction chemistry (Samanta & Sarkar, 2011) and hydrazide functionalised alkylthiols have

been utilised to immobilise glycans onto gold surfaces for use in glycoarrays (Zhi et al., 2008). DNA aptamers linked to a thiol with a spacer molecule have formed SAMs on gold electrodes for use as a protein sensor. These aptamers, able to bind lysozyme and thrombin, enabled label free detection of proteins in a sensitive and specific way (Goda & Miyahara, 2013).

Click chemistry

Click chemistry is being employed to covalently immobilise biomolecules on surfaces. The copper catalysed reaction of azide and alkyne is a fast, robust method (Berrade et al.,2011; Spiteri & Moses, 2010) and can link a biomolecule to a functionalised surface in a site-specific way. Alkyne terminated SAMs on gold or silicon surfaces have been linked to azide-containing molecules using this method (Ran et al., 2011; Shamsi et al., 2011; Sun et al., 2006), or vice versa (L. Wang et al., 2010). This offers advantages of mild conditions, high yield and stability of favourably orientated molecules, allowing for efficient electron transfer on the biosensors between the enzyme and the electrode. Biosensors are analytical devices capable of measuring an electrical signal detected by the transducer from the immobilised biological sensing element. This can be an enzyme, antibody or DNA. The inherent specific recognition or catalytic properties of these biomolecules is hugely beneficial to these systems, but careful immobilisation procedures need to be employed to retain the activity of these molecules.

Microarrays have also been created using the click reaction. Carbohydrates conjugated to alkyne groups were immobilised to azide SAMs on glass and silicon wafers in the presence of a copper containing solution and were able to specifically bind lectins in an array format (Michel & Ravoo, 2008). The utilisation of inert and biocompatible PEG linkers containing an alkyne end group was used to immobilise azide containing proteins and carbohydrates onto glass (X.-L. Sun et al., 2006). The application of click chemistry to DNA immobilisation has also been achieved by modification of the 5' end of oligonucleotides with an alkynyl and subsequent attachment to an azide functionalised glass slide. Hybridisation reactions confirmed the suitability of this reaction for producing DNA microarrays (Uszczynska et al., 2012). This provides a simple and efficient immobilisation strategy for high density probe attachment to solid surfaces. The Diels-Alder reaction is another example of click chemistry also employed for biomolecule immobilisation which involves a straightforward cycloaddition between a diene and an alkene (the dienophile) (Jose M. Palomo, 2010; Tasdelen, 2011). Diene functionalised biomolecules have been attached to a dienophile –terminated SAM to produce microarrays (Wendeln et al.,, 2010), or conversely dienophile-modified biomolecules immobilised on tetrazine-functionalised glass slides (Beckmann et al., 2012). This reaction is a fast and efficient conjugation tool which operates under mild conditions in aqueous solutions providing a favourable environment for the immobilised molecules.

Cross-linking

Cross-linking biomolecules to each other and to a surface using a biofunctional agent is a frequently used technique. It provides more stability than adsorption while still being a simple method of immobilisation. It can be used to join groups that react weakly together or not at all and can also act as a spacer, extending the biomolecule from the solid surface. In several cases cross-linking is a form of covalent bonding and hence the main problem relates to activity loss during the cross-linking process due to denaturing or altering the active site (Sassolas et al., 2012). The short linking groups common in covalent attachments can cause steric hindrance resulting in loss of activity. The addition of a linker molecule can moderate these effects by increasing distance between the molecule and the surface (Brady & Jordaan, 2009). Crosslinking reagents include glutaraldehyde, carbodiimide and succinimide (Andreescu & Marty, 2006; Coad et al., 2013).

Glutaraldehyde has been used to immobilise various enzymes onto electrodes for use in biosensors. It is a homo-bifunctional reagent that reacts with primary amine groups, for example, in lysine residues on the surface of proteins and onto amino functionalised surfaces. It is quite a complex reaction as glutaraldehyde forms dimers, or even longer polymers, which can provide a long spacer between the molecule and the surface and allow flexibility in the system (Scouten et al., 1995). The dimer form has been found to be more reactive than the monomer, as was shown when D-amino acid oxidase and GOD were cross-linked to an amine-activated agarose support (Betancor et al., 2006). At high ionic strength only the dimer form of glutaraldehyde was able to immobilise the enzymes. At low ionic strength there appears to be an initial fast adsorption step of the enzymes onto the amines via ionic interactions, which is followed by the covalent attachment of the glutaraldehyde. This indicates a level of control over the immobilisation by altering the ionic strength during the process. By combining adsorption and cross-linking a high level of immobilisation can be obtained which can produce a stable biosensor. B-galactosidase retained 90% activity when adsorbed and then cross-linked onto an anionic resin compared to 51% without the addition of glutaraldehyde. This linkage produces a stable immobilisation that is tolerant of a wider range of pH and temperature than purely adsorbed molecules (Guidini et al., 2010).

Cross-linking of alcohol dehydrogenase to gold and silver nanoparticles was shown to increase the activity of the enzyme compared to the adsorbed and covalently attached molecule. Although greater immobilisation occurred through physical adsorption and covalent coupling, the cross-linking method increased the stability of the enzyme and reduced the denaturing effect of the other process to show an overall increase in activity (Petkova et al., 2012). Glutaraldehyde, in the presence of detergent, enabled immobilisation of lipases with higher activity than covalently immobilised proteins, thought to be due to the optimal orientation and

conformation of the enzyme on the surface induced by the detergent and subsequent multiple attachments of the glutaraldehyde (Fernández-Lorente et al., 2006).

Using bovine serum albumin (BSA) along with the enzyme of interest is a common technique when using glutaraldehyde (Berezhetskyy et al., 2008; Luo et al., 2008; Yonemori et al., 2009). It is also cross-linked in the process to the surface and to the other biomolecule which helps with concentration and stability issues. Optimal ratios of the enzymes need to be determined; if it is too low the sensitivity of the biosensor is compromised, whereas if too high the enzymes aggregate and cause blocking of the active sites (Zhang et al., 2009). BSA layers cross-linked directly on the electrode, below the sensing layer of enzyme, can improve stability and provide a simple method for fabricating biosensors (Adeloju & Lawal, 2011).

Carbodiimide mediated immobilisation works by creating amine reactive surfaces using 1-ethyl-3-(3-dimethylaminopropyl) carbodiimide (EDC) to react with surface carboxylic acids. In the presence of NHS this forms an intermediate which can react with primary amines on proteins or other biomolecules (Talbert & Hotchkiss, 2012). This is a popular way of immobilising enzymes, peptides and nucleic acids to surfaces. Carbodiimide chemistry has been used to immobilise catalase onto gold nanoparticles. This method resulted in nanoparticles with high loading of the active enzyme compared to using biotin-streptavidin binding. These particles can be used as delivery mechanism for carrying the active enzyme in therapeutic applications (Chirra et al., 2011). The water soluble carbodiimide is also popular for immobilising molecules onto SAMs (Liu et al., 2013) or can be used for binding DNA to a glass surface for microarrays by conjugating the terminal amino of the oligonucleotides to a carboxyl surface (Scheicher et al., 2013).

Another heterobifunctional cross-linker commonly used contains a succinimidyl ester and a maleimidyl group, able to link amine and thiol groups (Xiao et al., 2004). Antibody fragments have been immobilised onto gold using this cross-linker. It is an effective way to join the amino terminated SAM to the exposed thiol generated on the immunoglobulin G (IgG), when it is split into fragments. This allowed orientated immobilisation creating an efficient immunosensor (Billah et al., 2010).

One method for linking carbohydrates to gold surfaces was through an amine linker which was achieved by coating a colloidal gold surface with polyamidoamine dendrimers. These branched molecules were then able to bind amino-modified carbohydrates, linking them to the gold, producing a sensitive and label free biosensor (Ogiso et al., 2013). Cross-linking can also be used to increase the loading of biomolecules by immobilising aggregates onto surfaces. This can greatly improve the sensitivity of the system over the monolayer formation (Z.-G. Wang et al., 2009).

Entrapment/encapsulation

In this method the biomolecule is trapped inside a membrane or 3D structure by polymerising a material network around it. The biomolecule is immobilised while the substrates and products are able to move freely through the membrane. This has the least impact on the structure of the molecule as it offers mild reaction conditions and protection from the environment, limiting the loss of activity. Leaching of the biomolecule from the surface, however, can be a problem and a diffusion barrier is introduced which may impede the performance of the catalytic reaction (Sassolas et al., 2012). This method has been used mainly to develop biosensors rather than arrays or other systems. Different methods can be employed for entrapment of biomolecules including electropolymerisation, photopolymerisation and the sol-gel process.

Electro/photo polymerisation

Electropolymerisation involves applying a potential to an electropolymerisable monomer and enzyme solution, with polymerisation occurring on the electrode surface (Teles & Fonseca, 2008). The degree of polymerisation and hence thickness of the film can be tightly controlled by managing the potential or current applied to the surface. Conducting polymers are the main type used for biomolecule entrapment and include polyacetylene, polythiophene, polyaniline and polypyrrole (Cosnier, 1999). They offer high response properties and therefore increased sensitivity. Conducting polymers have an organised molecular structure, enabling them to act as a monolayer for the immobilisation of the enzyme, retaining its biological activity. They are popular for the development of environmental and food monitoring tools and for diagnostics.

Numerous sensors based on polypyrrole have been described (Sassolas et al., 2012; Teles & Fonseca, 2008). Polypyrrole's popularity is due to good biocompatibility, conductivity, stability and efficient polymerisation at neutral pH. An amphiphilic pyrrole monomer solution containing the biomolecule can first be adsorbed on the electrode surface, before polymerisation. This allows greater control over the concentration of the enzyme and the composition of the entrapment layer, removing the need for a high concentration of monomer and catalyst in the aqueous solution (Cosnier, 1999). In addition to enzymes, DNA, antibodies and even cells have been immobilised with this method. Anti-mouse IgG has been successfully incorporated into a polypyrrol film for the detection of *p*-aminophenyl phosphate in a sandwich immunoassay, as a model system (Dong et al., 2006). Covalent bonding of the antibody, post polymerisation, using a carbodiimide crosslinker promoted the attachment of the protein and improved the sensitivity of the immunosensor compared to the purely entrapped protein. Polypyrrol films used to entrap oligonucleotides for the purposes of DNA sensors, allow for the detection of hybridisation reactions, which are useful in the environmental and medical field (Sassolas et al., 2008).

Interestingly, enzymes can also be used to catalyse the polymerisation. Horseradish peroxidase (HRP), for example, can create free radicals when catalysing the electron transfer from hydrogen peroxidase which can initiate polymerisation. Nanosponges (mesh-like nanostructures), can entrap HRP during the polymerisation for use in biosensors (Gopalan et al., 2013). These materials create a biocompatible environment for the immobilised molecule whilst enabling free movement of analytes through the porous membrane.

Photo polymerisation uses light to change the properties of the polymer. A photo-crosslinker incorporated into the polymer can be used to entrap various enzymes (Sassolas et al., 2012). Microarrays, fabricated with DNA or proteins in a hydrogel, can achieve higher density immobilisation than that of a flat surface. This is due to the increased surface area and greater intermolecular distances achieved in the 3D structure. Benzophenone, a photo initiator, mixed with a photopolymer and the biomolecule to be immobilised, forms hydrogels when exposed to UV (Rendl et al., 2011). The crosslinking binds not only the polymer to itself and the substrate, but also covalently binds the biomolecule to the polymer scaffold. 60% of the biomolecules were immobilised using this method yielding homogenous distribution over the array. Analysis of the binding reactions compared the fluorescent output of the arrays, showing reliable immobilisation on a variety of surfaces of flat and 3D structures.

Sol-gel process

The sol-gel technique is widely used to encapsulate biomolecules, as these sol-gel glasses are easily prepared and can be tailored for thermal and mechanical stability (Hanefeld, Gardossi, & Magner, 2009). It is a synthetic, inorganic procedure and involves the transition of a liquid phase (solution) into a gel through condensation reactions and dehydration. Typically, a silica gel network is used to trap the biomolecule (Andreescu & Marty, 2006). The silica gel can retain a large amount of water making a biocompatible environment for the entrapped molecule and increasing stability. This is also a room temperature procedure which avoids heat induced denaturing of the biomolecule (Kandimalla, Tripathi, & Ju, 2006). Enzymes are a major group of molecules immobilised by this method. In 1990, Braun et al, showed the entrapment of alkaline phosphatase in a silica sol-gel where at least 30% of the enzyme was immobilised and active. An improvement in the thermal and long term stability compared to the soluble enzyme demonstrated the protective environment of the matrix. The development of milder polymerisation strategies to maintain their structure has progressed this immobilisation strategy with applications utilising the entrapment of GOD, HRP, urease, tyrosinase and more. A study of the protein cytochrome encapsulated in a silica sol-gel has revealed information about the structure of the gel and its preparation. Alcohol is normally required for the process, however by adding buffer at a certain point, the need for alcohol was removed making this a more realistic approach for biomolecule immobilisation and increasing the stability of the protein. It also appears that the pores are formed around the protein, making them size specific and hence

separating them from external agents (Dunn et al., 1998). Butyrylcholinesterase was entrapped in silica nanospheres using a silica-condensing synthetic peptide to produce a bio-silica matrix (Luckarift et al., 2004). 90% of the enzyme was captured using this method, a huge increase compared to previously reported methods, accounted for by the mild conditions used. The enzyme was stable at room temperature for 30 days, retaining 100% activity, much greater than the free enzyme, indicating the advantages of immobilisation compared to using soluble proteins.

Although mild entrapment can be performed within sol-gels and bioactivity can be retained, the problem of slow diffusion of the analytes affects the reliability and sensitivity of detection. Thin films are therefore beneficial for analytical devices which can be controlled by the gelation behaviour of the sol, however, the immobilisation success also needs to be taken into account. Preservation of the bioactivity has been enhanced by the use of organically modified sol-gels. These can contain functional groups which help stabilise the molecules. Other additives, including PEG, can also increase stability in the system, by improving hydration of the films (Gupta & Chaudhury, 2007).

The sol-gel process is also used extensively to immobilise cells due to its biocompatibility, mechanical stability and porosity control (Carturan et al., 2004). The use of cells as biosensors or catalysts often requires their stabilisation inside a porous material to remain viable. Sol-gels can provide protection from the outside environment and increased stability (Alvarez et al., 2009; Michelini & Roda, 2012). For example, by using a gentle sol-gel process, genetically engineered *Moraxella* bacteria cells were entrapped in this matrix to detect organophosphate compounds. No leaching was observed and the entrapped cells showed greater stability over time compared to the free cells (D. Yu et al., 2005).

Encapsulation

Immobilising enzymes in capsules is another form of entrapment, creating a 3D structure enclosing the biomolecule. Numerous materials and methods are used for this process which can create a favourable environment to utilise the properties of an encapsulated molecule (B.-W. Park et al., 2010). GOD has been encapsulated in a polymer material for use as a biosensor. The formation of the capsules was achieved through the sequential adsorption of charged polyeletrolytes onto the enzyme particles. The capsules are then immobilised onto an electrode. By altering the wall thickness the permeability of the capsule, and therefore the diffusion rate of substrates, can be controlled (Trau & Renneberg, 2003).

A gelatine film and calcium shell around an alginate capsule was able to immobilise β-galactosidase. These multiple materials offered a biocompatible internal environment which prevented denaturation of the enzyme, while possessing a hard shell which prevented swelling and leakage. Additionally, this gave protection to the enzyme, creating a stable bioreactor (Shen

et al., 2011). Encapsulation of enzymes aims to sustain the activity by stabilising the molecule in a protected environment, creating long-term stable biosensors for use in a wide variety of applications and integration into large scale processes.

Encapsulation has also been employed to immobilise cells, with hydrogel immobilisation being a common method (Ben-Yoav et al., 2011). *E.coli* has been encapsulated inside PEG-based hydrogel microbeads, providing a biocompatible and robust environment for these microbes which were viable and capable of expressing fluorescent proteins upon induction (K. G. Lee et al., 2010). Porcine insulin-producing islets have been encapsulated inside alginate microcapsules and transplanted into a diabetic patient. These cells can then secrete insulin into the patient's body while the capsule protects the cells from the immune system (Elliott et al., 2007). Other types of cells, including stem cells, can also be encapsulated using this technology and clinical trials are being carried out in patients (http://www.lctglobal.com/).

Affinity

Affinity binding allows site-specific immobilisation of biomolecules using bio-affinity bonds between the activated surface and specific regions on the target. There are a large number of these affinity pairs which include lectin-carbohydrate, DNA hybridisation and avidin-biotin binding. This method allows for fast and easily controlled orientation of the molecule through non-covalent bonds, but does require the specific tag on the biomolecule.

Biotin/avidin

The biotin-avidin bond is one of the strongest non-covalent bonds making it extremely useful for immobilisation and detection techniques (Green, 1963). Avidin, and its close relative streptavidin, are homotetramer proteins capable of binding four biotin molecules strongly and specifically (Green, 1990). The wide availability of biotinylated molecules is also an advantage of this system. This site-specific immobilisation allows easy generation of arrays of biotinylated molecules onto an avidin-coated slide in a uniform orientation, and is a powerful and convenient method (Prieto-Simon et al., 2008; Yeo et al., 2004). A comparison of random versus orientated immobilised antibodies or antibody fragments, utilising this affinity binding was carried out on a streptavidin coated surface in a microarray format. The packing density of the capture molecules as well as their activity was shown to be consistently improved with orientated attachment, and highlights the advantages of being able to specifically orientate the biomolecule on the surface (Peluso et al., 2003).

The reproducible immobilisation of biotinylated-DNA onto streptavidin immobilised silica has been used to analyse the state of single stranded immobilised DNA and DNA hybridisation (Larsson et al., 2003) and to improve the binding kinetics of this reaction. Although two binding sites per streptavidin were free only one biotinylated DNA strand was shown to bind to each molecule, possibly due to steric hindrance or electrostatic repulsion. An atomic force

microscope (AFM) tip can deposit streptavidin and biotinylated molecules alternatively in precise positions on a functionalised glass surface to build nano-structures. Fluorescent dyes and single stranded DNA (ssDNA) were immobilised in this way and showed specific attachment to the spotted areas. Hybridisation of the ssDNA confirmed full functionality of the immobilised molecule (Breitenstein et al., 2010).

A novel approach to identify peptides involved in the innate immune system has exploited the avidin-biotin bond by capturing these proteins using an immobilised liposaccharide (LPS). This molecule was biotinylated and then adhered to a streptavidin coated agarose. After incubation with serum the proteins bound to the LPS were analysed, allowing investigation into the mechanism of LPS mediated recognition of the immune system (Giangrande et al., 2013). Microarrays, formed using biotinylated lectins bound to neutravidin (de-glycosylated avidin) slides, enabled profiling of the carbohydrate binding activity. This method proved gentler on the biomolecules than covalent attachment, where some activity was lost (Angeloni et al., 2005). A microarray of 172 biotinylated glycans were used to screen for the binding reactions of a sialic acid binding protein. This provided an efficient and high throughput assay, able to analyse the specific recognition of carbohydrate ligands (Bochner et al., 2005).

Biosensor electrodes functionalised with avidin or biotin are able to make use of this affinity binding. Biotinylated anti-human IgG was immobilised on a biotinylated polypyrrole, using avidin as the linker molecule to create a stable immunosensor (Ouerghi et al., 2002). HRP was conjugated to streptavidin and was then able to bind to a biotinylated ethanolamine SAM on a gold electrode, allowing sensitive detection of hydrogen peroxidase (Esseghaier et al., 2008). Immobilisation of urease, again on biotinylated polypyrrole, was carried out with the biotin-avidin-biotin layering (Barhoumi et al., 2008). Layers of enzymes on sensor surfaces can be constructed through avidin-biotin linkages. Deposition of multiple layers of biotinylated protein and avidin creates 3D structures, increasing the sensitivity of the sensor due to high loading of the enzyme in a spatially favourable arrangement (Takahashi et al., 2012). Immobilisation of multiple enzymes is also possible with this method by building them successively into the film allowing utilisation of more than one catalytic reaction.

Cellular array fabrication has also been achieved through the avidin-biotin linkage. A biotinylated lectin was used to attach biotin to the cell membranes, which were then printed onto streptavidin slides where they were immobilised (Hart et al., 2009). These cells were then able to be probed with various target proteins for analysis of cellular states in a high throughput manner. This provided an effective way of arraying a large number of cells for parallel screening.

Utilising the biotin-avidin bond presents an elegant strategy for biomolecule immobilisation. It provides site-specific, orientated attachment of strongly attracted molecules and ligands, utilising an inherent affinity to create ordered structures on non-biological surfaces.

Lectins

Lectins are sugar binding proteins which may bind a carbohydrate or a carbohydrate moiety on a glycoprotein or glycolipid. GOD is a widely studied enzyme because of its many applications in diagnostics, the food and beverage industry, and the chemical and biotechnology industries. It contains carbohydrate chains on its surface and can therefore be immobilised through reactions with lectins (Bankar et al., 2009). Glucose oxidase biosensors are extensively used for the measurement of blood glucose and its immobilisation is an important consideration. Attachment of GOD to a graphene oxide substrate utilising the sugar-binding properties of lectin Concanavalin A (Con A) has been performed (L. Zhou et al., 2012). This allows orientated immobilisation of the enzyme while preserving its activity, and produced greater stability of the enzyme over randomly orientated immobilisation. The use of graphene oxide provides a high surface area, hydrophilicity, oxygen surface functionalities and controllable electronic properties making it an appealing surface for biosensors.

Con A is a popular choice for immobilising glycoproteins. It contains four binding sites for D-glucose and D-mannose. Layers of enzyme on electrodes for biosensors have been formed using Con A, utilising the linking ability of the lectin with the polysaccharide chains on the surface of GOD or HRP (Takahashi et al., 2012). Four layers of Con A and HRP on a negatively charged gold surface were found to be optimal for sulphide detection. This stable and selective biosensor was shown to be efficient at detecting sulphide in water samples (Lijun Liu et al., 2008). The same method of layer-by-layer addition was used for another environmental biosensor detecting hydrogen peroxide (Yang et al., 2006). This was also shown to have sensitive and fast responses; important factors for developing these systems. Con A has shown attachment onto a galactomannan monolayer, adsorbed onto amino-terminated silicon wafers. The lectin is able to bind into the mannose backbone on the polysaccharide molecule (Valenga et al., 2012).

Chelators

The ability to attach metal ions onto surfaces through chelation allows for the immobilisation of histidine (His) -tagged proteins. Chelating agents like nitrilotriacetic acid (NTA) or iminodiacetic acid (IDA) are able to immobilise transition metals like Zn(II), Cu(II), Ni(II) or Co(II) onto solid supports. His residues are then able to bind to these metal ions. A polyhistidine sequence can be introduced to a protein using recombinant methods which is then able to be purified or immobilised via this tag. Five to six His residues are typically used in this affinity tag which is added to the C or N terminus of the protein, creating site-specific, controlled immobilisation (Knecht, et al., 2009; Nakanishi et al., 2008; You et al., 2009).

NTA, crosslinked to a chitosan surface, was used to immobilise His-tagged Green Fluorescent Protein (GFP). By activating the NTA with Ni, the His-tag was able to bind to the surface through this metal ion. This method allowed high levels of protein immobilisation whilst also enabling control over the orientation, since the protein is immobilised at a specific point (Oshige et al., 2013). Nickel particles have been used as the substrate for His-tagged enzyme attachment in a one-step procedure. The particles were deposited on the graphite electrode surface and enabled affinity binding between the His residue of the modified acetylcholinesterase enzyme directly to the nickel. The nanoparticles provided about a four times increase in the surface area compared to a flat surface for enzyme immobilisation, therefore increasing the efficiency and sensitivity of the pesticide sensor (Ganesana et al., 2011). Nickel bound to a polymer hydrogel was also utilised in a one-step immobilisation method. 90% conversion was seen and the His-tagged protein benefitted from increased thermal stability as a result of the hydrogel, making this an attractive method for biosensor fabrication (Ha et al., 2013).

Another comparison of His-tag immobilised enzymes over entrapped enzymes showed increased sensitivity of the affinity bound enzyme. The entrapment procedure limits diffusion rates through the polymer creating a disadvantage over the site-specific orientated immobilisation in this case (Istamboulie et al., 2007). The importance of the orientation of the immobilised biomolecule has frequently been demonstrated and can increase sensitivity, yield and stability of the system, by preserving the activity and structure of the molecule without using harsh reagents (You et al., 2009). The controlled orientation enables higher accessibility for the recognition molecule and can reduce denaturing of the immobilised molecule from multiple surface interactions, making affinity binding an attractive technique (Cha et al., 2005).

Sortase-mediated ligation

The catalytic activity of the sortase enzymes is being exploited to ligate tagged proteins to solid surfaces. Sortase A (SrtA) recognises a specific sequence in cell surface proteins that it cleaves to enable binding of the protein to bacterial cell walls. This sequence, LPETG, is cleaved between the threonine (T) and glycine (G), which leaves the carboxyl group of T free to bind to the amino group of the G on the peptidoglycan cell wall (Parthasarathy et al., 2007; Proft, 2010). Proteins expressing this sequence are therefore subject to the same ligation, enabling binding of glycines on solid surfaces. N-terminal glycine residues coated onto microspheres showed site-specific immobilisation of bacterial adhesions containing the specific tag and subsequent attachment of bacterial cells, using this method (S. Wu & Proft, 2010). Other recombinant proteins immobilised in this way include a fibronectin-binding protein (Clow et al., 2008), Blue, Red and Enhanced Green fluorescent proteins and Tus, a DNA binding protein (Chan et al., 2007). The sortase ligation allows selective and orientated attachment to any surface containing oligoglycine residues, making this an attractive method for biomolecule immobilisation, without using harsh conditions or complex procedures.

RGD peptides

The Arg-Gly-Asp (RGD) tripeptide sequence is a motif found in ligands for the integrin receptors. Integrins are cell membrane proteins that mediate cell adhesion and many will bind to extracellular matrix proteins containing this sequence (Kato & Mrksich, 2004). Immobilising these peptides onto surfaces can therefore mediate cell adhesion to these areas. Using a self-assembled monolayer (SAM) to attach the RGD peptide to a gold surface, Chinese hamster ovary (CHO) cells were immobilised on surfaces they were otherwise unable to attach to (Sánchez-Cortés et al., 2010). This research group had previously patterned gradients of the RGD peptide on SAMs which allowed efficient attachment of cells preferentially to the RGD areas. Tri(ethylene glycol) groups terminating the SAMs in non-RGD areas prevented non-specific binding of proteins and cells (Petty et al., 2007).

By modifying the RGD peptide with a cysteine (Cys) residue the oligopeptide itself can form a monolayer on a gold substrate. Binding of *E.coli* onto the surface can be used to detect phenol toxins in a sample, showing viability of the cells was maintained. This method could be applied to a variety of biosensors including drug and toxin detection (Choi et al., 2005). Porous silicon is popular for biomolecule adhesion due to its biocompatibility. By functionalising the surface with RGD peptides in specific regions it becomes selectively adhesive to cells. Epithelial cells have strongly attached to this surface in the patterned regions and were subsequently detected by fluorescence microscopy. This presents a solution for developing optical sensors for cellular process investigations (Flavel et al., 2011).

DNA

The use of DNA hybridisation for immobilising molecules and cells enables specific and orientated attachment to solid surfaces. SAMs of ssDNA and oligo(ethylene glycol) (OEG) have been produced on a gold surface through thiol linkages. The ssDNA demonstrated sequence specific immobilisation of antibodies conjugated to the complementary DNA strand. The OEG background provided a non-fouling surface that prevented non-specific binding of both the antibody conjugate and the analytes added to the surface (Boozer et al., 2004). Subsequently the same group have developed a multichannel biosensor based on the same binding technique. Three different antibodies with three separate DNA sequences were used for immobilisation onto patterned areas on the sensor surface. They showed specific and highly controlled placement of the biosensing molecules in an orientated manner. Also of note is that by dehybridising the DNA strands the surface can be regenerated and used for binding any molecule containing the complementary sequence, making this a technique for custom sensor development (Boozer et al., 2006).

DNA hybridisation is also a valid technique for immobilising cells. Douglas et al, (2007) have adhered a non-adherent T cell line to glass slides by covalently attaching ssDNA to the slide and then flowing over complementary DNA functionalised cells. They observed fast and specific

attachment of cells to the appropriate areas. Cell adhesion was tested with high flow rates through microfluidic channels and the cells remained attached to the surface. Using NHS-DNA (N-Hydroxysuccinimide -DNA) conjugates, the covalent attachment of DNA to the amines of the cell membrane proteins was achieved. This allows many cells to be modified with DNA and efficiently immobilised on surfaces for use in biosensors or microarrays, providing robust experimental tools for studying cellular behaviour (Hsiao et al., 2009).

Summary

The main methods of adsorption, covalent attachment, cross-linking, entrapment and affinity binding have been discussed with regards to immobilisation of biomolecules and their uses. Immobilisation can provide advantages over the free enzyme in regards to stability, storage, reusability and activity and has lead to the development of microarrays, biosensors and bioreactors now so useful to both research and in analytical devices. It has enabled miniaturisation and integration of various technologies meaning less reagent use, less waste, shorter reaction times and lower cost, whilst also increasing throughput.

The many methods available for biomolecule immobilisation indicate the interest in this area and the increasing research into maintaining activity and stability of the molecule. The immobilisation of the recognition elements or binding molecules is often the most challenging aspect for development of biosensors and array platforms, and there is no one technique that applies to all surfaces. There is an increasing tendency to incorporate more than one technique to enable the optimal system for a given enzyme, antibody, oligonucleotide or carbohydrate, and indeed it has been shown the optimisation for a particular molecule is important, along with the requirements of cost, time, availability of materials and throughput nature of the intended application. The orientation of the molecule is becoming increasingly important as methods to control this emerge, and the harsh conditions used in early procedures are being replaced with mild ones that better preserve the integrity of the biomolecule.

Understanding the immobilisation mechanics will help with obtaining the best trade-off between yield, activity, signal-to-noise ratio and cost to enable new devices and research tools to provide efficient analysis or detection of binding molecules.

1.1.2 Deposition techniques

Central to the immobilisation of biomolecules is the development of deposition and patterning technologies that retain the biological activity and allow high density and organised arrangement of the capture or sensing molecule. A variety of methods have been used to apply biomolecules to surface and include lithography, contact printing and non-contact printing.

Lithography is a popular way to create biomolecule patterned materials and includes photolithography, microcontact printing (μCP), nanoimprint lithography, electron beam lithography and scanning-probe lithography (Christman et al., 2006; C. Wu et al., 2011), which are generally a low cost and precise method for fabricating micro-architectures. Microcontact printing (μCP) is the transfer of the molecule, adsorbed onto a stamp, to the target surface through conformal contact. The surface properties need to be tailored to allow preferential transfer onto the surface. The polydimethylsiloxane (PDMS) stamp contains the pattern of the desired biomolecule immobilisation areas and hence transfers this pattern to the target surface. Proteins, lipids and oligonucleotides are common molecules deposited this way (Perl et al., 2009; Rożkiewicz et al., 2010). Scanning probe techniques can fabricate nanoscale patterns on a surface. For example, in dip-pen nanolithography, an ink-coated atomic force microscope (AFM) tip contacts and delivers the ink molecules directly to the surface, in a nanoscopic pattern (Mendes et al., 2007; C. Wu et al., 2011). Electron beam lithography is a maskless technique that relies on an electron beam to remove areas of polymeric film (or resist) on a surface, allowing biomolecule attachment to certain areas (Kolodziej & Maynard, 2011). Electron beam lithography, however, can be costly and time consuming compared to conventional lithography fabrication.

Microarrays are typically spotted on the surface by robotic contact printing. Here, metallic pins containing the solution of oligonucleotides, proteins or carbohydrates contact the target surface in a specific place and deposit the material by surface tapping. This is an extremely accurate method of depositing the droplet in defined areas (Auburn et al., 2005; Rożkiewicz et al., 2010). Many commercial robotic arrayers are available although it can be a complex and costly deposition method (Binder et al., 2011).

Inkjet printing is a technology rapidly becoming accessible to the biotechnology industry and is proving to be a valuable method for patterning biological molecules and cells for applications in diagnostics, analytical tests and tissue engineering (Komuro et al., 2013; Tasoglu & Demirci, 2013). This is a non-contact printing technique which can reduce contamination but can lead to lower resolution than contact printing, as the droplet has to travel between the printhead and the surface (Binder et al., 2011). It is a low cost and flexible technology that has many applications.

This research primarily uses inkjet printing as the deposition method for immobilising biological molecules onto non-biological surfaces. It will be discussed here in greater detail in regards to its relevance to patterning biomolecules on surfaces.

Inkjet printing

History and principle

Inkjet printing is the precise, non-contact deposition of small amounts of liquid on to a surface. Originally employed as an office tool to produce text and graphics, it is being utilised in many different industries to pattern different materials and molecules for a very varied array of uses. Inkjet printing is familiar to most people in the form of desktop printers, but a wide range of technologies fall into this category and it is the digitally controlled generation of small droplets of fluid as the end result that defines it. Below is described the growth of this technology and the principles behind it.

The first inkjet method to be used was the continuous inkjet method which, as the name implies, involves pressurised ink being forced through a nozzle in a continuous stream. A piezoelectric device applies pressure waves to the ink jet, causing it to break into individual droplets and an electrostatic field charging the drops causes them to be deflected on to its printed location. Drops not required are directed into a gutter for recirculation (Cooley et al., 2002; Le, 1998). Whilst continuous inkjet systems provided high throughput due to their speed, the less complex drop-on-demand (DOD) printing system, developed in the late 1970s proved more popular.

The DOD system propels ink droplets onto the surface only when required, hence reducing waste and contamination. A large degree of innovation led to market domination of DOD inkjet printers in homes and offices after its development. The two forms of DOD are thermal and piezoelectric. Thermal inkjet printing, developed mainly by Canon and Hewlett Packard (HP), uses a resistor to rapidly heat a small amount of ink which vaporises to form a bubble, causing a volume change in the ink chamber that forces ejection of a drop of ink from the nozzle. Piezoelectric systems create a physical displacement by applying a voltage to a piezoelectric crystal adjacent to the firing chamber, pushing out a drop of ink. DOD modes usually have an array of nozzles which only eject a drop of ink on to a specific area when needed (de Gans & Schubert, 2003; Le, 1998).

Whilst the common use of inkjet printers is in homes and offices, applications for this technology are expanding rapidly into industrial printing and manufacturing. Aside from just printing ink, DOD ejection is a way of delivering a controlled amount of material to a precise location on a target. Materials printed therefore extend into ceramics, polymers, and biological materials with the ability to manufacture photodiodes, displays, plastic electronics, sensors and medical devices, as well as being used in rapid prototyping and tissue engineering (Derby,

2010; Derby, 2011; M. Singh et al., 2010). The advantages of non-contact, digital control, low cost and low waste are appealing in these areas. Furthermore, the additive and mask-less nature of this technology allows for easy batch to batch variation, great flexibility in design and patterning, and reduction in material usage, compared to traditional techniques of photolithography or other deposition approaches. With increased understanding of how different materials can be inkjet printed, the applications are constantly being expanded, continuously growing the scope of this technology.

Inkjet printing biological molecules/markers

The biological field is widely employing inkjet printing for material deposition due to the ability to drop minute amounts of material onto solid surfaces, allowing precise patterning and assembling of biomolecules and cells. From research into binding interactions, drug screening and cell growth, to drug delivery systems and medical device fabrication, inkjet printing is becoming a feasible and attractive method, embracing the general trend towards miniaturisation, integration and automation.

Printing proteins

Manipulation and accurate deposition of picolitres of biomolecules is a valuable technological advancement that can be achieved through inkjet printing. The performance of various inkjet printers has been investigated for depositing proteins onto solid surfaces. Simple thermal desktop printers have been used to print the model enzyme HRP, useful due to ease of detection and availability. A simple system, such as the one used by Roda et al (2000), involves washing out a conventional black cartridge and inserting a solution of HRP. Here, dots were printed in an array format of differing sizes and the enzymatic activity assessed by a chemiluminescent substrate. Various papers and cellulose membranes were used as the solid support while the bio ink required adjustment by adding a surfactant to reduce the surface tension; a requirement of a thermal printer. Consistent distribution of the enzyme was observed across the array and activity was maintained over weeks at 4°C and months at -20°C. The same enzyme has been printed with a piezoelectric printer (Di Risio & Yan, 2007; Di Risio & Yan, 2008) and again the bioink was adjusted with a surfactant, to optimise the surface tension, allowing reproducible droplets. Carboxymethyl cellulose (CMC) was chosen as a viscosity modifier as it caused no change in activity of the enzyme and glycerol was added as a humectant. This optimisation of the ink properties enabled reproducible printing and any reduction in the HRP activity post-printing was not significant.

A comparison of thermal and piezoelectric printing of an immunoglobulin (Ig) conjugated to HRP was carried out to determine differences in printing and to evaluate damage to the printed molecules (Lonini et al., 2008), since the shear stresses that occur during droplet ejection may have detrimental effects. In this instance no additives were used in the bioink to alter the ink

properties. Using an enzyme-linked immunosorbent assay (ELISA) identical optical density results were observed between the piezoelectric and manual tests, indicating no damage to the Ig or the conjugated enzyme, since binding affinity was equal between printed and non-printed molecules. Unfortunately the thermal printer was not able to eject this liquid solution, probably due to surface tension properties not being optimal for this printhead. Solutions printed in thermal inkjet printers tend to need additives in the liquid to allow ease of ejection of the droplets (Khan et al., 2010; Roda et al., 2000; Setti et al., 2005).

Although many reports indicate printed proteins are still active after inkjet printing (Pardo et al., 2002; Setti et al., 2007; Watanabe et al., 2003) the damage of proteins during the printing process is a concern due to the shear stresses and heat experienced by these macromolecules during ejection which could cause them to denature. Some research does indicate a loss of activity of enzymes after inkjet printing (C. Cook et al., 2009; Nishioka et al., 2004). Compression rates of the bioink appear to be important and caused a reduction of activity of a peroxidase enzyme and GOD. This could be somewhat alleviated by the addition of sugars but compression and hence deposition rates had to be low to remove this risk. However, other researchers have reported the loss of enzyme activity with the increased addition of glycerol, probably due to the increased viscosity (C. Cook et al., 2009). Cook et al (2010) and T. Wang et al (2012), extensively investigated the effect of piezoelectric printing on GOD and discovered no change in structure or conformation, and indeed have shown a more linear response of inkjet printed GOD than the manually loaded sample (T. Wang et al., 2012).

Miniaturisation, integration and a high level of precision makes inkjet printing an attractive option for fabricating biosensors and immunoassays. DOD techniques provide contactless application of the biomolecules to the surface, reducing contamination. Being able to handle hydrated samples is an important consideration when working with proteins to keep them in their natural state, something which is difficult with other methods. Biosensors are devices used for the detection of an analyte, typically using antibodies, enzymes, nucleic acids, cells or microorganisms (Delaney et al., 2009). Sensors based on GOD and HRP have been realised by inkjet printing these enzymes on top of conducting polymers to transfer the signal detection of glucose or hydrogen peroxide respectively (Setti et al., 2005; Setti et al., 2007). A commercial thermal inkjet printer deposited both poly(3,4-ethylenedioxythio-phene/polystyrene sulphonic acid) (PEDOT/PSS) as the conducting polymer layer and either GOD or HRP as the active enzyme. Whilst the response of the GOD sensor was less than expected, possibly due to the thickness of the polymer film, the HRP performed well compared to other HRP sensors and the feasibility of using this technique to deposit these solutions, while keeping their functionality for use in bioelectronic devices, was shown. Although thermal inkjet printing involves increasing the surface temperature of the resistor quite dramatically, the small amount of time (~10 µs) that the sample is exposed to this temperature does not cause a rise in the bulk

temperature of the sample and enzyme activity has been clearly shown to survive the process (Khan et al., 2010).

Higher end custom made piezoelectric inkjet printheads have also been used to demonstrate the use of this technology in fabricating biosensors. Multi-analyte protein patterns on thiol surfaces were produced with a biotinylated-thiol (BAT) mix printed onto gold in an array format, and the remaining areas blocked with a polyethylene glycol (PEG)-thiol solution. The BAT was then allowed to bind to streptavidin and a final layer of two biotinylated proteins were printed onto the BAT regions. Specific and highly localised antibody binding to the two proteins was then shown (Hasenbank et al., 2008). This complex system not only uses the extremely strong biotin-streptavidin bond as a link between layers but has a non-fouling area, creating a robust biosensor capable of detecting multiple analytes. This is a convincing demonstration of how inkjet printing allows precise alignment of proteins, in a uniform layer, with high reproducibility.

Cellulose has long been used as support for chemical testing and biomolecule immobilisation. It is widely available, inexpensive and biologically compatible. Production of bioactive paper is a growing field as paper provides an attractive substrate for bioactive devices (Kong & Hu, 2012; Pelton, 2009). The high throughput nature of inkjet printing is well suited to the fabrication of low cost paper based devices. Di Risio and Yan (2010) have looked extensively at how biomolecules can be incorporated into cellulose-based functional materials. Their own experiments have concentrated mainly on HRP, and its adsorption onto different cellulose surfaces. Paper is available in many formats depending on the raw materials used, how it has been treated and the coating applied. Protein adsorption tends to increase with an increase in hydrophobicity of the surface, and hence a more crystalline paper structure was favourable due to less hydroxyl groups being accessible on the surface (Di Risio & Yan, 2009). No loss of enzyme activities occurred with these surfaces and the enzyme was also shown to preferentially attach to the cellulose fibres and not to pigments or fillers present in the paper (Di Risio & Yan, 2008).

An HP desktop inkjet printer has been used to print HRP onto cellulose paper of various weights, photo paper and plastic film (Roda et al., 2000). The cellulose paper gave the best results, with repeatability shown for dots down to 0.6 mm in diameter. However, some washing away of the protein occurred, highlighting the importance of protein optimisation of the immobilisation techniques and increasing the knowledge of their interactions with the solid support. This procedure shows a basic printer can be adapted to print proteins easily and quickly and illustrates how this technology holds great potential for microdeposition applications.

Paper-based analytical devices (μPADs) are microfluidic devices utilising the capillary action of porous paper. They are being developed as portable, simple diagnostic devices to be used in developing countries (Martinez et al., 2010). Hydrophilic and hydrophobic areas can be patterned easily onto paper due to its inherent porous structure. By inkjet printing an etching chemical onto a polymer-modified paper, defined hydrophilic channels were created into which chemical sensing inks could then be printed (Abe et al., 2008). Complex hydrophobic patterns have been printed onto unmodified filter paper using a waxy material as the ink. High resolution images, photos, text and concentration gradients have been created on paper by manipulating the colour management and greyscale of the printer (Khan et al., 2010). Printed in combination with biological molecules, bioanalytical devices can be produced in an efficient manner allowing the one-step approach for sensor fabrication in a low cost and scalable way (Li et al., 2010a; Li et al., 2010b).

Patterning cells

As far back at 1988 bioprinting, termed cytoscribing by Klebe (1988), was being used to deposit cell adhesion proteins onto a flexible plastic film for the patterned growth of cells. Using an HP desktop printer, tightly controlled spatial positioning of cells was achieved by printing fibronectin and monoclonal antibodies, to which the cells adhered. The functionality of the printed molecules was therefore shown to be retained due to the selective binding of the cells to this printed area, with the aim of increasing understanding of cell growth and differentiation.

Patterning of growth factors is a way of directing cell adhesion and is important for studies on cell behaviour, especially their proliferations and differentiation. A growth factor array as a cell-based analytical tool, fabricated using inkjet technology, has been shown to vary cell differentiation by altering the combination of different growth factors and their concentration in an array format (Watanabe et al., 2010; Watanabe et al., 2003). By using a desktop colour printer, multiple growth factors were able to be printed on the same substrate and were immobilised onto the surface. The growth of stem cells on this printed substrate was assessed and provided a system for analysing the influence of growth factors on cells and their environment. Other growth factor arrays have been developed using inkjet printing to produce concentration gradients to allow investigation into cell migration. Cell organisation and dose dependant behavioural responses to fibroblast growth factor-2 (FGF-2) patterns have been produced with this technology (Campbell et al., 2005). Miller et al, (2009) have used a piezoelectric system to deposit bone morphogenetic protein-2 (BMP-2) and insulin-like growth factor-II (IGF-II) onto fibrin-coated glass slides, which bound through natural affinity to the fibrin. The concentration gradients and patterns printed were retained for up to seven days on this surface and although the resolution of printed spots is below that able to be created with photolithography, it is adequate for this application and allows a known amount of biological material to be deposited in a known area.

Inkjet printed growth factor gradients of heparin-binding epidermal growth factor-like growth factor (HB-EGF) have shown unexpected stem cell migration influences. Using this methodology it was revealed that cells in this *in vitro* situation were directed primarily by cell diffusion from the cell source rather than individual cell migration, with HB-EGF spatial patterns maintaining the diffusion, rather than influencing it directly (Miller et al., 2011). Bioengineering these microenvironments by bioprinting patterns of these proteins has been shown to spatially guide stem cell differentiation. Fibroblast growth factor-2 (FGF-2) caused differentiation of stem cells, in a dose dependent manner, into tissue-specific tendon cells on the patterned areas, with myoblasts formed outside the printed areas (Ker et al., 2011), leading to multiple cell fates of a stem cell population on a solid phase platform. Inkjet delivered BMP-2 has also spatially engineered the fate of stem cells (Phillippi et al., 2008). Stem cell research could therefore benefit greatly from these approaches as it allows mimicking of the natural environment and evaluation of protein patterns to direct cell fate and increase understanding of cell behaviour, which could have advantages in regenerative medicine.

This tool is useful for patterning not only stem cells but also for investigating cell-cell interactions, drug screening and tissue engineering. Neurones have been patterned by creating cell adhesive micro-islands on a cell-repulsive background by printing a collagen mixture on top of a polyethylene (PEG) surface (Sanjana & Fuller, 2004). The neurones showed good conformity to the collagen areas after culture and had normal electrochemical physiology. Smooth muscle cells were cultured on a similar collagen patterned surface and control of cell adhesion and proliferation was achieved (Roth et al., 2004). This presents an attractive way to study the development of cells, as inkjet printing allows easy patterning of cell attachment molecules, with high resolution, high precision and digital control. With the resulting increase in understanding, applications in regenerative medicine and tissue engineering become achievable.

Printing DNA

Whilst proteins are the major group of biomolecules being printed, other types of molecules are also being patterned in this way and include nucleic acids. The printing of DNA has been demonstrated using a desktop thermal inkjet printer where radioactively labelled cDNA probes were hybridised to the printed DNA enabling visualisation of the printed area (Goldmann & Gonzalez, 2000). Oligonucleotides, inkjet printed onto a glass substrate, have formed a DNA microarray for detecting single-nucleotide polymorphisms (SNPs). The thermal inkjet technology used did not damage the 18-mer probes and allowed a fast, non-contact method for depositing DNA. This enabled fluorescent hybridisation reactions to be performed detecting one point mismatches in the *p*53 tumor suppressor gene (Okamoto et al., 2000). DNA microchip electrophoresis was carried out by inkjet printing the DNA samples into a straight separation channel. This negated the need for a T or cross channel injection method and hence

allowed for much simpler voltage programming. Only DNA strands over 20,000 base pairs were in danger of being cleaved due to shear stresses, and the small drop volumes (~20 pL) and direct loading enabled a much faster run time with high reproducibility (Yasui et al., 2012). Another use for inkjet printed DNA has been to immobilise cells on surfaces for cell interaction research. This involved printing specific DNA strands which hybridise to the complementary strand attached to the cell membrane through a lipid-PEG-DNA conjugate. This method of immobilising cells allows for patterning of different cells on the same substrate by printing varying DNA sequences, rather than using a cell adhesive protein which cannot differentiate between cells (Sakurai et al., 2011).

Printing carbohydrates

Since the initial development of microarray technology, DNA and protein arrays have advanced remarkably. However, the adaptation for carbohydrates has been slower, mainly due to the chemical and structural diversity of glycans. The majority of immobilised glycans have been spotted onto glass or other surfaces using robotic spotting techniques with little seen in the way of inkjet printing, although piezoelectric inkjet printing is showing promise in this area (Sørensen et al., 2009). Arrayjet (http://www.arrayjet.co.uk/) have developed arrayers that utilise an inkjet system and are suitable for use with carbohydrates. Another arrayer using piezoelectric non-contact printing has been used to deposit BSA-glycoconjugates onto silicon biosensor surfaces. This multiplex array showed specific binding to lectin molecules, indicating the full functionalities of the printed glycans, and also demonstrated the accuracy of the printer to deposit discrete droplets of different molecules (Kirk et al., 2011). Also of note is the applicability of inkjet printing to silicon photonic biosensors, as this does not damage the surface through contact and allows high density and fine control over the dispensing.

Inkjet printing cells

The shortage of organs for transplantation has advanced the approaches to engineer organs for repair and replacement of damaged or lost organs (Mironov et al., 2009). The success of printing proteins and other biomolecules has led to the printing of whole cells and given rise to a range of applications where exact cell positioning is of great importance (Derby, 2012). This has created a paradigm shift towards a bottom-up approach to tissue engineering, taking cues from the rapid prototyping industry where a layer-by-layer technique is employed to create 3D structures. A typical approach would involve implanting a biodegradable scaffold into which cells have been seeded and cultured. However, this presents problems of inadequate cell penetration, difficultly in placing specific cells at exact locations, and engineering a vascular system within the organ (Boland et al., 2006). Inkjet printing could potentially overcome some of these issues by placing all types of cells needed in exact, defined locations layer-by-layer, to self-assemble into a working organ or tissue, without the need for a scaffold.

Printing cells as opposed to molecules needs greater consideration of the nozzle diameter, the substrate being printed onto and the general printing conditions. Initial experiments merely showed proof of concept of cellular printing, and indeed cell survival is easily achieved following this process. An HP thermal printer, with the addition of specifically designed printheads to enable large cells to pass through the nozzles, and some software modifications, was used to print endothelial cells and smooth muscle cells onto Matrigen™ and collagen membranes respectively (W. C. Wilson & Boland, 2003). Printing was carried out in a sterile laminar flow hood at room temperature and took only one minute per sample. Following this the cells were transferred to a 37°C environment, where they grew and attached to their printed destinations. However, 25% death was observed in the population which was attributed to dehydration of the samples, a primary concern due to evaporation of the small droplets. Subsequent studies showed Chinese hamster ovary (CHO) and embryonic rat motorneurones printed into patterns with >90% survival. By printing onto hydrogels the cells were kept in a favourable state post printing, enabling their growth (Xu et al., 2005). Proliferation and differentiation was observed, therefore demonstrating a viable method for positioning mammalian cells. Having shown survival of cells after printing it was important to know whether these cells develop normally compared to non-printed cultures. Hippocampal and cortical neurones were printed in single layers and after two weeks of culture exhibited normal electrophysiology. They were able to fire action potentials with no significant differences in membrane properties measurable between the printed and control cells (Xu et al., 2006). A reasonable conclusion that thermal inkjet printing does not cause damage to these cells or cause cell death was drawn.

Time lapse observation and scanning electron microscope (SEM) imaging of piezoelectric printed endothelial cells was carried out to evaluate cell survival (Nakamura et al., 2005). These cells showed adherence to the culture dish following inkjet dispensing and retained normal morphology. Printed dots were roughly the same size as a cell and lines were able to be printed one dot thick, highlighting the inkjet advantages of high resolution and precision positioning of these cells.

A thorough study of cell death and damage was carried out to ensure the safety of inkjet printing (Cui et al., 2010). Whilst cells have been shown to be viable following printing (Lee et al., 2009; Xu et al., 2005), this study investigated the dead cell to live cell ratio, the level of apoptosis by examining DNA fragments, and cell membrane permeability, and concluded no increased loss of cells or apoptotic activity over normal cell handling. Pores appearing in the cell membrane closed after two hours resulting in normal cell morphology, and in fact revealed a new way of transfecting cells, since these transient pores offered an opening to insert plasmids if co-printed with the cells.

Cell settling is another concern with printing since an accurate cell concentration is required if tissue and organs are to be fabricated. Indeed, settling of cells has resulted in higher cell numbers per droplet than required (Lee et al., 2009) which can cause clogging of the nozzle, as well as unknown cell concentrations being delivered to the surface. This can later lead to a depletion of cells and hence a decrease in the number of cells being printed after a few runs have been performed (Saunders et al., 2008). Modelling of cell sedimentation whilst in the cartridge has shown a printing time window could be used where the cell concentration in the print area will be constant (Pepper et al., 2011).

The majority of cell printing has used a thermal inkjet system with Boland and Mironov initially demonstrating the proof of concept (Mironov et al., 2003; W. C. Wilson & Boland, 2003). However, few authors report on piezoelectric printers for this purpose. Saunders et al (2008) have successfully printed human fibroblast cells with a DOD piezoelectric actuator and performed a comprehensive study on the effects to the cell. The voltage applied to the transducer affects the drop velocity and hence the shear stress experienced by the cell. This stress can be minimised by decreasing the voltage. A drop from 80V to 40V increased cell survival from 94% to 98%, with samples printed at 40V having no significant difference from control cells. These cells proliferated at normal levels demonstrating the printed cells were viable.

Whilst cell printing has been demonstrated by numerous authors, being able to print functional tissue remains a challenge. This requires moving from 2D printing to 3D, being able to print an extracellular matrix with all the types of cells needed and to incorporate a vascular system capable of delivering oxygen and nutrients to the cells. Boland et al (2003), have shown the additive sequential layering of cell adhesive hydrogels and endothelial cell aggregates, where the aggregates fuse together forming a 3D structure, showing the feasibility of organ printing technology. Using self–assembled tissue spheroids or aggregates as the building blocks is attractive as they can be standardised, are scalable, and they will fuse together to build macro-tissue without the need for a scaffold (Mironov et al., 2009; Rezende et al., 2013). This mini-tissue based approach could potentially solve the vascularisation issue, where it is proposed that three types of spheroids could be used to build a vascular tree, printed simultaneously with the organ-specific spheroids, thus creating a self-assembled 3D tissue or organ. Post-printing is also an important step as the structure needs to maintain its shape and integrity. Most likely this will involve the addition of extracellular matrix molecules, for example collagen and fibronectin, which can increase cell cohesion. It could be possible to print these molecules along with the cells, mimicking the cellular environment and accelerating tissue maturation (Mironov et al., 2007). Tissue spheroids can be printed in prescribed 3D shapes, for example tubes and blocks, and become functional once fused together (Jakab et al., 2008). Cardiac fused

spheroids were able to synchronously beat, while endothelial cells grew into a tube like morphology signifying the potential for 3D fabrication of functional structures.

A modified thermal printer has fabricated tubes of polymerised fibrin gel using thrombin as the bioink and fibrinogen as the biopaper. Human endothelial cells were printed simultaneously onto the surface and aligned into the fibrin channel. The cells proliferated and formed tubular structures inside the fibrin walls, which had good integrity after 21 days of culture (Cui & Boland, 2009). This process utilises the ability of inkjet printing to deposit biomaterials along with cells, to give an immediate structure for the cells to position themselves against. This could be a promising approach to build micro vascular systems within engineered organs. Fibrin hydrogels have also been shown to support neural cells when printed together layer-by-layer. Growth factors embedded in the hydrogel were slowly released and together promoted migration and proliferation of the neural stem cells into neural tissue, demonstrating potential uses for cell and tissue replacement to treat neurological diseases (Y.-B. Lee et al., 2010).

Organ printing has been defined as computer-assisted inkjet-based 3D tissue engineering (Cui & Boland, 2009; Mironov et al., 2003). It allows the positioning of many types of cells as well as depositing nutrients, growth factors and other important molecules in exact positions thereby creating the right environment for living cells (Boland et al., 2006). It enables high cell density tissue creation and vascularisation while being scalable and reproducible (Mironov et al., 2009). This technology relies on the principles of developmental biology and the process of self-assembly (Elbert, 2011), in that cells placed together in the right environment will fuse and grow into tissue, similar to normal embryonic development, but in an accelerated and automated way. This interdisciplinary tactic promises to overcome problems associated with using scaffolds, presenting a more natural method for fabricating desired organs and tissues, not only for transplantation but for drug testing, cancer research and more. The idea of printing organs is indeed fascinating and has the potential to overcome organ shortage and rejection issues associated with this field.

Bacterial cells have been shown to survive the inkjet printing process as well as mammalian cells, with the view to printing high density cell arrays (Xu et al., 2004; Zheng et al., 2011). Very precise patterns of *E. coli* were delivered to an agar surface and were able to proliferate to form colony arrays. This proved to be a reproducible technique that allows full automation with a high level of flexibility for producing whole cell arrays, capable of detecting or responding to a panel of chemicals or toxins. A significant increase in applications for these arrays are appearing as the technology to fabricate them develops alongside. With cell immobilisation and long term viability being addressed, they are fast becoming important biosensing tools. Inkjet printing offers miniaturisation, precision, low cost and reproducibility, important features for producing assays for cell biology research as well as high throughput screening devices (Elad et al., 2008; Melamed et al., 2011).

Not only bacterial cells are being used for microarrays. For testing against pharmaceuticals, toxins, and for general cell research, single cells are being immobilised in an array format, with a variety of fabrication methods being investigated. Inkjet printing presents numerous advantages over microcontact printing and other techniques, including no contact with the surface and the ability to use picolitres of solutions, and has been used to produce cell arrays with the ability to print one cell per well (Liberski et al., 2010). Evaporation of the printed drops does pose a problem due to the volumes involved and can cause dehydration of the arrays, although a mineral oil layer can be added to alleviate this. Inkjet printed cell arrays have enabled the analysis of lipids in the cell membrane and in-depth profiling showed no change in composition between printed and non- printed cells (Ellis et al., 2012). Cell printing was compatible with the lipid analysis method used and showed great sensitivity of the single cell array. Inkjet printing offers a flexible method to enable analysis of a variety of cells in a large number, and also allows the use of them, as a whole, as detecting agents as opposed to their individual molecules.

Summary

The ability to inkjet print biological molecules or cells onto solid surfaces, whilst maintaining their binding or functional abilities, has led to a rapid increase in the varieties of applications of immobilised biological molecules. It is the ease and low cost of utilising this method that allows this interdisciplinary approach to make use of the advantages of both sides of this technology, as the high resolution and reliability of inkjet printing along with the very small amount of material deposited means valuable biological resources are not wasted and can be tested in an array format with relative ease.

1.2 KODE™ technology

KODE™ technology is a cell surface engineering technology that has the ability to add functionality to cell surfaces (Blake et al., 2011; Frame et al., 2007). This is achieved by Function-Spacer-Lipid (FSL) constructs modifying the cell membrane and displaying a functional moiety. These synthetic FSL constructs are capable of spontaneously inserting into the lipid bi-layer membrane and hence are able to create various landscapes on this surface, creating opportunities for studying cell surface molecules and opening up applications for designed cell surfaces (Korchagina et al., 2012). These constructs are composed of three parts, designed to allow almost any antigen, fluorophore, peptide, or other biological molecule to be employed as the functional part (F) of the construct. The lipid tail (L) embeds into the lipid bilayer of the cell anchoring the molecule to the membrane. The spacer (S) provides distance from the cell surface and also imparts solubility, allowing dispersion in water. The functional head group can be almost any functional moiety (provided it is not too hydrophobic) that is desired, and is attached to the cell through FSL immobilisation, to enable binding to ligands or antibodies, or to impart some other attribute or quality to the surface. Examples include fluorescent dyes allowing the cell to be tracked, biomarkers for diagnostics and blood group antigens for transfusion applications (Henry, 2009; Henry et al., 2011; Lan et al., 2012).

FSL constructs are amphiphilic molecules, having a polar and non-polar moiety with their structure being analogous to a flower (Figure 3). The lipid tail is the roots, the spacer is the stem and the functional moiety is the flower head, with the lipid anchoring into the membrane and the head group being extended out from the surface. The most common lipid chosen for FSL constructs is dioleoylphosphatidylethanolamine (DOPE). It is a membrane phospholipid compatible with biological assays with its diacyl structure capable of being retained in the cell membrane. Other lipids include a monoacyl lipid chain, sterol lipid (cholesterol) and ceramide. The spacers of FSL constructs can be a simple, short (1.9 nm) adipate linker or a longer (7.2 nm) carboxymethylglycine (CMG). The CMG spacer, developed for peptide FSLs, has recently been shown to improve the reactivity of ABO antigen kodecytes against monoclonal reagents by increasing the distance of the antigen from the cell surface. The functional head groups include a number of blood group carbohydrate antigens, peptide biomarkers, hyaluronic acid, biotin and fluorescent markers (Korchagina et al., 2012).

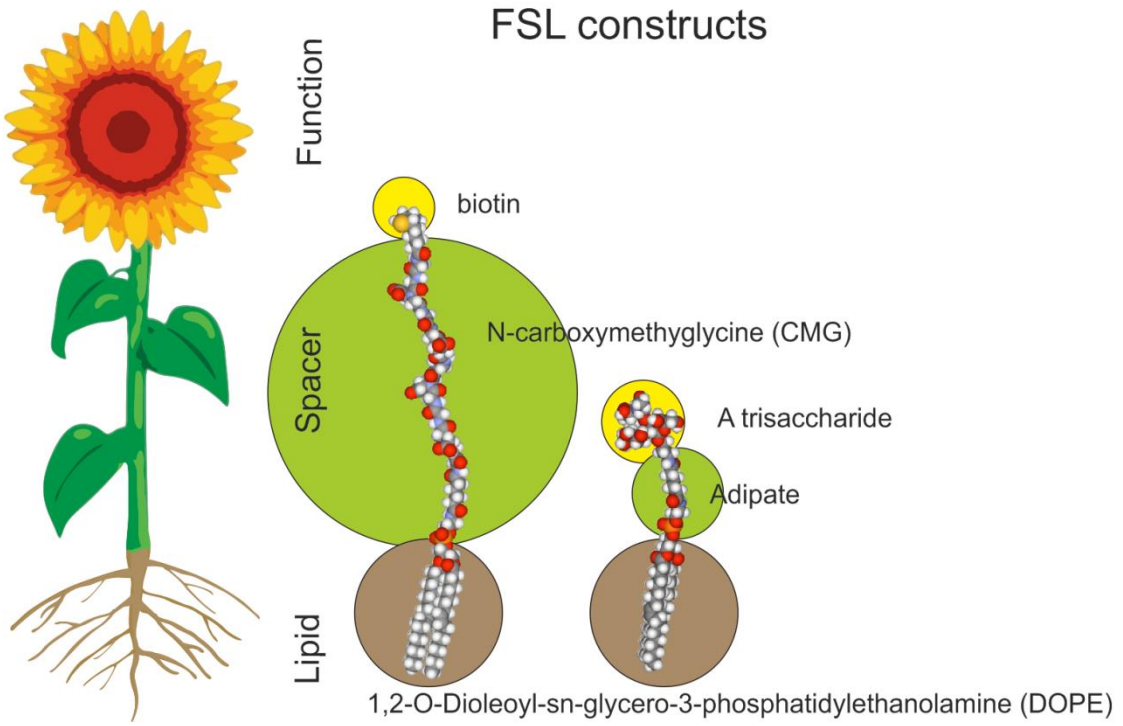

Figure 3. Examples of FSL constructs consisting of a lipid tail (DOPE), a spacer (CMG and adipate) and a functional head group (biotin and Atri) which can be thought of as similar to the parts of a flower.

It is the special features of these amphiphilic constructs that make them such a useful tool for biological surface engineering. Firstly, they will spontaneously and stably incorporate into a membrane. The method of 'koding' cells requires mixing of equal amounts of cells and a solution of FSLs, followed by a short incubation time (1-2 hours at 37°C) (Blake et al., 2011). The lipid tail will then integrate into the cell membrane upon contact. These cells are then known as kodecytes. By varying the concentration of the FSLs in a solution, full control over the amount of antigen (or other functional moiety) on the surface can be controlled and has enabled the production of control cells for blood testing (Henry, 2009; Hult et al., 2012). Secondly, they are non-toxic and do not affect the normal functioning of the cell, making them compatible with diagnostics and therapeutics. Thirdly, they are dispersible in water, and other biological solutions, making them very easy to handle and work with, especially when using cells and other sensitive biological systems (Blake et al., 2011). It is the spacer that helps imparts the water solubility, making the constructs easily compatible with biological systems, and also spaces the functional group away from the surface to allow interaction with other molecules.

The majority of experiments conducted in this research utilised FSL-Atri and FSL-Btri, two carbohydrate FSL constructs, and also FSL-biotin. This last construct is particularly useful due to its extremely strong bond to avidin and the use of this molecule can allow attachment of any biotinylated molecule through this avidin bridge. FSL-Atri contains the A trisaccharide

GalNAcα1-3(Fucα1-2)Galβ of the blood group A antigen joined to the DOPE tail with an adipate spacer (Figure 4). Similarly FSL-Btri contains the B trisaccharide Galα1-3(Fucα1-2)Galβ, of the blood group B antigen, with the adipate spacer and DOPE lipid. FSL-biotin uses the longer spacer of CMG, creating a larger space between the surface and biotin functional group (Figure 5).

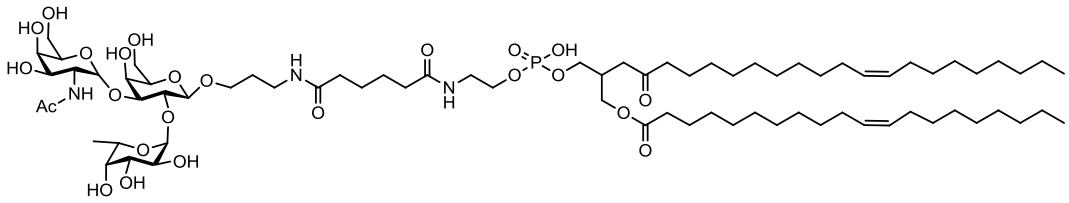

Figure 4: Schematic diagram of FSL-Atri

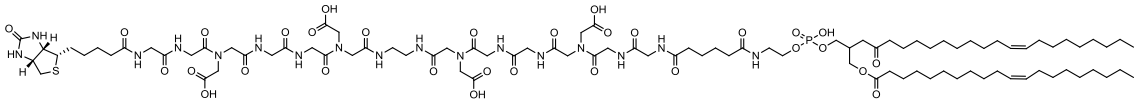

Figure 5. Schematic diagram of FSL-biotin

The ability to modify biological surfaces non-covalently and non-destructively is a powerful tool. It allows the investigation into the cell surface, tracking and studying of virions and cells, as well as diagnostic and therapeutic applications. Cells modified by KODE™ technology are termed 'kodecytes'. The amount of FSL attached to the surface is easily controlled by altering the FSL concentration during kodecyte production. Blood group antigen FSLs have been used to mimic natural weak ABO blood cells (Henry, 2009) and are being used in transfusion laboratories for control cells. The high reproducibility of preparing these kodecytes makes them extremely useful in these settings and also allows the creation of cells not present in nature, enabling the specific testing of certain antigens (Henry, 2009; Hult et al., 2012). Although they are synthetic molecules, these constructs produce serological results and flow cytometry profiles identical to the natural cells they are mimicking, making them extremely useful for antigen studies (Hult et al., 2012).

The *in vivo* use of blood group antigen kodecytes has also been demonstrated and the post transfusion cell survival studied (Henry et al., 2012; Oliver et al., 2011b). Compatible and incompatible transfusions were carried out in mice with blood group A antigen (FSL-Atri) kodecytes. FSL-biotin introduced to the cells allowed simple labelling and recovery of the transfused cells. The successful neutralisation of anti-A by injecting FSL-A allowed incompatible transfusions which may have applications in clinical settings (Oliver et al., 2011a).

These ABO blood group antigens are carbohydrates but peptides have also proven to be successfully attached to red blood cells using KODE™ technology. The main concern when designing peptide FSLs is its solubility, as all FSL must be soluble in saline. MUT and Mur are peptide Miltenberger antigens of the MNS blood group. The thiol group of a terminal cysteine of the peptides was coupled to a maleimide linker molecule attaching the peptide to the lipid tail and inserted into the cell membrane (Heathcote et al., 2010). An important feature of the spacer of the FSL is its non-reactivity with human sera or any cell components to ensure specific reactions when used in diagnostic panels. Screening cells have been prepared with Miltenberger FSL constructs to detect clinically significant antibodies within specific populations (Nadarajan et al., 2012), providing an improvement over the general screening panels commonly used. A cytomegalovirus (CMV) peptide epitope FSL has provided an improved method of Fc function assessment by removing the need for a continuous supply of red blood cells and the subsequent time consuming derivatisation of the surface (Georgakopoulos et al., 2012).

Fluorescent FSLs provide an attractive approach for visualising and imaging cell and virion behaviour. Live cells, sperm, mouse embryos and a variety of virions have been imaged this way. FSL-FLRO4 kodecytes prepared using adult zebrafish blood cells were transplanted into zebrafish embryos (Lan et al., 2012). Real time imaging allowed visualisation and tracking in vivo of the kodecytes, demonstrating the simple and effective use of kodecytes for investigating cell movements. The membrane of enveloped virions is another biological surface which can be modified with KODE™ technology. Using the same method for producing kodecytes, 'kodevirions' can be non-covalently coated in fluorescent molecules, enabling labelling and analysis of the virus particle. The FSLs did not affect its ability to bind to cells and have been used to label the measles virus for cell binding studies (Mesman et al., 2012). Radiolabelling of virions is also possible using ^{125}I radio-labelled FSL-tyrosine, showing another robust method of imaging these particles for *in vitro* and *in vivo* investigations (Hadac et al., 2011).

These applications show numerous uses of FSL constructs attaching to biological surfaces. The lipid tail is able to associate with the membrane and convey the FSLs functionality to that surface. The question addressed in this research is whether FSL constructs can attach to non-biological surfaces, functionalising supports other than cells and viruses for attachment of antibodies and other binding and recognition partners. Prior to this thesis the only surfaces modified with FSL constructs were cells and viruses. This thesis presents the first examples of modification of non-biological surfaces with KODE™ technology.

1.3 Aim

The aim of this research:

To evaluate modification of non-biological surfaces with FSL constructs by

1. Investigate and develop suitable methods of delivery for applying FSL constructs onto non-biological solid surfaces, with an emphasis on inkjet printing as a precise and controlled delivery method, and to establish an appropriate detection method.
2. Determine types of non-biological surfaces that FSL constructs are able to modify, determine limitations and where possible speculate on the mechanisms of actions for attachment.
3. Analyse the potential use of FSL modified non-biological surfaces in bioassays.
4. Evaluate the possibility of immobilising cells using FSL construct modified surfaces.

Chapter 2 Methods and Results

Function-Spacer-Lipid (FSL) constructs are water dispersible, amphiphilic molecules that are able to insert into the lipid bilayer of biological membranes upon contact. The focus of this research was to address whether these molecules can attach to solid non-biological surfaces and the possible mechanisms of action of this immobilisation. This section will firstly concentrate on the delivery of FSLs onto non-biological surfaces and then focus on the types of surfaces tested and their success and limitations at immobilising FSL constructs. The applicability of immobilised FSLs for use in bioassays will then be examined, involving validation of the inkjet printing method, carried out by comparing a range of inkjet printed blood group FSLs and testing against a range of monoclonal antibodies, and by using peptide FSLs to identify infectious disease markers. Finally the ability to attach cells or bacteria to a solid surface using various FSLs with appropriate linker molecules will be investigated.

2.1 Methods of delivery

This section focuses on developing the method of delivery of FSL constructs onto non-biological surfaces. FSL constructs are water dispersible making them ideal for use as "bio-paint" or "bio-ink" and the methods employed include painting, soaking and inkjet printing of FSLs on non-biological surfaces. The detection methods are also described here as they are required to establish the presence of FSL constructs. This involved either a simple method of staining with a general thin layer chromatography (TLC) stain (when a silica surface was used), or a more sensitive immunostaining protocol (used on all materials).

2.1.1 Detection method

Anisaldehyde staining

p-anisaldehyde stain (2 mL p-anisaldehyde, 4 mL sulphuric acid, 196 mL acetic acid) is a general purpose TLC stain which produces a range of diagnostic colours to various compounds including lipids and carbohydrates after baking. Silica TLC plates, when painted or printed with FSL constructs, were sprayed with anisaldehyde stain and baked in an oven at 200°C.

DACA staining

DACA (0.1% (w/v) 4-(dimethylamino)-cinnamaldehyde and 1% sulphuric acid in absolute ethanol) is a chromogenic reagent which reacts with biotin. Silica TLC plates, when painted or printed with FSL-biotin or biotin, were sprayed with DACA stain and baked in an oven at 200°C. The presence of biotin is revealed by a pink colour.

Immunostaining for carbohydrate molecules (blood group antigens)

To test for carbohydrate FSL attachment, the surface was immunostained. This is a simple enzyme immunoassay (EIA) which allows for the colorimetric detection of immobilised molecules using enzyme conjugated antibodies. Using monoclonal antibodies against the functional (F) part of the FSL as the primary antibody allows for monovalent detection of the FSL and hence is indicative of its immobilisation on the surface. The protocol of the assay is described here and based on the method reported in Svensson et al (2005), for staining on silica plates. All immunostaining was carried out at room temperature unless otherwise stated.

Monoclonal reagents:

1. Blocking step: 2% Bovine serum albumin (BSA) (Gibco, 30063572, USA) in phosphate buffered saline (PBS) was flooded onto surface for 1 hour, then removed. This was done to block the unoccupied spaces on the surface and prevent non-specific binding.
2. A monoclonal antibody reagent diluted 1:4 in 2% BSA was incubated on the surface for 1 hour by flooding the whole surface. The main reagents used were anti-A and anti-B (Epiclone anti-A 0261, Epiclone anti-B 0266, CSL, Australia).
3. The surface was washed 6 times in PBS, pH 7.2, each time by immersion for 20 seconds for each wash, using fresh PBS at each wash.
4. The secondary antibody, anti-mouse Ig conjugated to alkaline phosphatase (AQ502A, Millipore, USA) diluted 1:1000 in 2% BSA, was incubated on the surface for 30 minutes by flooding the whole surface.
5. The surface was washed again 6 times in PBS.
6. The substrate, NBT/BCIP (nitro-blue tetrazolium chloride and 5-bromo-4-chloro-3'-indolyphosphate p-toluidine salt, 11681451001, Roche, Germany) , was diluted in a tris substrate buffer (100 mM Tris, 100 mM NaCl, 50 mM $MgCl_{2)}$ pH 9.5, and flooded onto the surface for colour development of the assay.
7. The reaction was stopped by washing in water.
8. The surface was dried and stored unprotected at room temperature.

Polyclonal reagents/sera:

This method is the same as detailed for the monoclonal reagents apart from these steps:

2. A polyclonal reagent or serum diluted 0-1:4 in 2% BSA was incubated on the surface for 1 hour by flooding the whole surface.
4. The secondary antibody, anti-human Ig conjugated to alkaline phosphatase (AP318A, Chemicon, Australia) diluted 1 in 1000 in 2% BSA, was incubated on the surface for 30 minutes by flooding the whole surface.

Streptavidin conjugated staining for biotin molecules

For a sensitive staining method for biotin and FSL-biotin, streptavidin conjugated to alkaline phosphatase was used. Streptavidin has exceptionally high affinity for biotin making this an extremely sensitive reaction and an ideal method for detecting biotin.

1. Blocking step: 2% Bovine serum albumin in PBS was flooded onto the surface for 1 hour, then removed. This was done to block the unoccupied spaces on the surface and prevent non-specific binding.
2. Streptavidin conjugated to alkaline phosphatase (S2890-250UG, Sigma, USA), diluted in 2% BSA to 1 μg/mL, was incubated on the surface for 30 minutes.
3. The surface was washed 6 times in PBS, by immersion for 20 seconds for each wash.
4. The substrate, NBT/BCIP (nitro-blue tetrazolium chloride and 5-bromo-4-chloro-3'-indolyphosphate p-toluidine salt, 11681451001, Roche, Germany), was diluted in a Tris substrate buffer (100 mM Tris, 100 mM NaCl, 50 mM $MgCl_{2)}$ pH 9.5, and flooded onto the surface for colour development of the assay.
5. The reaction was stopped by washing in water.

All FSL constructs were obtained from KODE™ Biotech Materials, New Zealand.

2.1.2 Painting

Method overview

A simple method for applying FSL constructs to a solid surface was by painting with an artist's brush. Painting FSL constructs onto non-biological surfaces involved preparing a solution of FSLs in PBS, pH 7.2, at the required concentration and then painting them using a fine artist's paint brush (size 0). The brush was cleaned by washing 3 times in 70% ethanol before and after painting. The painted surface was then stained with anisaldehyde or immunostained as described above.

Results and interpretation

Figure 6 shows an example of FSL-A painted onto a silica TLC plate at various concentrations (2, 1, 0.5 and 0.25 mg/mL). 2 plates were produced for the two staining methods, anisaldehyde staining and immunostaining. Using a paint brush to deliver FSLs to surfaces proved successful and although not highly controllable it is useful for materials unable to pass through a printer.

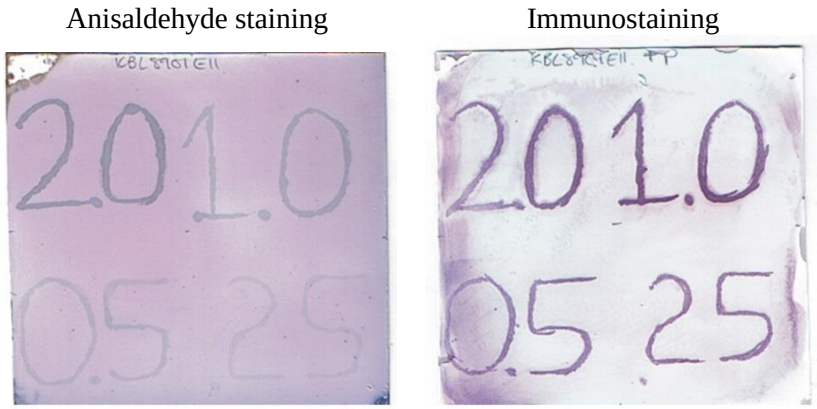

Figure 6. Examples of painted FSL-A onto a silica TLC plate and stained using two different methods, anisaldehyde staining and immunostaining.

2.1.3 Soaking/contact

Method overview

For some surfaces, for example microbeads, the surfaces were soaked in the FSL solution prepared in PBS at the required concentration for 30-60 minutes. The surfaces were then washed three times in PBS by centrifugation or by magnet induced sedimentation (for paramagnetic beads) to remove the remaining FSL solution. The surfaces were then either dried or kept in solution, as some types of beads could not be dried. For visualisation the materials were then either immunostained as normal, or in the instance of FSL-biotin microbeads, avidin-alexa fluor®488 (A-21370, Invitrogen) was used by incubating the FSL modified beads in a 0.1 mg/mL solution for 30 minutes and then washing the beads again in PBS. They were then analysed using fluorescent microscopy (488 nm excitation, Olympus Fluorescence Microscope BX51).

Results and interpretation

Figure 7 shows microbeads (20 µm) soaked in FSL-biotin and imaged using avidin conjugated to a fluorescent marker. This demonstrates the ability to attach FSL constructs to a surface by soaking them in an FSL solution.

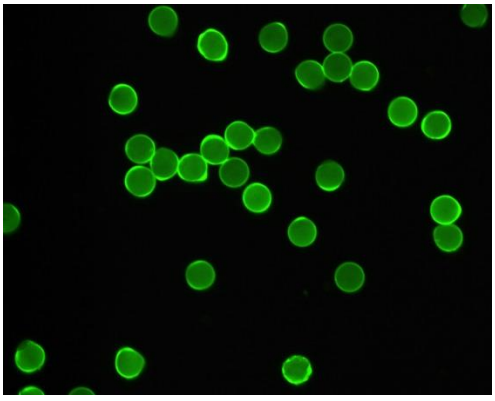

Figure 7. Image of microbeads soaked in FSL-biotin and stained using avidin-alexa fluor® 488 (×200).

2.1.4 Inkjet printing

Method overview

A standard desktop inkjet printer was used to print FSL constructs onto various surfaces. FSLs were dispersed in PBS (pH 7.2) at the required concentration and inserted into the cartridge. The cartridge was then inserted into the printer and printed from using Microsoft Word or CorelDraw.

Multiple printer manufacturers and cartridge types were tested, including thermal (HP and Canon) and piezoelectric (Epson) inkjet printers. Refillable cartridges and a continuous ink supply system (CISS) were investigated to find the best system for printing biological molecules. Requirements of the inkjet system include being able to clean the cartridge and printhead easily to remove contaminants, being able to use only a small amount (<1 ml) of printing solution to conserve valuable molecules and limiting air bubble introduction when removing and replacing cartridges.

The optimal printer was an Epson stylus T21 colour printer due to its ease of use, cleaning and ability to be modified. This printer uses a piezoelectric actuator in the printhead. Refillable cartridges were used which were modified by attaching a thin tube through the top of the cartridge to the small outlet chamber and sealing the other entrances to this chamber (Figure 8). This allowed the printing liquid to be injected directly through this tube to the outlet chamber without having to fill the whole cartridge, meaning small amounts of solution could be used (100-500 µL). The cosmetic cover of the printer was removed to allow access to the cartridges at all times (Figure 8). The cartridges are transparent which allows monitoring of the liquid injection into the ink outlet chamber, reducing the risk of introducing air bubbles to the system. Air bubbles in the print nozzles cause problems with ejection and can result in variable printing quality. They are also difficult to remove, so being able to minimise these is beneficial.

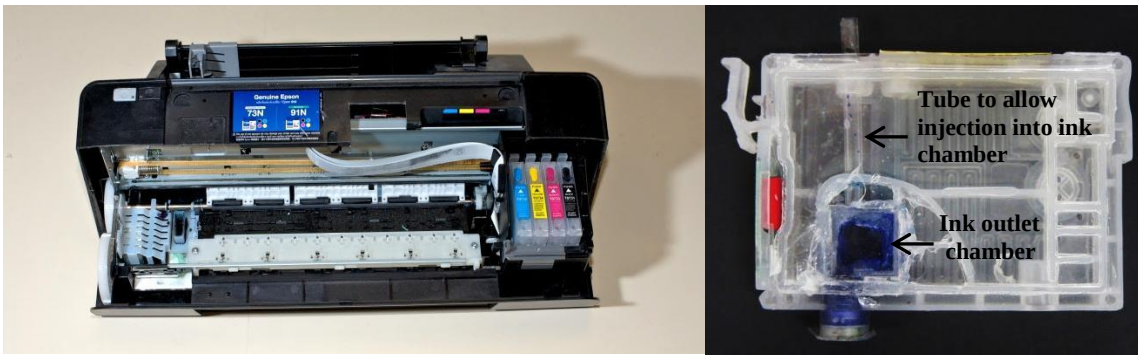

a b

Figure 8. The inkjet printer used for printing biological molecules (a) and the modified ink cartridge (b). The cosmetic cover has been removed from the printer to allow access to the cartridges. The cartridge has been adapted by sealing around the small ink outlet chamber and securing a tube from the top of the cartridge to this ink outlet chamber, for injecting the printing solution. The blue ink indicates the area that now holds the ink as opposed to before modification where the whole cartridge would be full of ink.

Colour printers with multiple cartridges apply their own colour adjustment, using the inbuilt profiles of their image colour management (ICM) system, and mix the ink from the different cartridges as it dispenses the droplets. It is therefore important to override this so that solutions in different cartridges are printed exactly when needed and molecules are not mixed on the printed surface. This is done through the printer controls, by selecting OFF in the colour management system in the advanced properties. This feature of mixing colour, although not employed here, could be used to add multiple FSL constructs to surfaces in different ratios. The print quality setting was also changed to photo, to achieve greater resolution.

A dye was added to the printing solution to provide a visual aid during and post printing. Bromophenol blue (20015, BDH Chemicals Ltd, UK) at a concentration of 0.025% was used in all printing solutions to ensure the printer was printing properly and as a guide to the printed area on the surface. This dye was removed either during washing with PBS, the initial blocking step or when incubated with samples (Figure 9). Once the dye is washed off, the surface becomes blank until specific staining of the FSLs is carried out. This dye caused no non-specific binding to any molecules used in these methods and was easily washed off all surfaces.

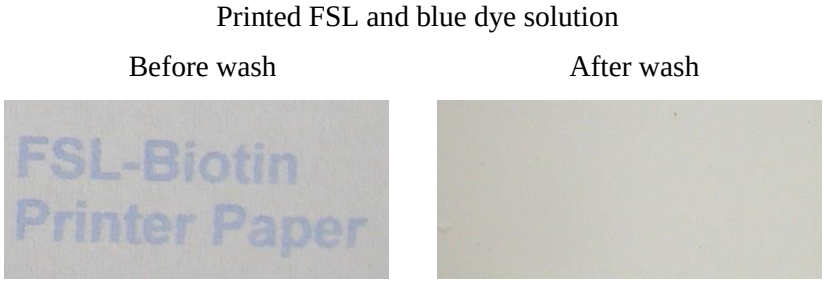

Figure 9. Example of printed FSL solution containing a blue dye for visualisation before and after washing which removed the dye. This leaves a blank surface which is then stained specifically for the FSL construct.

Results and interpretation

FSL constructs were able to be successfully delivered onto solid surfaces by inkjet printing. For an example, FSL-biotin at a concentration of 500 µM was printed onto a nitrocellulose membrane and stained using streptavidin conjugated to alkaline phosphatase (Figure 10).

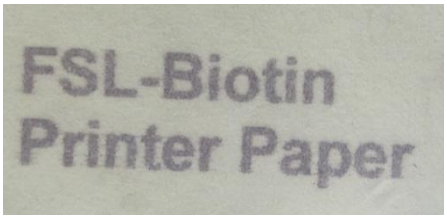

Figure 10. An example of FSL-biotin applied to a surface by inkjet printing. FSL-biotin was printed in the words "FSL-Biotin Printer Paper" onto printer paper and stained using streptavidin conjugated to alkaline phosphatase and NBT/BCIP substrate.

Degradation tests

Having established printing as a viable method of delivery of FSL constructs, the initial experiments involved investigations into any degradation of FSLs during the printing process. Sheer forces are imposed on the liquid as it travels through the nozzle of the printhead and this is a concern when printing biological molecules. Several authors have shown no significant loss of activity of several biomolecules after printing, including Horseradish peroxidase (HRP) (Khan et al., 2010; Setti et al., 2007), β-galactosidase (Setti et al., 2004), glucose oxidase (GOD) (Setti et al., 2005) and insulin (Watanabe et al., 2003), all using a thermal inkjet printer. Piezoelectric printers have also been shown to cause no damage to HRP (Di Risio & Yan, 2007; Lonini et al., 2008) and GOD (C. Cook et al., 2009), although Nishioka et al (2004), did find that the degree of compression on the solution during printing did alter the activity of the peroxidase enzyme and that a slow compression was favourable to reduce damage to the protein.

Here, the investigation was into the effect, if any, on the damage to the FSL as a construct, not on the specific head groups i.e. will FSL constructs remain intact with their lipid, spacer and head group after inkjet printing or can this method cause loss of some part of the construct?

The objective of this experiment was to determine any degradation of printed FSL constructs using thin layer chromatography (TLC). A change or degradation in the molecule will cause a different migration when compared to a non-degraded sample. This was tested with a thermal and piezoelectric printer to establish any differences between these two inkjet methods.

Method overview

Loading TLC: FSL-Atri at 600 µM was printed onto a 8x2 mm and a 8x1 mm line at the bottom of 2 marked lanes of a silica TLC plate (Alugram SIL G/UV, silica gel 60, Cat no. 818 133, Macherey-Nagel, Germany). The two different size lines were printed to print different amounts of the FSL. This was carried out using a thermal printer (Canon BJC2655P) and a piezoelectric printer (Epson stylus colour 460) on separate plates. 2 µL of the same FSL printing solution and a control FSL solution at the same concentration were manually loaded, using a syringe, into adjacent lanes and 2 µL of a TLC control loaded into the control lane. The TLC control contains a monoglycosyl ceramide, a triglycosyl ceramide, a sphingomyelin and a hexaglycosyl ceramide (Le^b). Two plates from each printer were prepared for two staining methods (anisaldehyde staining and immunostaining).

Developing TLC: The TLC was developed for 25 minutes in chloroform/methanol/water (60:35:8; v/v/v) solvent, then allowed to dry.

Anisaldehyde staining: *p*-anisaldehyde stain was sprayed onto the silica plate which was then baked in an oven at 200°C until the TLC control was visible.

Immunostaining: First the TLC control lane was cut off from the plate and stained with anisaldehyde as above. This was then aligned to the unstained part of the plate to allow removal of the top section of the plate above the blue sphingomyelin band, as the blood group FSLs will migrate below this band. The rest of the plate was plasticised by immersion into 4% polyisobutylmethacrylate in *n*-hexane solution for 1 minute, then removed and dried and immunostained with monoclonal anti-A according to the EIA protocol detailed above. This is common for TLC overlay procedures and leaves an acrylic layer over the TLC plate which helps with silica loss during washing steps and reduces non-specific binding of ligands (Hansson et al., 1985; Yiu & Lingwood, 1992).

Results and interpretation

Figure 11 and Figure 12 illustrate the results of a comparison between the migration rates of inkjet printed and manually loaded FSL-Atri constructs, and between thermal and piezoelectric printed FSL-Atri constructs. These TLC results show no difference between the migration distances of the printed samples and manually loaded control samples and reveal no degradation products, indicating no damage to the molecule during the printing process. To provide a more sensitive method an EIA overlay was also carried out to confirm the location of the FSL-Atri. Again, no difference is observed between the printed and non-printed samples and no other molecules are detected enabling a conclusion of no degradation of this FSL molecule due to inkjet printing.

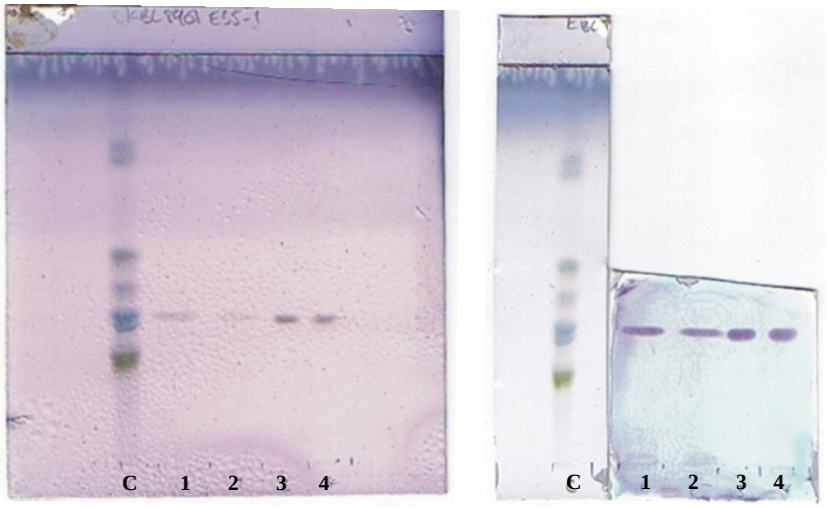

a b

Figure 11. Thermal inkjet printer. Anisaldehyde stained TLC (a) and TLC immunoassay overlay (b) of FSL-Atri degradation test printed at 600 µM. Lane C is a TLC control comprised of a monoglycosyl ceramide, a triglycosyl ceramide, a sphingomyelin and a hexaglycosyl ceramide (Le^b). Lanes 1 and 2 are printed samples and lanes 3 and 4 are manually loaded samples.

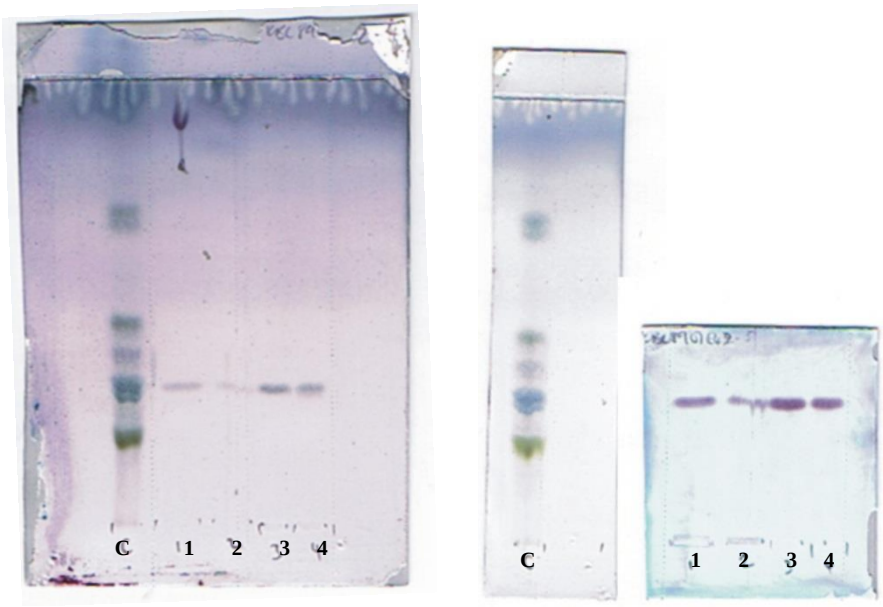

a b

Figure 12. Piezoelectric inkjet printer. Anisaldehyde stained TLC (a) and TLC immunoassay over lay (b) of FSL-Atri degradation test printed at 600 µM. Lane C is a TLC control comprised of a monoglycosyl ceramide, a triglycosyl ceramide, a sphingomyelin and a hexaglycosyl ceramide (Le^b). Lanes 1 and 2 are printed samples and 3 and 4 are manually loaded samples.

A lesser amount of printed FSL is detected compared to the manually loaded FSL. This is due to the low volume of liquid ejected from the printer compared to that manually loaded. However, the printed FSL moved at the same rate as the manually loaded sample indicating these molecules were the same and hence have remained intact during printing. The immunostained samples show the FSLs were able to bind to the antibodies, showing their activity was maintained and the FSL remained attached to the surface. As will be shown in the next section, the Atri antigen is unable to remain attached to the surface on its own, therefore if the FSL had been damaged the Atri may well have washed away during the immunostaining process, and would not have been detected. This therefore indicates the FSL remained as a whole molecule, immobilised on the silica surface.

It is also interesting to note that the results are the same for the thermal and piezoelectric printed samples, suggesting neither of these methods proves a problem for degradation of FSL constructs per se.

This has confirmed that FSL constructs can be inkjet printed and remain intact and able to bind to their binding partners after this process and has therefore established a printing method for FSLs.

Printing practices

In this thesis a number of different words and codes were used to describe what molecule or FSL construct was printed. In a lot of cases the name of the FSL construct, or other molecule, is printed to enable unambiguous detection of the immobilised molecule. The name of the surface

was also printed regularly in addition to the name of the printed molecule and occasionally the stain or immunostaining molecules to be used. In other cases, especially when material was limited or when printing for a small reaction well, a code was used. This code was used for ABO blood group FSLs and is detailed in section 2.4.2 (see later Figure 19).

Throughout this thesis there will be some instances where the printed area in the image looks stripy. This is due to the quality of the printing and not to the immobilisation of the constructs or a result of poor staining. Another problem sometimes seen is droplets of material outside the desired printing area, known as satellite droplets. These occur because of the lower surface tension of the FSL solution compared to the standard ink. Examples of these are shown in Figure 13 . As a few printers were trialled before deciding on the final one, imperfect printing was sometimes seen, especially with the old printers that were used initially, as they had blocked and dried nozzles.

Figure 13. a) An example of stripy staining of the printed area due to poor quality printing and not FSL immobilisation or staining and b) an example of satellite droplets

Having established the various delivery methods for FSL constructs onto non-biological surfaces the investigation into the types of materials able to immobilise these molecules was carried out.

2.2 Non-biological surfaces

This section is focused on the examination of the variety of surfaces that FSL constructs are able to attach to. Different FSLs were printed, soaked or painted onto these surfaces along with non-FSL control molecules and immunostained to reveal if they are able to be detected and retained on the surface following an EIA procedure.

It is known that FSL constructs will anchor into cell lipid membranes via their lipid tail (Korchagina et al., 2012) and so it was interesting to investigate whether they might attach to solid surfaces. A variety of laboratory surfaces were tested including silica TLC plates,

nitrocellulose and filter surfaces. This led to exploring other assay surfaces such as paper, polymers and metals. A wide variety of materials were also tested to establish limitations of FSL attachment, and to investigate the behaviour of these constructs.

There are a number of different mechanisms for adherence of an FSL construct to a solid surface. These include hydrophilic and hydrophobic binding of the various parts of the FSL, hydrophobic interaction or water exclusion due to aggregation of the amphiphilic molecules, entrapment of micelles within a porous membrane or encapsulation of fibres or microspheres. The results here have not attempted to group the results according to the potential mechanisms, as multiple mechanisms may be involved simultaneously on the same surface. Instead results are presented in groups of related material classes.

2.2.1 Cellulose membranes

Modified cellulose membranes have many uses for standard laboratory applications, for example blotting and filtering, and were some of the first materials to be used to immobilise enzymes (Lilly, 1976; Mitz & Summaria, 1961). The properties of the cellulose membranes depend mainly on the method of preparation and hence the modification it has been through. The binding of proteins covalently and non-covalently to different cellulose membranes is well documented (Fridley et al., 2013; Tovey & Baldo, 1989; Yin et al., 2010), however attachment of other classes of biomolecules, for example nucleic acids and carbohydrates, is less efficient (A. Yu et al., 2012). The abundance, low cost, stability, biocompatibility and well defined structure of cellulose derived materials makes them attractive assay surfaces and as a support for FSL constructs.

Nitrocellulose, a hydrophilic membrane formed by exposing cellulose to nitric acid, is widely used for blotting and binding assays (Tovey & Baldo, 1989), as well as a substrate for biosensors and microarrays (Fridley et al., 2013; Uttamchandani & Yao, 2008). Cellulose acetate and cellulose triacetate, mixed membranes of cellulose nitrate and cellulose acetate, and regenerated cellulose were also examined to compare different modified celluloses for their ability to adhere different FSL constructs.

Method overview

FSL-Atri was printed onto the cellulose membranes along with the Atri antigen, the functional head group of the FSL-Atri construct (see Figure 4 in section 1.2), at concentrations of 400-500 µM. The Atri antigen was printed as a control to compare the immobilisation of the functional part of the FSL compared to the whole FSL molecule. Other molecules printed include FSL-Btri and FSL-biotin. Btri and biotin, being the functional part of the respective FSL constructs, were also printed as controls. FSL-Atri and FSL-Btri contain the adipate spacer, whereas FSL-biotin contains the longer CMG spacer. Other FSL molecules printed include FSS-A and FSS-biotin. These molecules contain a sterol lipid tail instead of the diacyl DOPE

tail and were constructed to investigate the different binding abilities of FSLs containing variations in the lipid tail. FSL-B monoacyl is another variation which contains a monoacyl lipid instead of the diacyl lipid.

The modified cellulose materials printed onto include nitrocellulose, mixed cellulose esters, regenerated cellulose and cellulose acetate and triacetate (see Table 1 for details). Detailed images of the surfaces were obtained using a field emission scanning electron microscope (SEM) (Hitachi SU-70) after sputter coating with platinum and are shown in Table 2.

Table 1. Cellulose membrane material, ID names and supplier

Material	**ID/brand name***	**Manufacturer/Supplier**
Nitrocellulose membrane	Nitrocellulose	Invitrogen, USA
Cellulose triacetate filter membrane	CT or Metricel	Gelman Sciences, USA
Mixed cellulose esters filter membrane	MCE	Sterlitech, USA
Regenerated cellulose filter membrane	RC	Sterlitech, USA
Cellulose acetate filter membrane	CA	Sterlitech, USA

* Name printed onto surfaces

Table 2. SEM images of modified cellulose surfaces prior to FSL modification

Cellulose membrane ID	Magnification	
	×300	×5000
Nitrocellulose	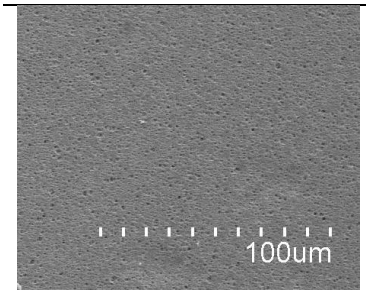	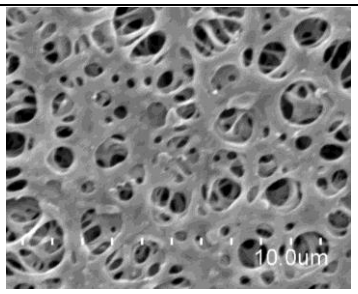
MCE	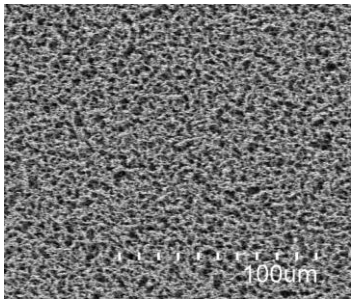	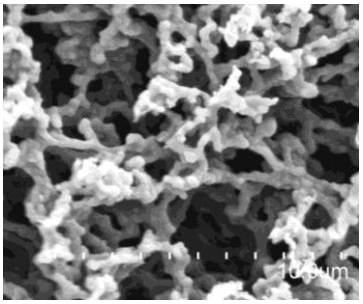
RC	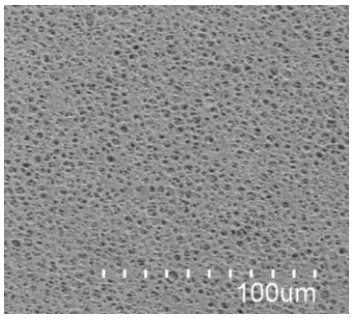	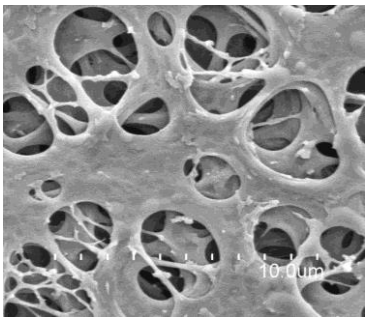
CT	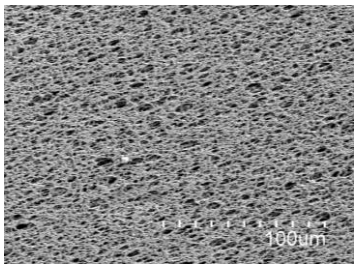	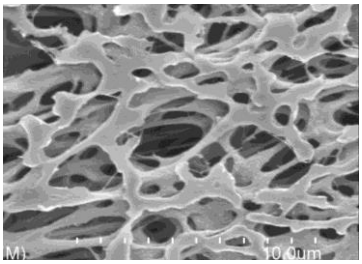
CA	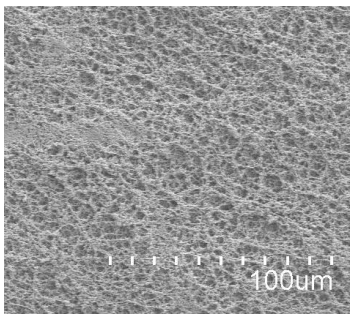	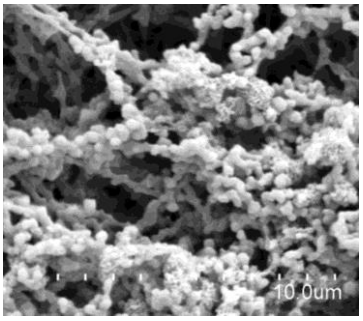

Results and interpretation

Table 3 indicates the success of each type of modified cellulose to be coated with various FSL constructs. Table 4 shows some examples of FSLs printed into these surfaces. Atri, Btri and

biotin were printed on some surfaces alongside the FSLs. All surfaces showed good attachment of FSL-constructs, apart from cellulose acetate which showed poor detection of FSL-Atri and FSL-Btri. This was due to especially high background staining of this surface resulting in poor sensitivity of FSL detection. The control molecule (the functional part of the FSL construct), when printed next to the FSL construct, was not detected on any of these surfaces, suggesting it washed away during the staining process.

Table 3. Cellulose surfaces that FSL molecules are able to attach to. ++ = strong positive detection, + = weak positive detection, - = no visible detection.

Cellulose membrane ID	Function-Spacer-Lipid							
	FSL	A/B × ×	A/B Ad DOPE	A Ad Sterol	B Ad Mono	Biotin × ×	Biotin CMG DOPE	Biotin CMG Sterol
Nitrocellulose		-	++	+	-	-	++	+
CT		-	++		-	-	++	+
MCE		-	++					
RC		-	++					
CA		-	+					

Table 4. FSL constructs immobilised on modified cellulose surfaces. + indicates detection of the molecule and – indicates no detection.

	Examples of FSL constructs immobilsed on modified cellulose surfaces			
Construct	FSL-Atri FSL-Btri	FSL-Atri FSL-Btri	FSL-B FSL-B mono	FSL-biotin
Concentration µM	400	400	400	500
Cellulose membrane ID	RC	MCE	CT/Metricel	Nitrocellulose
Control	Atri	Atri	Btri	Biotin
Result	FSL-Atri + FSL-Btri + Atri -	FSL-Atri + FSL-Btri + Atri -	FSL-Btri + FSL-B mono - Btri -	FSL-biotin + Biotin -
Printed words	3A0ad 3B0ad 3A000	3A0ad 3B0ad 3A000	FSL-B Metricel FSL-Bmono Metricel Btri Metricel	FSL-Biotin Nitrocellulose Biotin Nitrocellulose
Example		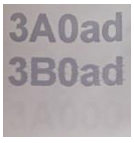		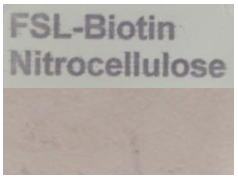

FSS-Atri and FSS-biotin were also printed onto these surfaces. These contain a sterol group as the lipid tail, not the DOPE of the standard FSL. Where tested they were detected poorly

compared to the DOPE FSL but were able to be seen. The FSL-B monoacyl construct was printed onto nitrocellulose and cellulose triacetate and was not detected. These results indicate the type of lipid tail is important in the constructs ability to attach to the surface, and as the functional moiety on its own did not adhere, suggests the lipid tail of the FSL is the part anchoring the molecule to the surface. The importance of the FSL construct as a whole is therefore shown, enabling the molecule to orientate itself with the functional part accessible for binding. Two different spacers were also tested (adipate on FSL-Atri and CMG on FSL-biotin) with no difference in attachment between the two observed, suggesting it is unlikely that the spacer affects the mechanism of attachment.

Due to the amphiphilic nature of FSL molecules it is probable that the adherence is driven by hydrophobic (water exclusion) forces, i.e. clustering of the hydrophobic components. Amphiphiles are composed of hydrophobic and hydrophilic parts which self-assemble into aggregates in aqueous solutions to shield the hydrophobic parts from water (Schmid et al., 2004). They can form a variety of structures including micelles, vesicles and bilayers, with this organisation being driven by the higher solubility of hydrocarbons in organic solvents than in water. This hydrophobic effect is complicated but can be thought of in terms of enthalpy and entropy where the thermodynamics and the order of the system direct the assembly (Chandler, 2005; Tanford, 1979). The opposing preference of the two ends of the molecule leads to the hydrophobic tail being removed from contact with the water molecules leaving the head groups at the surface of this aggregate. Liposomes, a bilayer vesicle structure, are known to break up and spread onto a surface they come into contact with, forming a bilayer on hydrophilic surfaces and a monolayer on hydrophobic ones (Jass et al., 2000), again driven by the hydrophobic effect.

Therefore the mechanism of binding of the FSL constructs to these surfaces could be a bilayer of these amphiphilic molecules. This would involve the head group interacting with these hydrophilic surfaces and removing the lipid tails from contact with the aqueous surrounding due to the bilayer formation. Other possible mechanisms include micelles of FSLs being trapped in the membrane, or encapsulation of the FSLs around the fibres of the membrane.

2.2.2 Paper

Paper is increasingly being used for bioassays due to its stability, availability, low cost, biodegradability and biocompatibility (Li et al., 2010a; Martinez et al., 2010; Pelton, 2009). Papers, constructed from cellulose pulp, can be coated with substances to impart certain attributes like gloss, smoothness or absorbency, or left uncoated. Tested here were a range of uncoated and coated papers with various degrees of gloss, thickness and whiteness.

Method overview

FSL-Atri and Atri were printed at concentrations of 500-600 µM onto a wide variety of coated and uncoated papers sourced from Spicers NZ, as well as standard office paper, and Whatman filter paper (see Table 5 for details). FSL-biotin and biotin were also printed as well as FSL-Btri, FSL-B monoacyl, FSS-Atri and FSS-biotin. SEM images of some of the papers tested are shown in Table 6 and include the most frequently tested paper surfaces.

Table 5. Paper material, name and supplier

Material	**ID/brand name***	**Manufacturer/Supplier**
Whatman 1 filter paper	Filter paper	Whatman, UK
Office copy paper	Printer paper	OfficeMax®, NZ
Media gloss paper	Media gloss	Spicers, NZ
9Lives gloss paper	9Lives	Spicers, NZ
Sapphire Cast coated paper	Sapphire	Spicers, NZ
Black velvet artboard paper	Black velvet	Spicers, NZ
Impress gloss paper	Impress gloss	Spicers, NZ
Impress silk paper	Impress silk	Spicers, NZ
G-Print matt paper	G-Print matt	Spicers, NZ
Alpine artboard paper	Alpine	Spicers, NZ
Superfine Hi gloss paper	Superfine	Spicers, NZ
Symbol freelife paper	Symbol	Spicers, NZ
Saxton paper	Saxton	Spicers, NZ
Hello silk paper	Hello silk	Spicers, NZ
Alpha matt paper	Alpha matt	Spicers, NZ
Alpha gloss paper	Alpha gloss	Spicers, NZ
Media silk paper	Media silk	Spicers, NZ
Photo gloss paper	Photo gloss	Spicers, NZ
Matt self adhesive paper	Matt self	Spicers, NZ
Motionjet paper	Motionjet	Spicers, NZ
Visual jet paper	Visual jet	Spicers, NZ
Scroll jet paper	Scroll jet	Spicers, NZ
Freelife satin paper	Freelife	Spicers, NZ
Digi artboard paper	Digi	Spicers, NZ

* Name printed onto surfaces

Table 6. SEM images of paper surfaces prior to FSL modification.

Paper ID	Magnification	
	×300	×5000
Media gloss	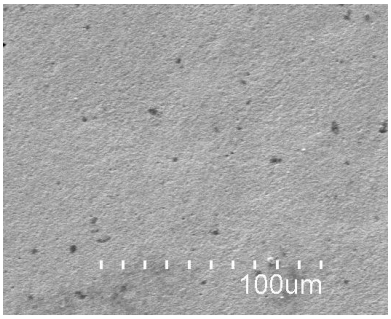	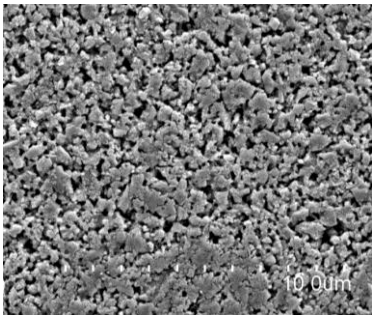
Printer paper	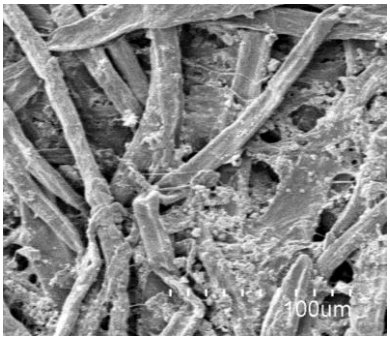	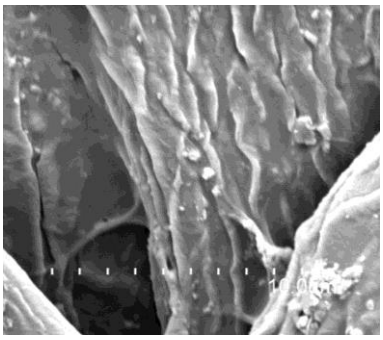
9 Lives	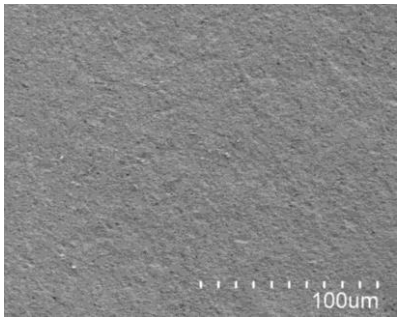	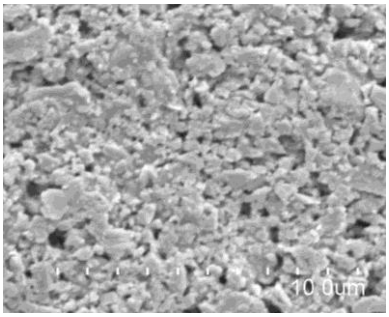
Filter	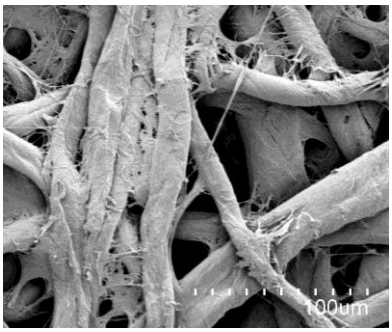	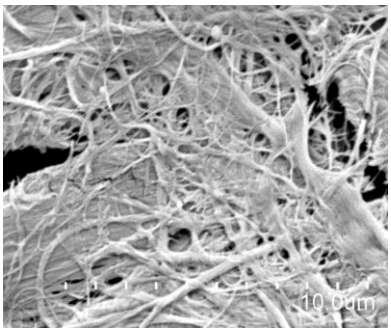

Results and interpretation

Table 7 shows the FSLs tested on different papers and their level of attachment. All papers performed well with regards to FSL attachment. Some examples are shown in Table 8. The Atri antigen and biotin printed separately were not detected on any papers suggesting these were removed during the staining process and indicates that the method of attachment is through the lipid tail of the FSL construct, since these control molecules could not adhere on their own. FSS-Atri, where printed, produced positive but weak results as regards detection on these paper

surfaces whereas FSS-biotin had good attachment to media gloss paper and Whatman 1 filter paper. FSL-B monoacyl was not detected on the papers it was printed onto. These results infer that the differences in the lipid tail can affect the immobilisation or the detection of the construct and show its importance in the attachment method. These surfaces are hydrophilic and so could interact with the head group of the FSL adsorbing it onto the surface. Formation of a bilayer through hydrophobic interactions would remove the non-polar lipids of the FSL from the polar solution surround it. Again micelles of FSLs could be entrapped in the porous surface, or encapsulation of the cellulose fibres could be taking place.

Table 7. Paper surface able to attach FSL constructs. . ++ = strong positive detection, + = weak positive detection, - = no visible detection.

Paper ID	Function-Spacer-Lipid							
	FSL	A/B × ×	A/B Ad DOPE	A Ad Sterol	B Ad Mono	Biotin × ×	Biotin CMG DOPE	Biotin CMG Sterol
Media gloss		-	++		-	-	++	++
Filter		-	++		-	-	++	++
Printer paper		-	++	+	-	-	++	+
9lives Gloss		-	++	+	-	-	++	+
Sapphire		-	++	+	-	-	++	
Black velvet		-	++	+	-	-	++	
Impress gloss		-	++	+			++	
G-print Matt		-	++	+			++	
Alpine		-	++	+		-	++	
Impress silk		-	++				++	
Superfine		-	++				++	
Symbol		-	++			-	++	
Saxton		-	++	+				
Hello silk		-	++					
Alpha Matt		-	++					
Alpha Gloss		-	++					
Media Silk		-	++					
Photo Gloss		-	++					
Matt Self		-	++					
Motionjet		-	++					
Visual jet,		-	++					
Scroll jet		-	++					
Freelife satin		-	++					
Digi artboard		-	++					

Table 8. FSL constructs printed onto and detected on various paper surfaces. + indicates detection of the molecule and – indicates no detection.

	Examples of FSL constructs immobilsed on paper			
Construct	FSL-Atri	FSL-Atri	FSL-biotin	FSL-biotin
Concentration µM	600	600	500	500
Paper ID	Impress silk	Printer paper	Sapphire	G-print
Control	Atri	Atri	Biotin	Biotin
Result	FSL-Atri + Atri -	FSL-Atri + Atri -	FSL-biotin + Biotin -	FSL-biotin + Biotin -
Printed words	FSL-A Impress silk Atri Impress silk	FSL-A Printer Paper Atri Printer Paper	FSL-Biotin Sapphire Biotin Sapphire	FSL-Biotin G-Print Biotin G-Print
Example		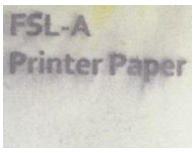	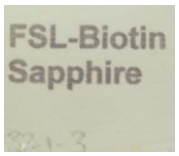	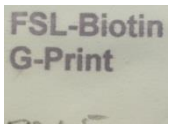

2.2.3 Silica

FSL constructs were tested on silica TLC plates since these are used to separate and therefore have affinity for glycolipids. Both normal (silica gel 60) and reverse phase (silica gel C18) silica layers were tested to investigate differences in attachment of the FSLs with differences in polarity of the surface. Octadecyl carbon chains (C18) modification produces a hydrophobic substance for reverse phase chromatography, while normal phase TLC uses hydrophilic silica.

Method overview

FSL-Atri, Atri and FSL-biotin and biotin were printed or painted onto the normal and reverse phase silica TLC plates at the concentrations 500-600 µM (see Table 9 for silica details). SEM images of the unmodified surfaces are shown in Table 10.

Table 9. Silica material, ID name and supplier.

Material	**ID/brand name***	**Manufacturer/Supplier**
Silica gel 60, Alugram Nano-SIL G	Silica	Machery-Nagel, Germany
Silica gel C18, Alugram RP-18W/UV	C18 silica	Machery-Nagel, Germany

* Name printed on surfaces

The normal phase silica surfaces were plasticised after FSL printing when required for immunostaining to reduce background staining, reduce silica loss during washing steps and potentially orientate the FSL, like glycolipids, in an advantageous position for antibody attachment due to their amphiphilic nature (Hansson et al, 1985, Yiu and Lingwood, 1992).

Table 10. SEM images of silica surfaces prior to FSL modification.

Silica ID	Magnification	
	×300	×5000
Silica	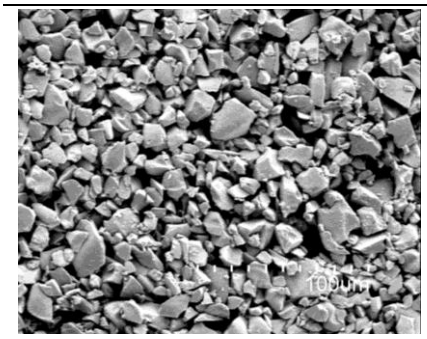	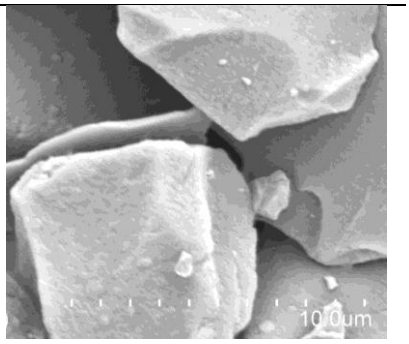
C18 silica	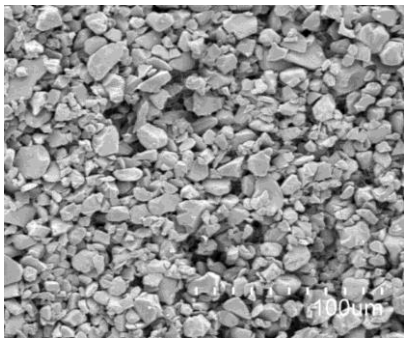	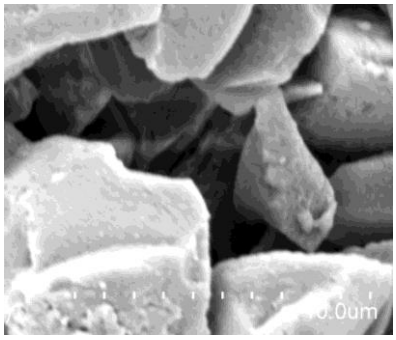

Results and interpretation

The FSL constructs where able to attach well to both of the silica surfaces (Table 11and Table 12). The Atri and biotin did not adhere to either silicas whereas the FSS-Atri bound to a lower level than the FSL-Atri. The FSL-B monoacyl construct was not detected at all. These results are consistent with results on other types of surfaces and indicate the whole FSL construct with the DOPE lipid tail is needed for attachment.

Table 11. Silica surfaces able to attach FSL constructs. ++ = strong positive detection, + = weak positive detection, - = no visible detection.

Silica ID	Function-Spacer-Lipid							
	F **S** **L**	A/B × ×	A/B Ad DOPE	A Ad Sterol	B Ad Mono	Biotin × ×	Biotin CMG DOPE	Biotin CMG Sterol
Silica		-	++	+	-	-	++	
C18 silica		-	++			-	++	

Table 12. FSL constructs printed and detected on silica surfaces+ indicates detection of the molecule and – indicates no detection.

	Examples of FSL constructs immobilsed on silca surfaces				
Construct	FSL-Atri	FSL-Atri	FSL-Atri	FSL-biotin	FSL-biotin
Concentration µM	600	600	600	500	500
Surface	Silica, plasticised	C18 silica	C18 silica, plasticised	Silica	C18 Silica
Staining method	Immunostain	Immunostain	Immunostain	DACA	DACA
Control	Atri	Atri	Atri	Biotin	Biotin
Result	FSL-Atri + Atri -	FSL-Atri + Atri -	FSL-Atri + Atri -	FSL-biotin + Biotin -	FSL-biotin + Biotin -
Printed/ painted words	FSL-A Silica Atri Silica	FSL-A C-18 Silica Atri C-18 Silica	FSL-A C-18 Silica Atri C-18 Silica	FSL-BIO BIOTIN	FSL-BIO BIOTIN
Example	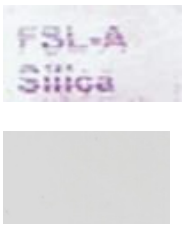	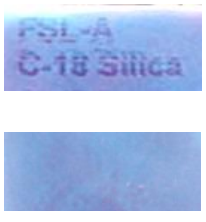	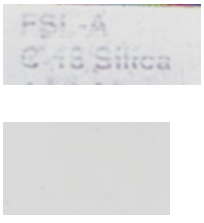		

These results are interesting as these two materials have very different functional groups exposed on their surface and therefore a major difference in attachment would be likely. The opposite polarity of the standard silica and the C18 surface however were both able to equally bind FSL constructs but not the functional head group on its own, indicating a more stable interaction when the whole FSL is involved. The hydrophilic silica, like the cellulose surfaces, may be binding the FSLs in a bilayer formation, whereas for the hydrophobic silica direct binding of the non-polar lipid tail seems more likely. The FSL-biotin DACA staining does appear slightly more intense on the C18 silica, implying possibly a larger degree of binding to this surface, although as they were painted on, the amount loaded onto the surface is less controllable.

The plasticising of the two surfaces also affects the immunostaining result. On hydrophilic silica the plasticising greatly reduces the background staining and improves the sensitivity of the FSL staining. With the hydrophobic surface, whilst the background staining is greatly reduced as well, the sensitivity of the FSL detection is also decreased. The plasticising of the already hydrophobic surface does not seem to orientate the molecule in the same way as the normal phase silica, suggesting differences in the binding mechanism on the two surfaces. The background staining is high with no plasticising of the C18 silica but the FSL is easily detected. On hydrophilic silica with no plasticising much lower detection is seen.

2.2.4 Polymers

Polymer membranes are commonly used for biological applications due to their mechanical and chemical stability. Synthetic polymeric membranes are able to be tailor made for a specific purpose or molecule, offering control over the chemical composition and by altering the pore size and distribution. This makes them very useful for dialysis, filtration and blotting.

Method overview

FSL-Atri, Atri antigen, FSL-Btri, FSL-biotin and FSS-biotin were printed at concentrations 100-400 µM. The surfaces printed onto mainly include filter membranes but also included polyester film, a polystyrene microwell plate and nylon used in a 3D printer, printed into a flexible 1mm layer. The filter membranes include polypropylene, nylon, poly-ethersulfone (PES), polyvinylidene fluoride (PVDF), polytetrafluoroethylene (PTFE) also known as Teflon, polyester (PE) and polycarbonate (PC) (see Table 13 for details). FSL-Atri, FSL-Btri and Atri were printed in a code, 3A0ad, 3B0ad and 3A000 respectively. All other FSLs were printed in words. SEM images of the surfaces tested are shown in Table 14a-c.

Table 13. Polymer material, ID name and supplier.

Material	**Pore size µm**	**ID/brand name***	**Manufacturer/ Supplier**
Polypropylene filter membrane	-	Polypropylene	Gelman Sciences, USA
Nylon filter membrane	0.45	Nylon filter	Schleicher and Schuell, USA
Polyethersulfone filter membrane	0.45	PES	Sterlitech, USA
Polyvinylidene fluoride filter membrane	0.45	PVDF	Sterlitech, USA
Polyvinylidene fluoride filter membrane	0.2	PVDF	Sterlitech, USA
Polytetrafluoroethylene filter membrane	0.2	PTFE or Teflon	Gelman, USA
Polytetrafluoroethylene filter membrane	1	PTFE or Teflon	Sterlitech, USA
Polytetrafluoroethylene filter membrane	10	PTFE or Teflon	Sterlitech, USA
Polyester filter membrane	1	PE	Sterlitech, USA
Polyester copier transparency film	-	Polyester film	OfficeMax, NZ
Polystyrene microplate	-	Polystyrene	Nunc, USA
Nanofibre material	-	Nanofibre	Confidential
Nylon PA2200, 3D printed	-	Printed nylon	EOS, Germany
Polycarbonate filter membrane	1	PC	Sterlitech, USA
Polycarbonate filter membrane	20	PC	Sterlitech, USA

* Name printed on surfaces

Table 14a. SEM images of polymer surfaces prior to FSL modification.

Polymer ID	Magnification	
	×300	×5000
Polypropylene	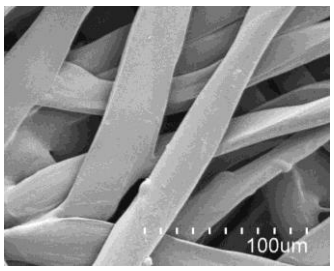	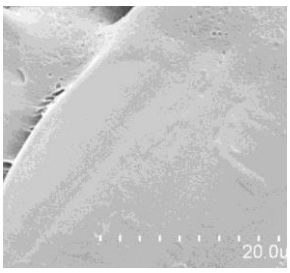
Nylon 0.45µm pores	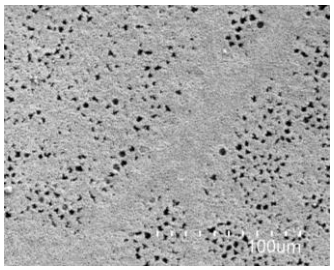	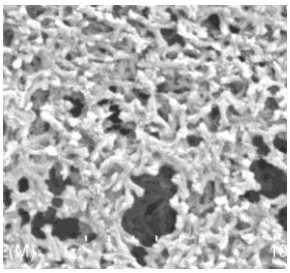
PES 0.45µm pores	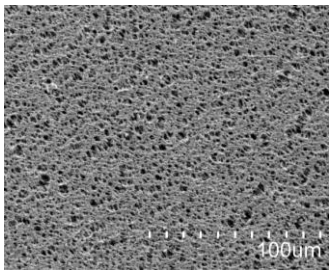	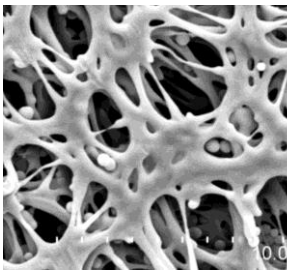
PVDF 0.45µm pores	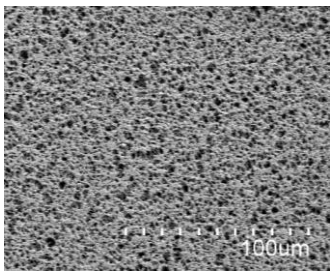	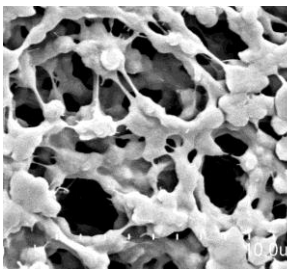
PVDF 0.2 µm pores	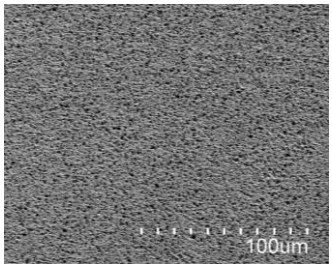	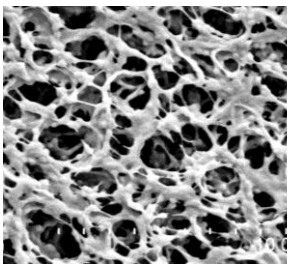
PTFE 0.2 µm pores	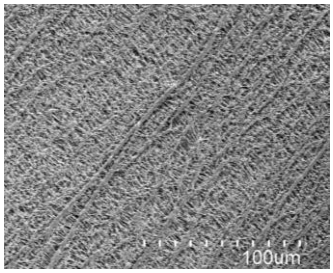	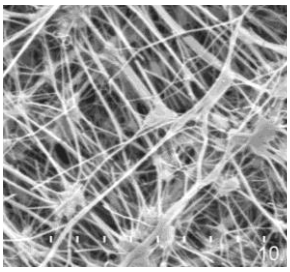

Table 14b. SEM images of polymer surfaces prior to FSL modification.

Polymer ID	Magnification	
	×300	×5000
PTFE 1µm pores	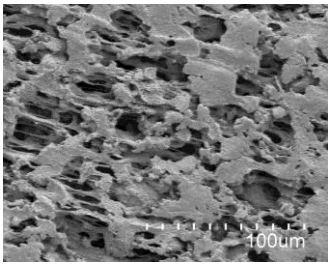	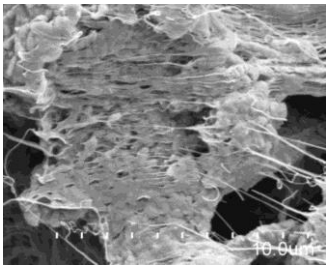
PTFE 10µm pores	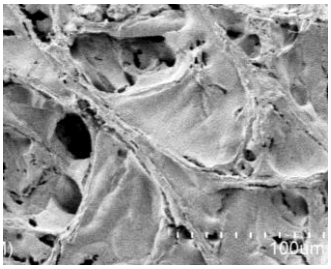	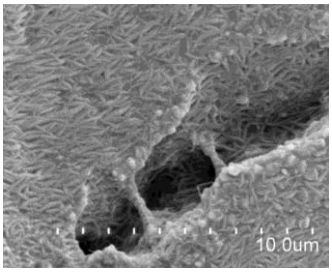
PE 1 µm pores	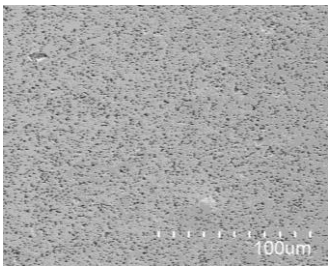	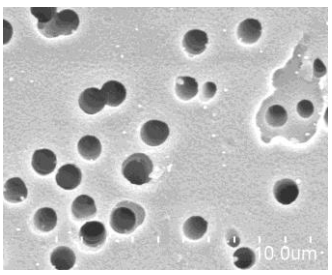
Polyester film	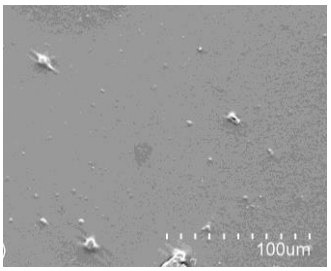	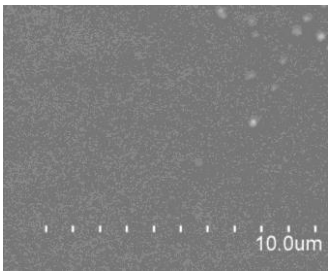
Polystyrene	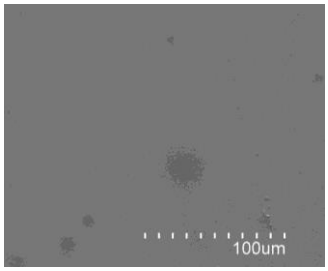	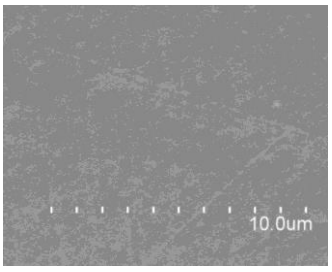
Nanofibres	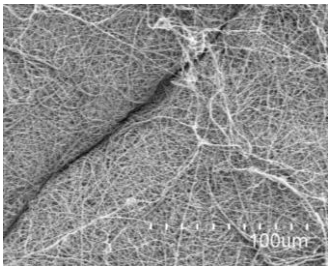	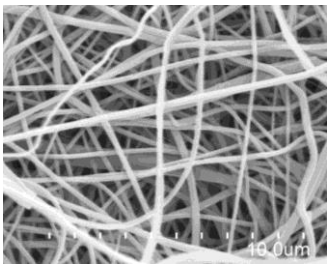

Table 14c. SEM images of polymer surfaces prior to FSL modification.

Polymer ID	Magnification	
	×300	×5000
3D Printer nylon printed	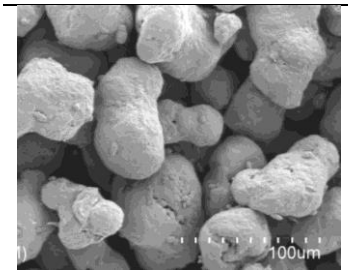	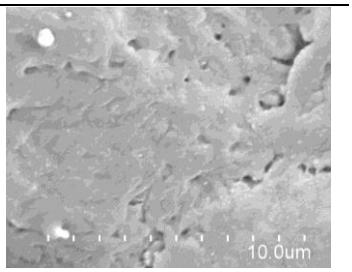
PC 1µm pores	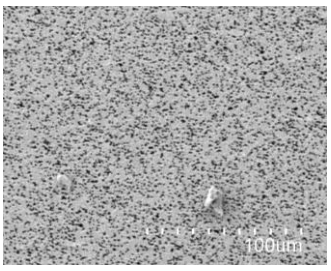	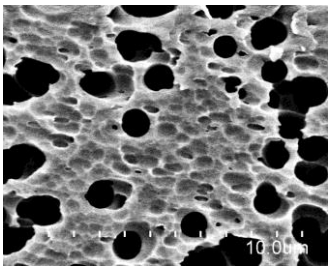
PC 20µm pores	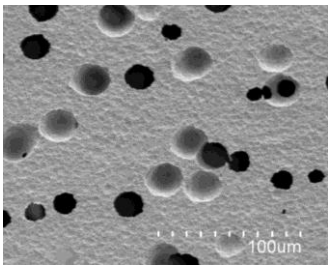	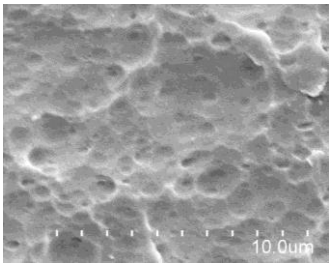

Results and interpretation

Of all the types of polymers tested, all were able to attach FSL constructs and allow them to be detected (Table 15). Some examples are shown in Table 16. Interestingly the pore size of the polymer did show some relationship in the ability to attach FSLs in the case of PDVF and polycarbonate. In the PVDF surfaces FSLs were less visible on the material with the smaller pore size of 0.2µm compared to 0.45µm. By looking at the SEM images of the two surfaces there is substantially less material available for adhering to the surface on the smaller pore size material. At ×5000 magnification the surface is composed of a string like surface rather than any flat areas, with large gaps between the threads, therefore reducing the amount of material available for FSL attachment compared to the larger pore surface. This might explain the lower level of FSL detection on this surface. The polycarbonate membrane with 20µm pores compared to 1µm pores showed lower detection of FSL constructs. This could again be due to less material to bind to, because of the large pores causing loss of FSL solution through them.

Table 15. Polymer surfaces that FSL molecules are able to attach to. ++ = strong positive detection, + = weak positive detection, - = no visible detection.

Polymer ID	Function-Spacer-Lipid							
	FSL	A/B × ×	A/B Ad DOPE	A Ad Sterol	B Ad Mono	Biotin × ×	Biotin CMG DOPE	Biotin CMG Sterol
PTFE 0.2µm		-	++		-	-	++	++
Polypropylene		-	++		-	-	++	++
Nylon 0.45µm		-	++		-	-	++	+
PES 0.45µm		-	++	++				
PVDF 0.45µm		-	++	++				
PE 1µm		-	++	++				
PTFE filter 1µm		-	++	++				
PTFE filter 10µm		-	++	++				
Polyester film		-	++			-	++	
Polystyrene		-	++			-	++	
Nanofibre		-	++			-	++	
Printed nylon		-	++					
PC 1µm		+	++					
PVDF 0.2µm		-	+					
PC 20µm		-	+					

Table 16. Various FSL constructs printed and detected on a variety of polymer surfaces. + indicates detection of the molecule and – indicates no detection.

	Examples of FSL constructs immobilsed on polymer surfaces				
Construct	FSL-Atri FSL-Btri	FSL-Atri FSL-Btri	FSL-Atri FSL-Btri	FSL-biotin FSS-biotin	FSL-biotin
Concentration µM	400	400	400	100	100
Polymer ID	PE	PTFE 0.45µm	PVDF 0.45µm	Nylon filter	Nanofibres
Control	Atri	Atri	Atri	Biotin	Biotin
Result	FSL-Atri + FSL-Btri + Atri -	FSL-Atri + FSL-Btri + Atri -	FSL-Atri + FSL-Btri + Atri -	FSL-biotin + FSS-biotin + Biotin -	FSL-biotin + Biotin -
Printed words	3A0ad 3B0ad 3A000	3A0ad 3B0ad 3A000	3A0ad 3B0ad 3A000	FSL-biotin Nylon Biotin Nylon	FSL-biotin Biotin
Example	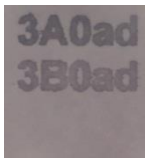	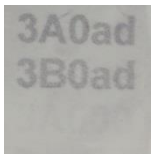	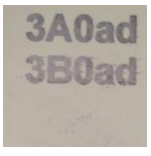	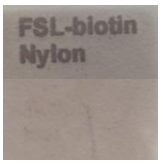	

The polycarbonate material did show some adherence of the Atri antigen molecule, although this was poor compared to the FSL-Atri printed at the same concentration. This indicates that

although the binding was greatly improved using the full FSL molecule, the antigen on its own did have some affinity for this hydrophilic surface.

The PTFE, polypropylene, PES, PVDF 0.45µm and polyester membranes showed equal attachment of the sterol (FSS) lipid tail compared to the standard DOPE lipid tail, whereas the nylon showed less attachment of FSL constructs with this sterol lipid. The surface properties can therefore affect the attachment of these constructs.

This polymer category is composed of hydrophilic and hydrophobic surfaces, however all showed they were able to attach FSL constructs, with pore size rather than material composition affecting the degree of attachment. Speculative methods of attachment here include direct attachment of the lipid tail to hydrophobic surfaces though hydrophobic interactions or bi-layering of the molecules on hydrophilic surfaces. This would be through interactions with the head group and subsequent hydrophobic interactions of the lipid tails between layers. On the fibrous surfaces this could be in the form of encapsulation of the molecules around the fibres. Interesting surfaces are the polyester film and polystyrene which are extremely flat. These hydrophobic surfaces are able to immobilise FSL constructs well and yet no micelle entrapment or encapsulation of fibres is possible. Direct physical adsorption seems possible in this situation where hydrophobic water exclusion interactions may be holding the FSLs to the surface. Amphiphilic molecules are known to assemble as aggregates or at interfaces due to the hydrophobic part removing itself from contact with the aqueous solution, which may be causing the attachment of FSLs on to these materials.

2.2.5 Natural fibres

Natural fibre surfaces were investigated to broaden the range of materials tested. Cotton fibres are composed of nearly pure cellulose, whereas silk is a natural protein fibre.

Method overview

FSL-Atri, FSL-biotin and FSS-biotin were inkjet printed onto cotton and silk material at 100-200 µM (see Table 17 for details). Images of the materials used were obtained using the SEM after sputter coating with platinum (Table 18).

Table 17.Natural fibre material, ID name and supplier.

Material	ID/brand name*	Manufacturer/Supplier
Cotton	Cotton	Centrepoint Fabrics, NZ
Silk	Silk	Centrepoint Fabrics, NZ

* Name printed on surfaces

Table 18. SEM images of natural fibre material surfaces

Fibre ID	Magnification	
	×300	×5000
Cotton	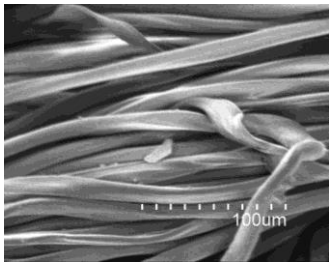	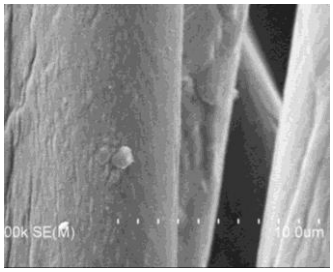
Silk	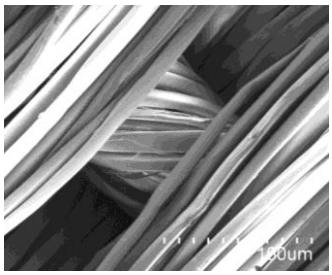	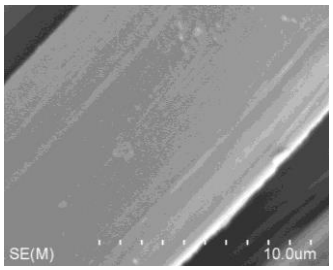

Results and interpretation

Table 19 presents the results of FSL attachment to cotton and silk. Table 20 shows some examples of FSL-Atri, FSL-biotin and FSS-biotin attached to different fibre surfaces. FSLs bind well to all these fibre surfaces and exhibit the same results as other surfaces in regards to the lipid tail, where Atri and biotin did not bind to these surfaces without being part of the whole FSL molecule. The monoacyl lipid did not attach to these surfaces whereas the sterol lipid adhered to the same degree as the diacyl lipid on cotton but to a lesser degree on silk.

The attachment mechanism in this situation could be encapsulation of the fibres in a liposome formation, as these are hydrophilic surfaces, or bilayers of FSLs forming on the surface of the fibres, but not encapsulating them. Again these could be formed by the hydrophobic effect.

Table 19. Natural fibre surfaces that FSL molecules are able to attach to. ++ = strong positive detection, + = weak positive detection, - = no visible detection.

Surface	Function-Spacer-Lipid							
	F **S** **L**	A/B × ×	A/B Ad DOPE	A Ad Sterol	B Ad Mono	Biotin × ×	Biotin CMG DOPE	Biotin CMG Sterol
Cotton		-	++		-	-	++	++
Silk		-	++		-	-	++	+

Table 20. Examples of FSL constructs inkjet printed and immunostained on fibre surfaces, + indicates detection of the molecule and – indicates no detection.

	Examples of FSL constructs immobilsed on natural fibres		
Construct	FSL-Btri	FSL-Atri	FSL-biotin FSS-biotin
Concentration µM	200	200	100
Fibre ID	Silk	Cotton	Cotton
Control	Btri	Atri	Biotin
Result	FSL-Btri + Btri -	FSL-Atri + Atri -	FSL-biotin + FSS-biotin + Biotin -
Printed words	FSL-B Silk Btri Silk	FSL-A Cotton Atri Cotton	FSL-biotin Biotin FSS-biotin
Example			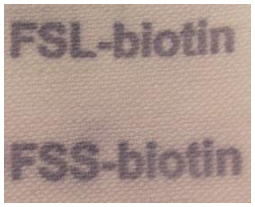

2.2.6 Glass

Glass is widely used as a substrate for biomolecule immobilisation, although usually through functionalisation for covalent attachment.

A range of borosilicate glass surfaces were trialled for attachment capabilities of FSL constructs.

Method overview

FSLs and control molecules were applied to the glass surfaces by painting and printing at concentrations of 100-300 µM. Two types of borosilicate glass were tested, in a fibre form and as a flat sheet (see Table 21 for details). SEM images of the surface were obtained after sputter coating with platinum (Table 22).

Table 21. Glass material, ID name and supplier.

Material	**ID/brand name***	**Manufacturer/Supplier**
Glass fibre filter membrane	Glass fibre	Whatman, UK
Glass microscope cover slip	Glass cover slip	Menzel Gläser, Germany

* Name printed/painted on surfaces

Table 22. SEM images of glass surfaces prior to FSL modification.

Glass ID	Magnification	
	×300	×5000
Glass fibre	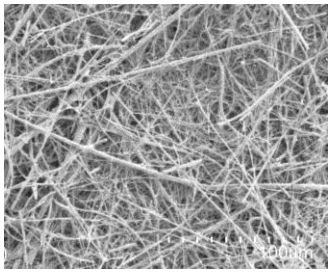	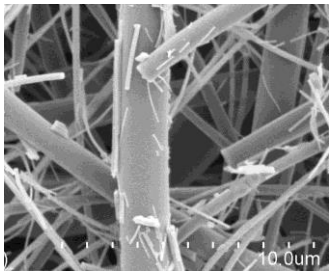
Glass cover slip	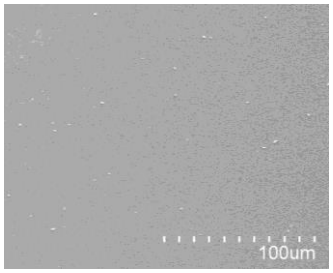	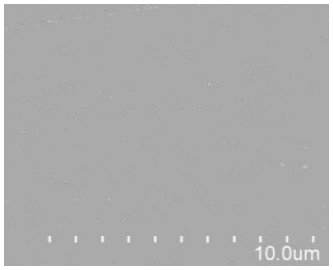

Results and interpretation

The FSL molecules bound well to both surfaces tested, whilst the biotin and Atri were washed away (Table 23 and Table 24). Again it seems the lipid tail is essential in adhering the molecule to the surface, as when no lipid was present attachment was prevented and the sterol lipid tail altered the attachment. Borosilicate is considered a hydrophilic surface able to adsorb water molecules (Bernett et al, 1968, Sumner et al, 2004). These two surfaces were extremely different topographically but exhibited the same binding behaviour towards FSLs. Possible binding theories include layering of the FSL constructs with hydrophilic head groups orientated to the surface with another layer in the opposite orientation in a bilayer formation, thus removing the lipid tails from contact with the surface or the surrounding solution.

Table 23. Glass surfaces that FSL molecules are able to attach to. ++ = strong positive detection, + = weak positive detection, - = no visible detection.

Surface	Function-Spacer-Lipid							
	F **S** **L**	A/B × ×	A/B Ad DOPE	A Ad Sterol	B Ad Mono	Biotin × ×	Biotin CMG DOPE	Biotin CMG Sterol
Glass fibre		-	++		-	-	++	+
Glass cover slip		-	++	+	-	-	++	

Table 24. FSL constructs immobilised on glass surfaces, + indicates detection of the molecule and -indicates no detection.

	Examples of FSL constructs immobilsed on glass		
Construct	FSL-Btri	FSL-biotin	FSL-biotin FSS-biotin
Concentration µM	300	300	100
Glass ID	Glassfibre	Glass cover slip	Glass fibre
Control	Btri	Biotin	Biotin
Result	FSL-Btri + Btri -	FSL-biotin + Biotin -	FSL-biotin + FSS-biotin + Biotin -
Printed/painted words	FSL-B Glass fibre Btri Glass fibre	FSL BIO	FSL-biotin Glass fibre FSS-biotin Glass fibre Biotin Glass fibre
Example			

2.2.7 Metals

Method overview

A variety of metal surfaces were tested for FSL immobilisation since they are common surfaces for biomolecule immobilisation, especially SAMs onto gold. Gold is a popular surface for biomolecule immobilisation as amines readily bind to thiol groups exposed on the gold surface and is a popular substrate for biosensors.

Metals tested for FSL immobilisation include gold leaf, silver filter, silver bandage, silver foil and aluminium foil (see Table 25 for details). FSLs were printed at concentrations of 100-300 µM. SEM images of the unmodified surface are shown in Table 26.

Table 25. Metal material, ID name and supplier.

Material	**ID/brand name***	**Manufacturer/Supplier**
Aluminium foil	Aluminium foil	Clorox, NZ
Golf leaf	Gold	The Gold Leaf Factory, Aus
Silver bandage	Silver bandage	Silverlon, USA
Silver filter membrane	Silver filter	Sterlitech, USA
Silver foil	Silver foil	The Gold Leaf Factory, Aus

* Name printed onto surfaces

Table 26. SEM images of metal surfaces tested prior to FSL modification.

Surface	Magnification	
	×300	×5000
Aluminium foil	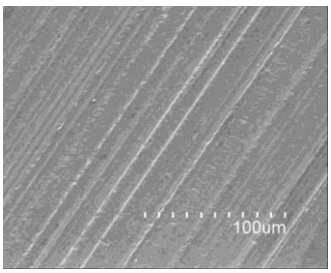	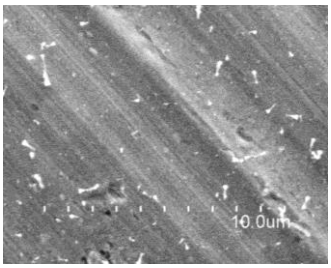
Gold leaf	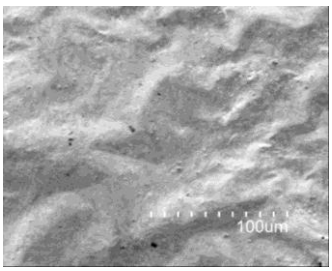	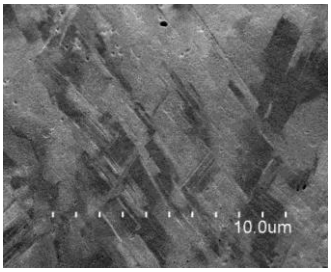
Silver bandage	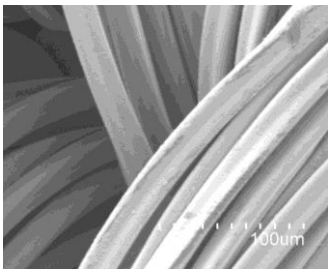	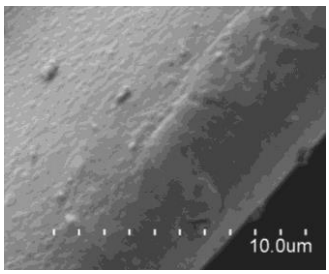
Silver filter	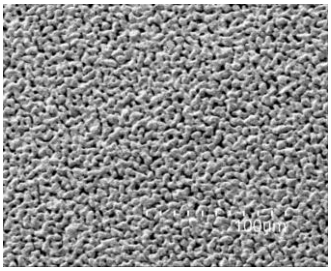	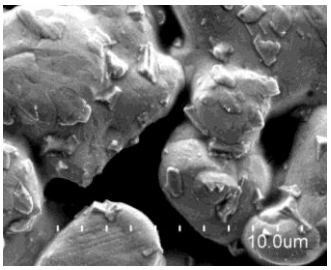
Silver foil	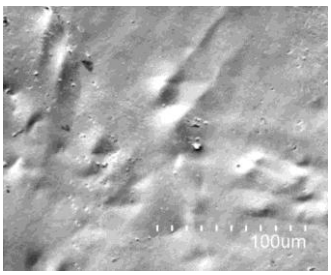	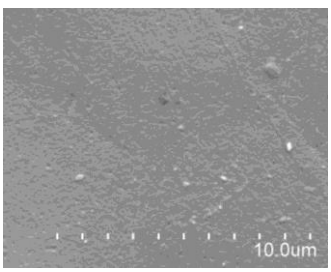

Results and interpretation

All metal surfaces tested were able to attach FSLs, with the functional group being washed away when printed on its own (Table 27, Table 28). One exception was biotin on gold, where there was some detection of this molecule on the gold leaf surface. This might suggest that the FSL construct is not causing the binding to the surface, however results of FSL-Atri and Atri show compete removal of the Atri antigen after washing, showing the FSL is indeed necessary for the immobilisation. Stronger detection is seen with FSL-biotin than biotin indicting an enhanced attachment with the FSL even though biotin itself has affinity for the gold surface.

Table 27. Metal surfaces that FSL molecules are able to attach to. . ++ = strong positive detection, + = weak positive detection, - = no visible detection.

Surface	Function-Spacer-Lipid							
	FSL	A/B × ×	A/B Ad DOPE	A Ad Sterol	B Ad Mono	Biotin × ×	Biotin CMG DOPE	Biotin CMG Sterol
Silver filter		-	++	++	-	-	++	
Aluminium foil		-	++	+	-	-	++	+
Silver bandage		-	++			-	++	
Gold leaf		-	++			+	++	+
Silver foil		-	++		-	-	++	

Table 28. FSLs tested on metal surfaces, + indicates detection of the molecule and – indicates no detection.

	Examples of FSL constructs immobilsed on metals			
Construct	FSL-Atri	FSL-Atri	FSL-Atri	FSL-biotin FSS-biotin
Concentration µM	300	300	300	100
Metal ID	Gold leaf	Silver filter	Silver bandage	Aluminium foil
Control	Atri	Atri	Atri	Biotin
Result	FSL-Atr + Atri -	FSL-Atri + Atri -	FSL-Atri + Atri -	FSL-Biotin + FSS-biotin + Biotin -
Printed/painted words	FSL-A Atri	FSL-A FSL-B Atri	FSL-A Atri	FSL-biotin Biotin FSS-biotin
Example				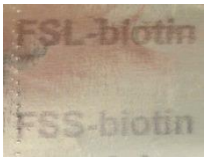

The sterol lipid showed reduced detection of the FSL except on the silver filter where equal detection was seen for DOPE FSL and sterol FSS. The lipid tail is therefore important in immobilisation of the FSL. Attachment of FSLs to these surfaces could be through hydrophobic interactions of the lipid tail on to the hydrophobic surfaces or hydrophilic binding though the head group in a bilayer formation. In fact there could be multiple layers of FSLs on all surfaces mentioned so far, in alternating orientation to the surface, through their amphiphilic nature.

2.2.8 Non-planar surfaces

Having discovered that FSL constructs will adhere to flat surfaces, non-planar surfaces were then investigated. The aim was to increase understanding of the attachment mechanism as different interactions may occur on these surfaces. Microbeads are popular in laboratory practises for a variety of assays and are extremely useful for binding, capture and filtration procedures. The applications for microbeads in a biological and medical environment are continually growing, making them an important tool in biotechnology. This also makes them readily available for testing FSL attachment. The objective of these experiments was to assess if FSLs can adhere to microbeads and fibreglass threads.

Method overview

The surfaces tested were polycarbonate microbeads (20µm), paramagnetic beads (1µm) and fibreglass threads (10µm wide) (for details see Table 29). SEM images of these surfaces are shown in Table 30.

Table 29. Microbead and thread material, name and supplier.

Material	**Manufacturer/Supplier**
Polycarbonate microbeads, 20 µm	Nanomi, Netherlands
Paramagnetic microbeads, 1µm	Millipore, France
Fibreglass threads	Standard fibre glass cloth

Table 30. SEM images of non-planar surfaces tested prior to FSL modification.

Surface	×300	×5000
Polycarbonate microbeads	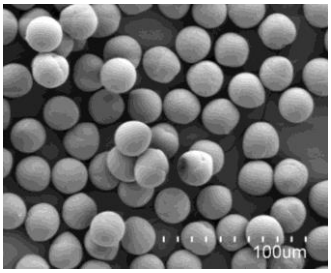	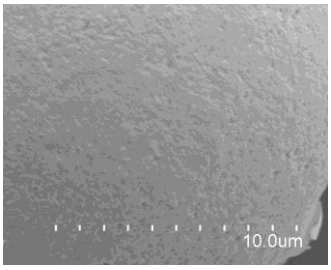
Paramagnetic microbeads	Beads too small at this magnification	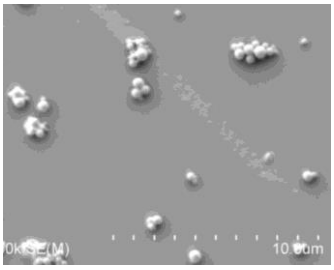
Fibreglass threads	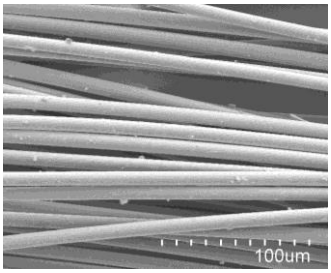	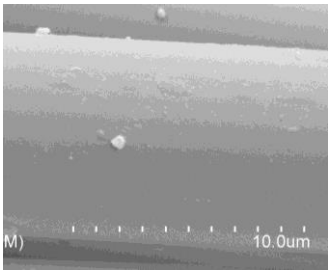

Polycarbonate microbeads: A small spatula amount of polycarbonate microbeads, 20 µm in diameter, were added to a 100 µL solution of FSL-biotin at 250 µM and mixed well. They were incubated for 30 minutes at room temperature then washed 3 times in PBS by centrifuging the solution on high for 10 seconds and removing the supernatant. A 100 µL solution of avidin-alexa fluor®488 (A-21370, Invitrogen, USA) was prepared at 0.1 mg/mL and added to the FSL-biotin modified beads. This reagent is avidin conjugated to a fluorescent label with excitation and emission wavelengths maxima at ~ 495/519 nm. They were incubated in the dark for 30 minutes and then washed two times in PBS. The beads were suspended in 200 µL PBS and examined on the fluorescent microscope at 488nm wavelength. For controls, beads that had no FSL contact were incubated with the avidin-alexa fluor®488 solution using the same protocol. Biotin, at 250 µM, was also incubated with the beads for 30 minutes and followed the same protocol of washing and avidin-alexa fluor®488 conjugate attachment.

Paramagnetic microbeads: 1 µL of packed paramagnetic beads, 1 µm in diameter, were added to a 100 µL solution of FSL-biotin at 50 µM in 0.1 % tween 20/PBS. They were mixed thoroughly and incubated at 4°C overnight. The beads were pulled into a pellet using a magnet (neodymium magnet) and the supernatant removed. 50 µL of avidin-alexa fluor®488 at 0.1 mg/mL was added to the beads and incubated at room temperature in the dark for 30 minutes,

then washed once in 0.1% tween 20/PBS using the magnet to hold the beads in the tube and then suspended in 100 µL of the tween/PBS solution. For controls, 1µL of beads was added to 100 µL of 50µM biotin and 1µL of beads added to 100µL PBS. These were incubated at 4°C overnight, as for the FSL beads, and tested with the avidin-alexa fluor®488 as described. The tween is added to prevent clumping of the beads.

Fibre glass: To test a fibre surface FSL-Atri and FSL-biotin at 250 µM were painted onto fibreglass threads in a specific region. This was allowed to dry and then the whole thread was immunostained to access the attachment of the FSL molecules using either monoclonal anti-A or streptavidin-alkaline phosphatase conjugate as appropriate. This was carried out by submerging the whole thread in a tube of each reagent.

Results and interpretation

FSL constructs were able to attach to both types of microbeads and to the fibreglass threads (Table 31). FSL-biotin coated the polycarbonate microspheres well and uniformly as seen in Table 32. Beads with no FSL incubation did not fluoresce after incubation with the fluorescent avidin, indicating the biotin nor the avidin bound to the beads.

Table 31. Immobilisation of FSLs on non-planar surfaces. ++ = strong positive detection, + = weak positive detection, - = no visible detection.

Surface	Function-Spacer-Lipid							
	F **S** **L**	A/B × ×	A/B Ad DOPE	A Ad Sterol	B Ad Mono	Biotin × ×	Biotin CMG DOPE	Biotin CMG Sterol
Polycarbonate microbeads			++			-	++	
Paramagnetic microbeads						-	++	
Fibreglass thread			++				++	

Table 32. Polycarbonate microspheres coated with 250µM FSL-biotin and visualised using avidin-alexa fluor® 488 using fluorescent microscopy.

Test/control	Images of polycarbonate microbeads with and without FSL attachment	
	×200 image	×200 Fluorescence image
Beads incubated with FSL-biotin	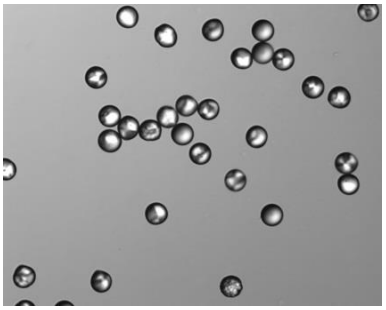	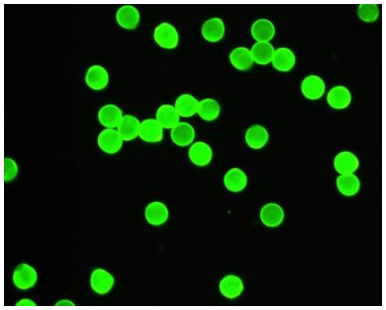
Beads incubated with control molecule biotin	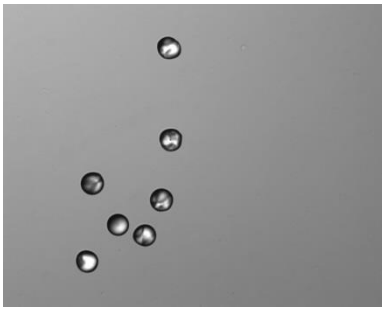	
Negative control beads	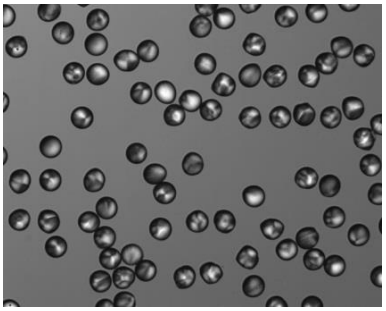	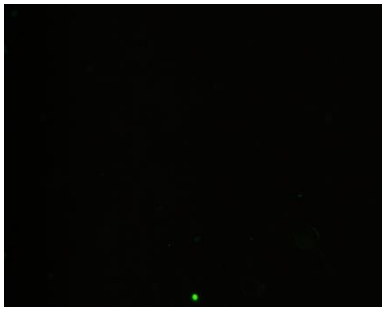

The paramagnetic microbeads also showed good attachment of FSL-biotin by fluorescing brightly after avidin incubation (Table 33). The beads incubated with biotin and avidin or the avidin alone did not fluoresce as brightly, although some fluorescence was observed indicating some background staining of the avidin on the beads.

Table 33. Paramagnetic microbeads coated with FSL-biotin and visualised with avidin-alexa fluor® 488. Beads were also incubated with biotin to test for biotin attachment to the beads, and also with the fluorescent avidin as a negative control.

Test/control	Images of beads with and without FSL attachment	
	×1000 image	×1000 Fluorescence image
Beads incubated with FSL-biotin	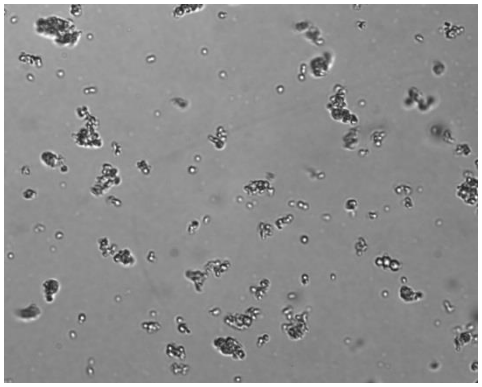	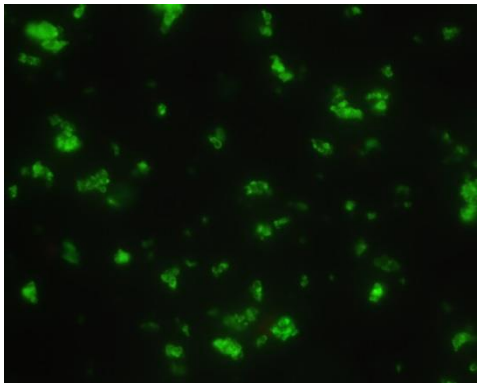
Beads incubated with control molecule	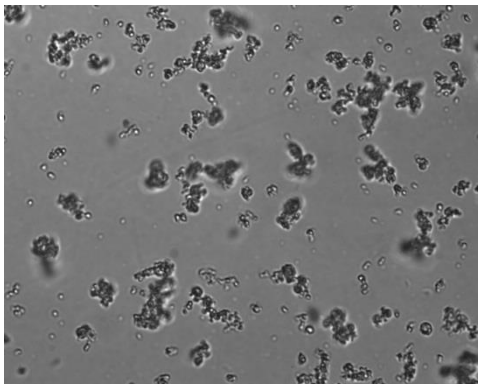	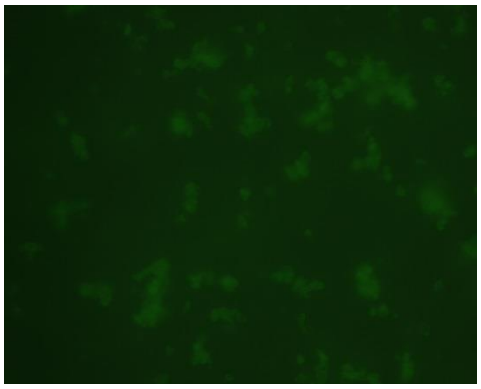
Negative control beads	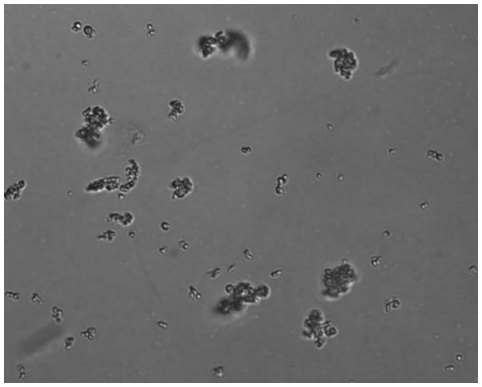	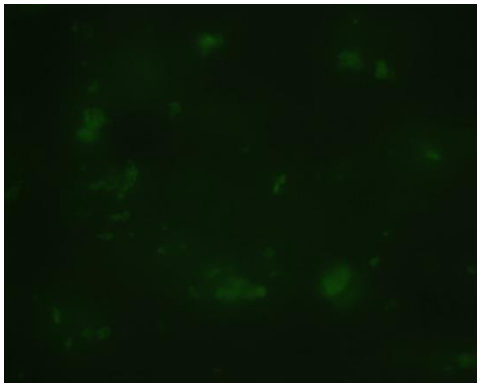

The fibreglass threads painted with FSLs showed staining only where the FSL had been applied, with the other half of the thread acting as a negative control (Figure 14). This again indicates the FSL had adhered to the fibres and were able to be detected.

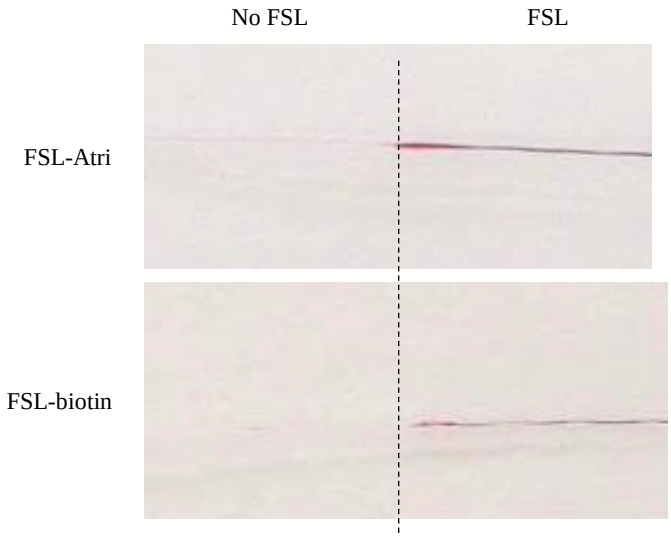

Figure 14. FSL-Atri and FSL-biotin painted onto the right hand side of fibre glass treads and stained. The left hand side acts as the negative control and shows no staining.

The FSL constructs were able to attach well to these surfaces. The attachment mechanisms possibly include encapsulation of the beads or threads by creating a layer of FSLs around the structure. This may be in a monolayer or bilayer organisation, involving hydrophobic forces removing the hydrophobic parts of the FSLs from the aqueous solution. They could also be attaching to these surfaces as micelles or layers directly onto the surface rather than surrounding it, again driven by hydrophobic forces.

2.2.9 Summary table of non-biological surfaces tested with FSLs

Table 34 a and b are summary tables of all the non-biological surfaces FSL constructs have been applied to and a score of how well they adhered to the surface. The immobilisation of the FSLs was scored with either -, + or ++, with - being no visible detection, + being weak detection and ++ being strong detection. All surfaces tested were able to immobilise FSL constructs. There was a wide variety of surfaces tested, including hydrophobic and hydrophilic, fibrous to extremely flat, which did not seem to determine FSL attachment. Indeed FSLs bound to all surfaces well, and were able to capture their binding molecules showing preserved activity after attachment. The hydrophobic effect, possibly driving the interaction, would enable the formation of mono or bi-layers of FSLs on the surfaces, arranging them in an oriented way for binding to their recognition molecules.

Table 34a. Score given to different surfaces for their ability to immobilise various FSL constructs. ++ = strong positive detection, + = weak positive detection, - = no visible detection. No score indicates this construct or molecule was not tested on this surface. A/B relates to carbohydrate blood group A or B antigen, Ad is adipate spacer, CMG is the longer carboxymethylglycine spacer, DOPE is standard lipid tail for FSL, sterol is the lipid tail for FSS, and mono is the lipid tail for monoacyl constructs.

Surface category	Surface ID	Function-Spacer-Lipid							
		FSL	A/B × ×	A/B Ad DOPE	A Ad Sterol	B Ad Mono	Biotin × ×	Biotin CMG DOPE	Biotin CMG Sterol
Modified cellulose	Nitrocellulose		-	++	+	-	-	++	+
	Cellulose triacetate		-	++		-	-	++	+
	Mixed cellulose esters		-	++					
	Regenerated cellulose		-	++					
	Cellulose acetate		-	+					
			-						
Paper	Media gloss		-	++		-	-	++	++
	Filter paper		-	++		-	-	++	++
	Printer paper		-	++	+	-	-	++	+
	9lives Gloss		-	++	+	-	-	++	+
	Sapphire		-	++	+	-	-	++	
	Black velvet		-	++	+	-	-	++	
	Impress gloss		-	++	+			++	
	G-print Matt		-	++	+			++	
	Alpine		-	++	+		-	++	
	Impress silk		-	++				++	
	Superfine		-	++				++	
	Symbol		-	++			-	++	
	Saxton		-	++	+				
	Hello silk		-	++					
	Alpha Matt		-	++					
	Alpha Gloss		-	++					
	Media Silk		-	++					
	Photo Gloss		-	++					
	Matt Self Adhesive		-	++					
	Motionjet		-	++					
	Visual jet		-	++					
	Scroll jet		-	++					
	Freelife satin		-	++					
	Digi artboard		-	++					
Silica	Silica		-	++	+	-	-	++	
	C18 silica		-	++			-	++	

Table 34b. Score given to different surfaces for their ability to immobilise various FSL constructs. ++ = strong positive detection, + = weak positive detection, - = no visible detection. No score indicates this construct or molecule was not tested on this surface. A/B relates to carbohydrate blood group A or B antigen, Ad is adipate spacer, CMG is the longer carboxymethylglycine spacer, DOPE is standard lipid tail for FSL, sterol is the lipid tail for FSS, and mono is the lipid tail for monoacyl constructs.

Surface category	Surface ID	Function-Spacer-Lipid							
		F **S** **L**	A/B × ×	A/B Ad DOPE	A Ad Sterol	B Ad Mono	Biotin × ×	Biotin CMG DOPE	Biotin CMG Sterol
Polymers	PTFE filter 0.2µm		-	++		-	-	++	++
	Polypropylene filter		-	++		-	-	++	++
	Nylon filter 0.45µm		-	++		-	-	++	+
	PES filter 0.45µm		-	++	++				
	PVDF 0.45µm filter		-	++	++				
	Polyester filter 1µm		-	++	++				
	PTFE filter 1µm		-	++	++				
	PTFE filter 10µm		-	++	++				
	Polyester film		-	++			-	++	
	Polystyrene microplate		-	++			-	++	
	Nanofibre		-	++			-	++	
	3D Printed nylon		-	++					
	Polycarbonate 1µm		+	++					
	PVDF 0.2µm filter		-	+					
	Polycarbonate 20µm		-	+					
Natural fibres	Cotton		-	++		-	-	++	++
	Silk		-	++		-	-	++	+
Glass	Glass fibre filter		-	++		-	-	++	+
	Glass cover slip		-	++	+	-	-	++	
Metal	Silver membrane filter		-	++	++	-	-	++	
	Aluminium foil		-	++	+	-	-	++	+
	Silver bandages		-	++			-	++	
	Gold leaf		-	++			+	++	+
	Silver foil		-	++		-	-	++	
Non-planar surfaces	Polycarbonate microbeads			++			-	++	
	Paramagnetic microbeads						-	++	
	Fibreglass thread			++				++	

2.3 Testing limitations of FSL immobilisation

This section looks more closely at the FSL immobilisation on non-biological surfaces. The limitations of this immobilisation are investigated to try to achieve a greater understanding of the attachment to solid surfaces. A number of experiments were carried out to assess which part of the construct maybe involved in the immobilisation, and if variations in the construct structure will alter the adherence and what effects detergents and solvents may have on the immobilisation. The stability of the FSL molecules attached to solid surfaces was also investigated.

FSL constructs were designed with a diacyl lipid tail capable of inserting into a cell membrane (Frame et al., 2007; Korchagina et al., 2012). Whilst FSLs have been shown to immobilise on a variety of solid surfaces with varying properties, it was important to ascertain if the lipid tail was vital to the adherence on these surfaces. Initial experiments determined whether the functional part (F) of the FSL could adhere without being part of an FSL construct. This involved printing both the functional moiety and the full FSL next to each other and staining them to test if they are both detectable and therefore immobilised and functional after being applied to the surface. Analysing the attachment of FSLs containing differences in the functional moiety, spacer and lipid tail was thought to be beneficial in understanding the limitations of the FSL binding. By contacting immobilised FSLs with various solvents or detergents, investigations into the nature and degree of binding to these surfaces were carried out.

2.3.1 F (functional head group) versus FSL

Method overview

FSL-Atri and Atri, the trisaccharide of the A blood group antigen, and Btri, the trisaccharide of the B blood group antigen, were applied at a concentration of 600 µM onto silica, C-18 silica and nitrocellulose. The B antigen was used as a negative immunological control. The surface was stained with anisaldehyde to check the molecules were present to start with, and then washed by immersing in DI water for 10 minutes then drying, and immunostained to test if they had adhered to the surface. Additionally FSL-Atri and Atri were printed between 400-600 µM alongside each other on various papers and other materials and immunostained to see if the same results occurred across a variety of materials.

FSL-biotin and biotin were also printed at 100-500 µM onto various surfaces to assess the degree of attachment of different functional head groups to determine the attachment of a range of FSLs. The surfaces were stained using streptavidin conjugated to alkaline phosphatase as previously described, during which the molecules may or may not stay attached to the surface.

Results and interpretation

FSL-Atri but not Atri was detected on all the surfaces tested (Table 35 and Table 36) after washing and immunostaining indicating that the FSL construct is necessary for immobilising these functional molecules onto these surfaces. Presence of the Atri was shown before washing by anisaldehyde staining but is removed during this process. The white area around the painted molecule on silica is due to the salts of the buffer solution (Table 35). This suggests the lipid tail (or possibly but unlikely the spacer) is required for attachment of FSLs since without this part the functional head group was unable to remain attached to these surfaces.

FSL-biotin was also detected on all surfaces, but not free biotin, except on gold leaf (Table 34). Some examples are shown in Table 37. These indicate again that the FSL construct as a whole is needed for attachment and that the functional group on its own cannot attach to the surface. By printing at the same concentration as FSL-biotin, it was shown that the biotin did not adhere to the same degree as the FSL on the gold surface, although it was visible, indicating the FSL construct may not be the immobilising factor. However, when FSL-Atri and Atri were then printed and immunostained on the gold surface only the FSL-Atri was detected confirming that the FSL construct is necessary for immobilisation of these molecules on gold.

Table 35. Water washing test of FSL-Atri on different surfaces

	Not washed	Washed by soaking in DI water for 10 minutes		
Construct	FSL-Atri	FSL-Atri	FSL-Atri	FSL-Atri
Concentration µM	600	600	600	600
Surface ID	Silica	Silica	C18 silica	Nitrocellulose
Control	Atri Btri	Atri Btri	Atri Btri	Atri Btri
Stain	Anisaldehyde	EIA	EIA	EIA
Result	FSL-Atri + Atri - Btri -	FSL-Atri + Atri - Btri -	FSL-Atri + Atri - Btri -	FSL-Atri + Atri - Btri -
Example				

Table 36. Different surfaces printed with FSL-Atri, FSL-Btri and Atri antigen to show detection of the immobilised FSL but not of the Atri antigen. In some cases the code 3A0ad, 3B0ad and 3A000 for FSL-Atri, FSL-Btri and the Atri antigen respectively were printed and in other cases the words were printed.

	Paper	Polymer	Natural fibre	Metal	Glass
Construct	FSL-Atri Atri	FSL-Atri FSL-Btri Atri	FSL-Atri Atri	FSL-Atri FSL-Btri Atri	FSL-Atri Atri
Concentration µM	600	400	600	400	600
Surface ID	Impress silk	PTFE	Cotton	Silver filter	Glass fibre filter
Printed words	FSL-A Impress Silk Atri Impress Silk	3A0ad 3Boad 3A000	FSL-A Cotton FSL-A Cotton	3A0ad 3Boad 3A000	FSL-A Glass fibre Atri Glass fibre
Example		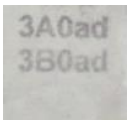			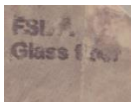

Table 37. Different surfaces printed with FSL-biotin and biotin to show detection of the FSL but not the biotin molecule (except on gold).

	Modified cellulose	Paper	Silica	Polymer	Metal
Construct	FSL-biotin Biotin	FSL-biotin Biotin	FSL-biotin Biotin	FSL-biotin Biotin	FSL-biotin Biotin
Concentration µM	500	500	500	100	100
Surface	Nitro-cellulose	G-print paper	Silica	Teflon	Gold leaf
Printed words	FSL-biotin Nitrocellulose Biotin Nitrocellulose	FSL-biotin G-Print Biotin G-Print	FSL-biotin Silica Biotin Silica	FSL-biotin Teflon Biotin Teflon	FSL BIO
Example	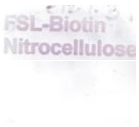	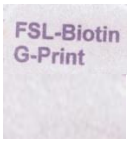	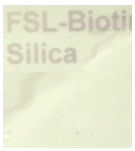	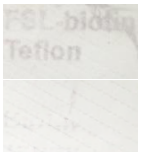	

2.3.2 Lipid tail variations

Method overview

FSL constructs with differing lipid tails were synthesized to establish any difference in the binding ability to non-biological surfaces. The sterol (FSS) and a monoacyl (FSL mono) lipid tail were constructed and tested against the standard diacyl DOPE FSL. FSL-Atri and FSS-Atri were printed onto silica, nitrocellulose and different papers and immunostained as detailed, with monoclonal anti-A. A TLC of the FSL-Atri and FSS-Atri printing solutions was carried out to check the presence and relative concentrations of the two molecules. 2 µL of each of the printing solutions and a control solution of FSL-Atri and FSS-Atri at the same concentration as

the printed construct were loaded on to a silica TLC plate (Alugram SIL G/UV, silica gel 60, Macherey-Nagel, Germany). A TLC control was run in lane C, alongside the samples. The TLC was allowed to develop for 25 minutes in Chloroform/methanol/water (60:35:8; v/v/v) chromatography solvent. It was then sprayed with anisaldehyde stain and transferred to an oven at 200°C, until the TLC control was visible.

FSL-Btri and FSL-B monoacyl were printed at the same concentration onto a variety of surfaces and immunostained with monoclonal anti-B, to investigate the binding difference of the diacyl versus the monoacyl lipid tail. A TLC of the printing solutions and control samples were again run on a TLC to confirm the identity of the construct. 2 µL of each solution were loaded onto a TLC plate (Alugram SIL G/UV, silica gel 60, Macherey-Nagel), as well as a TLC control in lane C. The TLC was allowed to develop for 25 minutes in CMH 60:35:8 solvent, sprayed with anisaldehyde and transferred to an oven at 200°C, until the control was visible.

FSL-biotin, FSS-biotin and biotin were printed at the same concentration of 100 µM onto a variety of surfaces and stained using streptavidin conjugated to alkaline phosphatase as previously described.

Results and interpretation

DOPE FSL-Atri was detected to a greater degree than sterol FSS-Atri on the surfaces tested (Table 34, Table 38a) suggesting the FSL lipid tail binds more strongly to these solid surfaces than the sterol tail. FSS-Atri was printed at a stronger concentration than FSL-Atri (1000µM compared to 600µM), so if it had adhered to the same degree it should have appeared stronger after staining. The TLC of FSL-Atri and FSS-Atri (Figure 15) shows the molecules were present in the printing solutions and that the FSS-Atri was printed at a stronger molar concentration. This indicates very low adherence capability of this molecule compared to the FSL, or possibly an altered presentation of the antigen due to the change in lipid, which may have caused a reduction in the binding capability of the antibody.

FSL-biotin and FSS-biotin were also compared and showed similar results to the FSS-Atri (Table 38a). Sterol FSS-biotin did not appear to adhere as well as the DOPE FSL on most surfaces tested (see summary Table 34), although it was detected equally well on the filter paper and on silk. Free biotin was not detected on any of the surfaces, suggesting it was washed off during the immunostaining process again showing being in the FSL format is essential for immobilisation to a solid surface.

FSL-B monoacyl did not adhere to any surfaces. Some examples are shown in Table 38b, where FSL-Btri can be clearly seen whereas nothing is visible below where the monoacyl construct was printed. The TLC (Figure 16) shows that the molecules were present at the same concentration in the printing solutions, and so FSL-B monoacyl would have been detected if it

had been present on the surface. This confirms that the type of lipid used is also an important consideration for FSL constructs as a great variation in immobilisation ability is seen between them.

Table 38a. Differences in attachment to surfaces of variations in the lipid tail of FSL constructs. + = construct was detected, - = construct wasn't detected.

	Examples of FSL constructs with cholesterol lipid tails printed onto different surfaces			
FSL-construct	FSS-Atri	FSS-biotin	FSS-biotin	FSS-biotin
Concentration µM	1000	100	100	100
Comparison construct	FSL-Atri	FSL-biotin	FSL-biotin	FSL-biotin
Concentration µM	600	100	100	100
Surface ID	Nitrocellulose	Glass fibre	Silk	Filter paper
Result	FSL-Atri + FSS-Atri + Atri -	FSL-biotin + FSS-biotin + Biotin -	FSL-biotin + FSS-biotin + Biotin -	FSL-biotin + FSS-biotin + Biotin -
Printed words	FSL-A Nitrocellulose FSS-A Nitrocellulose	FSL-biotin Glass fibre FSS-biotin Glass fibre	FSL-biotin Silk FSS-biotin Silk	FSL-biotin Filter FSS-biotin Filter
Example	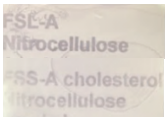		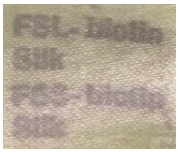	

Table 38b. Differences in attachment to surfaces of variations in the lipid tail of FSL constructs. + = construct was detected, - = construct wasn't detected.

	Examples of FSL constructs with monoacyl lipid tails printed onto different surfaces		
FSL-construct	FSL-B mono	FSL-B mono	FSL-B mono
Concentration µM	400	400	400
Comparison construct	FSL-Btri	FSL-Btri	FSL-Btri
Concentration µM	400	400	400
Surface ID	Metricel	Filter paper	Teflon
Result	FSL-Btri + FSL-B mono -	FSL-Btri + FSL-B mono -	FSL-Btri + FSL-B mono -
Printed words	FSL-B Metricel FSL-B mono Metricel	FSL-B Filter FSL-B mono Filter	FSL-B Teflon FSL-B mono Teflon
Example			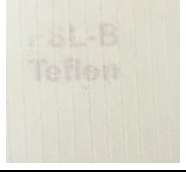

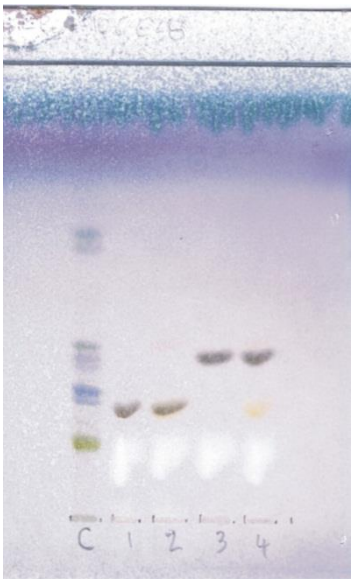

Figure 15. TLC of FSL-Atri and FSS-Atri printing solutions and fresh solutions at 1 mg/ml to check the constructs are present and to compare their relative concentration. Lane 1: FSL-Atri fresh sample, lane 2: FSL-Atri printing solution, lane 3: FSS-Atri fresh sample, lane 4: FSS-Atri printing solution.

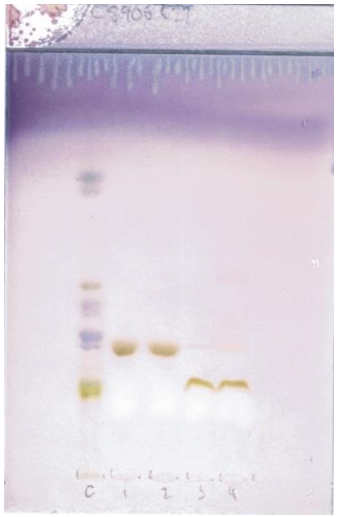

Figure 16. TLC of FSL-Btri and FSL-B monoacyl printing solutions and fresh solutions to check the constructs are present. Lane 1: FSL-Btri fresh solution, lane 2: FSL-Btri printing solution, lane 3: FSL-B monoacyl fresh solution, lane 4: FSL-B monoacyl printing solution

It is apparent from this that the lipid tail was needed to adhere the construct to the surface as free Atri or biotin were not detected on the various surfaces after washing. Changing the lipid tail from a diacyl lipid to a monoacyl or sterol lipid also either prevented or reduced the amount of FSL adhering to the surface respectively. This supports the theory that the lipid tail is the important part of the FSL construct for adhering to these surfaces. It should be noted that it

could not be established whether the effect was not due to the spacer, rather than the lipid, although this is unlikely given that two different spacers were used, with no difference in adherence observed. Also, changing the lipid tail changed the immobilisation of the construct.

2.3.3 Detergent/solvent washing tests

Testing the limitations of FSL constructs immobilised on non-biological surfaces requires investigation into the stability of the attachment and what agents might disrupt the binding. Printed surfaces were soaked in a number of solvents and detergents to examine what might cause elution of the FSL constructs. An examination into whether serum might have an effect on the attachment of FSLs to surfaces, due to lipids in the serum, was carried out against printed FSL constructs, as this may have sensitivity implications for diagnostics tests.

Method overview

Various materials were printed with FSL-Atri at 600 µM, then washed with 70% methanol by immersing them for 20 minutes, drying, then immunostaining them, to reveal if the FSLs had eluted from these surfaces. These were compared to the same printed surface washed in water for the equivalent time.

FSL-Atri was printed onto various surfaces at 600 µM. These surfaces were then soaked in a variety of detergents and solvents at various concentrations. These detergents/solvents were Tween 20, Triton X-100, methanol and ethanol, as well as PBS and water, and the surfaces were soaked for 1 hour at room temperature. The surfaces were then dried and immunostained with monoclonal anti-A as previously described.

Results and interpretation

Table 39 illustrates the difference between water washed and methanol washed FSL printed surfaces. For the surfaces washed in methanol the FSL is unable to be detected suggesting it is able to be eluted from the surface using this solvent. As the FSL can be removed with an alcohol, a popular solvent for lipids, but not water, this reinforces the theory that the lipid tail is required for attaching the construct to the surface.

Table 39. Comparison of FSL printed surfaces washed in water and washed in 70% methanol. W = washed in water, M= washed in methanol, + = construct was detected, - = construct was not detected.

	Examples of FSL constructs with different lipid tails printed onto different surfaces				
FSL construct	FSL-Atri	FSL-Atri	FSL-Atri	FSL-Atri	FSL-Atri
Concentration µM	600	300	300	300	400
Surface ID	Silica	Media gloss	Aluminium foil	Cotton	PVDF
Result	W + M -	W + M -	W + M -	W + M -	W + M -
Printed words	FSL-A Silica	FSL-A	FSL-A	FSL-A	3A0ad
Washed in water image	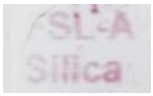	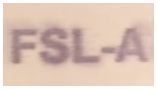			
Washed in methanol image				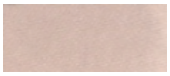	

Washing the surface with various detergents and solvents caused disruption of the immobilisation with some but not others (Table 40). Triton X-100 had a greater effect than tween 20, by removing all or greatly reducing the amount of the FSL on the surfaces, even at low concentrations. Ethanol and methanol also removed the FSLs, except at 100% where not all the FSL was removed. This was the case especially with ethanol on the paper and cotton surfaces, although it did remove the FSL on the plastic. In fact all the solutions tested removed the FSLs from the plastic surface, suggesting a possibly lower attachment to the plastic than the paper. Overall, detergent and solvent mixes can remove FSL molecules from surfaces once they have immobilised onto them.

Table 40. Elution test of printed FSL-Atri on a variety of surfaces. . ++ = strong positive detection, + = weak positive detection, - = no visible detection.

Wash test solution	%	Surface printed with FSL-Atri			
		Media gloss paper	Printer paper	Cotton	Polyester film
Tween 20	0.05	++	+	++	-
Tween 20	0.25	++	+	++	-
Tween 20	0.5	++	+	++	-
Tween 20	1	++	+	++	-
Tween 20	2.5	++	+	++	-
Tween 20	5	+	-	++	-
Triton X-100	0.05	-	-	+	-
Triton X-100	0.25	-	-	+	-
Triton X-100	0.5	-	-	+	-
Triton X-100	1	-	-	+	-
Triton X-100	2.5	-	-	+	-
Triton X-100	5	-	-	+	-
Ethanol	50	-	-	-	-
Ethanol	70	-	-	-	-
Ethanol	100	+	+	+	-
Methanol	50	+	-	+	-
Methanol	70	-	-	-	-
Methanol	100	-	+	-	-
PBS	-	++	++	++	++
Water	-	++	++	++	++

2.3.4 Detergents/solvents in printing solution

This investigation involved adding detergents and solvents into the printing solution along with the FSL constructs to see if this might influence the attachment of the FSL constructs to non-biological surfaces. Triton X-100 and methanol were chosen as these had the greatest effect on disturbing the attachment post printing.

Method overview

A solution of FSL-Atri at 120µM was prepared containing Triton X-100 at 0.05%, 0.2% and 0.5% and methanol at 70%. A solution at the same FSL concentration in PBS was also prepared as a control. These solutions were printed onto media gloss paper and polyester film to compare 2 different surfaces. It should be noted that triton X-100 solution at 0.5% was unable to be printed due to the large decrease in surface tension, causing the solution to run straight out of the print head. The surfaces were immunostained as standard using monoclonal anti-A.

Results and interpretation

Whilst triton X-100 was able to totally remove FSL constructs post printing at concentrations as low as 0.05%, there was no effect on the FSL attachment when present in the print solution (Table 41 and Table 42). The same cannot be said for methanol which caused much fewer FSL molecules to attach to the surface. Triton X-100 may be able to disrupt and absorb the FSL molecule back into solution but when they are dried together after printing the FSL is capable of fully attaching to the surface. The methanol however did, to some extent prevent full immobilisation of these molecules or possibly caused less solution to be printed due to the surface tension of the liquid.

Table 41. Effects on FSL immobilisation of detergent and solvent added to printing solution with FSL-Atri. . ++ = strong positive detection, + = weak positive detection, - = no visible detection.

Printing solution additive	%	Surface printed with FSL-Atri	
		Media gloss paper	Polyester film
Triton X-100	0.05	++	++
Triton X-100	0.2	++	++
Methanol	70	+	+
PBS (control)	-	++	++

Table 42. Examples of FSL-Atri printed in solution containing detergent or solvent on a paper and polymer surface

Printing solution additive	%	Surface printed with FSL-Atri	
		Media gloss paper	Polyester film
Triton X-100	0.05	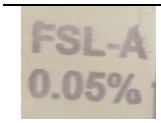	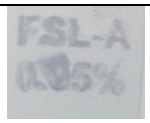
Triton X-100	0.2	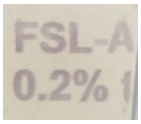	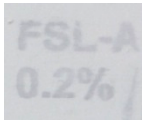
Methanol	70	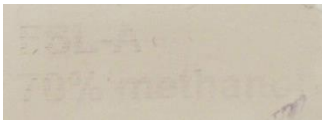	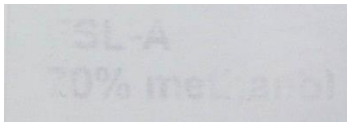
PBS (control)	-	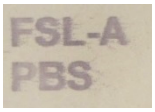	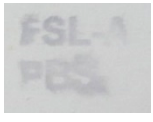

2.3.5 Serum washing tests

Having investigated the attachment of FSLs after being soaked in water, PBS, Tween 20, Triton X-100, methanol and ethanol, a similar investigation was carried out after being soaked in serum. If serum is able to disrupt the immobilisation of FSLs on solid surfaces this may have

implications for clinical applications. The lipids in the serum may affect the attachment of the FSL constructs to surfaces due to an interaction with the lipid tail. Kodecytes in circulation have been shown to lose FSL constructs from the cell membranes at a rate of 20% per day (Oliver et al., 2011b).

Method overview

Media gloss paper and nitrocellulose printed with FSL-Atri at 300 µM and FSL-biotin at 100 µM were soaked in Group AB serum, PBS and 2% BSA for 0.5, 1, 2, 4, 18 and 30 hours at room temperature. The surfaces in AB serum were then washed 3 times in PBS to remove any remaining serum and then all surfaces were immunostained with monoclonal anti-A or streptavidin- alkaline phosphatase as appropriate. 2% BSA was used as this is the blocking agent used during the EIA.

Results and interpretation

It can be seen from Table 43 that the serum had no effect on the immobilisation of FSL-biotin over these times periods, however some of the FSL-Atri was seen to be eluted after 18 hours on paper and 30 hours on nitrocellulose. 2% BSA and PBS solutions did not cause any elution of the FSL molecules, therefore it does not seem that proteins cause removal of the FSLs, but it is likely the lipids in the serum are interacting with the lipids of the FSL and eluting them into the serum, as has been seen with blood cells (Oliver et al., 2011b). The difference between the FSL-Atri and FSL-biotin is probably due to the staining sensitivity and not an actual difference in their binding, as the biotin staining has greater sensitivity.

Table 43. Serum wash test. FSL-Atri and FSL-biotin were soaked in AB serum, PBS and 2% BSA for different time periods to examine any elution from the surface. . ++ = strong positive detection, + = weak positive detection, - = no visible detection.

Time (hours)	FSL-Atri						FSL-biotin					
	Media gloss paper			Nitrocellulose			Media gloss paper			Nitrocellulose		
	Serum	PBS	BSA	Serum	PBS	BSA	Serum	PBS	BSA	Serum	PBS	BSA
0.5	++	++	++	++	++	++	++	++	++	++	++	++
1	++	++	++	++	++	++	++	++	++	++	++	++
2	++	++	++	++	++	++	++	++	++	++	++	++
4	++	++	++	++	++	++	++	++	++	++	++	++
18	+	++	++	++	++	++	++	++	++	++	++	++
30	+	++	++	+	++	++	++	++	++	++	++	++

2.3.6 Drying versus not drying tests

When the FSLs were painted or printed onto surfaces they were then dried before further washing and staining was carried out. This drying may have an effect on the immobilisation interactions with the surface. However, when working with microbeads these surfaces remained

in solution at all times as some microbeads cannot be dried. These microbeads were still able to immobilise the FSLs with strong affinity. It was therefore important to establish if there is a difference in FSL attachment, due to the surfaces being dried or not, to give insight into the binding mechanism. The surfaces used were polycarbonate microbeads, a solid glass cover slip and aluminium foil, as these surfaces will not absorb the FSL print solution and so drying can be prohibited.

Method overview

Microbeads: A small spatula amount of polycarbonate microbeads (Nanomi, Netherlands), 20 µm in diameter, were added to a 40 µL solution of FSL-biotin at 400 µM and 0.025 µM and mixed well. This very low concentration was used in case of saturation of the surface with FSL at the high concentration, which may not reveal differences between the wet and dried surfaces. Each tube of beads was then separated into two. One tube of each FSL concentration was kept at room temperature with the lid closed to keep the beads in solution. The other tube of each concentration was placed in a heat block at 60°C with the lid open to dry. They were all left for 90 minutes, which was the time taken to dry the beads. All beads were then washed 3 times in PBS by centrifugation and the supernatant was removed. A solution of avidin-alexa fluor®488 (Invitrogen) was prepared at 0.1 mg/mL and 40 µL was added to each tube of beads. They were incubated for 30 minutes and then washed again 2 times in PBS. The beads were suspended in 40 µL PBS and examined on the fluorescent microscope at 488nm wavelength. For a control, beads with no FSL contact were incubated with the avidin-alexa fluor®488 solution using the same protocol.

Glass cover slip and aluminium foil: A solution of FSL-biotin at 50 µM was prepared and painted onto two pieces of each of a glass cover slip (Menzel Gläser, Germany) and aluminium foil (Clorox, New Zealand) with the letters "FSL". One piece of each material was placed on a heat block at 60°C to dry the FSL solution whilst the other pieces were left at room temperature and maintained wet. The drying was completed in 2 minutes. At this point, the solution on the other materials was washed away before drying by immersing the surface into a beaker of PBS. All surfaces were then immediately stained with streptavidin- alkaline phosphatase as described (2.1.1).

Results and interpretation

The results on the microbeads and on the flat surfaces show no difference in FSL-biotin detection between drying and not drying the FSL (Table 44 and Table 45). Even at very low concentrations of FSL no difference was detectable. Some smudging was seen on the flat surfaces, especially the glass surface on the non-dried samples, which is probably caused when the FSL solution is washed off and runs across the surface briefly. It is interesting to note that on glass and aluminium the FSL was only in contact with the surface for 2 minutes before being

washed off and the amount detected was the same as when the same volume has been dried onto the surface. This indicates that only a very short contact time is necessary for FSL immobilisation.

Table 44. Dried versus not dried FSL as attachment method on microbeads. FSLs labelled with avidin-alex fluor® 488 and imgaed with fluorescent microscopy. These images are all taken at the same exposure of 300 ms.

Attachment method	FSL-biotin concentration	
	400 µM	0.025µM
Not dried	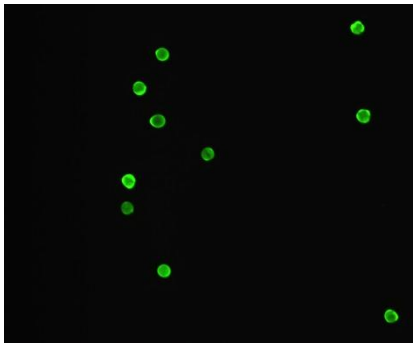	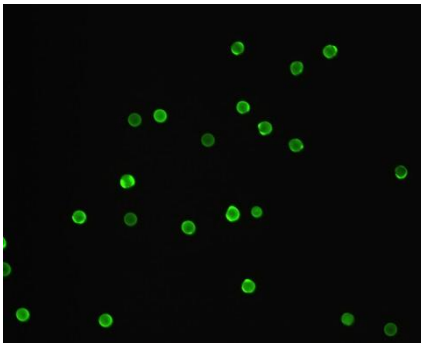
Dried	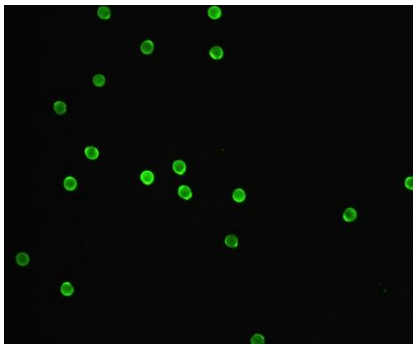	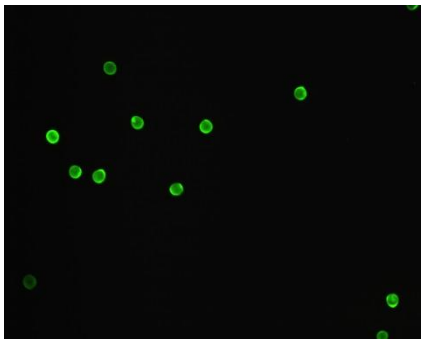

Table 45. Dried versus not dried FSL as attachment method on glass cover slip and aluminium foil. FSL-biotin was painted on the surface, then washed off after 2 minutes contact and then stained with streptavidin conjugated to alkaline phosphatase.

Attachment method	Surface	
	Glass cover slip	Aluminium foil
Not dried		
Dried	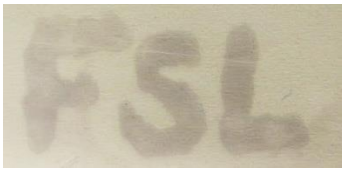	

2.3.7 Attachment time

The drying and non-drying tests revealed that the time it takes FSL constructs to attach to a surface was as short as 2 minutes and therefore the investigation into the actual time it takes FSL constructs to adhere to a solid surface was carried out.

Method overview

Media gloss paper (Spicers, New Zealand) and glass coverslips (Menzel Gläser, Germany) were used as the solid surfaces. FSL-biotin and FSL-Atri were prepared in PBS at 50 µM and 300 µM respectively. 2 µL was pipetted onto the surfaces at times intervals of 600, 300, 120, 60, 30, 20, 10 and 5 seconds. The surface was then dropped into a beaker of water to wash away the FSL solution and then immediately immunostained with monoclonal anti-A or streptavidin-alkaline phosphatase as appropriate.

Results and interpretation

The results showed that even after 5 seconds of contact with the surface, the FSL construct is able to attach and remain on the surface during washing and staining procedures (Table 46). There was no difference in intensity of the staining between the different time periods of FSL contact, suggesting the attachment is relatively instant and that leaving the FSL in contact with the surface does not cause an increase in the amount of FSL attachment that can be detected by these staining methods.

Table 46. FSL solution dropped onto a surface for different amounts of time to assess time needed for FSL attachment to solid surfaces. After washing, the surfaces were immunostained to reveal the degree of attachment of the FSL construct.

Surface and FSL construct	Amount of time FSL solution in contact with surface (seconds)							
	600	300	120	60	30	20	10	5
Paper FSL-Atri								
Glass FSL-biotin								

2.3.8 Stability tests

The stability of the FSL molecule once printed is also an important consideration as this will help with understanding the strength of the attachment, and also the general stability of the molecules. It will also influence any future applications as storage is a crucial factor. The principle of this assay was not to determine the immediate stability after inkjet printing, as was done previously (see section 2.1.4), but to determine any loss of construct or parts of the construct from the surface or any denaturing of the construct over time. If the lipid became detached from the head group it would be expected that the head group would then be lost during staining.

Method overview

Firstly, accelerated stability tests were carried out. FSL-Atri and FSL-biotin printed onto media gloss paper at 300 µM and 100 µM respectively were incubated in an oven at 80°C for 2, 4 and 12 hours. These surfaces were then immunostained along with a surface, printed at the same time but not incubated at 80°C, as a comparison control.

Secondly, two media gloss paper surfaces were printed with 10 different blood group FSL consisting of different types of FSL-A and FSL-B constructs in an 8 well format (see later Figure 19). One was immunostained immediately with 8 different monoclonal antibodies, a different one in each well; the other was stored at room temperature, in a box protected from light, for 8 months. After storage it was immunostained in exactly the same way as the first plate using the same antibodies.

Thirdly, FSL-Atri and FSL-biotin printed onto media gloss paper at 300 µM and 100 µM respectively were soaked in PBS or water overnight (~18 hours), then dried and immunostained as standard. This was to compare any difference in stability in water compared to a saline solution.

Results and interpretation

FSL-Atri and FSL-biotin attached to a paper surface showed no degradation or loss from the surface following 12 hours at 80°C in the accelerated stability assay (Table 47). The results showed the same level of detection of these two constructs after this high temperature incubation compared to the control surfaces. The stability of various FSL-A and FSL-B constructs was also shown in the 8 months storage test (Table 48). This example is a reaction well stained using a monoclonal anti-A,B reagent (Epiclone anti-A,B, CSL, Australia). There was no difference seen in sensitivity between the constructs stained immediately after printing compared to after 8 months storage at room temperature. FSL-Atri and FSL-biotin attached to a paper surface and soaked in water and PBS showed no difference in sensitivity suggesting the constructs are able to remain stable in water as well as saline solutions (Table 49). Together these results demonstrate the high stability of FSL constructs after they have been adhered to a solid surface.

Table 47. Accelerated stability test of FSL-biotin and FSL-Atri attached to a paper surface and incubated at 80°C for 12 hours, then immunostained and compared to a control surface.

Time at 80°C	FSL construct	
	FSL-Atri	FSL-biotin
0 hours		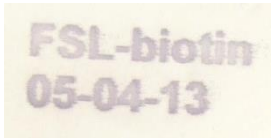
12 hours	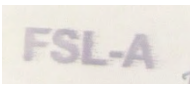	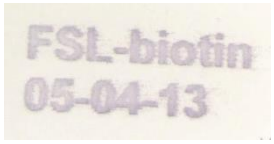

Table 48. Example of one well of stability test of printed FSL constructs immunostained immediately after printing and after 8 months of storage at room temperature.

		Storage time at room temperature after printing	
FSL construct	Printed code	0 months	8 months
FSL-Atri	3A0a		
FSL-Atetra type 1	4A1c		
FSL-Atetra type 2	4A2c		
FSL-Atetra type 3	4A3c		
FSL-Atetra type 4	4A4c		
FSL-Btri	3B0a		
FSL-Aquired Btri	3BQa		
FSL-Btetra type 1	4B1c		
FSL-Btetra type 2	4B2c		
FSL-Lewis a	3L1a		

Table 49. Water stability test. Printed FSL-Atri and FSL-biotin soaked in water and PBS for 18 hours to assess stability in those solutions.

Soaking solution	FSL construct	
	FSL-Atri	FSL-biotin
Water, 18 hours		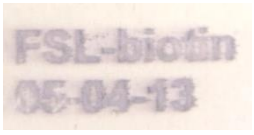
PBS, 18 hours	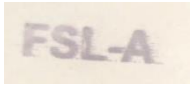	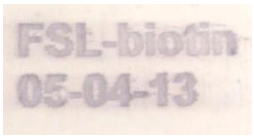

2.3.9 Resolution tests

Inkjet printer inks are designed to offer the optimum print quality in terms of resolution, clarity and colour on the paper. When printing biological inks as opposed to standard inks for inkjet printers, the quality is likely to be reduced due to different properties of the printing solution, and there may be scattering of the ink when it hits the paper. There may also be wicking of the solution within the membrane before it dries, causing a loss of resolution.

Method overview

A checkerboard pattern with increasing numbers of squares in the same area was used to observe the printing quality of FSL solutions compared to the printer's ink, to judge the clarity of the printing.

A 20×20 mm square pattern was used containing 8×8, 16×16, 24×24, 32×32 and 40×40 chequered squares in black and white. This was printed with FSL-Atri at 600 µM in a solution containing a blue dye onto media gloss paper, and then immunostained with monoclonal anti-A as previously described (2.1.1). The exact same pattern was printed onto the same type of paper in a standard inkjet black ink for comparison.

Results and interpretation

No obvious difference between the resolution of the ink, the blue dye solution and the FSL-Atri after immunostaining was seen (Table 50). Even down to 40×40 squares the chequered squares are distinguishable to a similar level in all 3 images. There is no running of the blue printed solution and there is no wicking of the FSL-Atri along the paper. At 40×40 in the immunostained image the squares are still well defined with some loss of sharpness along the edges (close up image in Table 50). The dots in the white square areas show some printing errors which are consistent across the whole test area, most likely due to the difference in the surface tension and viscosity of the printing solution compared to standard ink. The resolution of the FSL stained areas below 1 mm was good.

Table 50. Resolution tests of printed FSL-Atri. The patterns were printed in standard black ink and the FSL and dye solution. The dye is washed away before immunostaining leaving a blank surface. These images are the actual size of the printed area, 20×20 mm. A magnified imaged in shown at the bottom of a part of the 40×40 immunostained image.

Number of squares	Image of checkered square (20×20 mm)			
	Standard black ink	Blue dye + FSL-Atri solution	Blank surface after washing	Immunostained FSL-Atri
8×8	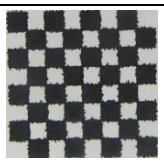	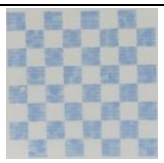		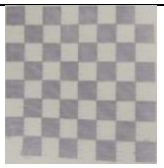
16×16				
24×24				
32×32				
40×40			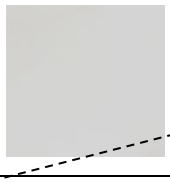	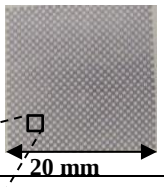

A ×200 image of a part of the 40×40 square of immunostained FSL-Atri

2.4 Inkjet printed FSL constructs for bioassays

The adaptation of inkjet printing technology allows repeatable, high-throughput and automated production of microarrays, microfluidic devices and biosensors allowing increased progress in the field of biological sciences. This section addresses the question of whether printed FSLs can be in used in bioassays, predominantly immunoassays, as diagnostic and research tools. Having shown that FSL constructs can be printed and detected on a wide variety of materials it was important to optimise the protocol to consider a proof of concept bioassay.

2.4.1 Different formats

Inkjet printing offers flexibility, precision and reliability for delivering biomolecules onto solid surfaces. A major advantage is the ability to create and alter patterns, images and words with ease, compared to other fabrication techniques.

The format of the bioassay is an important consideration. Creating reaction wells, for example, allows multiple samples to be tested side by side and utilising the multiple cartridges of the printer enables several molecules to be printed at the same time, into the same well, increasing the diagnostic or testing potential of small printed areas.

A number of different designs and methods were looked at for creating a bioassay/diagnostic test. A 2mm thick acrylic plate was laser cut to produce holes in the plastic which when adhered to a printed surface created many reaction wells on a single plate. The laser cutting technique allowed fast and accurate positioning of the wells which were deep enough to contain the reagents administered to them without contamination between wells. A 32 well and 8 well plate format are shown in Figure 17. These acrylic plates were glued to the FSL modified surfaces after printing to allow immunostaining in the wells. The 32 and 8 well formats are designed to be the same size as half a 96-well microplate, with the wells corresponding to well positions of a microplate. Control wells can also be incorporated, and engraving on the plastic allows easy numbering of wells for identification. Plates with different well sizes were investigated to allow larger number of molecules to be printed into each well.

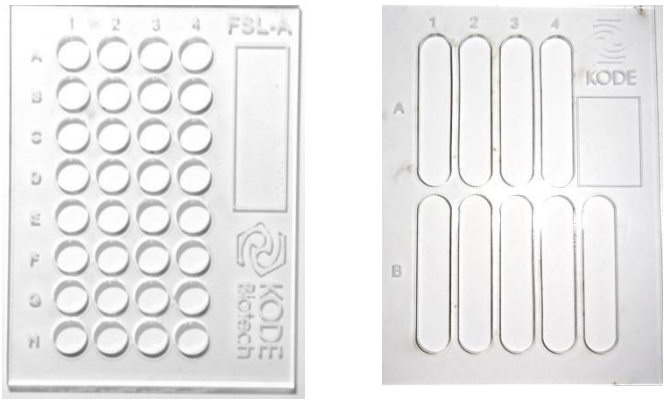

a b

Figure 17. 2mm thick acrylic plate with laser cut holes to make reaction wells. The acrylic is also engraved for labelling of the well coordinates. a) a 32 well plate and b) an 8 well plate.

The ability to print words and meaningful patterns or machine readable barcodes is a major advantage of inkjet printing. Examples of different formats and printing patterns are shown in Figure 18 and show the scope for inkjet printing as a tool for producing bioassays. Gradient ladders can also be printed, by printing in shades of grey, to dispense different amounts of FSL construct for a semi- quantitative assay (Figure 18d). Using the well coordinate as the printed pattern in the well reduces the ambiguity of the interpretation of the results, since there would be no doubt which well was positive. This example also demonstrates the simplicity of the assay, as positive results can be read, whereas negative results are blank. Being able to write the name of a disease, for example, would allow for direct reading of the result, hence easy deduction of the answer. Another advantage of printing words or patterns in wells is that each well contains its own negative control, the unprinted area, which can be compared to the printed area rather than comparing to a separate well, making the whole test more controlled. Alternatively, a control molecule printed in words such as “invalid” could be printed in a control well.

To demonstrate the flexibility of inkjet printing, different patterns were printed in FSLs and immunostained. These images show good resolution of complex designs, including a 2D barcode which was able to be read with a handheld barcode scanner (Figure 18e).

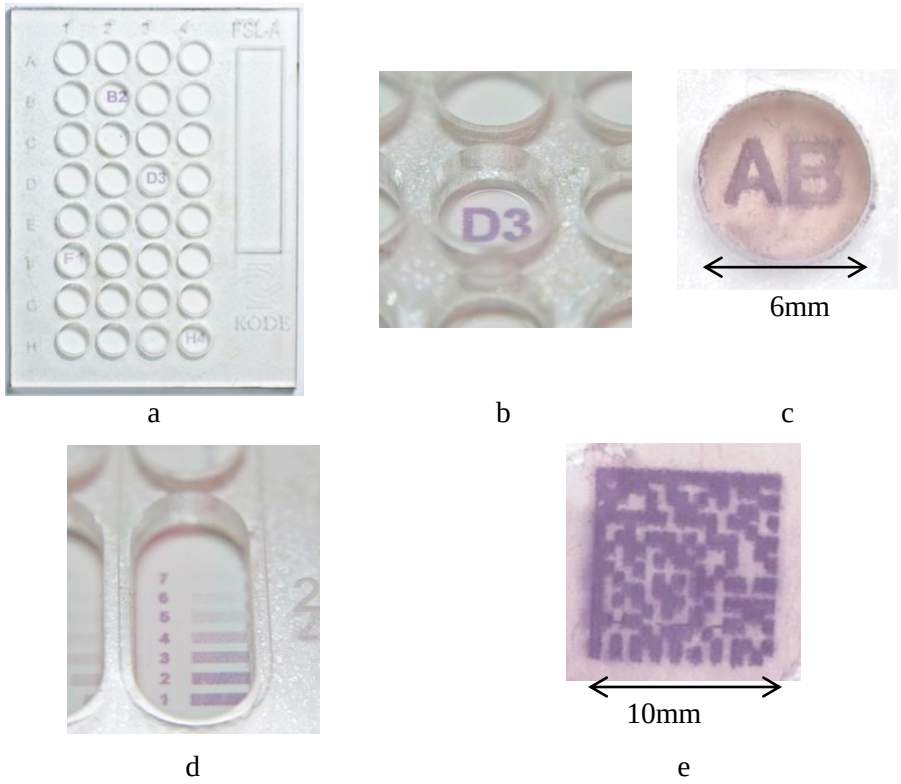

Figure 18. Examples of different printing patterns. a) and b) well coordinates printed with FSL, only positive i.e. samples containing antibody make the printed FSL visible, c) Two FSLs printed in the same well and immunostained, d) gradient ladders printed in a well achieved by reducing the percentage of colour printed, e) a 2D barcode printed in FSL constructs.

Optimal surface

Using monoclonal reagents to immunostain printed or painted ABO FSLs is a useful method to establish FSL attachment to surfaces and to assess sensitivity. However to test for non-specific binding and sensitivity, printed FSLs were tested against polyclonal sera to assess the optimal surface for FSL immobilisation for bioassays.

Method overview

The surfaces that performed the best against monoclonal reagents with carbohydrate FSLs and streptavidin with FSL-biotin, were further assessed for background staining and sensitivity by printing FSL-Atri and FSL-Btri and immunostaining them with human Group O serum containing low levels of anti-A,B. The surfaces were also immunostained with monoclonal anti-A,B (Epiclone, CSL Australia), containing high levels of anti-A and B to compare against. The surfaces tested included various papers, PTFE (Teflon), PVDF (polyvinylidene fluoride), PE (polyester), RC (regenerated cellulose), MCE (mixed cellulose esters) and nitrocellulose.

Results and interpretation

The results indicate that the paper surfaces offer the best sensitivity with the least background staining compared to the polymers and some of the cellulose membranes (Table 51). Media gloss, impress silk and G-print matt have similar levels of non-specific binding. Media gloss

has slightly greater sensitivity compared to the other papers. Further testing of these surfaces confirmed media gloss paper as the optimal surface, from those tested in this research, to use for a validation test to examine the use of inkjet printed FSL constructs for binding assays compared to a standard method.

Table 51. Assessing different surfaces printed with FSL-Atri and FSL-Btri with polyclonal serum to test for background staining and sensitivity. An 'A' represents FSL-Atri and a 'B' represents FSL-Btri. In some cases only FSL-Atri is shown.

Surface ID	Primary antibody used in immunostaining		
	Printed words	Monoclonal anti-A and B	Polyclonal anti-A,B
Printer paper	FSL-A Printer Paper	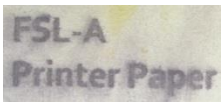	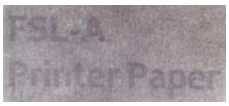
Media gloss paper	MG A MG B		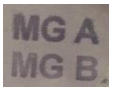
9 Lives paper	9L A 9L B		
Impress silk paper	FSL-A Impress Silk	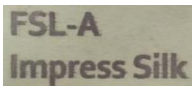	
G print matt paper	FSL-A G-print		
Black velvet Paper	FSL-A Black velvet	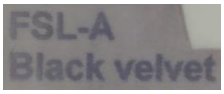	
Saxton paper	FSL-A Saxton		
PVDF 0.45µm	PVDF A PVDF B		
PTFE 1µm	PTFE A PTFE B	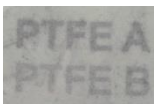	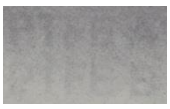
RC	RC A RC B		
PE	PE A PE B		
MCE	MCE A MCE B		
Nitrocellulose	FSL-A Nitrocellulose	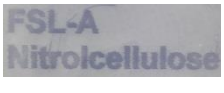	

2.4.2 Mapping monoclonal reagents with inkjet printed FSL constructs

To demonstrate a biological application for inkjet printing FSL constructs and to show some validation of the inkjet printing method a bioassay was designed to map a series of monoclonal reagents against specific blood group antigens. This mapping was also carried out using kodecytes and serology as a way of comparing the printed FSL results to a standard method. Monoclonal antibodies are relied upon to correctly detect patient blood types and are capable of broadly reacting with all antigenic variations. By using kodecytes and printed FSL constructs the reactivity of a wide range of commercial ABO reagents were assessed against variations in ABO antigens and used to reveal recognition patterns of these antibodies.

The printed FSL enzyme immunoassay (pFSL-EIA) was composed of a range of 10 blood group antigen FSLs of different types of A and B antigen, as well as the Lewis antigen as a negative control. FSLs were printed in the same reaction well to remove variations between wells and plates. A solution of PBS was also printed as a negative control to show no contamination from other cartridges and to indicate thorough cleaning of the printhead.

Method overview

FSL constructs: the FSL constructs printed and used to make kodecytes were (as in Figure 19)

- trisaccharide blood group A, B, Le^a and acquired B (deacetylated blood group A) FSL constructs with an adipate linker.
- tetrasaccharide blood group A type 1, A type 2, A type 3, A type 4, B type 1 and B type 2 with a carboxymethylglycine (CMG) linker.

Preparation of printed plates: the 10 FSL constructs were prepared at 600 µM in PBS. 0.025% bromophenol blue was added to the print solutions to act as a visualisation dye, which is lost during washing. A code for each construct was printed onto media gloss paper (Spicers, NZ) in a 8 well +control well format, which was cut to size, heat sealed with laser cut laminating plastic on both sides leaving the reaction areas exposed, and adhered to a laser cut 2mm thick acrylic plate to create wells 7 x 34 mm (Figure 19).

Function - Spacer - Lipid	Abbrev.	Code
GalNAcα1,3(Fucα1,2)Galβ1-ad-Lipid	A(tri)	3A0a
GalNAcα1,3(Fucα1,2)Galβ1,3GlcNAcβ1-CMG-Lipid	A type 1	4A1c
GalNAcα1,3(Fucα1,2)Galβ1,4GlcNAcβ1-CMG-Lipid	A type 2	4A2c
GalNAcα1,3(Fucα1,2)Galβ1,3GalNAcα1-CMG-Lipid	A type 3	4A3c
GalNAcα1,3(Fucα1,2)Galβ1,3GalNAcβ1-CMG-Lipid	A type 4	4A4c
Galα1,3(Fucα1,2)Galβ1-ad-Lipid	B(tri)	3B0a
GalNα1,3(Fucα1,2)Galβ1-ad-Lipid	Acquired B	3Q0a
Galα1,3(Fucα1,2)Galβ1,3GlcNAcβ1-CMG-Lipid	B type 1	4B1c
Galα1,3(Fucα1,2)Galβ1,4GlcNAcβ1-CMG-Lipid	B type 2	4B2c
Galβ1,3(Fucα1,4)GlcNAcβ1-ad-Lipid	Lewis a	3L1a
Phosphate Buffered Saline	PBS	PBS

ad = adipated based spacer (1.9 nm)
CMG = carboxymethylglycine based spacer (7.2 nm)
Lipid = dioleoyl phosphatidylethanolamine (DOPE)

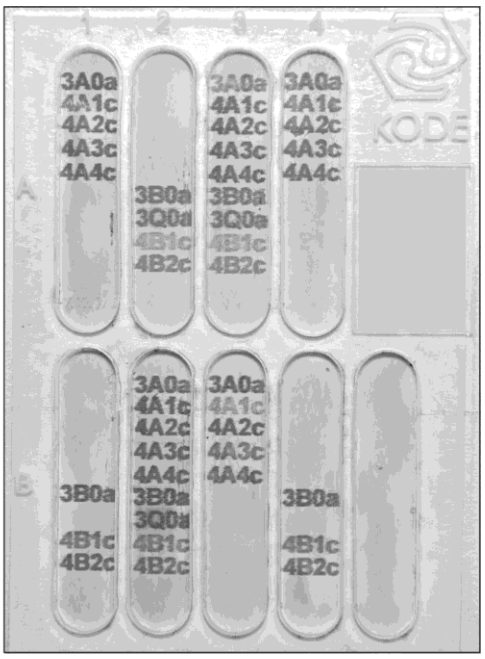

Figure 19. An example of a printed FSL enzyme immunoassay (pFSL-EIA). Ten different FSL constructs printed as unique codes onto paper with an acrylic plate adhered to produce separate reaction wells. The areas in the wells are immunostained with monoclonal or polyclonal reagents. Printed FSL codes only become visible if they have reacted with the primary antibody. Reagents in this plate are A1= A1, A2= A2, A3=A3, A4=A4, B1=B1, B2=B2, B3=B3, B4=B4, B5= reagent blank.

Preparation of kodecytes: the 10 FSL constructs were prepared at 50 µM, as well as acquired B at 3 mM. A 500 µL volume of FSLs was mixed with 500 µL of washed packed group O red blood cells and incubated for 2 hours at 37°C, then washed PBS by centrifugation for 1 minute and stored in Celpresol as a 3% suspension at 4°C.

pFSL-EIA: Printed plates were blocked with 2% BSA in PBS (pH7.2) for 1 hour. The 2% BSA in PBS was decanted and 150 µL of monoclonal antibody diluted 1 in 5 in 2% BSA in PBS was added to each well and incubated for 30 minutes at room temperature. 2% BSA in PBS was added to the control well. The plates were washed 6 times in PBS, by immersing the whole plate for 20 seconds using fresh PBS for each wash , then 150 µL of anti-mouse Ig conjugated to alkaline phosphatase diluted 1 in 1000 in 2% BSA in PBS was added to all wells and incubated for 30 minutes. For the human polyclonal reagents anti-human Ig conjugate was used. The primary reagents used are detailed in Table 52. After being washed 6 times in PBS 150 µL of NBT/BCIP substrate diluted 1 in 50 in a Tris substrate buffer was added to each well and incubated for 4 minutes. The reaction was stopped by washing with water (method detailed in 2.1.1).

Serology: 40 µL of kodecyte suspension was added to 40 µL of monoclonal or polyclonal reagent (Table 52) and left to incubate for 5 minutes at room temperature. The samples were centrifuged for 10 seconds on high in an immufuge centrifuge and the degree of agglutination assessed with a microscope eyepiece.

Table 52. Summary table of serologic ABO reagents used to compared printed FSLs against kodecytes.

	Reagent	Manufacturer	Clone(s)	Expiry	Batch/Lot
1A	Epiclone anti-A	CSL, Melbourne, Australia	4E7 & 8F2	Jan-12	26132801
2A	Anti-A	Immucor, Norcross, USA	Birma-1	May-09	AM109-2
3A	Anti-A (AB01)	Diagast, Loos, France	9113D10	Jun-07	403000
4A	Anti-A	Biotec, Kentford, UK	11H5	Mar-11	MA1881
5A	Spanclone Anti-A	Span Diagnostics, Surat, India	Spanclone	Dec-08	9263
6A	Anti-A	Millipore, Livingston, UK	Birma-1 (NI)	Aug-10	NIA0801B
7A	ALBAclone Anti-A	Alba Bioscience, Edinburgh, UK	LA2	Mar-09	V063311
8A	BioClone Anti-A	Ortho Clinical Diagnostics, High Wycombe, UK	MH04, 3D3	May-07	BAA557AX
9A	MolterClone Anti-A	Ortho Clinical Diagnostics, High Wycombe, UK	Birma-1	Nov-09	MC148
10A	Anti-A	Lateral Grifols, Melbourne, Australia	Birma-1	Mar-12	10090.14.6
11A	Anti-A	Millipore, Livingston, UK	Birma-1	Jul-13	JHF1108
12A	Anti-A	Lorne Laboratories, Reading, UK	9113D10	Jun-11	60083C
13A	DiaClon Anti-A	DiaMed, Cressier, Switzerland	LM297/LA2	Apr-12	10291.14.20
14A	Novaclone Anti-A	Dominion, Dartmouth, Canada	F98,7C6	Dec-11	102036
15A	Anti-A Series 1	Immucor, Norcross, USA	Birma-1	Mar-13	101811
16A	Anti-A Gammaclone	Immucor, Norcross, USA	Birma-1	Aug-12	104014.2
17A	R&D	Immucor, Norcross, USA	GAMA 120	N/A	A(120)020211P
18A	Series 2, R&D	Immucor, Norcross, USA	UNKNOWN	N/A	103004
19A	Anti-A (human)	Biological Laboratories, Auckland, NZ	Polyclonal	Oct-87	8636
20A	ALBAclone Anti-A	Diagnostics Scotland, Edinburgh, UK	Birma-1	Dec-04	Z0010770
1B	Epiclone Anti-B	CSL, Melbourne, Australia	B9	Aug-12	26633301
2B	Anti-B	Immucor, Norcross, USA	GAMA110	Jun-09	BM163-2
3B	Anti-B (AB02)	Diagast, Loos, France	9621A8	May-07	403000
4B	Anti-B	Biotec, Kentford, UK	6F9	Feb-11	unknown
5B	Spanclone Anti-B	Span Diagnostics, Surat, India	Spanclone	Feb-09	9474
6B	Anti-B	Millipore, Livingston, UK	LB2 (NJ)	Sep-10	NJC0801A
7B	ALBAclone Anti-B	Alba Bioscience, Edinburgh, UK	LB2	Jul-09	V066304
8B	Novaclone Anti-B	Dominion, Dartmouth, Canada	F84 3D6 & F97 2D6	Dec-08	NB09212
9B	BioClone Anti-B	Ortho Clinical Diagnostics, High Wycombe, UK	NB10.5A5, NG10.3B1 & NB1.19	Jul-07	BBB751AX
10B	MolterClone	Ortho Clinical Diagnostics, High Wycombe, UK	LB2	Mar-09	MC249
11B	Anti-B	Lateral Grifols, Melbourne, Australia	LB2	Apr-12	10091.14.7
12B	Anti-B	Millipore, Livingston, UK	LB2	Apr-13	JMD1105
13B	Anti-B	Millipore, Livingston, UK	ES-4	May-13	JED1108
14B	Anti-B	Lorne Laboratories, Reading, UK	9621A8	Jul-11	610111A
15B	DiaClon Anti-B	Bio-Rad Laboratories, DiaMed, Cressier, Switzerland	LM306/686(LB2)	Apr-12	10301.15.20
16B	Novaclone Anti-B	Dominion, Dartmouth, Canada	F84,F97	Dec-12	204043
17B	Anti-B Series 3	Immucor, Norcross, USA	LB2	Apr-13	203391
18B	Anti-B Gammaclone	Immucor, Norcross, USA	GAMA 110	Dec-12	205022-2
19B	R&D use	Immucor, Norcross, USA	GAMA 110	N/A	B(110)111003P
20B	ALBAclone Anti-B	Diagnostics Scotland, Edinburgh, UK	LB2	Jan-05	Z0100670
1AB	Epiclone Anti-A/B	CSL, Melbourne, Australia	4E7, B9 & ES15	Nov-11	26727501
2AB	Anti-A,B	Immucor, Norcross, USA	Birma-1, ES4 & ES15	Feb-09	ABM72-3
3AB	Anti-AB (AB03)	Diagast, Loos, France	9113D10 & 152D12	Jul-07	404000
4AB	ALBAclone Anti-AB	Alba Bioscience, Edinburgh, UK	LA2, LB2, ES15	Aug-09	V067330
5AB	Novaclone Anti-AB	Dominion, Dartmouth, Canada	F98 7C6, F84 3D6, F97 2D6 & F125 7B6	Jul-09	NAB05603
6AB	BioClone Anti-AB	Ortho Clinical Diagnostics, High Wycombe, UK	MH04, 3D3, NB10.4A5 & NB1.19	Oct-09	ABB688AX
7AB	MolterClone Anti-AB	Ortho Clinical Diagnostics, High Wycombe, UK	ES4 & ES15	Mar-10	MC337
8AB	Anti-A(B)	Millipore, Livingston, UK	ES15	Aug-13	VKH1102
9AB	Anti-A,B (human)	Biological Laboratories, Auckland, NZ	Polyclonal	Jan-88	8667
10AB	ALBAclone Anti-A,B	Diagnostics Scotland, Edinburgh, UK	LA2,LB2,ES15	Sep-04	Z0210450

Results and interpretation

The results were clustered in reaction patterns to allow comparison between the printed FSL assay and the kodecyte serology assay (Figure 20). The serological test is the standard method for identifying blood types where monoclonal reagents are reacted against patient blood cells for blood grouping. These results show excellent correlation between the two methods presented here, and demonstrate the potential use of printed FSL constructs in a bioassay. Numerous reaction patterns of the monoclonal and polyclonal reagents were discovered, identifying some issues surrounding the specificity of these antibodies. However, the printed FSLs were able to detect the subtle differences between them.

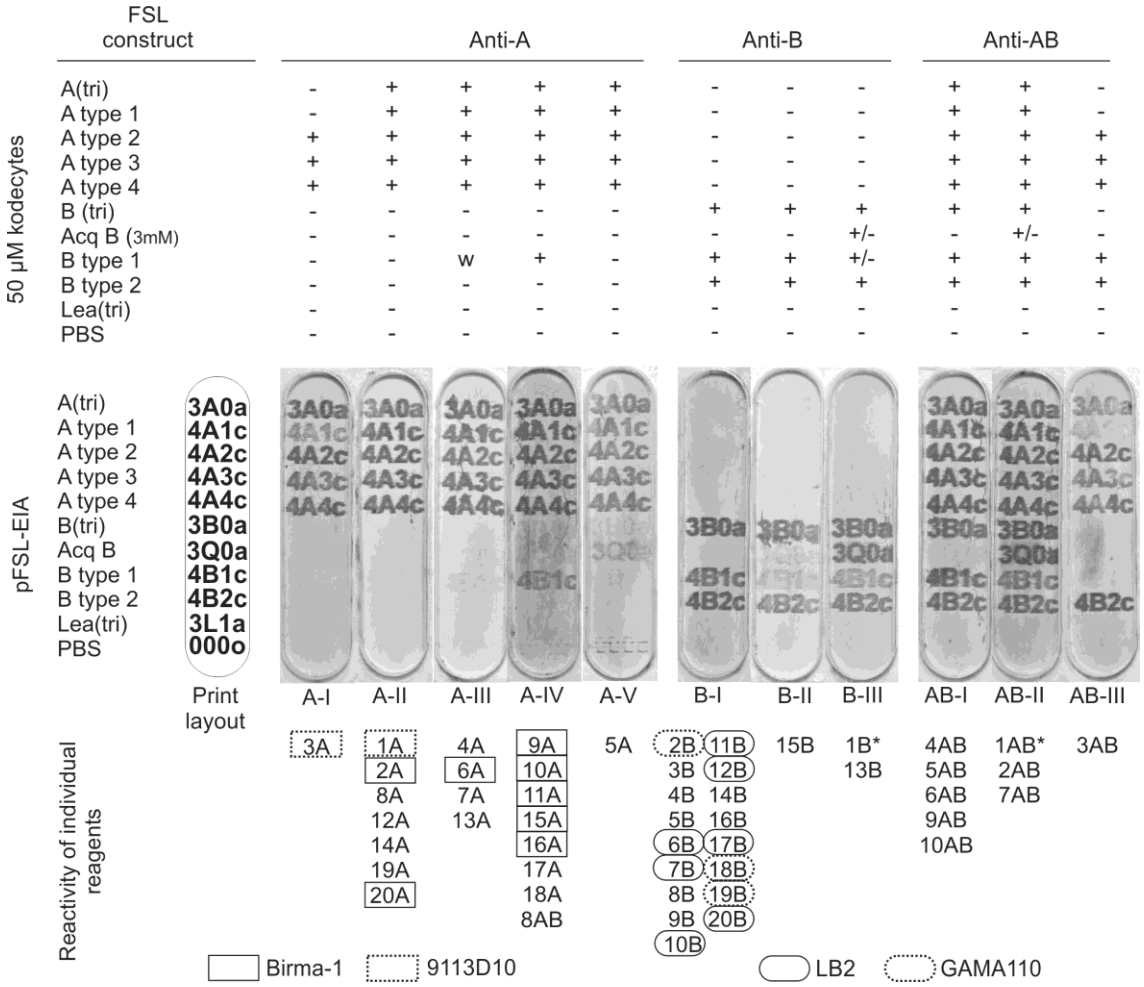

Figure 20. Comparison of kodecytes serological results and pFSL-EIA results against monoclonal and polyclonal ABO reagents. The serological (kodecyte) results are graded positive (+), negative (-) or weak (w). Reagents are clustered into common reaction patterns with kodecytes and pFSL-EIA analysis. Reagents identified by their ID number (see Table 52) are listed below the reaction patterns they associate with. Anti-A reaction patterns are identified as A-I, A-II, A-III, A-IV and A-V, anti-B reactions patterns are B-I, B-II and B-III and anti-AB as AB-I, AB-II and AB-III. Asterisks next to reagents 1B and 1AB indicate they gave negative results for the results graded +/-. Where common clones are present in the anti-A and anti-B reagents these have been indicated by outlines. Reagents 19A and 9AB are polyclonal human reagents.

In a couple of instances the printed FSLs gave a positive result where the kodecytes gave a negative result. Namely, in reaction patterns B-III and AB-II where reagents 1B and 1AB did not detect the FSL-Btetra type 1 or the FSL-acquired Btri. In the case of the FSL-Btetra type 1 the inkjet printed molecule was only weakly detected. However for the FSL-acquired Btri the concentration of the FSL on the kodecytes needed to be increased to 3M to get a positive result, where on the printed surface this was detected easily.

Another discrepancy is in the A-I pattern where reagent 3A did not detect the FSL-Atri and FSL-Atetra type 1 with the kodecytes but did on the printed FSL, albeit weakly with the FSL-Atetra type 1. This is seen again in the AB-III pattern with reagent 3AB. These reagents are in fact from the same manufacturer and contain the same anti-A clone. This implies the printed FSL is more sensitive than the cells as it was able to produce a positive result with these

antibodies. However it is known that some antigens react with antibodies in solid phase and do not do so when they are present on red blood cells. This is well documented for the Lewis blood group system where anti-Le^b reagents react with Le^a in solid phase but not when the Le^a is present on a red blood cell (Henry et al., 1995). A difference in avidity may also be observed between these two methods. Interestingly, these reagents gave positive results with kodecytes for the FSL-Atetra type 2, 3 and 4, highlighting the differences between the different antigens and the importance of the specificity of the reagents used for blood typing. This clone is also used in reagent 12A where the kodecyte reaction agreed fully with the printed result, giving a positive for FSL-Atri and FSL Atetra type 1, therefore suggesting differences between manufactures' reagents even when using the same clone of antibody.

Overall the majority of the antibody reagents gave the exact same results for kodecytes as they did with the pFSL-EIA, validating this printing method as a suitable technology for biological assays.

2.4.3 Using printed peptide FSL constructs as disease markers

The FSL constructs tested so far include carbohydrates and biotin. Being able to attach peptide FSLs to non-biological surfaces allows investigations into reactions that occur between peptides and antibodies or other molecules. Detection of disease markers in samples is one area where this can be utilised. In this section, Chagas disease FSL constructs (FSL-CHA) were printed onto a paper surface to create a peptide pFSL-EIA plate and used to try and detect the disease antibodies in a number of human sera.

Method overview

FSL-constructs:

- FSL-CHA1, FSL-CHA2, FSL-CHA4 and FSL-CHA5 are FSL constructs containing a 20 residue sequence of the Chagas antigen.
- FSL-CHA4N contains 3 identical 20 residue sequences on three branches and hence is 3 times larger than the other FSL-CHA constructs and was designed to potentially increase the sensitivity of the FSL.

All of these FSL constructs contain different peptide sequences to try and establish which has the greatest specificity and sensitivity against human sera.

Preparation of printed plates: FSL-CHA1, FSL-CHA2, FSL-CHA4 and FSL-CHA5 constructs were prepared at 600 µM in PBS. FSL-CHA4N was prepared at the 3 times lower concentration of 200 µM in PBS as it contains 3 identical peptide sequences. 0.025% bromophenol blue was added to the print solutions to act as a visualisation dye, which is lost during washing. Each construct was printed onto media gloss paper (Spicers, NZ) in a

16 well +control well format. CHA1, CHA2, CHA4, CHA5 and CHA4N were the words printed for the respective FSL constructs. The paper surface was cut to size, heat sealed with laser cut laminating plastic on both sides leaving the reaction areas exposed, and adhered to a laser cut 2mm thick acrylic plate to create wells 7 x 34 mm.

pFSL-EIA: Printed plates were blocked with 2% BSA in PBS (pH7.2) for 1 hour. The 2% BSA in PBS was decanted and 100 µL of neat serum was added to each well and incubated for 1 hour at room temperature. 2% BSA in PBS was added to the control well. The plates were washed 6 times in PBS, by immersing the whole plate for 20 seconds using fresh PBS for each wash, then 100 µL of anti-human Ig conjugated to alkaline phosphatase diluted 1 in 1000 in 2% BSA in PBS was added to all wells and incubated for 30 minutes. After being washed 6 times in PBS 100 µL of NBT/BCIP substrate diluted 1 in 50 in a Tris substrate buffer was added to each well and incubated for 15 minutes. The reaction was stopped by washing with water (method detailed in section 2.1.1). Sera were a gift from Dr Luiz Carlos De Mattos and are 44 known Brazilian Chagas patients positive sera and 27 Brazilian blood bank negative sera.

Preparation of kodecytes: the 4 FSL constructs were prepared at 60 µM in PBS. A 500µL volume of FSLs was mixed with 500 µL of washed packed group O red blood cells and incubated for 2 hours at 37°C, then washed PBS by centrifugation for 1 minute and stored in Celpresol as a 3% suspension at 4°C.

Serology: 30 µL of kodecyte suspension was added to 30 µL of serum and incubated for 60 minutes at 37°C. The samples were washed 4 times in PBS using an immufuge centrifuge. 30 µL of anti-AHG (Epiclone AHG poly, 03071305, CSL, Australia) was added and centrifuged for 10 seconds on high in an immufuge centrifuge. The degree of agglutination (positive reaction) assessed with a microscope eyepiece.

Results and interpretation

By comparing the kodecyte serology results against the inkjet printed EIA results, a difference in the number of positive sera detected was seen (Table 53). Only the FSL-CHA2, FSL-CHA4 and FSL-CHA4N result are shown as FSL-CHA1 and FSL-CHA5 did not show any reaction with any sera. The kodecytes were able to detect 40 out of 44 positive sera, whereas the inkjet printed plate detected less of the positive sera (example printed wells shown in Figure 21).

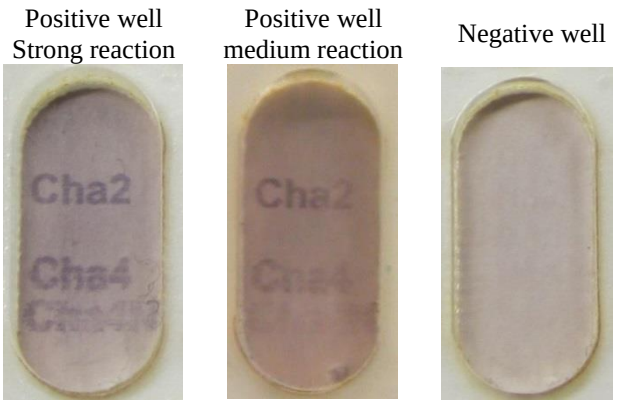

Figure 21. Examples of FSL-Chagas inkjet printed well tested against positive and negative sera. Printed in each well, using the appropriate FSL constructs, are the characters CHA1, CHA2, CHA4, CHA5, CHA4N. Only FSL-CHA2, FSL-CHA4 and FSL-CHA4N reacted against any sera.

Table 53. Number of Chagas sera detected positive by 3 different FSL constructs using FSL-Chagas kodecytes and the pFSL-EIA.

FSL-construct	Serology results of FSL-Chagas kodecytes			
	Positive sera (n=44)		Negative sera (n=27)	
	Kodecytes	pFSL-EIA	Kodecytes	pFSL-EIA
FSL-CHA2	14	33	0	1
FSL-CHA4	40	28	0	2
FSL-CHA4N	31	10	0	0

The 4 known positive samples that showed negative results with the kodecytes were negative for all FSL constructs. The same sera were also negative in the pFSL-EIA results for all constructs, and 10 sera overall were negative for all constructs in the printed assay. In the kodecytes results FSL-CHA4 was the construct that showed the greatest reactivity with the sera. Interestingly, in the inkjet printed results FSL-CHA2 was the construct that predominantly detected the positive sera. FSL-CHA4N proved not as reactive as the other two constructs. By comparing the FSL-CHA2 results, of the 33 out of 44 positive sera that were detected positive by the inkjet printed method, only 13 were detected positive using kodecytes (Table 54). However, when FSL-CHA4 was used, the kodecytes detected 40 out of 44, whereas inkjet printed constructs detected only 28. Of note are also the false positives that were observed when using the pFSL-EIA method. 3 negative sera overall, 1 by FSL-CHA2 and 2 by FSL-CHA4, were detected as positive, while no false positives were observed using kodecytes.

A comparison of the kodecyte and inkjet printed test results are shown in Table 54, Table 55 and Table 56 for FSL-CHA2, FSL-CHA4 and FSL-CHA4N respectively. FSL-CHA2 detected 33 positive sera as positive using the pFSL-EIA, whereas only 13 were detected positive by serology (Table 54). However, when FSL-CHA4 was used the pFSL-EIA detected only 28

positive sera as positive compared to 40 using the kodecytes (Table 55). The kodecytes also detected more positives using FSL-CHA4N then the pFSL-EIA (Table 56).

Table 54. Comparison of FSL-CHA2 results of positive sera tested using kodecytes and inkjet printed constructs. n=44.

		Kodecytes	
		+	-
Printed	+	13	20
	-	1	10

Table 55. Comparison of FSL-CHA4 results of positive sera tested using kodecytes and inkjet printed constructs. n=44.

		Kodecytes	
		+	-
Printed	+	28	0
	-	12	4

Table 56. Comparison of FSL-CHA4N results of positive sera tested using kodecytes and inkjet printed constructs. n=44.

		Kodecytes	
		+	-
Printed	+	9	1
	-	22	12

Overall the kodecytes showed greater sensitivity then the solid phase assay as only 4 out of 44 were not detected as positive. The difference in the reactivity of the FSL-CHA2 and FSL-CHA4 along with the lower sensitivity suggests different presentation of the antigen on the solid surface compared to the cell surface which is influencing the reactivity with the antibodies. However, optimisation was not done to any great extent.

To investigate the sensitivity of the pFSL-EIA, a second experiment involved printing FSL-CHA2 and FSL-CHA4 at different concentrations in the same well. The FSL solutions, at 600 μM (same as previous experiment), were printed in 1, 2 and 3 layers, thereby increasing the amount of FSL on the surface by 2 and 3 times (Figure 22). A subset of sera was then tested against this printed plate to try and increase sensitivity and to be able to see clearly the difference between the reactivity of the 2 constructs. The sera that were tested included the ones with a discrepancy between the kodecytes and pFSL-EIA results.

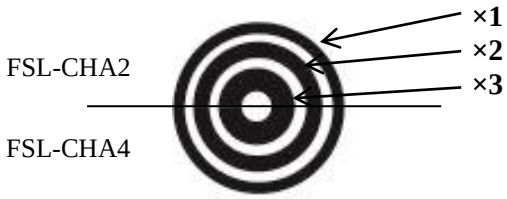

Figure 22. Design of printed reaction well with 2 FSL constructs at 3 concentrations. Top half printed with FSL-CHA2 and bottom half printed with FSL-CHA4. Outer circle is one layer, middle circle 2 layers and inner circle 3 layers of printed construct.

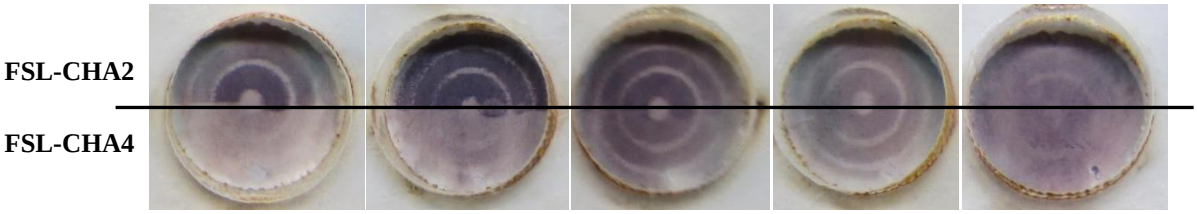

Figure 23. Examples of wells printed with 2 constructs, one in the upper and one in the lower half of the well. They were both printed at 3 different concentrations by layering the printing, 1 layer in the outside circle, 2 layers in the middle circle and 3 layers in the inner circle (see Figure 22). a) shows a serum that was sensitive to the concentration of the FSL as the circles are stained differently, b and c) show sera that bound equally to all concentrations of the printed FSL, d) shows similar sensitivity of FSL-CHA2 and FSL-CHA4 and e) shows high background staining where only the high printed concentration (inner circle) is seen.

By increasing the concentration of the printed constructs the ability to detect antibodies in the serum increased. More sera were detected as positive when using the higher concentration of printed constructs, showing greater sensitivity (Table 57 and Table 58). The pFSL-EIA with FSL-CHA2 detected all the sera (n=24) as positive compared to only 19 out of 24 in the previous experiment, and only one was detected as negative when using FSL-CHA4. Table 57 shows that the 5 sera detected negative with the low concentration of FSL-CHA2 printed construct are positive with the higher concentration, whilst 16 were detected as negative by the kodecytes. Table 58 shows that of the 11 sera detected as negative with the low concentration of FSL-CHA4 printed construct, 10 of them are positive with the higher concentration. All of these were correctly detected as positive by the kodecytes.

Table 57. FSL-CHA2 results of known positive sera tested using kodecytes and inkjet printed constructs. a is the results using the lower concentration of the printed construct and b is the results using the higher concentrations of the printed construct. n=24.

Low				High			
FSL-CHA2		Kodecytes		FSL-CHA2		Kodecytes	
		+	-			+	-
Printed	+	7	12	Printed	+	8	16
	-	1	4		-	0	0

Table 58. FSL-CHA4 results of known positive sera tested using kodecytes and inkjet printed constructs. a is the results using the lower concentration of the printed construct and b is the results using the higher concentrations of the printed construct. n=24.

Low				High			
FSL-CHA4		Kodecytes		FSL-CHA4		Kodecytes	
		+	-			+	-
Printed	+	13	0	Printed	+	23	0
	-	11	0		-	1	0

There was also a more similar reactivity between the FSL-CHA2 and FSL-CHA4 when using the printed constructs. However FSL-CHA2 did give stronger reactions, shown by stronger staining, than FSL-CHA4 even when both detected the positive sera (Figure 23 a, b and c). The difference in sensitivity between the 2 constructs was clearly seen in these samples and highlights the importance of selecting the right peptide for the specific assay, i.e. kodecytes may have difference requirements than the pFSL-EIA. Also, one negative sample was detected as positive by the FSL-CHA4 construct in the solid phase assay suggesting some non-specific binding with this construct.

Printing FSL-CHA2 and FSL-CHA4 in the 2 halves of the circles enabled a direct comparison between the 2 constructs and their selectivity (Figure 23). The 3 concentrations of the constructs, printed in the 3 circles, also allowed analysis of the sensitivity of each construct. In some cases an obvious difference was seen between the 3 circles, where the inner circle was much more strongly stained that the outer circle (Figure 23a). In other cases all 3 circles stained to a similar level although not necessarily very strongly (Figure 23 b, c and d). The background staining of the plates was a problem and can obscure the result as in seen in Figure 23e. Here, the increased concentration of the FSLs greatly improved detection of the antibodies as the inner circle (highest concentration) was the clearest circle seen and helps differentiate from the background staining. Some samples were negative in the first experiment and positive in the second due to this problem. There is still clearly a difference between the optimum antigen to use on kodecytes and the solid paper surface, suggesting differences in reactivity depending on the surface the construct is attached to, not just the structure of the peptide.

2.4.4 Attaching recombinant proteins to printed FSLs for immunoassays

Another method for creating a peptide or protein immunoassay is to attach the molecule to a surface using FSL constructs. This was tested by printing FSL-biotin onto a paper surface and then attaching a biotinylated protein to the printed FSL using streptavidin as a linker. This system enables the potential for any biotinylated molecule to be used as the antigen in the pFSL-EIA. In this experiment a biotinylated Human Leukocyte Antigen (HLA) protein was

coated onto a surface using FSL-biotin and streptavidin linkage, and tested against 3 antibodies. One antibody will detect this protein if it has denatured during attachment, whilst the others bind to the protein in its natural conformation. The recombinant protein used here contains a VLDL (very low density lipoprotein) tag which enables purification of the protein.

Method overview

The biotinylated protein and the 3 antibodies were a gift from PureProtein LLC, USA.

Preparation of printed plate: FSL-biotin was printed onto media gloss paper (Spicers, NZ) at a concentration of 500 µM in PBS and blue dye in the text 01323-P122, as this is the name of the protein to be attached. It was printed in a 32 well format (see Figure 17), in the first 3 columns. FSL-Atri, at 600 µM in PBS and blue dye, was printed in the fourth column as a control molecule for the conjugate antibody. The paper surface was cut to size, heat sealed with laser cut laminating plastic on both sides leaving the reaction areas exposed, and adhered to a laser cut 2mm thick acrylic plate to create wells 7mm x 34 mm.

Attaching the protein antigen: Printed plates were blocked with 2% BSA in PBS (pH7.2) for 1 hour. The 2% BSA in PBS was decanted and 50 µL of streptavidin (43-4301, Invitrogen, USA) at 8 ng/mL in 2%BSA in PBS was added to each test well and incubated for 30 minutes at room temperature, the plate was then washed 6 times in PBS, by immersing the whole plate for 20 seconds using fresh PBS for each wash. 2% BSA in PBS was added to the control wells. 50 µL of the biotinylated B*27:05VLDL protein (01323-P122) was added to the required wells at various concentrations to establish the sensitivity of this assay. It was incubated for 30 minutes at room temperature, and then the plate was washed 6 times in PBS, as described above and then immunostained immediately.

Immunostaining- 3 antibodies used to assess the success of attaching the HLA antigen:

- Anti-W6/32 is a monoclonal mouse antibody that recognises all HLA antigens but only in the structurally intact form.
- Anti-HC-10 is a monoclonal mouse antibody and is used as an indicator of structurally impaired HLA molecules. It recognises the heavy chain when not associated with the β_2-microglobulin subunit.
- Anti-β2m is a polyclonal rabbit antibody that recognises the β_2-microglobulin subunit.

The antibodies were diluted in 2% BSA in PBS to various concentrations to test the sensitivity of the assay. 50 µL of the antibody solutions was added to the test well and incubated for 1 hour. The plate was then washed 6 times in PBS as described, then 50 µL of a conjugate antibody (anti-mouse Aqu502A, Millipore, USA or anti-rabbit AP322A, Chemicon, Australia) diluted 1:1000 in 2% BSA in PBS was added to each well, incubated for 30 minutes, and then washed. 50 µL of the substrate was then added to each well (diluted 1:50 in substrate buffer)

for 3 minutes, then the plate was washed in water, dried and stored at room temperature (for details of method see section 2.1.1).

Control wells:

All control wells were blocked with 2% BSA in PBS with the rest of the plate. 2% BSA in PBS was added to the control wells when incubations with the streptavidin or biotinylated protein were carried out in the test wells.

Conjugate antibody control: 50 µL monoclonal anti-A (1:4 in 2% BSA in PBS) was added to each well printed with FSL-Atri and incubated for 1 hour. The wells were washed 6 times in PBS, then steps continued with conjugate anti-mouse antibody and substrate as above.

Control for streptavidin: streptavidin was added to the control well as per test well. After washing, biotinylated-alkaline phosphatase (50 µL at 0.1 mg/ml in 2% BSA in PBS) was added to the well and incubated for 30 minutes then washed. Staining continued with substrate step as above.

Control for FSL-biotin: streptavidin conjugated to alkaline phosphatase (50 µL at 2 ng/mL in 2% BSA in PBS) added to well and incubated for 30 minutes, then washed. Staining continued with substrate step as above.

For negative control of antigen: streptavidin and biotinylated 01323-P122 was added to the wells as for test wells. No primary antibody was added, 2% BSA in PBS was added instead, and then the staining continued with the conjugate antibody and substrate as above.

Results and interpretation

Anti-W6/32 and anti-β2m were able to detect the HLA antigen showing the antigen was present and able to bind to its recognition molecules after attachment to the paper surface (Table 59). The antigen was detected down to a concentration of 84 ng/mL. Since 50 µL of antigen solution was added to the wells, this equates to 4.2 ng of protein added to the printed FSL-biotin+streptavidin well at this concentration. It is assumed that not all the protein bound to the streptavidin, therefore a positive result was seen with less than 4.2 ng of protein attached to the surface. The low detection of the antigen by the anti-HC-10 antibody revealed that the antigen was mostly in its native conformation after attachment to the surface, as this antibody recognises structurally impaired molecules. This correlates to the high level of detection by the anti-W6/32 which only recognises the intact form. The concentrations of the recombinant protein trialled ranged from 835000 ng/mL to 84 ng/mL (some examples from 55700 ng/mL to 84 ng/mL shown in Table 59). All concentrations produced clear results with no non-specific binding seen. The control wells showed FSL-biotin and streptavidin were present and that there

was no non-specific binding to the protein by the secondary antibody (Table 60). This therefore shows a method for attaching biotinylated proteins to surfaces in a functional conformation using FSL-biotin and streptavidin as linkers, to be used in immunoassays.

Table 59. Example images of printed FSL-biotin used to attach a biotinylated HLA antigen to a surface for an immunostaining assay. "01323-P122" was printed in FSL-biotin, which then attached to biotinylated 01323-P122 HLA antigen.

Antibody	Antigen concentration (ng/mL)		
	55700	400	84
Anti-W6/32			
Anti-HC-10			
Anti-β2m			

Table 60. Example of control wells used for the printed FSL-biotin, HLA antigen immunoassay. AP= alkaline phosphatase.

Control	Example	FSL-biotin	FSL-A	Strept-avidin	Strept-avidin - AP	Biotin-AP	01323-P122	1° Ab	2° Ab
Negative control		+	-	+	-	-	+	-	+
FSL-biotin control		+	-	-	+	-	-	-	-
Streptavidin control		+	-	-	-	+	-	-	-
Conjugate control		-	+	-	-	-	-	+	+

2.5 Cell attachment

As well as being able to detect FSLs immobilised on solid surfaces, it was interesting to know if cells could be adhered to these surfaces using FSL constructs. The ability to pattern cells on selected membranes has applications from cell biosensors, research into cell growth and differentiation, to tissue engineering new organs for transplant, as well as regenerative medicine and wound healing. Using FSLs to attach cells to surfaces could potentially allow layers of cells to be built up using linker molecules to create 3D structures. Here the investigation was into the possibility of attaching kodecytes to non-biological surfaces using FSL constructs on the surface and a linker molecule to attach them together.

2.5.1 Establishing FSL attachment to bacteria

Initially bacteria were investigated for attachment to surfaces as they are smaller and more robust than mammalian cells. Up until now only mammalian cells and viruses have been modified with FSL constructs, so it was first established if FSLs could be attached to the bacteria cell wall.

Attaching FSLs to bacteria

A variety of microbes were tested with FSL-biotin and visualised with fluorescent avidin conjugate to analyse FSL attachment. Viability of the microbes after FSL modification was checked.

Method overview

Modifying bacteria: Various bacteria were cultured on nutriagar plates at 30°C for 2-3 days. One colony was removed and added to a 30 µL solution of FSL-biotin at 250 µM. After thorough mixing, they were incubated at 37°C for 2 hours, then washed 3 times in PBS by centrifugation (Sorvall Microcentrifuge 12V, 10 000 RPM).

Visualisation: 20 µl of avidin-alexa fluor® 488 at 0.1 mg/ml was added to each pellet, mixed and incubated for 30 minutes at 37°C in the dark. The culture was washed in PBS 3 times by centrifugation. Avidin-alexa fluor® 488 was also added to bacteria that had not been incubated with FSL-biotin, at the same concentrations, as a negative control. The bacteria were suspended 50 µL PBS and imaged under the fluorescent microscope at 488 nm excitation wavelength.

Bacteria tested were:

- *Micrococcus luteus*
- *Staphylococcus lugdunensis*
- *Stapylococcus saprophyticus*
- *Stapylococcus epidermidis*
- *Escherichia coli*
- *Bacillus subtilus*
- *Bacillus cereus*
- *Chrysobacterium*
- *Pseudomoas aeruginosa*
- *Klebsilla pneuoniae*
- *Proteus vulagaris*

For the viability tests *E. coli* and *S. saprophyticus* were chosen as representatives of a bacillus and coccus species. This experiment compared the colony count of bacteria that had been incubated with FSLs and those that had not. One colony from each species was added to a 500 µL solution of PBS and mixed well. This solution was then split into two tubes and one suspension of each species was added to a solution of 250 µM FSL-biotin. The other solution from each was added to the same volume of PBS. They were incubated at 37°C for 2 hours then washed 3 times in PBS and suspended in 200 µL PBS. The suspended cultures were then diluted 10 times by adding them to a volume of nutrient broth. A 10 times series dilution in nutrient broth was carried out, then spread onto nutriagar plates and incubated over night at 37°C. 4 plates of *E. coli* were counted at 10^{-5} dilution and 5 plates of *S. saprophyticus* at 10^{-4} dilution.

Results and interpretation

All bacteria tested were able to be visualised using fluorescent microscopy after 2 hour incubation with FSL-biotin followed by 30 minute incubation with avidin-alexa fluor® 488 and imaged immediately (examples shown in Figure 24). When avidin-alexa fluor® 488 was incubated with the bacteria without the FSL, nothing could be seen under fluorescence. This therefore indicates that the FSL is attaching to the outside of the bacteria with subsequent attachment of the fluorescent avidin.

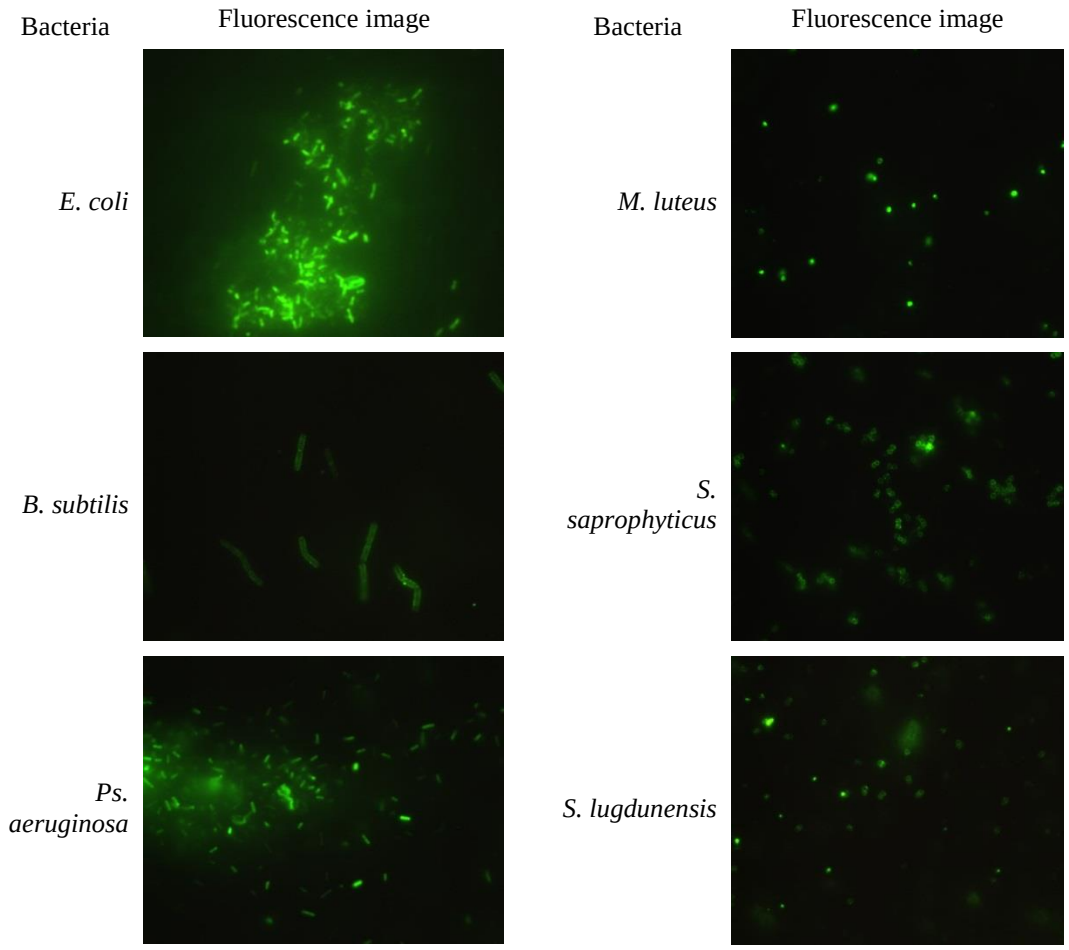

Figure 24. Examples of various bacteria incubated with FSL-biotin and then avidin-alexa fluor® 488 to be visualised under fluorescent microscopy

A Chi squared test was carried out on the data collected from the colony count to compare the FSL and non-FSL colonies (Table 61).

Table 61. Plate colony counts of *E.coli* and *Staphylococcus* with FSLs and without FSLs to establish viability of microbes with FSL insertion.

	E.coli 10-5 plate colony counts	*S. saprophyticus* 10-4 plate colony count
With FSL	160, 157, 124, 142	130, 112, 108, 121, 114
Without FSL	141, 149, 160, 161	104, 117, 114, 135, 125

E. coli:	p-value = 0.2133	Not significant
S. saprophyticus:	p-value = 0.771	Not significant

There was no significant difference between the number of colonies on plates of these two bacteria whether they have FSL-biotin attached to them or not. This indicates that FSLs do not affect the viability of microorganisms and so can be attached to these cells with no toxic effects.

Attaching FSL modified bacteria to FSL modified surfaces

Having determined that FSLs could be attached to bacterial surfaces, the attachment of these microbes to non-biological surfaces was then investigated. Firstly the study into whether bacteria could be stuck to microbeads was carried out, as visualising cells on beads is easier than on planar surfaces when using a microscope. Polycarbonate microbeads, 20µm in diameter, were used as they are easy to handle, have shown good attachment to FSL constructs and are easily visualised.

Method overview

Modifying bacteria: The bacteria *E. coli*, *S. saprophyticus* and *M. luteus* were cultured on nutriagar plates at 30°C for 2-3 days. One colony was removed and added to a 30 µL solution of FSL-biotin at 100 µM. After thorough mixing, they were incubated at 37°C for 2 hours and then washed 3 times in PBS by centrifugation. They were then suspended in 300 µL PBS. The bacteria tested were *E. coli*, *Staphylococcus saprophyticus* and *Micrococcus luteus*.

Modifying microbeads: Polycarbonate microbeads (Nanomi, Netherlands) were also modified with FSL-biotin at concentration of 250 µM in PBS. This was carried out by mixing the beads in 100 µL of FSL solution and incubating for 30 minutes at room temperature. The beads were washed 3 times in PBS by centrifugation and the supernatant removed. Avidin (A-9275, Sigma) was then attached to the biotin coated microbeads by adding 100 µL avidin at 2 mg/mL in PBS to the beads and incubating for 30 minutes. The beads were washed 3 times by centrifugation, the supernatant removed and 100 µL of the FSL modified bacteria suspended in PBS added. They were mixed and incubated for 2 hours at room temperature. The microbeads were diluted by adding 100 µL PBS to the mixture. They were then imaged under the microscope at ×1000 magnification.

To be imaged under the SEM the bacteria first needed to be fixed. This was carried out after modifying the bacteria with FSLs but before attaching them to the microbeads. This fixing procedure involved adding 100 µL of 2.5% glutaraldehyde to the pellet of bacteria after washing, mixing and incubating for 10 minutes. The bacteria were then washed 3 times in PBS by centrifugation and then incubated with the microbeads as described above.

Results and interpretation

All bacteria cells tested (*E. coli*, *S. saprophyticus* and *M. luteus*) were able to adhere to the surface of the microbeads (Table 62). Microbeads that had not been coated with FSL-biotin and avidin did not adhere any bacteria, showing that the FSL is needed for attachment of these cells to the polymer bead. Figure 25 shows a scanning electron microscope image of these bacteria on the surface of the microbeads. The bacteria cells do not cover the whole of the surface, probably due to washing off of the cells during handling. However, this could also be due to the liquid nature of the attachment, as it is likely the FSL constructs are able to move over the

surface of the bead, and hence the bacteria attached through the FSL linkage may also move on the surface.

Table 62.Images of FSL-biotin modified bacteria after incubation with FSL-biotin/avidin microbeads. Control beads had no FSL attached. ×1000 magnification.

Bacteria	FSL-biotin beads	Control beads (no FSL)
E. coli	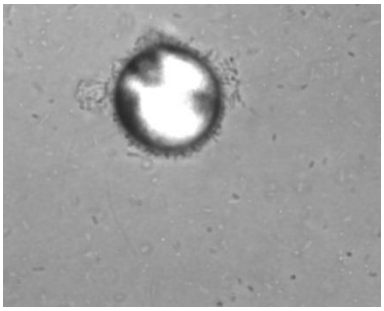	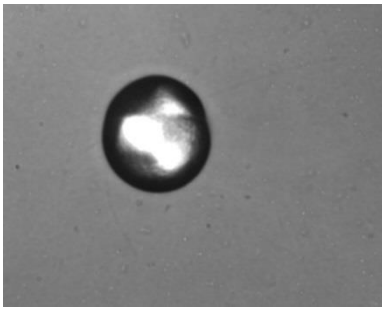
S. saprophyticus	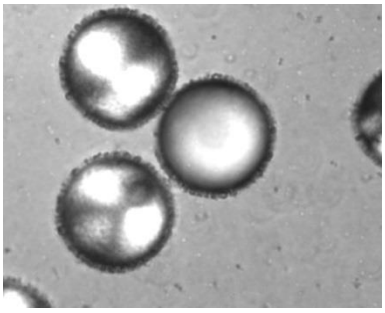	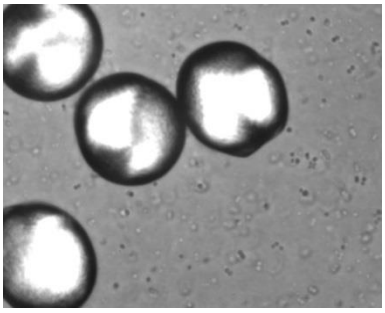
M. luteus	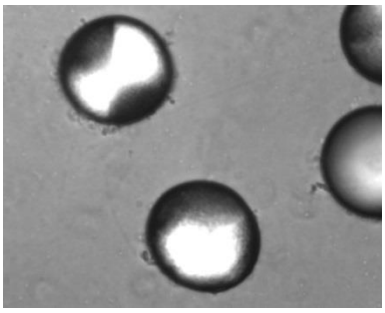	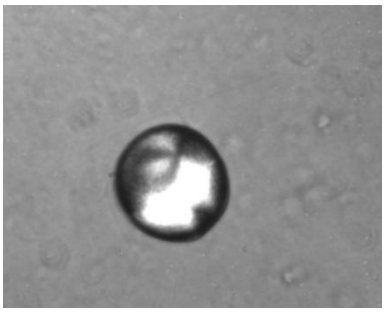

E. coli

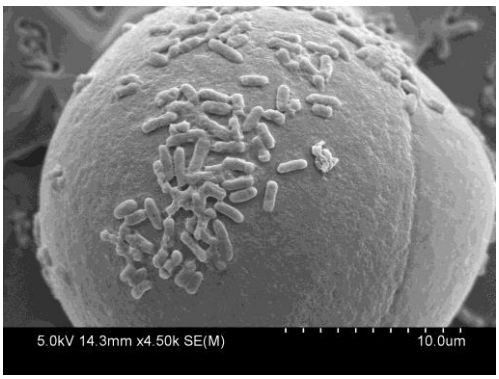

S. saprophyticus

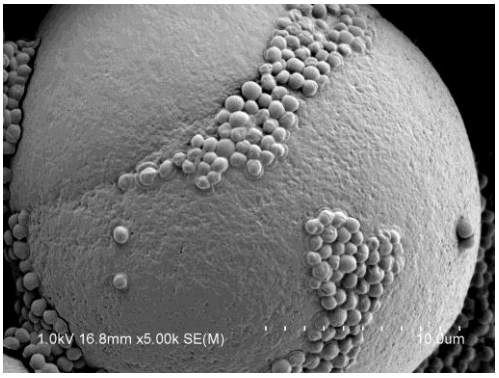

M. luteus

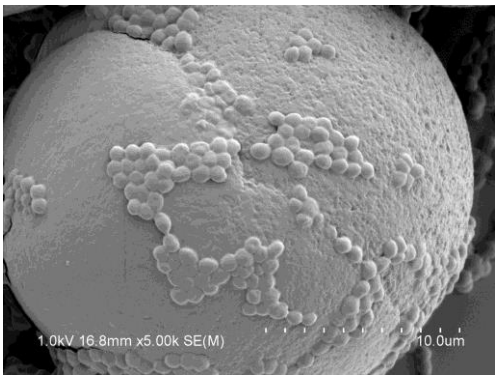

Figure 25. Scanning electron microscope images of different FSL-biotin modified bacteria adhered to FSL-biotin modified polycarbonate microbeads using avidin as the linker.

2.5.2 Mammalian cells

Attaching blood cells to microbeads

Having shown attachment of bacteria cells to solid surfaces, mammalian cells were then tested in the same way. Red blood cells (RBCs) were used as the test cell as they are easily obtainable and require no culturing. Additionally RBCs are relatively rigid and would be expected to be harder to attach than more fluid cells. Group O blood cells were used to produce kodecytes (cells containing FSL molecules in their membrane). Microbeads coated with the same FSL as used to make the kodecytes, plus a linker molecule (avidin or antibody), were prepared to see if the kodecytes would attach to the solid surface via these molecules.

Polycarbonate beads

Method overview

FSL-biotin: Fresh Group O RBCs, were modified with100 µM FSL-biotin to produce FSL-biotin kodecytes by incubating packed RBCs with an equal volume of the FSL-biotin solution for 2 hours at 37°C (see method in section 2.4.2). Polycarbonate microbeads (Nanomi, Netherlands) were FSL modified with 100 µM FSL-biotin by incubating them with in the FSL solution for 30 minutes at room temperature and then washing them 3 times in PBS by centrifugation. They were then coated with streptavidin by incubating them in a 200 µg/ml streptavidin solution for 30 minutes at room temperature, and then washing them 3 times in PBS by centrifugation and suspending them in 100 µL PBS. An equal volume of the FSL-biotin+streptavidin beads suspended in PBS and a 20% FSL-biotin kodecyte suspension was mixed and incubated at 37°C for 1 hour. 100 µL of PBS was added to dilute the free cells to allow analysis of the attachment of the cells to the microbeads. Control samples were also prepared, which included 1) mixing FSL-biotin beads containing no streptavidin with FSL-biotin kodecytes, and 2) preparing FSL-Atri beads at the same concentration and mixing them with FSL-biotin kodecytes.

FSL-Atri: Kodecytes were produced with FSL-Atri by incubating equal volumes of packed RBCs and 120 µM FSL-Atri in PBS solution at 37°C for 2 hours (see section 2.4.2). Microbeads were modified with FSLs by incubating them with a 300 µM FSL-Atri solution in PBS for 30 minutes at room temperature and then washing them 3 times in PBS by centrifugation. The supernatant was removed and the 50 µL monoclonal anti-A was added to the FSL modified beads and incubated for 1 hour at room temperature. After washing 3 times in PBS by centrifugation and removing the supernatant the beads were mixed with 50 µL of a 20% suspension of the FSL-Atri kodecytes, The control samples were composed of 1) FSL-Atri-beads+antiA with group O RBCs (no FSL-Atri), and 2) FSL-Atri beads with FSL-Atri kodecytes and no anti-A.

Kodecytes attached to microbeads were imaged on the SEM to analyse the degree of attachment. This was carried out using FSL-biotin and streptavidin, as above, except the kodecytes were fixed in 0.5% glutaraldehyde for 10 minutes after FSL modification, and then washed in dH_2O to remove salts, prior to mixing with the FSL-biotin+streptavidin beads. Once the cells and beads had incubated, 5 µL was taken and placed onto a 7 mm x 5 mm silicon wafer and allowed to dry overnight.

The degree of washing needed to remove the beads was also investigated to see how well the cells were adhered. Washing by centrifugation involved a 2 second spin, repeated 6 times. Washing by sedimentation involved letting the beads settle in the tube for 10 minutes, then removing the supernatant. 500 µL of PBS was then added and the beads mixed by inversion.

Results and interpretation

RBCs were able to be attached to the surface of the microbeads using FSL constructs and a linker molecule. FSL-biotin or FSL-Atri were attached onto the surface of the cells and microbeads, and by using streptavidin or anti-A respectively as the joining molecule, allowed immobilisation of the cells. Only when all linking molecules were present was attachment seen, ruling out non-specific attachment of the cells to the beads or to other FSLs (Table 63 and Table 64).

Table 63. Images of FSL-biotin kodecytes attached to FSL-biotin+streptavidin microbeads with two control samples.

Test/control	Images of beads and cells attached using FSL-biotin	
	×200	×1000
Test beads: FSL-biotin+ streptavidin beads + FSL-biotin kodecytes	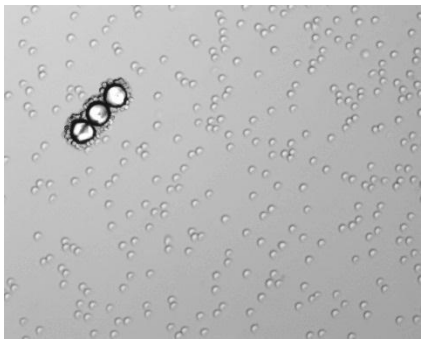	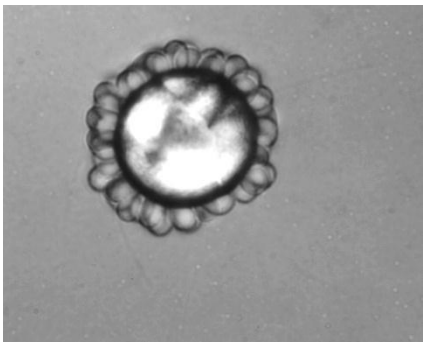
Control 1: FSL-biotin beads+FSL-biotin kodecytes. No streptavidin		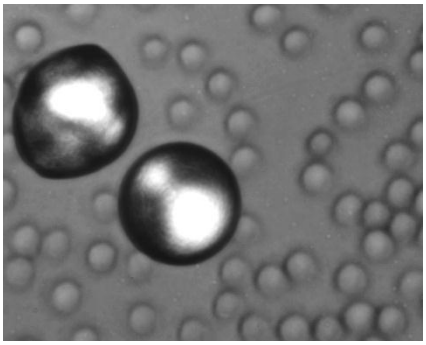
Control 2: FSL-Atri beads, with FSL-biotin kodecytes	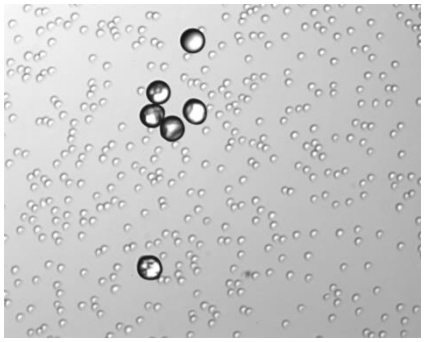	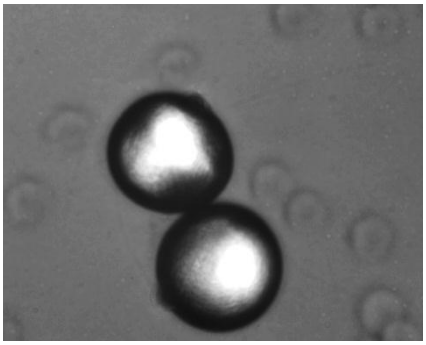

Table 64. Images of FSL-Atri kodecytes attached to FSL-Atri+anti-A microbeads with two control samples.

Test/control	Images of beads and cells attached using FSL-Atri	
	×200	×1000
Test beads: FSL-Atri+anti-A beads + FSL-Atri kodecytes	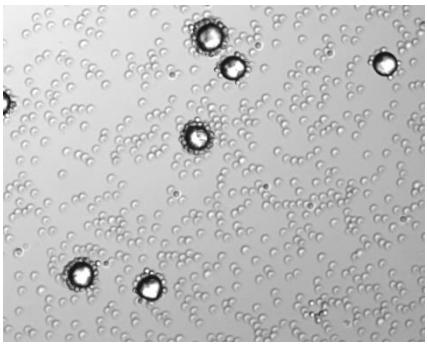	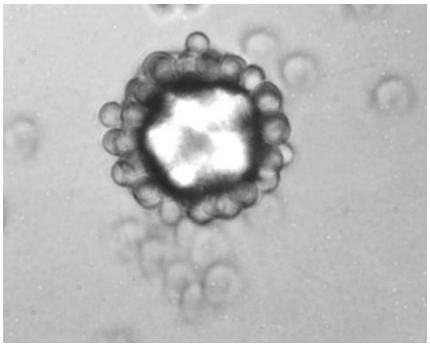
Control 1: FSL-Atri beads + FSL-Atri kodecytes. No anti-A	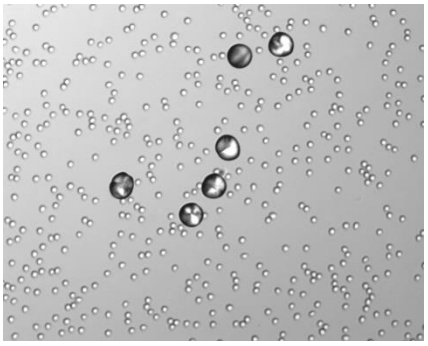	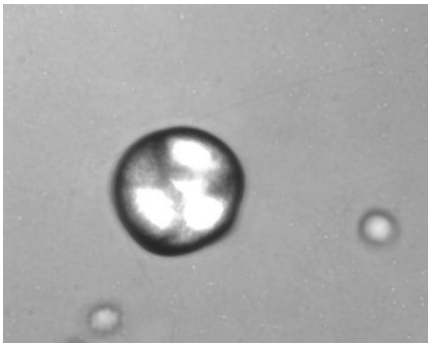
Control 2: FSL-Atri beads+anti-A + group O RBCs		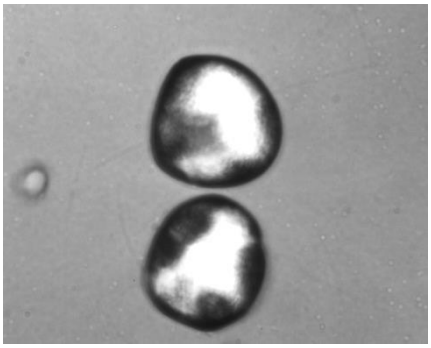

From these images it appears that the cells are not covering the whole of the bead but adhering only to the side and not the top. However, this is down to the focal point of the microscope and the cells have indeed adhered to all parts of the microbead (Figure 26).

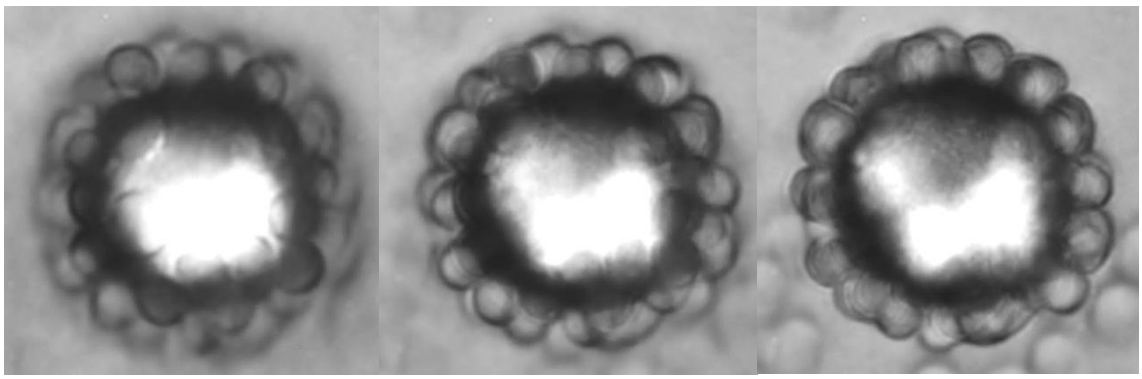

a b c

Figure 26. Images showing different focal points of the same microbead with cells adhered to the outside using FSL-biotin and streptavidin. It appears that the cells are not attached evenly over the surface of the microbead, however this is due to the different microscope planes which are imaged. As can be seen in image a, cells are present on the top of the bead, which is less obvious in b and not seen in c, purely because of the focal point of the image.

Figure 27 shows some examples of the SEM images captured of RBCs adhered to microbeads. This shows successful attachment of cells to a solid surface using FSL molecules. As is clear from the images the cells are not completely covering the beads. In fact, more attachment seems to be visible in the microscope images (Table 63 and Table 64). This could be due to the increased handling and drying of the SEM samples, which may have caused some cells to fall off. What can be seen in the SEM images is that the cells have attached to the top as well as the sides of the beads, which is not always obvious from the microscope images.

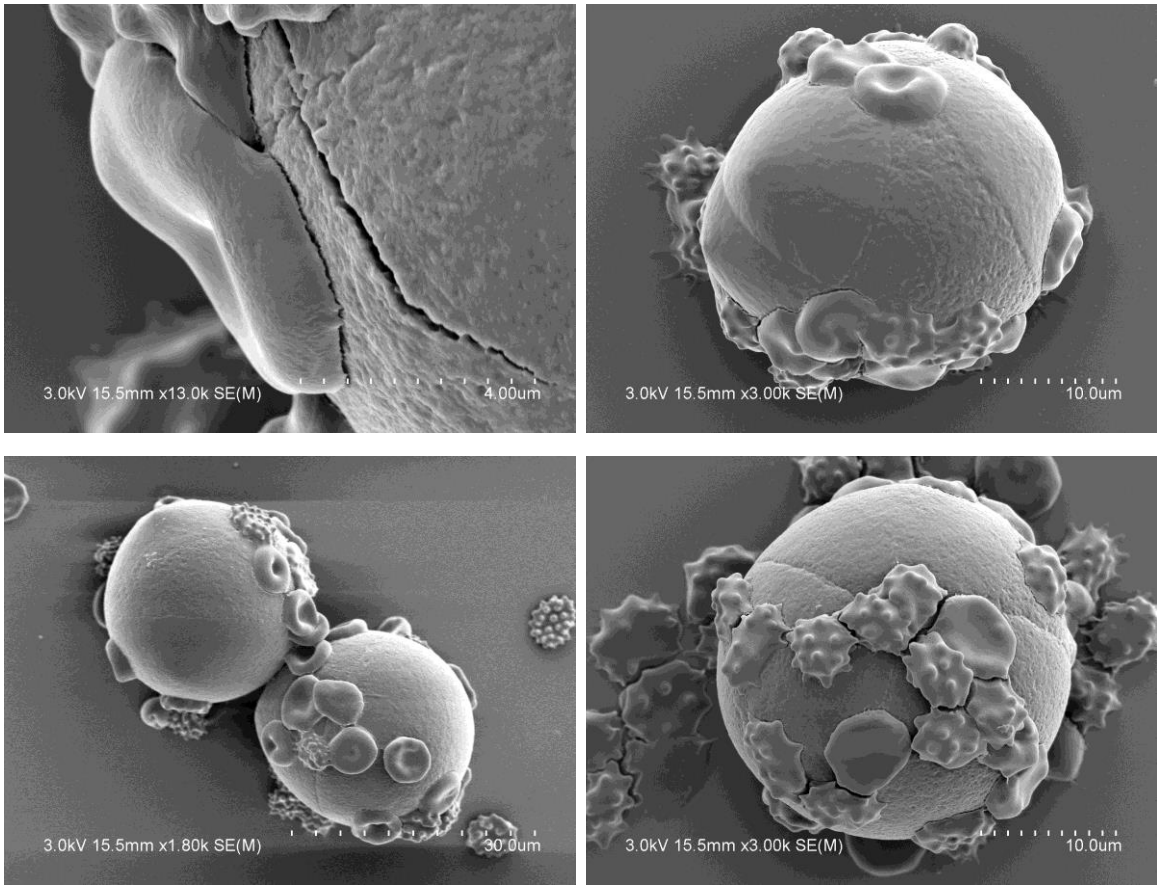

Figure 27. SEM images of FSL-biotin kodecytes immobilised on the surface of FSL-biotin+streptavidin microbeads.

In these SEM images, different shapes of the RBCs are observed. These crenated cells are called echinocytes and this is due to storage of the cells in a saline solution at 4°C. The cells change shape during storage from disks to spheres but remain viable and can return to the disk shape *in vivo* (Mollison, 2005).

The washing of the beads was investigated to assess how well these cells have stuck to the surface. Initial experiments involving washing by centrifugation proved to be too harsh and removed most of the cells from the surface of the beads. Washing by sedimentation was much gentler on the cells and 6 washes by this method were needed to see a reduction in the amount of cells on the surface (Table 65). The cell attachment is therefore quite weak, with the cells being removed easily by centrifugation and less easily by inversion and settling during the sedimentation washing.

Table 65. Washing of cells adhered to microbeads through FSL linkages and the different wash methods used to assess degree of attachment. For centrifugation one wash removed the cells, after 6 sedimentation washes cells were still attached to the microbeads.

Washing method	Cells adhered to beads through FSL linkages	
	Not washed	Washed
Centrifugation	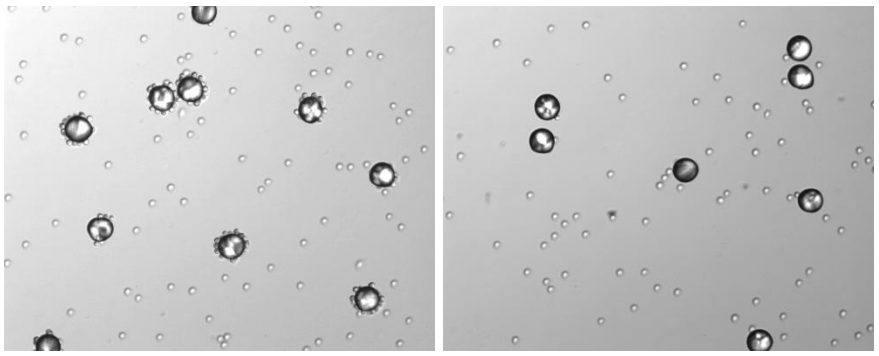	
Sedimentation	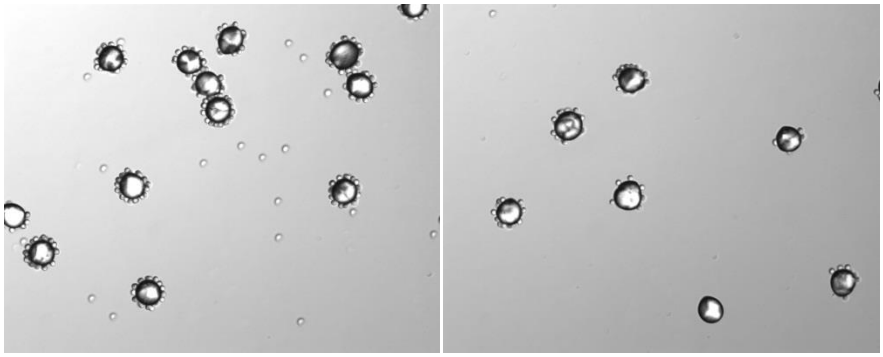	

Paramagnetic beads

Method overview

Microbeads: 1 µL of packed paramagnetic beads (Millipore, France), 1 µm in diameter, were added to a 100 µL solution of FSL-biotin at 50 µM in 0.1 % tween 20/PBS. They were mixed thoroughly and incubated at 4°C overnight. The beads were pulled into a pellet using a magnet

(neodymium magnet) and the supernatant removed. The microbeads were then washed once in 0.1% tween 20/PBS using the magnet to hold the beads in the tube and then suspended in 200 µL of the tween/PBS solution. The tween was added to prevent clumping of the beads. 50µl of the bead suspension was removed and the liquid discarded. 100µL 0.5 mg/mL streptavidin (43-4301, Invitrogen) was added and incubated for 1 hour at room temperature. The beads were then washed once in PBS, and the suspended in 100 µL 0.1% tween in PBS.

Kodecytes: Kodecytes were prepared with 0.1 mg/m FSL-biotin as standard by mixing equal amounts of the FSL solution with packed O cells and incubating them for 2 hours at 37°C.

Beads+cells: equal volumes of the FSL-biotin+streptavidin beads suspension plus a 10% kodecyte suspension were mixed together and incubated for 1 hour at room temperature. For a control the same method was carried using O cells instead of kodecytes.

Results and interpretation

Table 66 shows the attachment of the kodecytes to the streptavidin beads. All the cells are clumped together and are covered in the microbeads. When O cells are used instead of kodecytes no clumping of the cells is observed. This demonstrates that the FSL-biotin on the cells is able to bind to the streptavidin on the beads. There were no free cells spotted in this sample, with all cells being bound by the beads to other cells and beads. Once attached to the beads, the cells can be moved using the magnet (Figure 28). This does not occur when group O cells are using instead of kodecytes. This movement is rapid and hence reveals a strong interaction of the cells with the beads which are able to remain attached during this movement.

Table 66. Images of FSL-biotin kodecytes attached to FSL-biotin+streptavidin paramagnetic microbeads compared to a control using group O cells.

Test/control	Microbeads attached to cells using FSL-biotin	
	×200	×1000
FSL-biotin+ streptavidin beads + FSL-biotin kodecytes	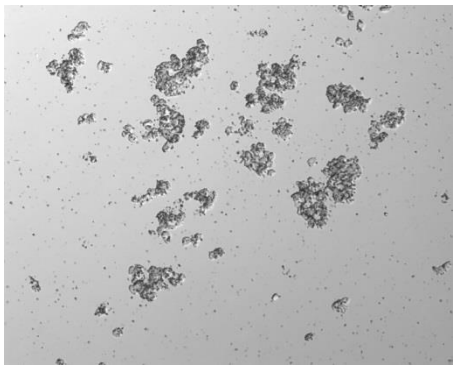	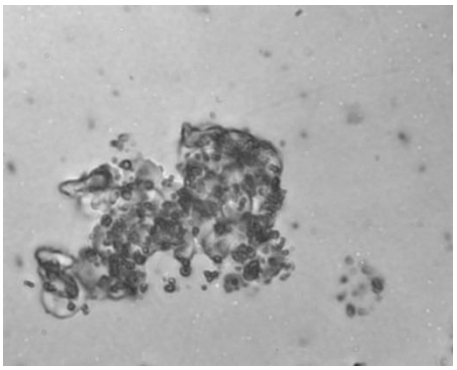
FSL-biotin+ streptavidin beads + Group O cells	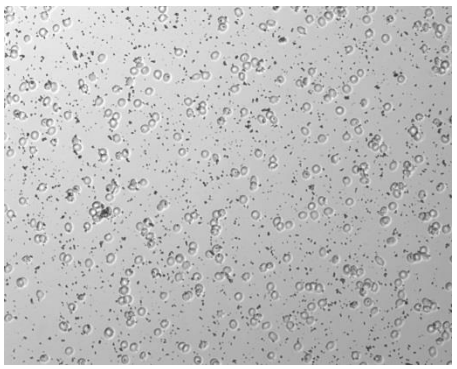	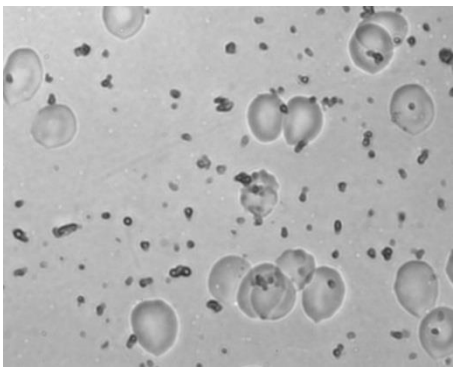

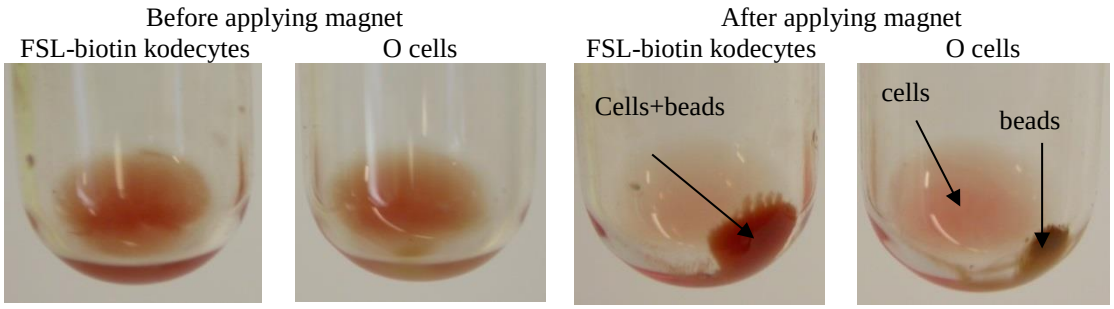

Figure 28. Paramagnetic beads modified with FSL-biotin and streptavidin able to bind to FSL-biotin kodecytes. When kodecytes are mixed with the beads they are able to be moved with the magnet, however O cells remain in the solution and only the brown beads are seen to move to the side of the tube.

Attaching cells to printed FSLs

Having demonstrated the ability to attach cells to different microbeads using FSL constructs the possibility of immobilising cells onto planer surfaces was then established. The surfaces tested included papers, cotton, metals and plastics and the mechanism of attachment was through FSL-Atri and anti-A.

Method overview

Printing FSLs: FSL-Atri was printed at 600 µM onto media gloss paper, printer paper, cotton, polyester film, aluminium foil and nitrocellulose. "FSL-A" was printed in bold in font size 10pt.

Adding linker molecule: The printed surface was blocked in 2% BSA for 1 hour by flooding the surface. After removal of the BSA, monoclonal anti-A diluted 1 in 5 in 2% BSA was flooded onto the surface for 1 hour. The surface was then washed 6 times in PBS by immersing the whole material in the PBS solution for 20 seconds for each wash.

Preparing kodecytes: 100 µL of packed group O red blood cells were mixed with 100 µL of 600 µM FSL-Atri in PBS. They were mixed thoroughly and incubated at 37°C for 2 hours. The cells were then washed 3 times in PBS and stored in celpresol at a 5% suspension at 4°C until needed.

Attaching cells to surfaces: A 5% suspension of FSL-Atri kodecytes was flooded onto the FSL-Atri+Anti-A surface and incubated for 1 hour. A 5% suspension of natural A1 cells were also flooded over the media gloss paper surface to investigate the attachment of these compared to kodecytes. To remove unbound cells the surface was washed very gently in PBS with a slight rocking motion.

Preparing attached cells for SEM: after gentle washing of the surface containing immobilised cells, a solution of 0.5% glutaraldehyde was flooded over the cells for 10 minutes. The surface was then washed gently in dH_2O to remove the glutaraldehyde and any salts and left to dry overnight. The surfaces were then sputter coated in platinum for SEM imaging.

Results and interpretation

FSL-Atri, printed onto a variety of non-biological surfaces was able to attach FSL-Atri kodecytes to the surface using an antibody as the linker (Figure 29 a-f). The text "FSL-A" was printed in this FSL construct onto which anti-A was attached, which was then able to attach FSL-A kodecytes. The cells show good confinement to the printed areas with the edge of the printed area well defined. The SEM images reveal almost a monolayer of cells on the surfaces indicating good attachment of the cells. Figure 30 shows that when O cells or FSL-biotin kodecytes are flooded on the surface, or when no anti-A has been added, there is no attachment of the cells, demonstrating that it is the FSL-Atri and the anti-A linking the cells to the surface. Similarly, the immunostaining of the printed FSL-Atri confirms it was FSL-Atri printed onto the surface.

These surfaces were quite varied in topography from extremely flat surfaces like the polyester film and aluminium foil to very uneven surfaces like the cotton. Looking at the media gloss paper images it can be seen that the cells adhere very closely to the printed areas as the streakiness of the printing seems to be enhanced. On other examples, like the nitrocellulose, the edge of the printed area is very obvious with hardly any cells observed beyond the printed line.

Figure 31 shows the attachment of FSL-Atri kodecytes and natural A cells. Both these types of cells were able to adhere well to the surface. This is important as it shows not only synthetic antigens are able to attach cells to surfaces but also natural ones, and presents opportunities for assays utilising natural molecules on cells for adhering them to surfaces.

Overall, these results have established the ability to attach and capture cells containing different FSL constructs to a variety of non-biological surfaces, showing how KODE™ technology provides a tool for immobilisation of cells.

Figure 29a. FSL-Atri kodecytes attached to paper which has been printed with FSL-Atri and had subsequent attachment of monoclonal anti-A. The stripy nature of the printing can be seen (refer to section 2.1.4), as the cells have adhered in a stripy fashion. This is due to the uneven printing of the FSL, not due to the cell immobilisation. A clear monolayer can be observed in the printed area. The ×1500 image shows the cells have a normal morphology after they have been attached to the surface.

Surface	Photo	SEM image
Media gloss paper	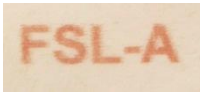	×35 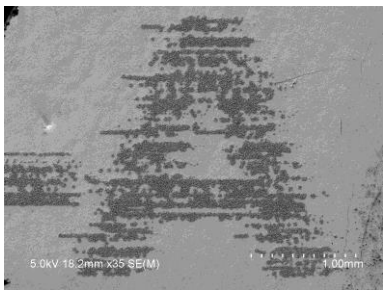
		×300 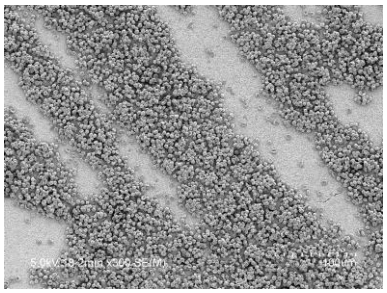
Un-printed area →		×1500 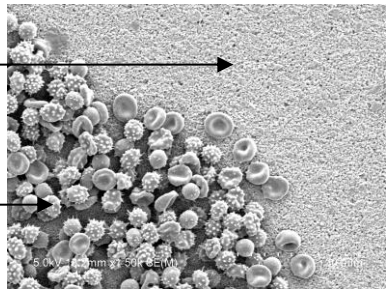
Printed area →		

Figure 29b. FSL-Atri kodecytes attached to printer paper which has been printed with FSL-Atri and had subsequent attachment of monoclonal anti-A. The ×300image reveals a monolayer of cells over the printed area.

Surface	Photo		SEM image
Printer paper		×300	
		×4000	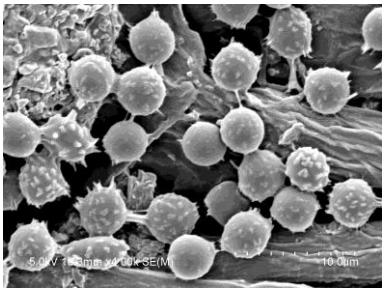

Figure 29c. FSL-Atri kodecytes attached to polyester film which has been printed with FSL-Atri and had subsequent attachment of monoclonal anti-A. A clear line is observed between where the cells have and have not attached, which correlated to the printed and non-printed areas.

Surface	Photo		SEM image
Polyester film		×700	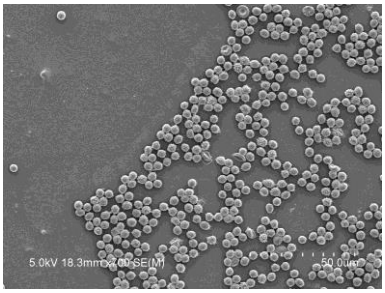
		×7000	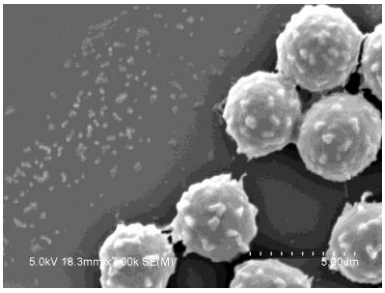

Figure 29d. FSL-Atri kodecytes attached to nitrocellulose which has been printed with FSL-Atri and had subsequent attachment of monoclonal anti-A. A clear monolayer of cells is observed in the ×350 and ×700 images and a clear line is seen between the printed and non-printed areas. The photo shows some cells adhered to other areas than the printed area, but the "FSL-A" clearly has a denser layer of cells attached.

Surface	Photo	SEM image	
Nitro-cellulose		×350	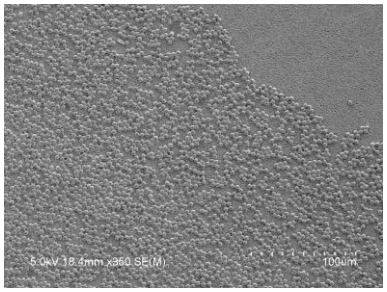
		×700	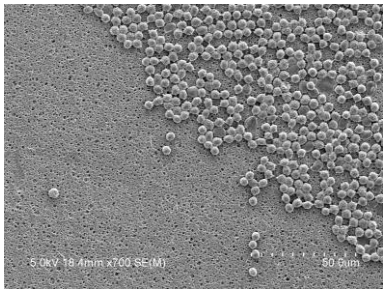
		×4000	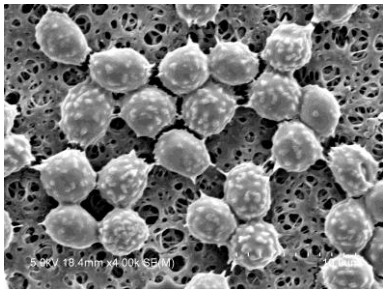

Figure 29e. FSL-Atri kodecytes attached to cotton which has been printed with FSL-Atri and had subsequent attachment of monoclonal anti-A. The cells have clearly attached to the printed area and not to the un-printed area. Interestingly in the ×900 image the cells seemed to have aligned along the cotton fibres.

Surface	Photo	SEM image
Cotton		×300 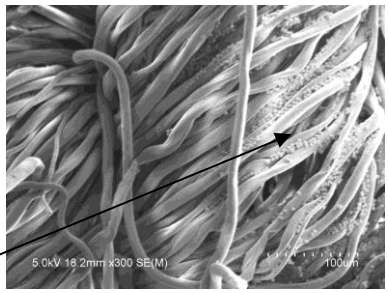
	Printed area	×900 

Figure 29f. FSL-Atri kodecytes attached to aluminium foil which has been printed with FSL-Atri and had subsequent attachment of monoclonal anti-A. The cells have attached to the foil in a monolayer in the printed areas. The photo is not clear due to the difficulty in photographing the foil.

Surface	Photo	SEM image
Aluminium foil		×300 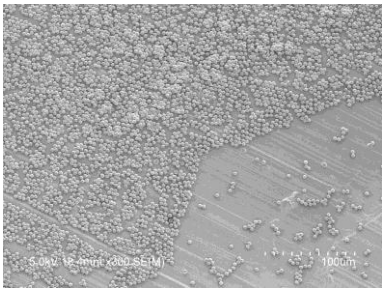
		×1200 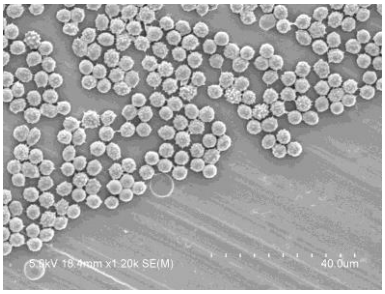

Figure 30. Controls for attaching cells to printed FSLs. FSL-Atri is printed on all surfaces and tested with different cells, or with a missing linker for negative control. The surface was also immunostained with monoclonal anti-A for a positive control. There is no attachment to the printed FSL-A by cells that are not FSL-A kodecytes. The immunostain shows the FSL-A was present on the surface.

Controls	Photo
FSL-Atri, anti-A, Group O cells	
FSL-Atri, anti-A, FSL-biotin kodecytes	
FSL-Atri, no anti-A, FSL-Atri kodecytes	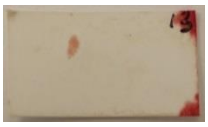
Immunostain positive control	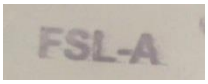

FSL-Atri kodecytes

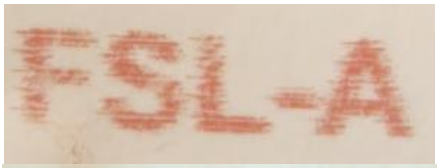

Natural A1 cells

Figure 31. Images comparing FSL-Atri kodecytes and natural A cells attached to printed FSL-Atri on paper using monoclonal anti-A to link the cells to the surface. Cells containing natural A antigen were able to bind to the printed area just as well as the FSL-A kodecytes.

Chapter 3 Discussion

Retaining active biomolecules in a defined area on a surface is the goal of immobilisation. High density loading, long term stability, control over orientation and accessibility for the binding agent are critical parameters for producing microarrays, biosensors and other assays or devices that can utilise immobilised biomolecules. Immobilisation of enzymes, antibodies, DNA, carbohydrates and other biomolecules onto a solid phase allows analysis of multiple biomolecules simultaneously, leading to the development of miniaturised and multiplex systems. It enables sensitive, high-throughput analysis of protein-protein interactions, DNA hybridisation, carbohydrate research, as well as the development of many biotechnology applications (Datta et al., 2013; Larsen et al., 2006; V. Singh et al., 2011). The rapid growth of biochips has led to a demand for reproducible devices with consistent immobilisation procedures, which likely need to be tailored to a specific molecule.

KODE™ technology enables the modification of biological membranes by attaching function-spacer-lipid (FSL) constructs onto the surface of a cell or virion, to impart a new functionality to that surface (Korchagina et al., 2012). Utilising FSL constructs for attaching biological molecules onto solid non-biological surfaces can potentially provide a controllable and reliable approach for immobilisation of a wide variety of molecules for various applications.

This research focussed on determining the ability of FSL constructs to adhere to non-biological surfaces. Prior to this research FSL constructs have been used to modify cells and viruses but not to modify other types of surfaces. Therefore the opportunity existed to explore the immobilisation of these molecules onto different solid surfaces, to investigate the possible mechanisms of attachment and explore uses for this immobilisation.

Methods of delivery

The first research aim was to investigate suitable methods of delivery for the application of FSL constructs onto solid surfaces. Of the methods tested, including painting, soaking and inkjet printing, all were able to deliver FSL constructs onto the relevant surface, and each were useful in certain situations. The emphasis here was to establish inkjet printing as a means of delivery which proved to be a successful method, using a standard desktop inkjet printer.

Inkjet printing has evolved from the printing of text or graphics with traditional ink on paper. Its applications now range from deposition of polymers and inorganic particles (M. Singh et al., 2010; Tekin et al., 2008) to DNA/peptide/carbohydrate microarrays and biosensors (Delaney et al., 2009) and tissue engineering (Mironov et al., 2009). It provides a precise and cost effective method for depositing any material that can be expelled through inkjet nozzles and is able to produce bio-devices in a high-throughput manner. Therefore, this seemed a good choice of

delivery method for FSL constructs, given they are easily dispersed in water, making them an ideal “bioink”.

Inkjet printing allowed very controllable, flexible and precise patterning of these biological molecules onto various surfaces with no degradation observed, demonstrating its excellent use in a biotechnological setting. The printing solution used in this research was a saline solution containing the FSL construct at the required concentration, and a small amount of blue dye to enable visualisation of the printed area. This solution was easily printed from the Epsom printer used, with no modification of the solution necessary. Other authors have reported adjustment of the printing solution by adding agents to alter the surface tension or viscosity, to enable dispensing of biological molecules with this method (Di Risio & Yan, 2008; Setti et al., 2005). The FSLs with this printer required no adjustment, possibly due to the surfactant nature of the molecule reducing the surface tension enough to allow easy ejection of the molecules without causing leaking from the printhead. Although blue dye was used to visualise the printed area this was washed away before immunostaining, leaving a blank surface which only revealed the printed constructs when a specific antibody or binding molecule attached to it. Therefore, a positive reaction allowed the printed text to be read, producing a clear result.

The cleaning of the printing cartridge and of the printhead became an important consideration to reduce contamination between printing cycles of different constructs. As FSLs were able to bind to all the surfaces tested, they were assumed to be attaching to all surfaces they came into contact with, including pipette tips, tubes, and the printing apparatus. This revealed a limitation of this FSL attachment as some undesirable binding to surfaces was probably occurring. Cleaning involved multiple washes with 70% methanol of the cartridge and then running cleaning cycles of the printer with this solution. This was sufficient to remove any detectable FSL constructs from these surfaces.

Inkjet printing allows for text, barcodes, symbols or any meaningful image to be applied to a surface using a biological ink. This can enable unambiguous reading of the result of a diagnostic test or a binding reaction and could also be used to store patient or assay details, by incorporating a unique ID into a specific sample. It is flexible, in that the image or text can be readily changed without having to alter the hardware of the system, allowing printing of different assay formats easily and immediately. By applying FSL constructs to surfaces in this manner, disease markers, carbohydrates or proteins, as well as other useful molecules, can be attached to non-biological surfaces. They can be applied in an area of the surface that is precise and informative to allow fabrication of diagnostic tests, research platforms such as microarrays or capture surfaces for a multitude of applications.

Painting and soaking, as delivery methods, were also investigated. Painting proved useful for materials that could not be put through a printer, requiring a simpler form of dispensing liquid to

a surface. The main difference in the two approaches is the contact versus non-contact technique. However, no difference was observed in ability to attach to a surface. The advantage of non-contact methods i.e. inkjet printing, is the reduction of contamination between the surface and the solution. Soaking surfaces in FSL solution was suitable when attaching FSLs to microbeads. In this case, the beads did not need to be dried but could be taken straight into the assay. Microbeads are valuable tools for capturing and filtering biomolecules or cells, and KODE™ technology provided a straightforward approach for modifying these beads.

Types of surfaces for immobilisation

The second research aim was to determine what types of non-biological surfaces FSL constructs are able to be immobilised on. Remarkably, FSLs were able to attach to all the surfaces tested, which included modified cellulose membranes, papers, synthetic polymers, natural fibrous material, metals and glass. The surface chemistry can play an important part in immobilisation and can affect what will adhere to them. These surfaces consisted of a mixture of porous and non-porous materials, hydrophilic and hydrophobic surfaces, planar and non-planar surfaces. All of these various surface properties did not affect the ability of FSL constructs to immobilise to these solid surfaces, as all types of surface allowed good detection of the FSL molecules, even after going through multiple washing stages of an immunoassay. The attachment to all surfaces was shown to be robust and stable. Staining of surfaces months after printing, revealed no difference compared to those stained immediately after printing. The same specificity and sensitivity was shown. This implies a strong interaction between the FSL and the surface which is not usually seen when molecules are adsorbed onto surfaces. This is encouraging for storage of surfaces printed with FSL constructs.

The main methods of immobilisation of biomolecules onto surfaces include physical adsorption, covalent bonding, cross-linking, entrapment and affinity binding (Kong & Hu, 2012; Sassolas et al., 2012). The method employed in this research involved adsorbing the molecules on the surfaces by simply applying or contacting the surface with a solution of FSL constructs. This was a simple and effective method. In some cases the constructs were dried onto the surface (after printing or painting) and in others the surface was kept in solution (microbeads). No difference was observed when the two methods were directly compared on the same surface, indicating that drying was not necessary for attachment. The constructs, therefore, favoured adsorption onto the surface, over staying in solution. The spontaneous attachment of FSLs to solid surfaces was also demonstrated implying a fast attachment process. No difference in the staining was observed between 5 seconds contact and 600 seconds (10 minutes) contact of the FSL with the surface. This has advantages over other methods of immobilisation, for example covalent attachment methods, which require longer time periods.

Investigations into the attachment of variations of the FSL construct, namely differences in the lipid tail and the functional group without the lipid, gave insights into how these molecules might be adhering to the surfaces. It is clear that of the functional groups tested, immobilisation was not achieved unless the molecule was part of an FSL construct. In addition, alterations of the lipid tail i.e. a sterol lipid or a monoacyl lipid caused reduced or no attachment of the molecule respectively, compared to the diacyl tail. These results taken together suggest the lipid part of the FSL molecule is essential for immobilisation. However, if it was the lipid directly adsorbing to the surfaces it would be expected that these would be observed only on hydrophobic surfaces. However the hydrophilic surfaces retained the FSLs to the same degree as the hydrophobic surfaces. This leads to a theory that it is the amphiphilic nature of these molecules that drives their attachment to the solid surfaces, and it is possible that they are adsorbing onto solid surfaces due to the hydrophobic effect.

Amphiphiles contain a hydrophilic part and a hydrophobic part, known as the head group and the tail respectively. They possess the exceptional ability to spontaneously self-assemble to form complex structures in aqueous solutions (Ramanathan et al., 2013). The dichotomous nature of the molecule causes orientation and aggregation into various formations including micelles, liposomes and bilayers (Evans & Ninham, 1986; Schmid et al., 2004; Tanford, 1987), driven by what is known as the hydrophobic effect (Ben-Naim, 2003; Bergström, 2011). These molecules play important roles in biology due to their role in cell and organelle membranes.

It was Kausmann in 1959 that gave the first insights into the hydrophobic effect in his review of protein folding mechanisms (Kauzmann, 1959). This theory was widely accepted and is now known to be the dominant force in stabilising cell membranes and controlling protein conformation by causing the aggregation of non-polar moieties in aqueous solution (Ben-Naim, 2003; Tanford, 1997). Simply, it is the repulsion of oil and water causing the hydrocarbons to orientate together to remove their contact with water molecules. However it is much more complex, and is actually the attraction of water-to-water that forces the clustering of hydrocarbons or folding of proteins (Southall et al., 2002; Tanford, 1997), although the mechanism is still not fully understood.

The hydrophobic effect is due to the favourable energy state of grouping of non-polar molecules in polar solutions. There is an energy cost saving by separating the polar and non-polar molecules due to their preference for the aqueous and non-aqueous medium respectively (Chandler, 2005; Tanford, 1979). The free energy is composed of enthalpy and entropy, where the enthalpy is the potential energy of interactions between molecules, and entropy is the order of the system. Whilst it is thermodynamically favourable for hydrophobic molecules to self-assemble to remove or reduce contact with water, there is an ordering of the system and hence a change in the entropy (Bergström, 2011). The free energy of the solvation of a cluster of

hydrophobic solutes is lower than the free energy of solvation of the individual molecules, due to the low surface area to volume ratio, resulting in a drive towards aggregation (Chandler, 2005). In terms of entropy, the water molecules become more ordered around the non-polar groups causing a decrease in entropy, which is unfavourable. However, the clustering results in fewer water molecules breaking their hydrogen bonds at the interface of the aggregate, and hence increases the entropy compared to individual molecules (Vance & Vance, 2008). The complex enthalpy and entropy factors are still not fully understood and continue to be debated (Baldwin, 2013; Blokzijl & Engberts, 1993; Southall et al., 2002).

Amphiphiles form structures in water to shield their hydrophobic parts while the hydrophilic group remains in solution. They typically form spherical or cylindrical micelles or bilayers. Micelles are spherical assemblies with a hydrophobic core and hydrophilic surface. Larger structures can be formed resulting from the packing constraints of the specific molecules that prevent the simple micelle formation (Israelachvili et al., 1976). The geometry of the assemblies is determined by the shape of the amphiphile. Small amphiphiles, such as surfactants, will form spheres whereas phospholipids, with their two acyl tails, generally form bilayer structures (Tanford, 1979; C. Wang et al., 2012). These two tails increase the volume of molecule compared to one-tailed molecules, prohibiting globular or cylindrical micelles. Phospholipids tend to form stable, homogenous bilayers, with low critical micelle concentrations, hence their importance in cell and other biological membranes (Israelachvili et al., 1976). It is therefore possible that FSL constructs, with their two-tailed structure assemble into bilayer vesicles (liposomes) in solution, although the size of the head group will play a part in the structure.

Liposomes are known to adsorb onto solid surfaces and form planar layers. This can be a monolayer on a hydrophobic surface or a bilayer on a hydrophilic surface (Jass et al., 2000). Amphiphilic polymers have been shown to absorb onto hydrophobic surfaces by their hydrophobic parts, leaving the hydrophilic section extending out (Freij-Larsson, et al., 1996). Driven by the hydrophobic effect, micelles and individual molecules were adsorbed onto the surface when present in an aqueous solution. FSL constructs, therefore, in liposome or micelle formation in water or as individual molecules, could be adsorbing onto solid surfaces and forming a mono- or bi-layer, depending on the hydrophobicity of the surface. This correlates to what has been observed, in that FSLs are able to attach to hydrophilic and hydrophobic surfaces, which is likely due to their amphiphilic nature.

Of the delivery methods used for FSL dispensing most of them involved drying of the FSL constructs onto the surface. This dehydration could be playing a part in the adherence to solid surfaces. However, as was shown, there was no difference in attachment when the FSL solution was dried onto the surface or not. This implies that the molecules intrinsically adsorb onto these solid surfaces when they come into contact, and do not rely on being dried and forced onto the

surface. This supports the theory that adsorption and the favourable thermodynamics of adhering to the surface and removing the hydrophobic parts of the molecule from contact with water, is the mechanism of attachment.

An advantage of using FSL constructs to immobilise biological molecules to surfaces is the wide variety of molecules that are able to be attached. This included carbohydrates, peptides and biotin, and it is envisaged that any FSL, with due consideration to the size and type of F, will be able to be immobilised onto non-biological surfaces. This is an advantage of using FSLs, as a problem with adsorbing peptides and other small biomolecules onto surfaces is the large degree of desorption that occurs with these molecules (Butler et al., 1992; Uttamchandani & Yao, 2008). Peptide FSLs of 20 residues and carbohydrates containing only 3 or 4 sugars were easily attached onto paper, showing the opportunity of using this technology for immobilising small molecules, which were able to attach strongly to all surfaces tested. These FSLs showed specific binding to various antibodies, demonstrating their retained activity after immobilisation.

One problem encountered with adsorption as a method for immobilisation is the random orientation of the biomolecule on the surface. Presentation of the biomolecule is an important factor and inadequate orientation can impede the activity of the molecule by blocking active sites. It also offers limited control over the immobilisation. Orientation can be controlled by using affinity binding or by covalent process (Prieto-Simon et al., 2008). These are often time consuming as they involve attaching the correct tag or functional group to the molecule. FSL immobilisation is inherently orientated due to the way it is perceived that they adhere to surfaces. This would mean the functional head group is exposed on the surface in an orientated way, able to bind to its binding partner, and is fully controllable by adjusting the concentration of the FSL solution that is used.

The stability of FSL attachment to non-biological surfaces was tested by washing in various detergent and solvent solutions. Some of these solutions caused removal, to various degrees, of the immobilised FSLs, with total removal seen for methanol and triton X-100 at certain concentrations. This strengthens the theory that the lipid tail is involved in the immobilisation as lipids are more soluble in these solutions than in water. These detergents and solvents were able to desorb the FSL molecules back into solution, whereas water and other aqueous solutions did not. This also presents a limitation of FSL immobilisation as some detergents and solvents cannot be used with these bioassays.

Leaching of biomolecules adsorbed onto surfaces is a problem with the physical adsorption method of immobilisation. Therefore, the temporal stability of the immobilised FSLs was also examined to analyse any loss of the FSL constructs from the surface over time. Accelerated trials were carried out at 80°C for 2-12 hours and showed no difference in detection levels

compared to the same sample with no heat treatment. A printed paper surface featuring a range of blood group FSLs was tested at day 1 and after 8 months at room temperature, and no observable difference was detected in sensitivity or specificity. This suggests FSLs are stable at room temperature for at least 8 months and probably longer. Of note is the stability of the immobilised FSL constructs in water as opposed to PBS. No difference was observed after 18 hours soaking in these solutions. FSL constructs are known to be less stable in water than saline solution (FSL data sheets, http://www.sigmaaldrich.com), whereas after immobilisation they are able to survive many hours in water. Compared to other mechanisms for immobilising biomolecules, this shows great benefits of KODE™ technology as stability is a huge factor when assessing immobilisation of biological molecules.

Speculation of the attachment mechanisms of FSL constructs onto surfaces has been discussed but it is still unknown what exact mechanisms apply to each surface. It is probable they are attaching in multiple layers and single layers, encapsulating fibres when present, and binding as aggregates, with combinations of these different mechanisms existing on different surfaces. However, it seems the amphiphilic nature is important and hence the hydrophobic effect seems likely as a binding mechanism.

Bioassays

The third research aim was to analyse the potential use of FSL constructs immobilised onto non-biological surfaces in bioassays. The ability to immobilise biomolecules onto surfaces enables the fabrication of devices that measure the binding reactions of antigens and antibodies, complementary DNA strands, enzymes and ligands, and allows research into variations of epitopes or binding reactions that occur between different molecules.

Three different assays were investigated in this research, including using carbohydrate blood group FSLs to map different monoclonal reagents against different antigens, using peptide FSL constructs as disease markers in a diagnostic assay, and to attach recombinant proteins to a surface using FSL constructs and a linker molecule.

When mapping the monoclonal reagents, good correlation was observed between the printed carbohydrate blood group FSLs and the serological results. Various reaction patterns were identified between different manufacturers of monoclonal antibodies. The serological assay is a standard method for identifying blood groups by analysing the agglutination of the red blood cells after contact with antibodies. The attachment of FSL constructs to a paper surface allowed detection of the antibodies in a solid phase, using an immunostaining technique. 10 different antigens were simultaneously analysed in the same reaction well, eliminating any variations between wells, plates or time differences. The unprinted areas of the wells were used as negative controls, allowing simple comparison between the sensitivity of the different antigens.

Similarly with the Chagas inkjet printed assay, the different epitopes tested were examined side by side, reducing the amount of serum needed, by testing all constructs in the same well. This also allowed direct comparison of the sensitivity and specificity of the different FSL constructs, where FSL-CHA2 proved to give the most accurate results. This assay was carried out to present an example of using an infectious disease marker on a solid surface, using FSL constructs. Chagas was chosen as it was being concurrently developed as a serological test in the laboratory. This allowed comparison between the inkjet printed test and the serological results, and provided an example of peptide FSL constructs immobilised onto solid surfaces.

The different concentrations of the FSL Chagas constructs, printed next to each other in the circular assay, gave insight into the sensitivity of the reaction and enabled optimisation of the printed assay. Interestingly there was a difference seen between the optimal FSL construct to use with kodecytes and the optimal one to use in a solid phase. FSL-CHA2 detected almost all the positive sera when printed onto paper at the stronger concentration, but was much weaker at detecting them when on the surface of a cell. In kodecytes, FSL-CHA4 was able to detect nearly all the positive sera. This illustrates a difference in sensitivity of the same construct depending on the method used, which could relate to the presentation or availability of the antigen on the surface, and demonstrates the importance of the surface when considering sensitivity, not just the peptide structure.

No great optimisation was carried out when examining these assays. In fact, the peptide FSLs were applied to the paper surface optimised for carbohydrate FSLs. There was no investigation of other surfaces for this specific assay, which leaves the opportunity to possibly improve the signal to noise ratio by choosing a different surface. Here, proof of concept applications have been addressed with the aim of identifying certain areas where FSL immobilisation on solid surfaces could be used, and to show some validation of this method compared to standard assays. It was shown that FSLs can be inkjet printed on non-biological surfaces and provide a robust approach to determining antibody attachment from monoclonal or polyclonal samples. It can also provide a standard platform for attaching biotinylated biomolecules to surfaces for further analysis or detection.

Inkjet printing these assays proved to be a simple method for attaching FSL constructs onto precise locations on the surface, in a reproducible manner. By simply loading a reusable ink cartridge with an FSL solution, these assays were printed in a few minutes using a cost effective method. Using standard software, the design of the printed area can be quickly changed. This was shown for the Chagas assay, where a design incorporating concentration levels added more complexity, enabling a greater amount of information to be gained from a single reaction well.

Surfaces printed with FSLs were washed in serum to establish any removal of the constructs in this solution, due to lipids that are present. This did not seem to disrupt the attachment of FSLs

to surfaces, except after 30 hours where some removal was seen. Therefore, diagnostic assays for testing various sera can be carried out on solid phase FSL platforms, without causing impairment to the test.

As well as using FSL constructs produced with a specific antigen, FSLs can also be used to attach various molecules to surfaces, as a more general method to produce assays. FSL-biotin, containing the biotin molecule as its functional head group can used, with avidin, to anchor biotinylated proteins to a surface, which in turn can be used in binding assays. This was tested with a biotinylated HLA protein attached to a paper surface via FSL-biotin and streptavidin. The protein showed specific binding to the FSL-biotin printed area. Even when high concentrations of the protein were loaded into the well, very low background staining was observed. The protein was also shown to be in an active, complete state. The antibodies that were used to react with the protein were able to detect denatured and undenatured forms, which showed low and high staining respectively. Also of note is the low level of protein that was able to be detected. <4 ng of the HLA protein was able to bind and be detected by the appropriate antibodies. Proteins are known to change conformation when adsorbing to a surface (Rabe et al., 2011). KODE™ technology presents a method for adhering proteins to surfaces through FSL-biotin and avidin, where large proteins can bind in an orientated way, probably without disrupting their conformation.

All these bioassays were printed onto a paper surface, as paper was shown to give the best signal to noise ratio of the surfaces tested. Paper is becoming a popular surface for various micro analytical systems, including diagnostics tests and environmental and food testing (Pelton, 2009). Antibodies, enzymes, DNA aptamers, biotin, and cells have been immobilised onto paper through different strategies, to create biosensors. Bioactive paper, i.e. paper containing biomolecules that have recognition properties, has potential uses in developing countries, in the field and in home healthcare applications, where inexpensive, fast reactions and low operating skill requirements are important factors (X. Y. Liu et al., 2011). Colorimetric detection of analytes, for example for tumour markers (S. Wang et al., 2012) or foodborne pathogens (Jokerst et al., 2012), is ideal on paper and lends itself well to analytical paper devices. It is easy to interpret and requires no complex machinery which may not be available where paper based devices are being used.

Microfluidic paper-based analytical devices (μPAD) were introduced by the Whitesides group (Martinez, 2011; Martinez et al., 2007; Martinez et al., 2010). These systems require the creation of hydrophilic and hydrophobic areas using photolithography, to direct the fluid flow, although inkjet has also been utilised for this purpose (Abe et al., 2008). These systems are usually based on enzymatic reactions, which use a colorimetric detection system. Multistep assays can also be achieved on this platform, for example an immunoassay for a malaria protein

has been developed where several inlets allow multiple reagents to be used (Fu et al., 2012). This broadens the scope for paper based assays, which can still be produced cheaply and do not require equipment for testing. Single stranded DNA probes have also been immobilised on paper, to be used in a wicking test to capture target DNA. This has potential use in forensics and other diagnostic tests (Araújo et al., 2012). The use of paper in medical and environmental testing devices has advantages of biocompatibility, low cost, abundance and biodegradability. Being able to immobilise FSL constructs onto paper for use in bioassays can utilise these advantages and enable multiplex assays for use in settings where equipment free testing is required. The simple attachment process of FSLs to solid surfaces and their stability once immobilised, could enhance the advantages of these systems.

Attaching cells

The final research question was to evaluate the binding of cells to immobilised FSL constructs. This involved making kodecytes or using natural cells with the appropriate antigen and attaching them to a surface printed with FSLs and using affinity binding of a linker molecule. This linker was either avidin when using FSL-biotin or an antibody when using blood group FSLs. The ability to attach cells to surface has the potential to be used to create cell arrays or whole cell sensors, and also for building up layers of cells on surfaces to create tissue.

This research has shown the ability to anchor blood cells onto a variety of surfaces where they adhered well to the area printed with FSL constructs, or onto microbeads modified with FSLs. This was a simple technique involving the attachment of the FSL to the surface and attaching the same type of FSL to the cell. This was followed by attaching the linker molecule to the surface then incubating with the modified cells, where they successfully bound to the linker molecule and hence attached to the surface. Inkjet printing the FSL constructs onto the surface enable patterned cell-adhesive surfaces to be generated. The ability to attach live cells to surfaces opens up opportunities for using them as biosensors, although their extracellular environment would need to be controlled.

The methods of attachment of cells to surfaces can be through affinity binding through the RGD sequence, using growth factor molecules or even DNA. The RGD sequence found in integrin receptors is an attractive method for immobilising cells as many cells will adhere to this motif. This peptide does however need to be attached to the surface in some way, for example though self- assembled monolayers (SAMs), or by chemisorption methods (Choi et al., 2005; Sánchez-Cortés et al., 2010). DNA hybridisation can also be utilised to attach cells to surfaces. Covalent methods have been used to attach ssDNA to a surface and the complementary strand to a cell for immobilisation on glass (Hsiao et al., 2009). Both these strategies could be employed using KODE™ technology, where instead of biotin or an antigen, RGD or ssDNA could be incorporated into an FSL construct to bind cells to surfaces. This would remove the covalent

requirement of the procedure, which is inherently more costly and time consuming, and would simply involve adsorbing FSL constructs onto surfaces and producing kodecytes. In fact RGD FSLs would remove the need to modify the cell at all, and so would only require a one step procedure of adhering the FSL to the surface, to produce a patterned surface for precise cell immobilisation.

Other than cell arrays and biosensors, there is potential to use immobilised cells in live bandages, where white blood cells could be attached to a suitable bandage material to provide enhanced wound care to an affected area. Sophisticated bandages exist that contain extracellular matrix molecules to aid wound and tissue repair. Positioning of cells in layers can also be advantageous to create tissue with a view to fabricating grafts or even organs for transplantation. This is currently being researched by groups exploring organ printing (Cui & Boland, 2009; Cui et al., 2010; Rezende et al., 2013).

To continue this research, investigation into the state of the cells once immobilised needs to be carried out. Whilst their attachment has been shown, the viability, stability and protection remains to be examined. For use in assays, bandages or as tissue, the cells would need to be protected from the outside environment, to be kept hydrated and be provided with nutrients to remain viable. Cells other than red blood cells would also be required, so investigation into the attachment of various cell types onto surfaces would need to be determined. This research has provided a starting point for patterning cells on solid surfaces using KODE™ technology.

Conclusion

Immobilisation of FSL constructs is an easily controlled, orientated, fast and simple procedure, which can be used to modify non-biological surfaces with virtually any biological molecule able to be incorporated into an FSL construct. KODE™ technology is a powerful tool for creating surfaces functionalised with biological molecules which could be useful for diagnostic assays, for profiling immune responses, to detect or identify biomarkers or specific epitopes, to fabricate biosensors, for capture assays or cellular immobilisation, and has the potential to be used in many biological assays where stable immobilisation of biomolecules is required. Its significance is in its broad, general applicability to surfaces, whether they are cells, paper, metals or polymers. This technology possesses the capability of being a universal tool for bio-modification of surfaces.

Future applications for KODE™ technology need not be limited to diagnostics or microarrays. With the ability to potentially modify any surface with biological molecules, any anchoring or detection application can be investigated. Further, it need not be limited to medical or environmental testing but could be extended to industrial uses such as anti- counterfeiting using an advanced ink. This research provided insights into the extent of FSL attachment, its limitations, and the potential for KODE™ to be used as a broad surface modification technology.

References

Abe, K., Suzuki, K., & Citterio, D. (2008). Inkjet-printed microfluidic multianalyte chemical sensing paper. *Analytical Chemistry, 80*(18), 6928-6934. doi:10.1021/ac800604v

Adeloju, S. B., & Lawal, A. T. (2011). Fabrication of a bilayer potentiometric phosphate biosensor by cross-link immobilization with bovine serum albumin and glutaraldehyde. *Analytica Chimica Acta, 691*(1–2), 89-94. doi:10.1016/j.aca.2011.02.020

Aissaoui, N., Bergaoui, L., Landoulsi, J., Lambert, J.-F., & Boujday, S. (2011). Silane Layers on Silicon Surfaces: Mechanism of Interaction, Stability, and Influence on Protein Adsorption. *Langmuir, 28*(1), 656-665. doi:10.1021/la2036778

Alvarez, G., Foglia, M., Copello, G., Desimone, M., & Diaz, L. (2009). Effect of various parameters on viability and growth of bacteria immobilized in sol–gel-derived silica matrices. *Applied Microbiology and Biotechnology, 82*(4), 639-646. doi:10.1007/s00253-008-1783-9

Andreescu, S., & Marty, J.-L. (2006). Twenty years research in cholinesterase biosensors: From basic research to practical applications. *Biomolecular Engineering, 23*(1), 1-15. doi:10.1016/j.bioeng.2006.01.001

Angeloni, S., Ridet, J. L., Kusy, N., Gao, H., Crevoisier, F., Guinchard, S., ... Sprenger, N. (2005). Glycoprofiling with micro-arrays of glycoconjugates and lectins. *Glycobiology, 15*(1), 31-41. doi:10.1093/glycob/cwh143

Angenendt, P., Glökler, J., Murphy, D., Lehrach, H., & Cahill, D. J. (2002). Toward optimized antibody microarrays: a comparison of current microarray support materials. *Analytical Biochemistry, 309*(2), 253-260. doi:10.1016/S0003-2697(02)00257-9

Araújo, A. C., Song, Y., Lundeberg, J., Ståhl, P. L., & Brumer, H. (2012). Activated Paper Surfaces for the Rapid Hybridization of DNA through Capillary Transport. *Analytical Chemistry, 84*(7), 3311-3317. doi:10.1021/ac300025v

Auburn, R. P., Kreil, D. P., Meadows, L. A., Fischer, B., Matilla, S. S., & Russell, S. (2005). Robotic spotting of cDNA and oligonucleotide microarrays. *Trends in Biotechnology, 23*(7), 374-379. doi:10.1016/j.tibtech.2005.04.002

Baldwin, R. L. (2013). The new view of hydrophobic free energy. *FEBS Letters, 587*(8), 1062-1066. doi:10.1016/j.febslet.2013.01.006

Bankar, S. B., Bule, M. V., Singhal, R. S., & Ananthanarayan, L. (2009). Glucose oxidase — An overview. *Biotechnology Advances, 27*(4), 489-501. doi:10.1016/j.biotechadv.2009.04.003

Barhoumi, H., Maaref, A., Cosnier, S., Martelet, C., & Jaffrezic-Renault, N. (2008). Urease immobilization on biotinylated polypyrrole coated ChemFEC devices for urea biosensor development. *IRBM, 29*(2–3), 192-201. doi:10.1016/j.rbmret.2007.11.004

Beckmann, H. S. G., Niederwieser, A., Wiessler, M., & Wittmann, V. (2012). Preparation of Carbohydrate Arrays by Using Diels–Alder Reactions with Inverse Electron Demand. *Chemistry – A European Journal, 18*(21), 6548-6554. doi:10.1002/chem.201200382

Ben-Naim, A. (2003). Hydrophobic hydrophilic phenomena in biochemical processes. *Biophysical Chemistry, 105*(2–3), 183-193. doi:10.1016/S0301-4622(03)00088-7

Ben-Yoav, H., Melamed, S., Freeman, A., Shacham-Diamand, Y., & Belkin, S. (2011). Whole-cell biochips for bio-sensing: integration of live cells and inanimate surfaces. *Critical Reviews in Biotechnology, 31*(4), 337-353. doi:10.3109/07388551.2010.532767

Berezhetskyy, A. L., Sosovska, O. F., Durrieu, C., Chovelon, J. M., Dzyadevych, S. V., & Tran-Minh, C. (2008). Alkaline phosphatase conductometric biosensor for heavy-metal ions determination. *IRBM, 29*(2–3), 136-140. doi:10.1016/j.rbmret.2007.12.007

Bergström, L. M. (2011). *Thermodynamics of Self-Assembly, Application of Thermodynamics to Biological and Materials Science, Prof. Mizutani Tadashi (Ed.), ISBN: 978-953-307-980-6, InTech, DOI: 10.5772/13711* Retrieved from http://www.intechopen.com/books/application-of-thermodynamics-to-biological-and-materials-science/thermodynamics-of-self-assembly

Berrade, L., Garcia, A., & Camarero, J. (2011). Protein Microarrays: Novel Developments and Applications. *Pharmaceutical Research, 28*(7), 1480-1499. doi:10.1007/s11095-010-0325-1

Betancor, L., López-Gallego, F., Hidalgo, A., Alonso-Morales, N., Mateo, G. D.-O. C., Fernández-Lafuente, R., & Guisán, J. M. (2006). Different mechanisms of protein immobilization on glutaraldehyde activated supports: Effect of support activation and immobilization conditions. *Enzyme and Microbial Technology, 39*(4), 877-882. doi:10.1016/j.enzmictec.2006.01.014

Bhatia, S. K., Shriver-Lake, L. C., Prior, K. J., Georger, J. H., Calvert, J. M., Bredehorst, R., & Ligler, F. S. (1989). Use of thiol-terminal silanes and heterobifunctional crosslinkers for immobilization of antibodies on silica surfaces. *Analytical Biochemistry, 178*(2), 408-413. doi:10.1016/0003-2697(89)90662-3

Billah, M. M., Hodges, C. S., Hays, H. C. W., & Millner, P. A. (2010). Directed immobilization of reduced antibody fragments onto a novel SAM on gold for myoglobin impedance immunosensing. *Bioelectrochemistry, 80*(1), 49-54. doi:10.1016/j.bioelechem.2010.08.005

Binder, K. W., Allen, A. J., Yoo, J. J., & Atala, A. (2011). Drop-On-Demand Inkjet Bioprinting: A Primer. *Gene Therapy and Regulation, 06*(01), 33-49. doi:10.1142/S1568558611000258

Blake, D. A., Bovin, N. V., Bess, D., & Henry, S. M. (2011). FSL Constructs: A Simple Method for Modifying Cell/Virion Surfaces with a Range of Biological Markers Without Affecting their Viability. *J Vis Exp*(54), e3289. doi:doi:10.3791/3289

Blixt, O., Head, S., Mondala, T., Scanlan, C., Huflejt, M. E., Alvarez, R., ... Paulson, J. C. (2004). Printed covalent glycan array for ligand profiling of diverse glycan binding proteins. *Proceedings of the National Academy of Sciences of the United States of America, 101*(49), 17033-17038. doi:10.1073/pnas.0407902101

Blokzijl, W., & Engberts, J. B. F. N. (1993). Hydrophobic Effects. Opinions and Facts. *Angewandte Chemie International Edition in English, 32*(11), 1545-1579. doi:10.1002/anie.199315451

Bochner, B. S., Alvarez, R. A., Mehta, P., Bovin, N. V., Blixt, O., White, J. R., & Schnaar, R. L. (2005). Glycan Array Screening Reveals a Candidate Ligand for Siglec-8. *Journal of Biological Chemistry, 280*(6), 4307-4312. doi:10.1074/jbc.M412378200

Boland, T., Mironov, V., Gutowska, A., Roth, E. A., & Markwald, R. R. (2003). Cell and organ printing 2: Fusion of cell aggregates in three-dimensional gels. *The Anatomical Record Part A: Discoveries in Molecular, Cellular, and Evolutionary Biology, 272A*(2), 497-502. doi:10.1002/ar.a.10059

Boland, T., Xu, T., Damon, B., & Cui, X. (2006). Application of inkjet printing to tissue engineering. *Biotechnology Journal, 1*(9), 910-917. doi:10.1002/biot.200600081

Boozer, C., Ladd, J., Chen, S., & Jiang, S. (2006). DNA-Directed Protein Immobilization for Simultaneous Detection of Multiple Analytes by Surface Plasmon Resonance Biosensor. *Analytical Chemistry, 78*(5), 1515-1519. doi:10.1021/ac051923l

Boozer, C., Ladd, J., Chen, S., Yu, Q., Homola, J., & Jiang, S. (2004). DNA Directed Protein Immobilization on Mixed ssDNA/Oligo(ethylene glycol) Self-Assembled Monolayers for Sensitive Biosensors. *Analytical Chemistry, 76*(23), 6967-6972. doi:10.1021/ac048908l

Bora, U., Sharma, P., Kannan, K., & Nahar, P. (2006). Photoreactive cellulose membrane—A novel matrix for covalent immobilization of biomolecules. *Journal of Biotechnology, 126*(2), 220-229. doi:10.1016/j.jbiotec.2006.04.013

Brady, D., & Jordaan, J. (2009). Advances in enzyme immobilisation. *Biotechnology Letters, 31*(11), 1639-1650. doi:10.1007/s10529-009-0076-4

Braun, S., Rappoport, S., Zusman, R., Avnir, D., & Ottolenghi, M. (1990). Biochemically active sol-gel glasses: the trapping of enzymes. *Materials Letters, 10*(1–2), 1-5. doi:10.1016/0167-577X(90)90002-4

Breitenstein, M., Holzel, R., & Bier, F. (2010). Immobilization of different biomolecules by atomic force microscopy. *Journal of Nanobiotechnology, 8*(1), 10. doi:10.1186/1477-3155-8-10

Bryan, M. C., Plettenburg, O., Sears, P., Rabuka, D., Wacowich-Sgarbi, S., & Wong, C.-H. (2002). Saccharide Display on Microtiter Plates. *Chemistry and Biology, 9*(6), 713-720. doi:10.1016/S1074-5521(02)00155-2

Butler, J. E., Ni, L., Nessler, R., Joshi, K. S., Suter, M., Rosenberg, B., ... Cantarero, L. A. (1992). The physical and functional behavior of capture antibodies adsorbed on polystyrene. *Journal of Immunological Methods, 150*(1–2), 77-90. doi:10.1016/0022-1759(92)90066-3

Butterfield, D. A., Bhattacharyya, D., Daunert, S., & Bachas, L. (2001). Catalytic biofunctional membranes containing site-specifically immobilized enzyme arrays: a review. *Journal of Membrane Science, 181*(1), 29-37. doi:10.1016/S0376-7388(00)00342-2

Campbell, P. G., Miller, E. D., Fisher, G. W., Walker, L. M., & Weiss, L. E. (2005). Engineered spatial patterns of FGF-2 immobilized on fibrin direct cell organization. *Biomaterials, 26*(33), 6762-6770. doi:10.1016/j.biomaterials.2005.04.032

Carturan, G., Dal Toso, R., Boninsegna, S., & Dal Monte, R. (2004). Encapsulation of functional cells by sol-gel silica: actual progress and perspectives for cell therapy [10.1039/B401450B]. *Journal of Materials Chemistry, 14*(14), 2087-2098. doi:10.1039/b401450b

Cha, T., Guo, A., & Zhu, X.-Y. (2005). Enzymatic activity on a chip: The critical role of protein orientation. *PROTEOMICS, 5*(2), 416-419. doi:10.1002/pmic.200400948

Chaki, N. K., & Vijayamohanan, K. (2002). Self-assembled monolayers as a tunable platform for biosensor applications. *Biosensors and Bioelectronics, 17*(1–2), 1-12. doi:10.1016/S0956-5663(01)00277-9

Chan, L., Cross, H., She, J., Cavalli, G., Martins, H., & Neylon, C. (2007). Covalent Attachment of Proteins to Solid Supports and Surfaces via Sortase-Mediated Ligation. *PLoS ONE, 2*(11). doi:10.1371/journal.pone.0001164

Chandler, D. (2005). Interfaces and the driving force of hydrophobic assembly. *Nature 437*, 640-647. doi:10.1038/nature04162

Chang, S.-H., Han, J.-L., Tseng, S. Y., Lee, H.-Y., Lin, C.-W., Lin, Y.-C., ... Wong, C.-H. (2010). Glycan Array on Aluminum Oxide-Coated Glass Slides through Phosphonate Chemistry. *Journal of the American Chemical Society, 132*(38), 13371-13380. doi:10.1021/ja1046523

Chirra, H. D., Sexton, T., Biswal, D., Hersh, L. B., & Hilt, J. Z. (2011). Catalase-coupled gold nanoparticles: Comparison between the carbodiimide and biotin–streptavidin methods. *Acta Biomaterialia, 7*(7), 2865-2872. doi:10.1016/j.actbio.2011.01.003

Choi, J.-W., Park, K.-W., Lee, D.-B., Lee, W., & Lee, W. H. (2005). Cell immobilization using self-assembled synthetic oligopeptide and its application to biological toxicity detection using surface plasmon resonance. *Biosensors and Bioelectronics, 20*(11), 2300-2305. doi:10.1016/j.bios.2004.11.019

Christman, K. L., Enriquez-Rios, V. D., & Maynard, H. D. (2006). Nanopatterning proteins and peptides [10.1039/B611000B]. *Soft Matter, 2*(11), 928-939. doi:10.1039/b611000b

Clow, F., Fraser, J., & Proft, T. (2008). Immobilization of proteins to biacore sensor chips using Staphylococcus aureus sortase A. *Biotechnology Letters, 30*(9), 1603-1607. doi:10.1007/s10529-008-9718-1

Coad, B. R., Jasieniak, M., Griesser, S. S., & Griesser, H. J. (2013). Controlled covalent surface immobilisation of proteins and peptides using plasma methods. *Surface and Coatings Technology*(0). doi:10.1016/j.surfcoat.2013.05.019

Cook, C., Wang, T., & Derby, B. (2009). Inkjet printing of enzymes for glucose biosensors Symposium conducted at the meeting of the Materials Research Society Symposium Proceedings Retrieved from http://www.scopus.com/inward/record.url?eid=2-s2.0-77649124711&partnerID=40&md5=8333926f987f3edab82d09d6210e5ca7

Cook, C. C., Wang, T., & Derby, B. (2010). Inkjet delivery of glucose oxidase [10.1039/C0CC00567C]. *Chemical Communications, 46*(30), 5452-5454. doi:10.1039/c0cc00567c

Cooley, P., Wallace, D., & Antohe, B. (2002). Applicatons of Ink-Jet Printing Technology to BioMEMS and Microfluidic Systems. *Journal of the Association for Laboratory Automation, 7*(5), 33-39. doi:10.1016/S1535-5535(04)00214-X

Cosnier, S. (1999). Biomolecule immobilization on electrode surfaces by entrapment or attachment to electrochemically polymerized films. A review. *Biosensors and Bioelectronics, 14*(5), 443-456. doi:10.1016/S0956-5663(99)00024-X

Cui, X., & Boland, T. (2009). Human microvasculature fabrication using thermal inkjet printing technology. *Biomaterials, 30*(31), 6221-6227. doi:10.1016/j.biomaterials.2009.07.056

Cui, X., Dean, D., Ruggeri, Z. M., & Boland, T. (2010). Cell damage evaluation of thermal inkjet printed Chinese hamster ovary cells. *Biotechnology and Bioengineering, 106*(6), 963-969. doi:10.1002/bit.22762

Cui, X., Gao, G., & Qiu, Y. (2013). Accelerated myotube formation using bioprinting technology for biosensor applications. *Biotechnology Letters, 35*(3), 315-321. doi:10.1007/s10529-012-1087-0

Cunha, A., Fernández-Lorente, G., Bevilaqua, J., Destain, J., Paiva, L. C., Freire, D. G., ... Guisán, J. (2008). Immobilization of Yarrowia lipolytica Lipase—a Comparison of Stability of Physical Adsorption and Covalent Attachment Techniques. *Applied Biochemistry and Biotechnology, 146*(1-3), 49-56. doi:10.1007/s12010-007-8073-3

Datta, S., Christena, L. R., & Rajaram, Y. (2013). Enzyme immobilization: an overview on techniques and support materials. *3 Biotech, 3*(1), 1-9. doi:10.1007/s13205-012-0071-7

de Boer, A. R., Hokke, C. H., Deelder, A. M., & Wuhrer, M. (2007). General Microarray Technique for Immobilization and Screening of Natural Glycans. *Analytical Chemistry, 79*(21), 8107-8113. doi:10.1021/ac071187g

de Gans, B.-J., & Schubert, U. S. (2003). Inkjet Printing of Polymer Micro-Arrays and Libraries: Instrumentation, Requirements, and Perspectives. *Macromolecular Rapid Communications, 24*(11), 659-666. doi:10.1002/marc.200350010

Delaney, J. T., Smith, P. J., & Schubert, U. S. (2009). Inkjet printing of proteins. *Soft Matter, 5*(24), 4866-4877.

Derby, B. (2010). Inkjet Printing of Functional and Structural Materials: Fluid Property Requirements, Feature Stability, and Resolution. *Annual Review of Materials Research, 40*(1), 395-414. doi:doi:10.1146/annurev-matsci-070909-104502

Derby, B. (2011). Inkjet printing ceramics: From drops to solid. *Journal of the European Ceramic Society, 31*(14), 2543-2550. doi:10.1016/j.jeurceramsoc.2011.01.016

Derby, B. (2012). Printing and Prototyping of Tissues and Scaffolds. *Science, 338*(6109), 921-926. doi:10.1126/science.1226340

Di Risio, S., & Yan, N. (2007). Piezoelectric Ink-Jet Printing of Horseradish Peroxidase: Effect of Ink Viscosity Modifiers on Activity. *Macromolecular Rapid Communications, 28*(18-19), 1934-1940. doi:10.1002/marc.200700226

Di Risio, S., & Yan, N. (2008). Piezoelectric ink jet printing of horseradish peroxidase on fibrous supports. *Journal of Pulp and Paper Science, 34*(4), 203-211.

Di Risio, S., & Yan, N. (2009). Adsorption and inactivation behavior of horseradish peroxidase on cellulosic fiber surfaces. *Journal of Colloid and Interface Science, 338*(2), 410-419. doi:10.1016/j.jcis.2009.07.005

Di Risio, S., & Yan, N. (2010). Bioactive Paper Through Inkjet Printing [Article]. *Journal of Adhesion Science and Technology, 24*(3), 661-684. doi:10.1163/016942409x12561252292387

Dong, H., Li, C. M., Chen, W., Zhou, Q., Zeng, Z. X., & Luong, J. H. T. (2006). Sensitive Amperometric Immunosensing Using Polypyrrolepropylic Acid Films for Biomolecule Immobilization. *Analytical Chemistry, 78*(21), 7424-7431. doi:10.1021/ac060657o

Douglas, E. S., Chandra, R. A., Bertozzi, C. R., Mathies, R. A., & Francis, M. B. (2007). Self-assembled cellular microarrays patterned using DNA barcodes [10.1039/B708666K]. *Lab on a Chip, 7*(11), 1442-1448. doi:10.1039/b708666k

Dunn, B., Miller, J. M., Dave, B. C., Valentine, J. S., & Zink, J. I. (1998). Strategies for encapsulating biomolecules in sol–gel matrices. *Acta Materialia, 46*(3), 737-741. doi:10.1016/S1359-6454(97)00254-1

Duroux, M., Skovsen, E., Neves-Petersen, M. T., Duroux, L., Gurevich, L., & Petersen, S. B. (2007). Light-induced immobilisation of biomolecules as an attractive alternative to microdroplet dispensing-based arraying technologies. *PROTEOMICS, 7*(19), 3491-3499. doi:10.1002/pmic.200700472

Ekblad, T., & Liedberg, B. (2010). Protein adsorption and surface patterning. *Current Opinion in Colloid & Interface Science, 15*(6), 499-509. doi:10.1016/j.cocis.2010.07.008

Elad, T., Lee, J. H., Belkin, S., & Gu, M. B. (2008). Microbial whole-cell arrays. *Microbial Biotechnology, 1*(2), 137-148. doi:10.1111/j.1751-7915.2007.00021.x

Elbert, D. L. (2011). Bottom-up tissue engineering. *Current Opinion in Biotechnology, 22*(5), 674-680. doi:10.1016/j.copbio.2011.04.001

Elliott, R. B., Escobar, L., Tan, P. L. J., Muzina, M., Zwain, S., & Buchanan, C. (2007). Live encapsulated porcine islets from a type 1 diabetic patient 9.5 yr after xenotransplantation. *Xenotransplantation, 14*(2), 157-161. doi:10.1111/j.1399-3089.2007.00384.x

Ellis, S. R., Ferris, C. J., Gilmore, K. J., Mitchell, T. W., Blanksby, S. J., & in het Panhuis, M. (2012). Direct Lipid Profiling of Single Cells from Inkjet Printed Microarrays. *Analytical Chemistry, 84*(22), 9679-9683. doi:10.1021/ac302634u

Esseghaier, C., Bergaoui, Y., ben Fredj, H., Tlili, A., Helali, S., Ameur, S., & Abdelghani, A. (2008). Impedance spectroscopy on immobilized streptavidin horseradish peroxidase layer for biosensing. *Sensors and Actuators B: Chemical, 134*(1), 112-116. doi:10.1016/j.snb.2008.04.016

Evans, D. F., & Ninham, B. W. (1986). Molecular forces in the self-organization of amphiphiles. *The Journal of Physical Chemistry, 90*(2), 226-234. doi:10.1021/j100274a005

Feizi, T., Fazio, F., Chai, W., & Wong, C.-H. (2003). Carbohydrate microarrays -- a new set of technologies at the frontiers of glycomics. *Current Opinion in Structural Biology, 13*(5), 637-645. doi:10.1016/j.sbi.2003.09.002

Fernández-Lorente, G., Palomo, J. M., Mateo, C., Munilla, R., Ortiz, C., Cabrera, Z., ... Fernández-Lafuente, R. (2006). Glutaraldehyde Cross-Linking of Lipases Adsorbed on Aminated Supports in the Presence of Detergents Leads to Improved Performance. *Biomacromolecules, 7*(9), 2610-2615. doi:10.1021/bm060408+

Flavel, B. S., Sweetman, M. J., Shearer, C. J., Shapter, J. G., & Voelcker, N. H. (2011). Micropatterned Arrays of Porous Silicon: Toward Sensory Biointerfaces. *Acs Applied Materials & Interfaces, 3*(7), 2463-2471. doi:10.1021/am2003526

Frame, T., Carroll, T., Korchagina, E., Bovin, N., & Henry, S. (2007). Synthetic glycolipid modification of red blood cell membranes. *Transfusion, 47*(5), 876-882. doi:10.1111/j.1537-2995.2007.01204.x

Freij-Larsson, C., Nylander, T., Jannasch, P., & Wesslén, B. (1996). Adsorption behaviour of amphiphilic polymers at hydrophobic surfaces: effects on protein adsorption. *Biomaterials, 17*(22), 2199-2207. doi:10.1016/0142-9612(96)00050-6

Fridley, G. E., Holstein, C. A., Oza, S. B., & Yager, P. (2013). The evolution of nitrocellulose as a material for bioassays. *MRS Bulletin, 38*(04), 326-330. doi:10.1557/mrs.2013.60

Fu, E., Liang, T., Spicar-Mihalic, P., Houghtaling, J., Ramachandran, S., & Yager, P. (2012). Two-Dimensional Paper Network Format That Enables Simple Multistep Assays for Use in Low-Resource Settings in the Context of Malaria Antigen Detection. *Analytical Chemistry, 84*(10), 4574-4579. doi:10.1021/ac300689s

Fukui, S., Feizi, T., Galustian, C., Lawson, A. M., & Chai, W. (2002). Oligosaccharide microarrays for high-throughput detection and specificity assignments of carbohydrate-protein interactions. *Nature Biotechnology, 20*(10), 1011. doi:10.1038/nbt735

Galanina, O., Chinarev, A., Shilova, N., Sablina, M., & Bovin, N. (2012). Immobilization of Polyacrylamide-Based Glycoconjugates on Solid Phase in Immunosorbent Assays. In Y. Chevolot (Ed.), *Carbohydrate Microarrays* (Vol. 808, pp. 167-182): Humana Press. doi:10.1007/978-1-61779-373-8_12

Ganesana, M., Istarnboulie, G., Marty, J.-L., Noguer, T., & Andreescu, S. (2011). Site-specific immobilization of a (His)6-tagged acetylcholinesterase on nickel nanoparticles for highly sensitive toxicity biosensors. *Biosensors and Bioelectronics, 30*(1), 43-48. doi:10.1016/j.bios.2011.08.024

Gao, J., Ma, L., Liu, D., & Wang, Z. (2012). Microarray-Based Technology for Glycomics Analysis. *Combinatorial Chemistry & High Throughput Screening, 15*(1), 90-99. doi:10.2174/138620712798280808

Georgakopoulos, T., Komarraju, S., Henry, S., & Bertolini, J. (2012). An improved Fc function assay utilizing CMV antigen-coated red blood cells generated with synthetic function–spacer–lipid constructs. *Vox Sanguinis, 102*(1), 72-78. doi:10.1111/j.1423-0410.2011.01512.x

Giangrande, C., Colarusso, L., Lanzetta, R., Molinaro, A., Pucci, P., & Amoresano, A. (2013). Innate immunity probed by lipopolysaccharides affinity strategy and proteomics. *Analytical and Bioanalytical Chemistry, 405*(2-3), 775-784. doi:10.1007/s00216-012-6204-3

Goda, T., & Miyahara, Y. (2013). Label-free and reagent-less protein biosensing using aptamer-modified extended-gate field-effect transistors. *Biosensors and Bioelectronics, 45*(0), 89-94. doi:10.1016/j.bios.2013.01.053

Goddard, J. M., & Hotchkiss, J. H. (2007). Polymer surface modification for the attachment of bioactive compounds. *Progress in Polymer Science, 32*(7), 698-725. doi:10.1016/j.progpolymsci.2007.04.002

Godula, K., & Bertozzi, C. R. (2010). Synthesis of Glycopolymers for Microarray Applications via Ligation of Reducing Sugars to a Poly(acryloyl hydrazide) Scaffold. *Journal of the American Chemical Society, 132*(29), 9963-9965. doi:10.1021/ja103009d

Goldmann, T., & Gonzalez, J. S. (2000). DNA-printing: utilization of a standard inkjet printer for the transfer of nucleic acids to solid supports. *Journal of Biochemical and Biophysical Methods, 42*(3), 105-110. doi:10.1016/s0165-022x(99)00049-4

Gopalan, A. I., Komathi, S., Sai Anand, G., & Lee, K.-P. (2013). Nanodiamond based sponges with entrapped enzyme: A novel electrochemical probe for hydrogen peroxide. *Biosensors and Bioelectronics, 46*(0), 136-141. doi:10.1016/j.bios.2013.02.036

Gray, J. J. (2004). The interaction of proteins with solid surfaces. *Current Opinion in Structural Biology, 14*(1), 110-115. doi:10.1016/j.sbi.2003.12.001

Green, N. M. (1963). Avidin. 3. The nature of the biotin-binding site. *Biochem. J.* (89), 599-609.

Green, N. M. (1990). [5] Avidin and streptavidin. In W. Meir & A. B. Edward (Eds.), *Methods in Enzymology* (Vol. Volume 184, pp. 51-67): Academic Press. Retrieved from http://www.sciencedirect.com/science/article/pii/007668799084259J. doi:10.1016/0076-6879(90)84259-J

Grönbeck, H., Curioni, A., & Andreoni, W. (2000). Thiols and Disulfides on the Au(111) Surface: The Headgroup−Gold Interaction. *Journal of the American Chemical Society, 122*(16), 3839-3842. doi:10.1021/ja993622x

Guidini, C. Z., Fischer, J., Santana, L. N. S., Cardoso, V. L., & Ribeiro, E. J. (2010). Immobilization of Aspergillus oryzae β-galactosidase in ion exchange resins by combined ionic-binding method and cross-linking. *Biochemical Engineering Journal, 52*(2–3), 137-143. doi:10.1016/j.bej.2010.07.013

Gupta, R., & Chaudhury, N. K. (2007). Entrapment of biomolecules in sol–gel matrix for applications in biosensors: Problems and future prospects. *Biosensors and Bioelectronics, 22*(11), 2387-2399. doi:10.1016/j.bios.2006.12.025

Ha, E.-J., Kim, K., Park, H., Lee, S.-G., Lee, J.-O., An, S., & Paik, H.-j. (2013). One-step immobilization and purification of his-tagged enzyme using poly(2-acetamidoacrylic acid) hydrogel. *Macromolecular Research, 21*(1), 5-9. doi:10.1007/s13233-013-1007-8

Hadac, E. M., Federspiel, M. J., Chernyy, E., Tuzikov, A., Korchagina, E., Bovin, N. V., ... Henry, S. M. (2011). Fluorescein and radiolabeled Function-Spacer-Lipid constructs allow for simple in vitro and in vivo bioimaging of enveloped virions. *Journal of Virological Methods, 176*(1–2), 78-84. doi:10.1016/j.jviromet.2011.06.005

Hanefeld, U., Gardossi, L., & Magner, E. (2009). Understanding enzyme immobilisation [10.1039/B711564B]. *Chemical Society Reviews, 38*(2), 453-468. doi:10.1039/b711564b

Hansson, G. C., Karlsson, K.-A., Larson, G., Strömberg, N., & Thurin, J. (1985). Carbohydrate-specific adhesion of bacteria to thin-layer chromatograms: A rationalized approach to the study of host cell glycolipid receptors. *Analytical Biochemistry, 146*(1), 158-163. doi:10.1016/0003-2697(85)90410-5

Hart, T., Zhao, A., Garg, A., Bolusani, S., & Marcotte, E. M. (2009). Human Cell Chips: Adapting DNA Microarray Spotting Technology to Cell-Based Imaging Assays. *PLoS ONE, 4*(10), e7088. doi:10.1371/journal.pone.0007088

Hasenbank, M. S., Edwards, T., Fu, E., Garzon, R., Kosar, T. F., Look, M., ... Yager, P. (2008). Demonstration of multi-analyte patterning using piezoelectric inkjet printing of multiple layers. *Analytica Chimica Acta, 611*(1), 80-88. doi:10.1016/j.aca.2008.01.048

Heathcote, D., Carroll, T., Wang, J.-J., Flower, R., Rodionov, I., Tuzikov, A., ... Henry, S. (2010). IMMUNOHEMATOLOGY: Novel antibody screening cells, MUT+Mur kodecytes, created by attaching peptides onto red blood cells. *Transfusion, 50*(3), 635-641. doi:10.1111/j.1537-2995.2009.02480.x

Henry, S., Oriol, R., & Samuelsson, B. (1995). Lewis Histo-Blood Group System and Associated Secretory Phenotypes. *Vox Sanguinis, 69*(3), 166-182. doi:10.1111/j.1423-0410.1995.tb02591.x

Henry, S. M. (2009). Modification of red blood cells for laboratory quality control use. *Current Opinion in Hematology, 16*(6), 467-472 doi:10.1097/MOH.0b013e328331257e

Henry, S. M., Barr, K. L., & Oliver, C. A. (2012). Modeling transfusion reactions with kodecytes and enabling ABO-incompatible transfusion with function-spacer-lipid constructs. *ISBT Science Series, 7*(1), 106-111. doi:10.1111/j.1751-2824.2012.01563.x

Henry, S. M., Komarraju, S., Heathcote, D., & Rodionov, I. L. (2011). Designing peptide-based FSL constructs to create Miltenberger kodecytes. *ISBT Science Series, 6*(2), 306-312. doi:10.1111/j.1751-2824.2011.01505.x

Herbert, C. B., McLernon, T. L., Hypolite, C. L., Adams, D. N., Pikus, L., Huang, C. C., ... Hu, W.-S. (1997). Micropatterning gradients and controlling surface densities of photoactivatable biomolecules on self-assembled monolayers of oligo(ethylene glycol) alkanethiolates. *Chemistry and Biology, 4*(10), 731-737. doi:10.1016/S1074-5521(97)90311-2

Hernandez, K., & Fernandez-Lafuente, R. (2011). Control of protein immobilization: Coupling immobilization and site-directed mutagenesis to improve biocatalyst or biosensor performance. *Enzyme and Microbial Technology, 48*(2), 107-122. doi:10.1016/j.enzmictec.2010.10.003

Hlady, V., & Buijs, J. (1996). Protein adsorption on solid surfaces. *Current Opinion in Biotechnology, 7*(1), 72-77. doi:10.1016/S0958-1669(96)80098-X

Homs, M. C. i. (2002). DNA SENSORS. *Analytical Letters, 35*(12), 1875-1894. doi:10.1081/al-120014280

Horlacher, T., & Seeberger, P. H. (2008). Carbohydrate arrays as tools for research and diagnostics [10.1039/B708016F]. *Chemical Society Reviews, 37*(7), 1414-1422. doi:10.1039/b708016f

Hsiao, S. C., Shum, B. J., Onoe, H., Douglas, E. S., Gartner, Z. J., Mathies, R. A., ... Francis, M. B. (2009). Direct Cell Surface Modification with DNA for the Capture of Primary Cells and the Investigation of Myotube Formation on Defined Patterns. *Langmuir, 25*(12), 6985-6991. doi:10.1021/la900150n

Huang, X.-J., Yu, A.-G., & Xu, Z.-K. (2008). Covalent immobilization of lipase from Candida rugosa onto poly(acrylonitrile-co-2-hydroxyethyl methacrylate) electrospun fibrous membranes for potential bioreactor application. *Bioresource Technology, 99*(13), 5459-5465. doi:10.1016/j.biortech.2007.11.009

Hult, A. K., Frame, T., Chesla, S., Henry, S., & Olsson, M. L. (2012). Flow cytometry evaluation of red blood cells mimicking naturally occurring ABO subgroups after modification with variable amounts of function-spacer-lipid A and B constructs. *Transfusion, 52*(2), 247-251. doi:10.1111/j.1537-2995.2011.03268.x

Israelachvili, J. N., Mitchell, D. J., & Ninham, B. W. (1976). Theory of self-assembly of hydrocarbon amphiphiles into micelles and bilayers [10.1039/F29767201525]. *Journal of the Chemical Society, Faraday Transactions 2: Molecular and Chemical Physics, 72*(0), 1525-1568. doi:10.1039/f29767201525

Istamboulie, G., Andreescu, S., Marty, J.-L., & Noguer, T. (2007). Highly sensitive detection of organophosphorus insecticides using magnetic microbeads and genetically engineered acetylcholinesterase. *Biosensors and Bioelectronics, 23*(4), 506-512. doi:10.1016/j.bios.2007.06.022

Jakab, K., Norotte, C., Damon, B., Marga, F., Neagu, A., Besch-Williford, C. L., ... Forgacs, G. (2008). Tissue Engineering by Self-Assembly of Cells Printed into Topologically Defined Structures. *Tissue Engineering Part A, 14*(3), 413-421. doi:10.1089/tea.2007.0173

Jass, J., Tjärnhage, T., & Puu, G. (2000). From Liposomes to Supported, Planar Bilayer Structures on Hydrophilic and Hydrophobic Surfaces: An Atomic Force Microscopy Study. *Biophysical Journal, 79*(6), 3153-3163. doi:10.1016/S0006-3495(00)76549-0

Jokerst, J. C., Adkins, J. A., Bisha, B., Mentele, M. M., Goodridge, L. D., & Henry, C. S. (2012). Development of a Paper-Based Analytical Device for Colorimetric Detection of Select Foodborne Pathogens. *Analytical Chemistry, 84*(6), 2900-2907. doi:10.1021/ac203466y

Kandimalla, V. B., Tripathi, V. S., & Ju, H. (2006). Immobilization of Biomolecules in Sol–Gels: Biological and Analytical Applications. *Critical Reviews in Analytical Chemistry, 36*(2), 73-106. doi:10.1080/10408340600713652

Kato, M., & Mrksich, M. (2004). Rewiring Cell Adhesion. *Journal of the American Chemical Society, 126*(21), 6504-6505. doi:10.1021/ja039058e

Kauzmann, W. (1959). Some Factors in the Interpretation of Protein Denaturation. *Adv Protein Chem., 14*, 1-63.

Ker, E. D. F., Chu, B., Phillippi, J. A., Gharaibeh, B., Huard, J., Weiss, L. E., & Campbell, P. G. (2011). Engineering spatial control of multiple differentiation fates within a stem cell population. *Biomaterials, 32*(13), 3413-3422. doi:10.1016/j.biomaterials.2011.01.036

Khan, M. S., Fon, D., Li, X., Tian, J., Forsythe, J., Garnier, G., & Shen, W. (2010). Biosurface engineering through ink jet printing. *Colloids and Surfaces B: Biointerfaces, 75*(2), 441-447. doi:10.1016/j.colsurfb.2009.09.032

Khan, M. S., Li, X., Shen, W., & Garnier, G. (2010). Thermal stability of bioactive enzymatic papers. *Colloids and Surfaces B: Biointerfaces, 75*(1), 239-246. doi:10.1016/j.colsurfb.2009.08.042

Kirk, J. T., Fridley, G. E., Chamberlain, J. W., Christensen, E. D., Hochberg, M., & Ratner, D. M. (2011). Multiplexed inkjet functionalization of silicon photonic biosensors. *Lab on a Chip, 11*(7), 1372-1377. doi:10.1039/c0lc00313a

Klebe, R. J. (1988). Cytoscribing: a method for micropositioning cells and the construction of two-and three-dimensional synthetic tissues. *Experimental Cell Research, 179*(2), 362-373.

Knecht, S., Ricklin, D., Eberle, A. N., & Ernst, B. (2009). Oligohis-tags: mechanisms of binding to Ni2+-NTA surfaces. *Journal of Molecular Recognition, 22*(4), 270-279. doi:10.1002/jmr.941

Kolodziej, C. M., & Maynard, H. D. (2011). Electron-Beam Lithography for Patterning Biomolecules at the Micron and Nanometer Scale. *Chemistry of Materials, 24*(5), 774-780. doi:10.1021/cm202669f

Komuro, N., Takaki, S., Suzuki, K., & Citterio, D. (2013). Inkjet printed (bio)chemical sensing devices. *Analytical and Bioanalytical Chemistry, 405*(17), 5785-5805. doi:10.1007/s00216-013-7013-z

Kong, F., & Hu, Y. (2012). Biomolecule immobilization techniques for bioactive paper fabrication. *Analytical and Bioanalytical Chemistry, 403*(1), 7-13. doi:10.1007/s00216-012-5821-1

Korchagina, E., Tuzikov, A., Formanovsky, A., Popova, I., Henry, S., & Bovin, N. (2012). Toward creating cell membrane glyco-landscapes with glycan lipid constructs. *Carbohydrate Research, 356*(0), 238-246. doi:10.1016/j.carres.2012.03.044

Kralovec, J. A., Laycock, M. V., Richards, R., & Usleber, E. (1996). Immobilization of small molecules on solid matrices: A novel approach to enzyme-linked immunosorbent assay screening for saxitoxin and evaluation of anti-saxitoxin antibodies. *Toxicon, 34*(10), 1127-1140. doi:10.1016/0041-0101(96)00063-3

Kubiak-Ossowska, K., & Mulheran, P. A. (2010). What Governs Protein Adsorption and Immobilization at a Charged Solid Surface? *Langmuir, 26*(11), 7690-7694. doi:10.1021/la101276v

Lan, C.-C., Blake, D., Henry, S., & Love, D. (2012). Fluorescent Function-Spacer-Lipid Construct Labelling Allows for Real-Time in Vivo Imaging of Cell Migration and

Behaviour in Zebrafish (Danio Rerio). *Journal of Fluorescence, 22*(4), 1055-1063. doi:10.1007/s10895-012-1043-3

Larsen, K., Thygesen, M. B., Guillaumie, F., Willats, W. G. T., & Jensen, K. J. (2006). Solid-phase chemical tools for glycobiology. *Carbohydrate Research, 341*(10), 1209-1234. doi:10.1016/j.carres.2006.04.045

Larsson, C., Rodahl, M., & Höök, F. (2003). Characterization of DNA Immobilization and Subsequent Hybridization on a 2D Arrangement of Streptavidin on a Biotin-Modified Lipid Bilayer Supported on SiO2. *Analytical Chemistry, 75*(19), 5080-5087. doi:10.1021/ac034269n

Le, H. P. (1998). Progress and Trends in Ink-jet Printing Technology *Journal of Imaging Science and Technology, 42*(1), 49-62.

Lee, K. G., Park, T. J., Soo, S. Y., Wang, K. W., Kim, B. I. I., Park, J. H., ... Lee, S. J. (2010). Synthesis and utilization of E. coli-encapsulated PEG-based microdroplet using a microfluidic chip for biological application. *Biotechnology and Bioengineering, 107*(4), 747-751. doi:10.1002/bit.22861

Lee, W., Debasitis, J. C., Lee, V. K., Lee, J.-H., Fischer, K., Edminster, K., ... Yoo, S.-S. (2009). Multi-layered culture of human skin fibroblasts and keratinocytes through three-dimensional freeform fabrication. *Biomaterials, 30*(8), 1587-1595. doi:10.1016/j.biomaterials.2008.12.009

Lee, Y.-B., Polio, S., Lee, W., Dai, G., Menon, L., Carroll, R. S., & Yoo, S.-S. (2010). Bio-printing of collagen and VEGF-releasing fibrin gel scaffolds for neural stem cell culture. *Experimental Neurology, 223*(2), 645-652. doi:10.1016/j.expneurol.2010.02.014

Lei, L., Bai, Y., Li, Y., Yi, L., Yang, Y., & Xia, C. (2009). Study on immobilization of lipase onto magnetic microspheres with epoxy groups. *Journal of Magnetism and Magnetic Materials, 321*(4), 252-258. doi:10.1016/j.jmmm.2008.08.047

Li, X., Tian, J., Garnier, G., & Shen, W. (2010a). Fabrication of paper-based microfluidic sensors by printing. *Colloids and Surfaces B: Biointerfaces, 76*(2), 564-570. doi:10.1016/j.colsurfb.2009.12.023

Li, X., Tian, J., & Shen, W. (2010b). Quantitative biomarker assay with microfluidic paper-based analytical devices. *Analytical and Bioanalytical Chemistry, 396*(1), 495-501. doi:10.1007/s00216-009-3195-9

Liberski, A. R., Delaney, J. T., & Schubert, U. S. (2010). "One Cell−One Well": A New Approach to Inkjet Printing Single Cell Microarrays. *ACS Combinatorial Science, 13*(2), 190-195. doi:10.1021/co100061c

Lilly, M. D. (1976). [4] Enzymes immobilized to cellulose. In M. Klaus (Ed.), *Methods in Enzymology* (Vol. Volume 44, pp. 46-53): Academic Press. Retrieved from http://www.sciencedirect.com/science/article/pii/S0076687976440065. doi:10.1016/S0076-6879(76)44006-5

Liu, L., Chen, Z., Yang, S., Jin, X., & Lin, X. (2008). A novel inhibition biosensor constructed by layer-by-layer technique based on biospecific affinity for the determination of sulfide. *Sensors and Actuators B: Chemical, 129*(1), 218-224. doi:10.1016/j.snb.2007.07.137

Liu, L., Deng, D., Xing, Y., Li, S., Yuan, B., Chen, J., & Xia, N. (2013). Activity analysis of the carbodiimide-mediated amine coupling reaction on self-assembled monolayers by cyclic voltammetry. *Electrochimica Acta, 89*(0), 616-622. doi:10.1016/j.electacta.2012.11.049

Liu, X., Xing, J., Guan, Y., Shan, G., & Liu, H. (2004). Synthesis of amino-silane modified superparamagnetic silica supports and their use for protein immobilization. *Colloids and Surfaces A: Physicochemical and Engineering Aspects, 238*(1–3), 127-131. doi:10.1016/j.colsurfa.2004.03.004

Liu, X. Y., Cheng, C. M., Martinez, A. W., Mirica, K. A., Li, X. J., Phillips, S. T., ... Whitesides, G. M. (2011, 23-27 Jan. 2011). A portable microfluidic paper-based device for ELISA Symposium conducted at the meeting of the Micro Electro Mechanical Systems (MEMS), 2011 IEEE 24th International Conference on doi:10.1109/MEMSYS.2011.5734365

Liu, Z., Xiao, L., Xu, B., Yu, Z., Mak, A., Man, W.-y., & Yang, M. (2012). Covalently immobilized biomolecule gradient on hydrogel surface using a gradient generating microfluidic device for a quantitative mesenchymal stem cell study. *Biomicrofluidics, 6*(2), 024111-024111-024112. doi:10.1063/1.4704522

Lonini, L., Accoto, D., Petroni, S., & Guglielmelli, E. (2008). Dispensing an enzyme-conjugated solution into an ELISA plate by adapting ink-jet printers. *Journal of Biochemical and Biophysical Methods, 70*(6), 1180-1184. doi:10.1016/j.jbbm.2007.05.003

Luckarift, H. R., Spain, J. C., Naik, R. R., & Stone, M. O. (2004). Enzyme immobilization in a biomimetic silica support [Article]. *Nature Biotechnology, 22*(2), 211-213. doi:10.1038/nbt931

Luo, P., Liu, Y., Xie, G., Xiong, X., Deng, S., & Song, F. (2008). Determination of serum alcohol using a disposable biosensor. *Forensic Science International, 179*(2–3), 192-198. doi:10.1016/j.forsciint.2008.06.002

MacBeath, G., & Schreiber, S. L. (2000). Printing Proteins as Microarrays for High-Throughput Function Determination. *Science, 289*(5485), 1760-1763. doi:10.1126/science.289.5485.1760

Martinez, A. W. (2011). Microfluidic paper-based analytical devices: from POCKET to paper-based ELISA. *Bioanalysis, 3*(23), 2589-2592. doi:10.4155/bio.11.258

Martinez, A. W., Phillips, S. T., Butte, M. J., & Whitesides, G. M. (2007). Patterned paper as a platform for inexpensive, low-volume, portable bioassays. *Angewandte Chemie - International Edition, 46*(8), 1318-1320. doi:10.1002/anie.200603817

Martinez, A. W., Phillips, S. T., Whitesides, G. M., & Carrilho, E. (2010). Diagnostics for the Developing World: Microfluidic Paper-Based Analytical Devices. *Analytical Chemistry, 82*(1), 3-10. doi:10.1021/ac9013989

Mateo, C., Fernández-Lorente, G., Abian, O., Fernández-Lafuente, R., & Guisán, J. M. (2000). Multifunctional Epoxy Supports: A New Tool To Improve the Covalent Immobilization of Proteins. The Promotion of Physical Adsorptions of Proteins on the Supports before Their Covalent Linkage. *Biomacromolecules, 1*(4), 739-745. doi:10.1021/bm000071q

Mateo, C., Palomo, J. M., Fernandez-Lorente, G., Guisan, J. M., & Fernandez-Lafuente, R. (2007). Improvement of enzyme activity, stability and selectivity via immobilization techniques. *Enzyme and Microbial Technology, 40*(6), 1451-1463. doi:10.1016/j.enzmictec.2007.01.018

Mateo, C., Torres, R., Fernández-Lorente, G., Ortiz, C., Fuentes, M., Hidalgo, A., ... Fernández-Lafuente, R. (2003). Epoxy-Amino Groups: A New Tool for Improved Immobilization of Proteins by the Epoxy Method. *Biomacromolecules, 4*(3), 772-777. doi:10.1021/bm0257661

Melamed, S., Ceriotti, L., Weigel, W., Rossi, F., Colpo, P., & Belkin, S. (2011). A printed nanolitre-scale bacterial sensor array [10.1039/C0LC00243G]. *Lab on a Chip, 11*(1), 139-146. doi:10.1039/c0lc00243g

Mendes, P., Yeung, C., & Preece, J. (2007). Bio-nanopatterning of Surfaces. *Nanoscale Research Letters, 2*(8), 373-384. doi:10.1007/s11671-007-9083-3

Mesman, A., de Vries, R., McQuaid, S., Duprex, W., de Swart, R., & Geijtenbeek, T. (2012). A Prominent Role for DC-SIGN+ Dendritic Cells in Initiation and Dissemination of Measles Virus Infection in Non-Human Primates. *PLoS ONE, 7*(12). doi:10.1371/journal.pone.0049573

Michel, O., & Ravoo, B. J. (2008). Carbohydrate Microarrays by Microcontact "Click" Chemistry. *Langmuir, 24*(21), 12116-12118. doi:10.1021/la802304w

Michelini, E., & Roda, A. (2012). Staying alive: new perspectives on cell immobilization for biosensing purposes. *Analytical and Bioanalytical Chemistry, 402*(5), 1785-1797. doi:10.1007/s00216-011-5364-x

Miller, E. D., Li, K., Kanade, T., Weiss, L. E., Walker, L. M., & Campbell, P. G. (2011). Spatially directed guidance of stem cell population migration by immobilized patterns of growth factors. *Biomaterials, 32*(11), 2775-2785. doi:10.1016/j.biomaterials.2010.12.005

Miller, E. D., Phillippi, J. A., Fisher, G. W., Campbell, P. G., Walker, L. M., & Weiss, L. E. (2009). Inkjet Printing of Growth Factor Concentration Gradients and Combinatorial Arrays Immobilized on Biologically-Relevant Substrates. *Combinatorial Chemistry & High Throughput Screening, 12*(6), 604-618. doi:10.2174/138620709788681907

Mironov, V., Boland, T., Trusk, T., Forgacs, G., & Markwald, R. R. (2003). Organ printing: computer-aided jet-based 3D tissue engineering. *Trends in Biotechnology, 21*(4), 157-161. doi:10.1016/S0167-7799(03)00033-7

Mironov, V., Kasyanov, V., Drake, C., & Markwald, R. R. (2007). Organ printing: promises and challenges. *Regenerative Medicine, 3*(1), 93-103. doi:10.2217/17460751.3.1.93

Mironov, V., Visconti, R. P., Kasyanov, V., Forgacs, G., Drake, C. J., & Markwald, R. R. (2009). Organ printing: Tissue spheroids as building blocks. *Biomaterials, 30*(12), 2164-2174. doi:10.1016/j.biomaterials.2008.12.084

Mitz, M. A., & Summaria, L. J. (1961). Synthesis of Biologically Active Cellulose Derivatives of Enymes. *Nature 189*, 576-577. doi:10.1038/189576a0

Mollison, P. L. (2005). *Blood transfusion in clinical medicone* (11th ed.): Blackwell publishing.

Nadarajan, V. S., Laing, A. A., Saad, S. M., & Usin, M. (2012). Prevalence and specificity of red-blood-cell antibodies in a multiethnic South and East Asian patient population and influence of using novel MUT+Mur+ kodecytes on its detection. *Vox Sanguinis, 102*(1), 65-71. doi:10.1111/j.1423-0410.2011.01507.x

Nakamura, M., Kobayashi, A., Takagi, F., Watanabe, A., Hiruma, Y., Ohuchi, K., ... Takatani, S. (2005). Biocompatible inkjet printing technique for designed seeding of individual living cells. *Tissue Engineering, 11*(11-12), 1658-1666.

Nakanishi, K., Sakiyama, T., Kumada, Y., Imamura, K., & Imanaka, H. (2008). Recent Advances in Controlled Immobilization of Proteins onto the Surface of the Solid Substrate and Its Possible Application to Proteomics. *Current Proteomics, 5*, 161-175.

Nan, G., Yan, H., Yang, G., Jian, Q., & Li, Z. (2009). The Hydroxyl-Modified Surfaces on Glass Support for Fabrication of Carbohydrate Microarrays. *Current Pharmaceutical Biotechnology, 10*(1), 138-146. doi:10.2174/138920109787048652

Nishioka, G. M., Markey, A. A., & Holloway, C. K. (2004). Protein damage in drop-on-demand printers. *J. Am. Chem. Soc, 126*(50), 16320-16321. doi:10.1021/ja044539z

Ogiso, M., Kobayashi, J., Imai, T., Matsuoka, K., Itoh, M., Imamura, T., ... Minoura, N. (2013). Carbohydrate immobilized on a dendrimer-coated colloidal gold surface for fabrication of a lectin-sensing device based on localized surface plasmon resonance spectroscopy. *Biosensors and Bioelectronics, 41*(0), 465-470. doi:10.1016/j.bios.2012.09.003

Okamoto, T., Suzuki, T., & Yamamoto, N. (2000). Microarray fabrication with covalent attachment of DNA using Bubble Jet technology [10.1038/74507]. *Nat Biotech, 18*(4), 438-441. doi:10.1038/74507

Oliver, C., Blake, D., & Henry, S. (2011a). In vivo neutralization of anti-A and successful transfusion of A antigen–incompatible red blood cells in an animal model. *Transfusion, 51*(12), 2664-2675. doi:10.1111/j.1537-2995.2011.03184.x

Oliver, C., Blake, D., & Henry, S. (2011b). Modeling transfusion reactions and predicting in vivo cell survival with kodecytes. *Transfusion, 51*(8), 1723-1730. doi:10.1111/j.1537-2995.2010.03034.x

Oshige, M., Yumoto, K., Miyata, H., Takahashi, S., Nakada, M., Ito, K., ... Katsura, S. (2013). Immobilization of His-Tagged Proteins on Various Solid Surfaces Using NTA-Modified Chitosan. *Open Journal of Polymer Chemistry, 3*(1), 6-10. doi:10.4236/ojpchem.2013.31002

Ouerghi, O., Touhami, A., Jaffrezic-Renault, N., Martelet, C., Ouada, H. B., & Cosnier, S. (2002). Impedimetric immunosensor using avidin–biotin for antibody immobilization. *Bioelectrochemistry, 56*(1–2), 131-133. doi:10.1016/S1567-5394(02)00029-4

Palomo, J. M. (2010). Diels–Alder Cycloaddition in Protein Chemistry. *European Journal of Organic Chemistry, 2010*(33), 6303-6314. doi:10.1002/ejoc.201000859

Palomo, J. M., Segura, R. L., Fernández-Lorente, G., Pernas, M., Rua, M. L., Guisán, J. M., & Fernández-Lafuente, R. (2004). Purification, Immobilization, and Stabilization of a Lipase from Bacillus thermocatenulatus by Interfacial Adsorption on Hydrophobic Supports. *Biotechnology Progress, 20*(2), 630-635. doi:10.1021/bp0342957

Pardo, L., Wilson, W. C., & Boland, T. (2002). Characterization of Patterned Self-Assembled Monolayers and Protein Arrays Generated by the Ink-Jet Method *Langmuir, 19*(5), 1462-1466. doi:10.1021/la026171u

Parida, S. K., Dash, S., Patel, S., & Mishra, B. K. (2006). Adsorption of organic molecules on silica surface. *Advances in Colloid and Interface Science, 121*(1–3), 77-110. doi:10.1016/j.cis.2006.05.028

Park, B.-W., Yoon, D.-Y., & Kim, D.-S. (2010). Recent progress in bio-sensing techniques with encapsulated enzymes. *Biosensors and Bioelectronics, 26*(1), 1-10. doi:10.1016/j.bios.2010.04.033

Park, S., Gildersleeve, J. C., Blixt, O., & Shin, I. (2013). Carbohydrate microarrays. *Chemical Society Reviews, 42*(10), 4310-4326. doi:10.1039/c2cs35401b

Park, S., Lee, M.-r., Pyo, S.-J., & Shin, I. (2004). Carbohydrate Chips for Studying High-Throughput Carbohydrate−Protein Interactions. *Journal of the American Chemical Society, 126*(15), 4812-4819. doi:10.1021/ja0391661

Park, S., Lee, M.-R., & Shin, I. (2009). Construction of Carbohydrate Microarrays by Using One-Step, Direct Immobilizations of Diverse Unmodified Glycans on Solid Surfaces. *Bioconjugate Chemistry, 20*(1), 155-162. doi:10.1021/bc800442z

Park, S., & Shin, I. (2002). Fabrication of Carbohydrate Chips for Studying Protein–Carbohydrate Interactions. *Angewandte Chemie, 114*(17), 3312-3314. doi:10.1002/1521-3757(20020902)114:17<3312::aid-ange3312>3.0.co;2-k

Parthasarathy, R., Subramanian, S., & Boder, E. T. (2007). Sortase A as a Novel Molecular "Stapler" for Sequence-Specific Protein Conjugation. *Bioconjugate Chemistry, 18*(2), 469-476. doi:10.1021/bc060339w

Pelton, R. (2009). Bioactive paper provides a low-cost platform for diagnostics. *TrAC Trends in Analytical Chemistry, 28*(8), 925-942. doi:10.1016/j.trac.2009.05.005

Peluso, P., Wilson, D. S., Do, D., Tran, H., Venkatasubbaiah, M., Quincy, D., ... Nock, S. (2003). Optimizing antibody immobilization strategies for the construction of protein microarrays. *Analytical Biochemistry, 312*(2), 113-124. doi:10.1016/S0003-2697(02)00442-6

Pepper, M. E., Seshadri, V., Burg, T., Booth, B. W., Burg, K. J. L., & Groff, R. E. (2011, Aug. 30 2011-Sept. 3 2011). Cell settling effects on a thermal inkjet bioprinter Symposium conducted at the meeting of the Engineering in Medicine and Biology Society,EMBC, 2011 Annual International Conference of the IEEE doi:10.1109/iembs.2011.6090605

Perl, A., Reinhoudt, D. N., & Huskens, J. (2009). Microcontact Printing: Limitations and Achievements. *Advanced Materials, 21*(22), 2257-2268. doi:10.1002/adma.200801864

Petkova, G., Zaruba, K., Zvatora, P., & Kral, V. (2012). Gold and silver nanoparticles for biomolecule immobilization and enzymatic catalysis. *Nanoscale Research Letters, 7*(1), 287. doi:10.1186/1556-276X-7-287

Petty, R. T., Li, H.-W., Maduram, J. H., Ismagilov, R., & Mrksich, M. (2007). Attachment of Cells to Islands Presenting Gradients of Adhesion Ligands. *Journal of the American Chemical Society, 129*(29), 8966-8967. doi:10.1021/ja0735709

Phillippi, J. A., Miller, E., Weiss, L., Huard, J., Waggoner, A., & Campbell, P. (2008). Microenvironments Engineered by Inkjet Bioprinting Spatially Direct Adult Stem Cells Toward Muscle- and Bone-Like Subpopulations. *Stem Cells, 26*(1), 127-134. doi:10.1634/stemcells.2007-0520

Pijanowska, D. G., Remiszewska, E., Łysko, J. M., Jaźwiński, J., & Torbicz, W. (2003). Immobilisation of bioreceptors for microreactors. *Sensors and Actuators B: Chemical, 91*(1–3), 152-157. doi:10.1016/S0925-4005(03)00081-9

Prieto-Simon, B., Campas, M., & Marty, J. L. (2008). Biomolecule immobilization in biosensor development: tailored strategies based on affinity interactions. *Protein and Peptide Letters, 15*, 757-763. doi:10.2174/092986608785203791

Proft, T. (2010). Sortase-mediated protein ligation: an emerging biotechnology tool for protein modification and immobilisation. *Biotechnology Letters, 32*(1), 1-10. doi:10.1007/s10529-009-0116-0

Pyun, J.-C., Cheong, M.-Y., Park, S.-H., Kim, H.-Y., & Park, J.-S. (1997). Modification of short peptides using ε-aminocaproic acid for improved coating efficiency in indirect enzyme-

linked immunosorbent assays (ELISA). *Journal of Immunological Methods, 208*(2), 141-149. doi:10.1016/S0022-1759(97)00136-1

Rabe, M., Verdes, D., & Seeger, S. (2011). Understanding protein adsorption phenomena at solid surfaces. *Advances in Colloid and Interface Science, 162*(1–2), 87-106. doi:10.1016/j.cis.2010.12.007

Ramanathan, M., Shrestha, L. K., Mori, T., Ji, Q., Hill, J. P., & Ariga, K. (2013). Amphiphile nanoarchitectonics: from basic physical chemistry to advanced applications [10.1039/C3CP50620G]. *Physical Chemistry Chemical Physics*. doi:10.1039/c3cp50620g

Ran, Q., Peng, R., Liang, C., Ye, S., Xian, Y., Zhang, W., & Jin, L. (2011). Covalent immobilization of horseradish peroxidase via click chemistry and its direct electrochemistry. *Talanta, 83*(5), 1381-1385. doi:10.1016/j.talanta.2010.11.024

Ravi Kumar, M. N. V. (2000). A review of chitin and chitosan applications. *Reactive and Functional Polymers, 46*(1), 1-27. doi:10.1016/S1381-5148(00)00038-9

Rendl, M., Bönisch, A., Mader, A., Schuh, K., Prucker, O., Brandstetter, T., & Rühe, J. r. (2011). Simple One-Step Process for Immobilization of Biomolecules on Polymer Substrates Based on Surface-Attached Polymer Networks. *Langmuir, 27*(10), 6116-6123. doi:10.1021/la1050833

Rezende, R. A., Pereira, F. D. A. S., Kasyanov, V., Kemmoku, D. T., Maia, I., da Silva, J. V. L., & Mironov, V. (2013). Scalable Biofabrication of Tissue Spheroids for Organ Printing. *Procedia CIRP, 5*(0), 276-281. doi:10.1016/j.procir.2013.01.054

Roda, A., Guardigli, M., Russo, C., Pasini, P., & Baraldini, M. (2000). Protein microdeposition using a conventional ink-jet printer. *Biotechniques, 28*, 492-496.

Roth, E. A., Xu, T., Das, M., Gregory, C., Hickman, J. J., & Boland, T. (2004). Inkjet printing for high-throughput cell patterning. *Biomaterials, 25*(17), 3707-3715. doi:10.1016/j.biomaterials.2003.10.052

Rożkiewicz, D. I., Ravoo, B. J., & Reinhoudt, D. N. (2010). Immobilization and Patterning of Biomolecules on Surfaces. In *The Supramolecular Chemistry of Organic-Inorganic Hybrid Materials* (pp. 433-466): John Wiley & Sons, Inc. doi:10.1002/9780470552704.ch14

Sakurai, K., Teramura, Y., & Iwata, H. (2011). Cells immobilized on patterns printed in DNA by an inkjet printer. *Biomaterials, 32*(14), 3596-3602. doi:10.1016/j.biomaterials.2011.01.066

Salam, F., & Tothill, I. E. (2009). Detection of Salmonella typhimurium using an electrochemical immunosensor. *Biosensors and Bioelectronics, 24*(8), 2630-2636. doi:10.1016/j.bios.2009.01.025

Salis, A., Bhattacharyya, M. S., & Monduzzi, M. (2010). Specific Ion Effects on Adsorption of Lysozyme on Functionalized SBA-15 Mesoporous Silica. *The Journal of Physical Chemistry B, 114*(23), 7996-8001. doi:10.1021/jp102427h

Samanta, D., & Sarkar, A. (2011). Immobilization of bio-macromolecules on self-assembled monolayers: methods and sensor applications. *Chemical Society Reviews, 40*(5), 2567-2592. doi:10.1039/C0CS00056F

Sánchez-Cortés, J., Bähr, K., & Mrksich, M. (2010). Cell adhesion to unnatural ligands mediated by a bifunctional protein. *Journal of the American Chemical Society, 132*(28), 9733-9737.

Sanjana, N. E., & Fuller, S. B. (2004). A fast flexible ink-jet printing method for patterning dissociated neurons in culture. *Journal of Neuroscience Methods, 136*(2), 151-163. doi:10.1016/j.jneumeth.2004.01.011

Sassolas, A., Blum, L. J., & Leca-Bouvier, B. D. (2012). Immobilization strategies to develop enzymatic biosensors. *Biotechnology Advances, 30*(3), 489-511. doi:10.1016/j.biotechadv.2011.09.003

Sassolas, A., Leca-Bouvier, B. D., & Blum, L. J. (2008). DNA Biosensors and Microarrays. *Chemical Reviews, 108*(1), 109-139. doi:10.1021/cr0684467

Saunders, R. E., Gough, J. E., & Derby, B. (2008). Delivery of human fibroblast cells by piezoelectric drop-on-demand inkjet printing. *Biomaterials, 29*(2), 193-203. doi:10.1016/j.biomaterials.2007.09.032

Scheicher, S. R., Kainz, B., Köstler, S., Reitinger, N., Steiner, N., Ditlbacher, H., ... Ribitsch, V. (2013). 2D crystalline protein layers as immobilization matrices for the development of DNA microarrays. *Biosensors and Bioelectronics, 40*(1), 32-37. doi:10.1016/j.bios.2012.05.037

Schmid, F., Düchs, D., Lenz, O., & Loison, C. (2004). Amphiphiles at Interfaces: Simulation of Structure and Phase Behavior. *Condensed Matter > Soft Condensed Matter, 23*, 323. doi:arXiv:cond-mat/0405685

Scouten, W. H., Luong, J. H. T., & Stephen Brown, R. (1995). Enzyme or protein immobilization techniques for applications in biosensor design. *Trends in Biotechnology, 13*(5), 178-185. doi:10.1016/S0167-7799(00)88935-0

Seidel, M., & Niessner, R. (2008). Automated analytical microarrays: a critical review. *Analytical and Bioanalytical Chemistry, 391*(5), 1521-1544. doi:10.1007/s00216-008-2039-3

Seo, J. H., Kim, C. S., Hwang, B. H., & Cha, H. J. (2010). A functional carbohydrate chip platform for analysis of carbohydrate–protein interaction. *Nanotechnology, 21*(21), 215101. doi:10.1088/0957-4484/21/21/215101

Setti, L., Fraleoni-Morgera, A., Ballarin, B., Filippini, A., Frascaro, D., & Piana, C. (2005). An amperometric glucose biosensor prototype fabricated by thermal inkjet printing. *Biosensors and Bioelectronics, 20*(10), 2019-2026. doi:10.1016/j.bios.2004.09.022

Setti, L., Fraleoni-Morgera, A., Mencarelli, I., Filippini, A., Ballarin, B., & Di Biase, M. (2007). An HRP-based amperometric biosensor fabricated by thermal inkjet printing. *Sensors and Actuators B: Chemical, 126*(1), 252-257. doi:10.1016/j.snb.2006.12.015

Setti, L., Piana, C., Bonazzi, S., Ballarin, B., Frascaro, D., Fraleoni-Morgera, A., & Giuliani, S. (2004). Thermal Inkjet Technology for the Microdeposition of Biological Molecules as a Viable Route for the Realization of Biosensors. *Analytical Letters, 37*(8), 1559-1570. doi:10.1081/AL-120037587

Shamsi, F., Coster, H., & Jolliffe, K. A. (2011). Characterization of peptide immobilization on an acetylene terminated surface via click chemistry. *Surface Science, 605*(19–20), 1763-1770. doi:10.1016/j.susc.2011.05.027

Sharma, S. K., Sehgal, N., & Kumar, A. (2003). Biomolecules for development of biosensors and their applications. *Current Applied Physics, 3*(2–3), 307-316. doi:10.1016/S1567-1739(02)00219-5

Sheldon, R. A. (2007). Enzyme Immobilization: The Quest for Optimum Performance. *Advanced Synthesis & Catalysis, 349*(8-9), 1289-1307. doi:10.1002/adsc.200700082

Shen, Q., Yang, R., Hua, X., Ye, F., Zhang, W., & Zhao, W. (2011). Gelatin-templated biomimetic calcification for β-galactosidase immobilization. *Process Biochemistry, 46*(8), 1565-1571. doi:10.1016/j.procbio.2011.04.010

Shin, I., Park, S., & Lee, M.-r. (2005). Carbohydrate Microarrays: An Advanced Technology for Functional Studies of Glycans. *Chemistry - A European Journal, 11*(10), 2894-2901. doi:10.1002/chem.200401030

Shipp, E. L., & Hsieh-Wilson, L. C. (2007). Profiling the Sulfation Specificities of Glycosaminoglycan Interactions with Growth Factors and Chemotactic Proteins Using Microarrays. *Chemistry and Biology, 14*(2), 195-208. doi:10.1016/j.chembiol.2006.12.009

Sigrist, H., Collioud, A., Clemence, J.-F., Gao, H., Luginbuehl, R., Saenger, M., & Sundarababu, G. (1995). Surface immobilization of biomolecules by light. *Optical Engineering, 34*(8), 2339-2348. doi:10.1117/12.201815

Singh, M., Haverinen, H. M., Dhagat, P., & Jabbour, G. E. (2010). Inkjet Printing—Process and Its Applications. *Advanced Materials, 22*(6), 673-685. doi:10.1002/adma.200901141

Singh, V., Zharnikov, M., Gulino, A., & Gupta, T. (2011). DNA immobilization, delivery and cleavage on solid supports. *Journal of Materials Chemistry, 21*(29), 10602-10618.

Smith, J. E. (2004). *Biotechnology* (Fourth ed.): Cambridge University Press.

Song, E.-H., & Pohl, N. L. B. (2009). Carbohydrate arrays: recent developments in fabrication and detection methods with applications. *Current Opinion in Chemical Biology, 13*(5–6), 626-632. doi:10.1016/j.cbpa.2009.09.021

Sørensen, I., Pedersen, H. L., & Willats, W. G. T. (2009). An array of possibilities for pectin. *Carbohydrate Research, 344*(14), 1872-1878. doi:10.1016/j.carres.2008.12.008

Southall, N. T., Dill, K. A., & Haymet, A. D. J. (2002). A View of the Hydrophobic Effect. *The Journal of Physical Chemistry B, 106*(3), 521-533. doi:10.1021/jp015514e

Spiteri, C., & Moses, J. E. (2010). Copper-Catalyzed Azide–Alkyne Cycloaddition: Regioselective Synthesis of 1,4,5-Trisubstituted 1,2,3-Triazoles. *Angewandte Chemie International Edition, 49*(1), 31-33. doi:10.1002/anie.200905322

Su, S., Nutiu, R., Filipe, C. D. M., Li, Y., & Pelton, R. (2007). Adsorption and Covalent Coupling of ATP-Binding DNA Aptamers onto Cellulose. *Langmuir, 23*(3), 1300-1302. doi:10.1021/la060961c

Sun, J., Zhang, H., Tian, R., Ma, D., Bao, X., Su, D. S., & Zou, H. (2006). Ultrafast enzyme immobilization over large-pore nanoscale mesoporous silica particles [10.1039/B516930E]. *Chemical Communications, 0*(12), 1322-1324. doi:10.1039/b516930e

Sun, X.-L., Stabler, C. L., Cazalis, C. S., & Chaikof, E. L. (2006). Carbohydrate and Protein Immobilization onto Solid Surfaces by Sequential Diels−Alder and Azide−Alkyne Cycloadditions. *Bioconjugate Chemistry, 17*(1), 52-57. doi:10.1021/bc0502311

Svensson, L., Rydberg, L., Hellberg, Å., Gilliver, L. G., Olsson, M. L., & Henry, S. M. (2005). Novel glycolipid variations revealed by monoclonal antibody immunochemical analysis of weak ABO subgroups of A. *Vox Sanguinis, 89*(1), 27-38. doi:10.1111/j.1423-0410.2005.00642.x

Takahashi, S., Sato, K., & Anzai, J.-i. (2012). Layer-by-layer construction of protein architectures through avidin–biotin and lectin–sugar interactions for biosensor applications. *Analytical and Bioanalytical Chemistry, 402*(5), 1749-1758. doi:10.1007/s00216-011-5317-4

Talbert, J. T., & Hotchkiss, J. H. (2012). Chemical modification of lactase for immobilization on carboxylic acid-functionalized microspheres. *Biocatalysis and Biotransformation, 30*(5-6), 446-454. doi:10.3109/10242422.2012.740020

Tanford, C. (1979). Interfacial free energy and the hydrophobic effect. *Proc Natl Acad Sci U S A, 76*(9), 4175-4176.

Tanford, C. (1987). Amphiphile orientation: physical chemistry and biological function. *Biochem Soc Trans. , 15*, Suppl:1S-7S.

Tanford, C. (1997). How protein chemists learned about the hydrophobic factor. *Protein Science, 6*(6), 1358-1366. doi:10.1002/pro.5560060627

Tasdelen, M. A. (2011). Diels-Alder "click" reactions: recent applications in polymer and material science. *Polymer Chemistry, 2*(10), 2133-2145. doi:10.1039/C1PY00041A

Tasoglu, S., & Demirci, U. (2013). Bioprinting for stem cell research. *Trends in Biotechnology, 31*(1), 10-19. doi:10.1016/j.tibtech.2012.10.005

Tekin, E., Smith, P. J., & Schubert, U. S. (2008). Inkjet printing as a deposition and patterning tool for polymers and inorganic particles [10.1039/B711984D]. *Soft Matter, 4*(4), 703-713. doi:10.1039/b711984d

Teles, F. R. R., & Fonseca, L. P. (2008). Applications of polymers for biomolecule immobilization in electrochemical biosensors. *Materials Science and Engineering: C, 28*(8), 1530-1543. doi:10.1016/j.msec.2008.04.010

Tovey, E. R., & Baldo, B. A. (1989). Protein binding to nitrocellulose, nylon and PVDF membranes in immunoassays and electroblotting. *Journal of Biochemical and Biophysical Methods, 19*(2–3), 169-183. doi:10.1016/0165-022X(89)90024-9

Trau, D., & Renneberg, R. (2003). Encapsulation of glucose oxidase microparticles within a nanoscale layer-by-layer film: immobilization and biosensor applications. *Biosensors and Bioelectronics, 18*(12), 1491-1499. doi:10.1016/S0956-5663(03)00119-2

Ulman, A. (1996). Formation and Structure of Self-Assembled Monolayers. *Chemical Reviews, 96*(4), 1533-1554. doi:10.1021/cr9502357

Uszczynska, B., Ratajczak, T., Frydrych, E., Maciejewski, H., Figlerowicz, M., Markiewicz, W. T., & Chmielewski, M. K. (2012). Application of click chemistry to the production of DNA microarrays [10.1039/C2LC21096G]. *Lab on a Chip, 12*(6), 1151-1156. doi:10.1039/c2lc21096g

Uttamchandani, M., & Yao, S. Q. (2008). Peptide Microarrays: Next Generation Biochips for Detection, Diagnostics and High-Throughput Screening. *Current Pharmaceutical Design, 14*(24), 2428-2438. doi:10.2174/138161208785777450

Valenga, F., Petri, D. F. S., Lucyszyn, N., Jó, T. A., & Sierakowski, M. R. (2012). Galactomannan thin films as supports for the immobilization of Concanavalin A and/or dengue viruses. *International Journal of Biological Macromolecules, 50*(1), 88-94. doi:10.1016/j.ijbiomac.2011.10.005

Vance, D. E., & Vance, J. E. (2008). *Biochemistry of lipids, lipoproteins and membranes* (5th ed.): Elsevier.

Venkatasubbarao, S. (2004). Microarrays - status and prospects. *Trends in Biotechnology, 22*(12), 630-637. doi:10.1016/j.tibtech.2004.10.008

Vericat, C., Vela, M. E., Benitez, G., Carro, P., & Salvarezza, R. C. (2010). Self-assembled monolayers of thiols and dithiols on gold: new challenges for a well-known system [10.1039/B907301A]. *Chemical Society Reviews, 39*(5), 1805-1834. doi:10.1039/b907301a

Wan, Y., Su, Y., Zhu, X., Liu, G., & Fan, C. (2013). Development of electrochemical immunosensors towards point of care diagnostics. *Biosensors and Bioelectronics, 47*(0), 1-11. doi:10.1016/j.bios.2013.02.045

Wang, C., Wang, Z., & Zhang, X. (2012). Amphiphilic Building Blocks for Self-Assembly: From Amphiphiles to Supra-amphiphiles. *Accounts of Chemical Research, 45*(4), 608-618. doi:10.1021/ar200226d

Wang, D., Liu, S., Trummer, B. J., Deng, C., & Wang, A. (2002). Carbohydrate microarrays for the recognition of cross-reactive molecular markers of microbes and host cells. *Nature Biotechnology, 20*(3), 275. doi:10.1038/nbt0302-275

Wang, H., Zhang, Y., Yuan, X., Chen, Y., & Yan, M. (2011). A universal protocol for photochemical covalent immobilization of intact carbohydrates for the preparation of carbohydrate microarrays. *Bioconjugate Chemistry, 22*(1), 26-32. doi:10.1021/bc100251f

Wang, L., Ran, Q., Tian, Y., Xu, J., Xian, Y., Peng, R., & Jin, L. (2010). Covalent immobilization of redox protein via click chemistry and carbodiimide reaction: Direct electron transfer and biocatalysis. *Journal of Colloid and Interface Science, 350*(2), 544-550. doi:10.1016/j.jcis.2010.07.018

Wang, S., Ge, L., Song, X., Yu, J., Ge, S., Huang, J., & Zeng, F. (2012). Paper-based chemiluminescence ELISA: Lab-on-paper based on chitosan modified paper device and wax-screen-printing. *Biosensors and Bioelectronics, 31*(1), 212-218. doi:10.1016/j.bios.2011.10.019

Wang, T., Cook, C. C., Serban, S., Ali, T., Drago, G., & Derby, B. (2012). *Fabrication of glucose biosensors by inkjet printing*. Retrieved from http://arxiv.org/abs/1207.1190

Wang, W., Wang, Y., Tu, L., T, K., Feng, Y., & Wang, J.-P. (2013). Surface Modification for Protein and DNA <newline/>Immobilization onto GMR Biosensor. *Magnetics, IEEE Transactions on, 49*(1), 296-299. doi:10.1109/tmag.2012.2224327

Wang, X., Matei, E., Deng, L., Koharudin, L., Gronenborn, A. M., Ramström, O., & Yan, M. (2013). Sensing lectin–glycan interactions using lectin super-microarrays and glycans labeled with dye-doped silica nanoparticles. *Biosensors and Bioelectronics, 47*(0), 258-264. doi:10.1016/j.bios.2013.03.014

Wang, Z.-G., Wan, L.-S., Liu, Z.-M., Huang, X.-J., & Xu, Z.-K. (2009). Enzyme immobilization on electrospun polymer nanofibers: An overview. *Journal of Molecular Catalysis B: Enzymatic, 56*(4), 189-195. doi:10.1016/j.molcatb.2008.05.005

Watanabe, K., Fujiyama, T., Mitsutake, R., Watanabe, M., Tazaki, Y., Miyazaki, T., & Matsuda, R. (2010). Fabrication of Growth Factor Array Using an Inkjet Printer. In B. R. Ringeisen, B. J. Spargo, & P. K. Wu (Eds.), *Cell and Organ Printing* (pp. 203-222): Springer Netherlands. doi:10.1007/978-90-481-9145-1_12

Watanabe, K., Miyazaki, T., & Matsuda, R. (2003). Growth Factor Array Fabrication Using a Color Ink Jet Printer. *Zoological Science, 20*(4), 429-434. doi:10.2108/zsj.20.429

Weetall, H. (1993). Preparation of immobilized proteins covalently coupled through silane coupling agents to inorganic supports. *Applied Biochemistry and Biotechnology, 41*(3), 157-188. doi:10.1007/bf02916421

Wendeln, C., Heile, A., Arlinghaus, H. F., & Ravoo, B. J. (2010). Carbohydrate Microarrays by Microcontact Printing. *Langmuir, 26*(7), 4933-4940. doi:10.1021/la903569v

Willats, W. G. T., Rasmussen, S. E., Kristensen, T., Mikkelsen, J. D., & Knox, J. P. (2002). Sugar-coated microarrays: A novel slide surface for the high-throughput analysis of glycans. *PROTEOMICS, 2*(12), 1666-1671. doi:10.1002/1615-9861(200212)2:12<1666::aid-prot1666>3.0.co;2-e

Wilson, D. S., & Nock, S. (2002). Functional protein microarrays. *Current Opinion in Chemical Biology, 6*(1), 81-85. doi:10.1016/S1367-5931(01)00281-2

Wilson, W. C., & Boland, T. (2003). Cell and organ printing 1: Protein and cell printers. *The Anatomical Record Part A: Discoveries in Molecular, Cellular, and Evolutionary Biology, 272A*(2), 491-496. doi:10.1002/ar.a.10057

Wu, C.-C., Reinhoudt, D. N., Otto, C., Subramaniam, V., & Velders, A. H. (2011). Strategies for Patterning Biomolecules with Dip-Pen Nanolithography. *Small, 7*(8), 989-1002. doi:10.1002/smll.201001749

Wu, S., & Proft, T. (2010). The use of sortase-mediated ligation for the immobilisation of bacterial adhesins onto fluorescence-labelled microspheres: a novel approach to analyse bacterial adhesion to host cells. *Biotechnology Letters, 32*(11), 1713-1718. doi:10.1007/s10529-010-0349-y

Xiao, S.-J., Brunner, S., & Wieland, M. (2004). Reactions of Surface Amines with Heterobifunctional Cross-Linkers Bearing Both Succinimidyl Ester and Maleimide for Grafting Biomolecules. *The Journal of Physical Chemistry B, 108*(42), 16508-16517. doi:10.1021/jp047726s

Xu, T., Gregory, C. A., Molnar, P., Cui, X., Jalota, S., Bhaduri, S. B., & Boland, T. (2006). Viability and electrophysiology of neural cell structures generated by the inkjet printing method. *Biomaterials, 27*(19), 3580-3588. doi:10.1016/j.biomaterials.2006.01.048

Xu, T., Jin, J., Gregory, C., Hickman, J. J., & Boland, T. (2005). Inkjet printing of viable mammalian cells. *Biomaterials, 26*(1), 93-99. doi:10.1016/j.biomaterials.2004.04.011

Xu, T., Petridou, S., Lee, E. H., Roth, E. A., Vyavahare, N. R., Hickman, J. J., & Boland, T. (2004). Construction of high-density bacterial colony arrays and patterns by the ink-jet method. *Biotechnology and Bioengineering, 85*(1), 29-33. doi:10.1002/bit.10768

Yang, S., Chen, Z., Jin, X., & Lin, X. (2006). HRP biosensor based on sugar-lectin biospecific interactions for the determination of phenolic compounds. *Electrochimica Acta, 52*(1), 200-205. doi:10.1016/j.electacta.2006.04.059

Yasui, T., Inoue, Y., Naito, T., Okamoto, Y., Kaji, N., Tokeshi, M., & Baba, Y. (2012). Inkjet Injection of DNA Droplets for Microchannel Array Electrophoresis. *Analytical Chemistry, 84*(21), 9282-9286. doi:10.1021/ac3020565

Yates, E. A., Jones, M. O., Clarke, C. E., Powell, A. K., Johnson, S. R., Porch, A., ... Turnbull, J. E. (2003). Microwave enhanced reaction of carbohydrates with amino-derivatised labels and glass surfaces. *Journal of Materials Chemistry, 13*(9), 2061-2063. doi:10.1039/b305248f

Yeo, D. S. Y., Panicker, R. C., Tan, L. P., & Yao, S. Q. (2004). Strategies for Immobilization of Biomolecules in a Microarray. *Combinatorial Chemistry & High Throughput Screening, 7*(3), 213-221. doi:10.2174/1386207043328823

Yin, L.-T., Lin, Y.-T., Leu, Y.-C., & Hu, C.-Y. (2010). Enzyme immobilization on nitrocellulose film for pH-EGFET type biosensors. *Sensors and Actuators B: Chemical, 148*(1), 207-213. doi:10.1016/j.snb.2010.04.042

Yiu, S. C. K., & Lingwood, C. A. (1992). Polyisobutylmethacrylate modifies glycolipid binding specificity of verotoxin 1 in thin-layer chromatogram overlay procedures. *Analytical Biochemistry, 202*(1), 188-192.

Yonemori, Y., Takahashi, E., Ren, H., Hayashi, T., & Endo, H. (2009). Biosensor system for continuous glucose monitoring in fish. *Analytica Chimica Acta, 633*(1), 90-96. doi:10.1016/j.aca.2008.11.023

You, C., Bhagawati, M., Brecht, A., & Piehler, J. (2009). Affinity capturing for targeting proteins into micro and nanostructures. *Analytical and Bioanalytical Chemistry, 393*(6-7), 1563-1570. doi:10.1007/s00216-008-2595-6

Yu, A., Shang, J., Cheng, F., Paik, B. A., Kaplan, J. M., Andrade, R. B., & Ratner, D. M. (2012). Biofunctional Paper via the Covalent Modification of Cellulose†. *Langmuir, 28*(30), 11265-11273. doi:10.1021/la301661x

Yu, D., Volponi, J., Chhabra, S., Brinker, C. J., Mulchandani, A., & Singh, A. K. (2005). Aqueous sol–gel encapsulation of genetically engineered Moraxella spp. cells for the detection of organophosphates. *Biosensors and Bioelectronics, 20*(7), 1433-1437. doi:10.1016/j.bios.2004.04.022

Zhang, Z., Xia, S., Leonard, D., Jaffrezic-Renault, N., Zhang, J., Bessueille, F., ... Silveira, C. M. (2009). A novel nitrite biosensor based on conductometric electrode modified with cytochrome c nitrite reductase composite membrane. *Biosensors and Bioelectronics, 24*(6), 1574-1579. doi:10.1016/j.bios.2008.08.010

Zheng, Q., Lu, J., Chen, H., Huang, L., Cai, J., & Xu, Z. (2011). Application of inkjet printing technique for biological material delivery and antimicrobial assays. *Analytical Biochemistry, 410*(2), 171-176. doi:10.1016/j.ab.2010.10.024

Zhi, Z.-L., Laurent, N., Powell, A. K., Karamanska , R., Fais , M., Voglmeir, J., ... Turnbull, J. E. (2008). A Versatile Gold Surface Approach for Fabrication and Interrogation of Glycoarrays. *ChemBioChem, 9*(10), 1568-1575. doi:10.1002/cbic.200700788

Zhi, Z.-l., Powell, A. K., & Turnbull, J. E. (2006). Fabrication of Carbohydrate Microarrays on Gold Surfaces: Direct Attachment of Nonderivatized Oligosaccharides to Hydrazide-Modified Self-Assembled Monolayers. *Analytical Chemistry, 78*(14), 4786-4793. doi:10.1021/ac060084f

Zhou, L., Jiang, Y., Gao, J., Zhao, X., Ma, L., & Zhou, Q. (2012). Oriented immobilization of glucose oxidase on graphene oxide. *Biochemical Engineering Journal, 69*(0), 28-31. doi:10.1016/j.bej.2012.07.025

Zhou, X., & Zhou, J. (2006). Oligosaccharide microarrays fabricated on aminooxyacetyl functionalized glass surface for characterization of carbohydrate–protein interaction. *Biosensors and Bioelectronics, 21*(8), 1451-1458. doi:10.1016/j.bios.2005.06.008

Zimmermann, J. L., Nicolaus, T., Neuert, G., & Blank, K. (2010). Thiol-based, site-specific and covalent immobilization of biomolecules for single-molecule experiments. *Nat. Protocols, 5*(6), 975-985. doi:10.1038/nprot.2010.49